ol. 116 No. 2, May 1, 1980
ompleting Vol. 116
ISSN 0003-2670

ANALYTICA CHIMICA ACTA

International journal devoted to all branches of analytical chemistry

ELSEVIER SCIENTIFIC PUBLISHING COMPANY

ANALYTICA CHIMICA ACTA

International journal devoted to all branches of analytical chemistry
Revue internationale consacrée à tous les domaines de la chimie analytique
Internationale Zeitschrift für alle Gebiete der analytischen Chemie

PUBLICATION SCHEDULE FOR 1980 (incorporating the section on Computer Techniques and Optimization).

	J	F	M	A	M	J	J	A	S	O	N	D
Analytica Chimica Acta	113/1 113/2	114	115	116/1	116/2	117	118/1	118/2	119	120/1	120/2	121
Section on Computer Techniques and Optimization			122/1			122/2			122/3			122/4

Scope. *Analytica Chimica Acta* publishes original papers, short communications, and reviews dealing with every aspect of modern chemical analysis, both fundamental and applied. The section on *Computer Techniques and Optimization* is devoted to new developments in chemical analysis by the application of computer techniques and by interdisciplinary approaches, including statistics, systems theory and operation research. The section deals with the following topics: Computerized acquisition, processing and evaluation of data. Computerized methods for the interpretation of analytical data including chemometrics, cluster analysis, and pattern recognition. Storage and retrieval systems. Optimization procedures and their application. Automated analysis for industrial processes and quality control. Organizational problems.

Submission of Papers. Manuscripts (three copies) should be submitted as designated below for rapid and efficient handling:

Papers from the Americas to: Professor Harry L. Pardue, Department of Chemistry, Purdue University, West Lafayette, IN 47090, U.S.A.

Papers from all other countries to: Dr. A. M. G. Macdonald, Department of Chemistry, The University, P.O. Box 363, Birmingham B15 2TT, England.

For the section on *Computer Techniques and Optimization:* Dr. J. T. Clerc, Universität Bern, Pharmazeutisches Institut, Sahlistrasse 10, CH-3012 Bern, Switzerland.

American authors are recommended to send manuscripts and proofs by INTERNATIONAL AIRMAIL.

Information for Authors. Papers in English, French and German are published. There are no page charges. Manuscripts should conform in layout and style to the papers published in this Volume. Authors should consult Vol. 111, p. 343 for detailed information. Reprints of this information are available from the Editors or from: Elsevier Editorial Services Ltd., Mayfield House, 256 Banbury Road, Oxford OX2 7DE (Great Britain).

Reprints. Fifty reprints will be supplied free of charge. Additional reprints (minimum 100) can be ordered. An order form containing price quotations will be sent to the authors together with the proofs of their article.

Advertisements. Advertisement rates are available from the publisher.

Subscriptions. Subscriptions should be sent to: Elsevier Scientific Publishing Company, P.O. Box 211, 1000 AE Amsterdam, The Netherlands. The section on *Computer Techniques and Optimization* can be subscribed to separately.

Publication. *Analytica Chimica Acta* (including the section on *Computer Techniques and Optimization*) appears in 10 volumes in 1980. The subscription for 1980 (Vols. 113–122) is Dfl. 1390.00 plus Dfl. 160.00 (postage) (total approx. U.S. $795.00). The subscription for the *Computer Techniques and Optimization* section only (Vol. 122) is Dfl. 139.00 plus Dfl.16.00 (postage) (total approx. U.S. $79.50). Journals are sent automatically by airmail to the U.S.A. and Canada at no extra cost and to Japan, Australia and New Zealand for a small additional postal charge. All earlier volumes (Vols. 1–112) except Vols. 23 and 28 are available at Dfl. 150.00 (U.S. $77.00), plus Dfl. 10.00 (U.S. $5.00) postage and handling, per volume.

Claims for isssues not received should be made within three months of publication of the issue, otherwise they cannot be honoured free of charge.

Customers in the U.S.A. and Canada who wish to obtain additional bibliographic information on this and other Elsevier journals should contact Elsevier/North Holland Inc., Journal Information Center, 52 Vanderbilt Avenue, New York, NY 10017. Tel: (212) 867-9040.

JOURNAL OF ORGANOMETALLI CHEMISTRY LIBRARY

A series of books presenting reviews of recent developments and techniques in the expanding field of organometallic chemistry.

Coordinating Editor: D. SEYFERTH, *Massachusetts Institute of Technolog Cambridge, Mass., U.S.A.*

Volume 7: Organometallic Chemistry Reviews

CONTENTS: Non-catalytic hydrogenation via organoboranes *(K. Avasthi, D. Devapi bhakara and A. Suzuki).* Allyl derivatives of the Group IVA metals and mercury *(J. Mangravite).* Silyl-mercurials in organic synthesis *(W. P. Neumann and K. Reuter).* C ganosiliciumverbindungen des Schwefels, Selens und Tellurs *(D. Brandes).* Ferrocen carbocations and related species *(W. E. Watts).* The chemistry of cobaltocene, cob ticinium salts and other cobalt sandwich compounds *(J. E. Sheats).*

1979 viii + 522 pages US $105.00/Dfl. 215.00 ISBN: 0-444-41788-5

Volume 6: Organometallic Chemistry Reviews (1976); Annual Surveys: Silicor Germanium - Tin - Lead

1978 viii + 550 pages US $89.25/Dfl. 183.00 ISBN: 0-444-41698-6

Volume 5: Organometallic Chemistry Reviews

1977 viii + 320 pages US $73.25/Dfl. 150.00 ISBN: 0-444-41633-1

Volume 4: Organometallic Chemistry Reviews (1975); Annual Surveys - Silicon Tin - Lead

1977 viii + 548 pages US $73.25/Dfl. 150.00 ISBN: 0-444-41591-2

Volume 3: Organometallic Chemistry Reviews

1977 viii + 342 pages US $73.25/Dfl. 150.00 ISBN: 0-444-41538-6

Volume 2: Organometallic Chemistry Reviews: Organosilicon Reviews

1976 viii + 404 pages US $73.25/Dfl. 150.00 ISBN: 0-444-41488-6

Volume 1: New Applications of Organometallic Reagents in Organic Synthe

Out of Print

ELSEVIER

P.O. Box 211,
1000 AE Amsterdam
The Netherlands

52 Vanderbilt Ave
New York, N.Y. 10017

The Dutch guilder price is definitive. US $ prices are subject to exchange rate fluctuations.

JOURNAL OF ORGANOMETALLIC CHEMISTRY LIBRARY

A series of books presenting reviews of recent developments and techniques in the expanding field of organometallic chemistry.

Coordinating Editor: D. SEYFERTH, *Massachusetts Institute of Technology, Cambridge, Mass., U.S.A.*

Volume 9: ORGANOMETALLIC CHEMISTRY REVIEWS

CONTENTS: Applications of organomagnesium compounds in polymerization *(D. B. Malpass).* Formation and reactivity of the complexes of carbonyl compounds with organoaluminium compounds and aluminium chloride *(A. Sprozynski and K. B. Starowieyski).* Organofluorosilanes *(R. M. Pike and K. A. Koziski).* Structural evidence of coordination interactions in organic derivatives of mercury, tin and lead *(N. G. Furmanova, L. G. Kuz'mina and Yu. T. Struchkov).* The preparation of organotin compounds by the direct reaction *(J. Murphy and R. C. Poller).* Recent advances in the chemistry of arsonium ylides *(R. K. Bansal and S. K. Sharma).*

Selected plenary lectures from the Fifth International Symposium on Organosilicon Chemistry held in Karlsruhe, August 14-18, 1978: The environmental chemistry of liquid polydimethylsiloxanes, an overview *(C. L. Frye).* Cyclic silanes *(E. F. Hengge).* Silicon as a substituent and a link of heterocyclic rings *(L. Birkofer).* Recent developments in silyl-transition metal chemistry *(B. J. Aylett).* Mechanism of nucleophilic substitution at silicon. The nature of the driving force of stereochemistry *(R. Corriu).* Silicon-containing derivatives of carbonic acid *(V. F. Mironov).* Novel aspects of silicone chemistry *(W. Buechner).*

1980 viii + 432 pages US $105.00/Dfl. 215.00 ISBN: 0-444-41840-7

Volume 8: ORGANOMETALLIC CHEMISTRY REVIEWS; ANNUAL SURVEYS: SILICON - GERMANIUM - TIN - LEAD

CONTENTS: Silicon - Synthesis and reactivity; Annual Survey covering the year 1977 *(J. Y. Corey).* Organosilicon reaction mechanisms; Annual Survey for the year 1977 *(F. K. Cartledge).* Silicon: Bonding and Structure; Annual Survey covering the year 1977 *(P. R. Jones).* Silicon - Application to organic synthesis; Annual Survey covering the year 1977 *(G. M. Rubottom).* Germanium; Annual Survey covering the year 1977 *(D. Quane).* Tin; Annual Survey covering the year 1977 *(P. G. Harrison).* Lead; Literature Survey covering the year 1977 *(J. Wolters).*

1979 viii + 608 pages US $105.00/Dfl. 215.00 ISBN: 0-444-41789-3

ELSEVIER

The Dutch guilder price is definitive. US $ prices are subject to exchange rate fluctuations.

P.O. Box 211,
1000 AE Amsterdam
The Netherlands

52 Vanderbilt Ave
New York, N.Y. 10017

7157

Analytica Chimica, Acta, 116 (1980) 217—254

Review

NORMAL LEVELS OF TRACE ELEMENTS IN HUMAN BLOOD PLASMA OR SERUM

JACQUES VERSIECK* and RITA CORNELIS

Department of Internal Medicine, Division of Gastroenterology, University of Ghent, De Pintelaan 135, B-9000 Ghent (Belgium)

and

Institute for Nuclear Sciences, Laboratory for Analytical Chemistry, University of Ghent, Proeftuinstraat 86, B-9000 Ghent (Belgium)

(Received 19th November 1979)

SUMMARY

This review scrutinizes published information on the levels of 18 trace elements in blood plasma or serum of apparently healthy individuals. The disparities between the values reported by different investigators are examined critically. There is solid experimental evidence that much of the existing controversy is due to inadequate sampling and sample handling or to defective analysis. The data show that much work remains to be done to establish the normal levels of most trace elements. The development of adequate measures for contamination control is the most important prerequisite. Efforts should also be directed towards improving the accuracy and precision of the procedures applied.

During recent decades, great progress in analytical methodology has provided sensitive techniques for trace element research in man. Much interest has centred on plasma or serum levels in health and disease. Yet, a survey of the available information discloses serious inconsistencies. Confusion exists about the interpretation of the results. Some investigators [1] consider a serum chromium level of 0.5 ng ml^{-1} as the upper limit in normal individuals; others [2] accept a value of 5 ng ml^{-1} as definitive proof of chromium deficiency. Furthermore, the values found in apparently healthy subjects in the same laboratory may vary considerably. In 1962 the mean serum aluminium concentration in 17 volunteers was reported to be 800 ng ml^{-1} [3], but in 1971 the level in 68 subjects was found to be only 109 ng ml^{-1} [4]. Finally, analytical techniques with working curves or detection limits much higher than previously determined normal values are still being recommended. Thus, Maessen et al. [5] developed a method for the determination of cobalt in plasma at the μg ml^{-1} level although numerous investigators previously obtained values lower than the ng ml^{-1} level. Moreover, Ward and Ryan [6] recently presented a neutron activation analysis procedure which was said to permit the determination of 23 or more elements in plasma or

serum. A critical evaluation, however, shows that the literature values which are mentioned are far from complete and that, in fact, the detection limits of the recommended method for Al, As, Co, Cr, Hg, Mn, Mo, Ni, Rb, and V are markedly higher than the normal values reported by several investigators.

A living organism contains numerous intrinsic regulatory mechanisms. Many observations illustrate that the plasma or serum level of an essential element such as manganese is homeostatically controlled [7—10]. It has also been shown that the elevated level, after loading, of a non-essential element such as aluminium gradually returns to the control value [11]. As a consequence, values with a rather small range would be expected in healthy individuals who are not environmentally or occupationally exposed.

The purpose of this review is to summarize the available information about the concentration of 18 trace elements in plasma or serum of normal humans, and to examine which differences may be due to analytical errors rather than to biological variations. Twelve of these elements have also been studied at Ghent University. All the tabulated results were obtained in apparently healthy adults. The literature on trace elements also includes values determined in children or in "control subjects", i.e., in patients with generally minor, systemic diseases which are supposed not to interfere with normal trace element metabolism. As these values are regularly quoted as reference values, some of them are also discussed in the text. The figures reported by Burger [12] (Cr, Co, Cu, Mn, Mo, Ni, V, and Zn), Mertz et al. [13] (Cr, Mn, Mo, Ni, and Ag), and Webb et al. [14] (Al, Cs, Cr, Cu, Mn, Mo, Ni, Sn, and Zn) however, will not be considered further. Most of the results determined by these investigators differ substantially from those which, by more or less common consensus, are considered as the most reliable.

In this review all values are expressed in $\mu g\ ml^{-1}$ or $ng\ ml^{-1}$. Concentrations published as ppm (parts per million, 10^{-6}, $\mu g\ g^{-1}$) or in ppb (parts per billion, 10^{-9}, $ng\ g^{-1}$) have been multiplied by 1.026 (serum specific gravity). The following abbreviations are used: a.a.s. (atomic absorption spectrometry), c.l. (chemiluminescence), col. (colorimetry), e.s. (emission spectrometry), fluor. (fluorimetry), g.c.—e.c.d. (gas chromatography—electron capture detector), g.c.—m.e.e.d. (gas chromatography—microwave excited emission detector), n.a.a. (neutron activation analysis), spect. (spectrophotometry), and x.r.f. (x-ray fluorescence spectrometry).

ALUMINIUM

Recent reports that aluminium is toxic in the presence of renal failure has brought about an upsurge of interest in analyses for this element. Table 1 shows the levels published by different investigators. Nine sets of results were obtained by a.a.s., 4 by e.s., 3 by n.a.a., and 1 by spectrophotometry. Widely divergent values were found, varying from 3.72 $ng\ ml^{-1}$ up to 1460 $ng\ ml^{-1}$. As regulatory mechanisms for plasma aluminium have been docu-

TABLE 1

Plasma or serum aluminium concentration

Authors and reference numbers	Analytical technique	Mean (ng ml^{-1})	S.d. (ng ml^{-1})	Range (ng ml^{-1})	Number of subjects
De Baets et al., 1978 [15]	A.a.s.	3.72	1.20	2.1—6.2	8
Kaehny et al., 1977 [16]	A.a.s.	6	3		13
Salvadeo et al., 1972 [17]	A.a.s.	12.0	4.0		12
Valentin et al., 1976 [18]	A.a.s.	14.2	7.1	4.0—34.5	♂40
Clavel et al., 1978 [19]	A.a.s.	24	8	10—45	59
Ward et al., 1978 [20]	N.a.a.	25		10—50	10
Gorsky and Dietz, 1978 [21]	A.a.s.	28	9	12—46	23
Fuchs et al., 1974 [22]	A.a.s.	38		10—92	29
Clarkson et al., 1972 [23]	N.a.a.	72	70		10
Niedermeier and Griggs, 1971 [4]	E.s.	109	159	<60—790[a]	68
Seibold, 1960 [25]	Spect.	172	80		536
Panteliadis, 1975 [26]	E.s.	175			300
Julshamn et al., 1978 [27]	A.a.s.	210			pool
Berlyne et al., 1970 [28]	A.a.s.	240		200—300	5
Butt et al., 1964 [29]	E.s.	400	277		48
Niedermeier et al., 1962 [3]	E.s.	800		103—1930	17
Berlyne et al., 1970 [28]	N.a.a.	1460		1100—1800	5

[a]Values mentioned by Niedermeier et al., 1971 [24].

mented [11], doubt arises about the large spread of these figures.

Several factors may interfere with accurate determinations of aluminium at low levels. Because of the ubiquity of the element, stringent precautions must be taken to avoid extraneous additions. Some investigators such as Salvadeo et al. [17], Ward and associates [20], Panteliadis [26], and Berlyne et al. [28] give no details concerning their sample collecting and handling techniques. The samples analysed by De Baets et al. [15] were collected by using the procedure developed for other trace element determinations at Ghent University [30]. Whereas some investigators avoid pretreatment, others apply extensive sample preparation procedures before the actual measurement. De Baets et al. [15], Clavel and his colleagues [19], Gorsky and Dietz [21], and Fuchs et al. [22], all using a.a.s., introduces the samples directly into the graphite furnace. Kaehny et al. [16] first add Triton X-100 to prevent build-up of organic residues. Valentin et al. [18] dilute their serum samples with twice-distilled water. Julshamn et al. [27] perform a wet mineralization using a 1:1 mixture of concentrated nitric acid and 70% perchloric acid and, after evaporating the digest to dryness, dissolve the residue in 5% nitric acid. Several researchers using other analytical techniques also applied wet [4] or dry ashing procedures [3, 23, 25, 29]. Many other manipulations are sometimes added: mixing of the ash with spectroscopic-quality graphite [3], dissolution of the ash in hydrochloric acid followed by

ion exchange [25], or dissolution of the ashed residue in a spectroscopic buffer [4, 29]. Seibold [25] reports his technique to yield a blank value of 54 ng Al ml^{-1}. It is striking that the reported aluminium content is going up with the increasing complexity of the procedure before the actual detection. As far as emission spectrometry is concerned, besides the elaborate sample preparation, even the Spec-pure graphite used for the electrodes can be a major source of contamination. A matrix similar to plasma or serum but free of aluminium is not yet available for a true blank to be run. Only De Baets et al. [15] and Gorsky and Dietz [21] use a deuterium background corrector when employing atomic absorption spectrometry.

The determination of aluminium by n.a.a. is severely jeopardized by the fast neutron interference reaction $^{31}P\ (n,\alpha)^{28}Al$ ($\bar{\sigma}_f = 1.9$ mb). For a thermal-to-fast flux ratio of 5, the amount of phosphorus in plasma or serum (about 132 $\mu g\ ml^{-1}$ [31]) produces interference equivalent to about 190 ng Al ml^{-1}. Ward and associates [20] and Clarkson et al. [23] mention that a correction was made, but the interference probably accounts in part for the very high result found by Berlyne et al. [28] (1460 ng ml^{-1} by n.a.a. versus 240 ng ml^{-1} by a.a.s.).

In this survey of published aluminium levels, the work of Elliot et al. [32], who determined the aluminium content in 20 random serum samples from the routine biochemistry laboratory should also be mentioned. In the original publication a value of 0.06 $\mu mol\ l^{-1}$ is mentioned. This is a clerical error, the real value being 0.6 $\mu mol\ l^{-1}$ or 16.2 ng ml^{-1} as was ascertained by Fell [33].

ANTIMONY

Antimonials have been shown to be of value in tropical medicine, but the element has no known biological function in living organisms. Few investigators have determined its concentration in plasma or serum. The results, all obtained by n.a.a., are summarized in Table 2. The reported means vary from 0.52 to 5.2 ng ml^{-1}.

Antimony is a common impurity of quartz. Large differences exist for various types [39—42]. During irradiation at high neutron fluxes, recoil of

TABLE 2

Plasma or serum antimony concentration, all by n.a.a.

Authors and reference numbers	Mean (ng ml^{-1})	S.d. (ng ml^{-1})	Range (ng ml^{-1})	Number of subjects
Kasperek et al., 1979 [34]	0.52	0.19		7
Wester, 1973 [35]	0.75	0.51		8
Kasperek et al., 1972 [36]	2.5	1.37		149
Behne and Diel, 1972 [37]	3.3	2.7		4
Giovannetti et al., 1967 [38]	5.2		1.0—15	9

antimony may occur. Furthermore, serum specimens suffer from irradiation damage. Thus, the samples have to be separated from the container by wet ashing, i.e. by dissolution with a mixture of strong acids. In this way, impurities may also be leached from the quartz vial, forming an irreproducible "wet ashing blank", Mazière et al. [41] found <0.01—0.04 ng g^{-1} for Quartex, whereas Tjioe et al. [43] obtained 0.6 ± 0.5 ng and 1.4 ± 0.6 ng per vial for Vitreosil and Spectrosil, respectively. It is evident that the way the irradiation container is opened (snap cutting or crushing) may influence the wet ashing blank.

No specifications are available about the impurities in the quartz ampoules or silica containers used by Wester [35], Kasperek et al. [36], and Behne and Diel [37]. In the most recent studies of Kasperek et al. [34], which yielded the lowest antimony concentration (0.52 ± 0.19 ng ml^{-1}), Suprasil tubes were used. In the most recent experiments of Behne and Jürgensen [42], yielding one additional value of 0.11 ng ml^{-1}, high silica quartz made to specification by Heraeus (containing 0.02 ± 0.03 ng Sb g^{-1}) was used [42]. Moreover, as most of the impurities were believed to be located in the surface layers, the vials were cleaned by etching with 40% hydrofluoric acid (Suprapur; Merck). The authors do not mention the other values obtained in the 25 normal subjects they investigated.

Giovannetti et al. [38] irradiated lyophilized samples of ca. 0.1 g (corresponding to about 1 ml of fresh plasma) wrapped in high-purity aluminium foils. No data are available about the impurities in this material.

ARSENIC

Arsenic compounds have long been known to be toxic. Recently, evidence has been presented that arsenic may be an essential trace element. Table 3 mentions 8 reported mean values, ranging from 1.07 to 190 ng ml^{-1}. The 5

TABLE 3

Plasma or serum arsenic concentration

Authors and reference numbers	Analytical technique	Mean (ng ml^{-1})	S.d. (ng ml^{-1})	Range (ng ml^{-1})	Number of subjects
Damsgaard et al., 1973 [45]	N.a.a.	1.07	0.45	0.46—1.82	11
Giovannetti et al., 1967 [38]	N.a.a.	1.7		0.9—3.0	13
Heydorn, 1970 [46]	N.a.a.	2.4	1.9		16[a]
Wester, 1973 [35]	N.a.a.	8.9	6.2		8
Heydorn, 1970 [46]	N.a.a.	15.4	1.39		17[b]
Kingsley and Schaffert, 1951 [47]	Spect.	53	10.5	35—72	53
Gerhardt et al., 1978 [48]	Spect.			50—80	unknown
Schroeder and Nason, 1971 [49]	Spect.	190			unknown

[a]Normal Danish subjects. [b]Normal Taiwanese subjects.

lowest results were obtained by n.a.a., and the others by spectrophotometry.

Careful studies on arsenic were done at Risø National Laboratory in Denmark. The first results (2.4 ± 1.9 ng ml^{-1}) published by Heydorn were obtained on samples taken under good, standard hospital conditions [46]. The analysis of precision, as outlined by Heydorn in another publication [50], clearly indicated the presence of unsuspected sources of variability not accounted for in the expected precision of the analytical method. Two uncontrolled factors were identified: sampling conditions and bromine interference [50]. Thus, a new set of serum samples was taken under almost perfect conditions. The results of this study (1.07 ± 0.45 ng ml^{-1}) were published by Damsgaard et al. [45]. The observations illustrate how apprehension of unsuspected errors may lead to changes in methodology yielding both better precision and improved accuracy. Heydorn also reported a value of 15.4 ± 1.39 ng ml^{-1} in Taiwanese subjects [46]. However, it is not known if these samples were taken in the fasting state. In a recent study [51] Heydorn et al. showed that food intake has a marked influence on the serum arsenic concentration.

The arsenic level found by Giovannetti et al. [38] is only slightly higher than that mentioned by Damsgaard et al. [45]. Failure to observe the necessary strict precautions during sampling may explain the value of 8.9 ± 6.2 ng ml^{-1} obtained by Wester [35] as well as the other high values summarized in Table 3. Furthermore, Kingsley and Schaffert [47], Gerhardt et al. [48], and Schroeder and Nason [49] applied more or less extensive separations before the actual detection of the element. Taking into account the observations of Heydorn [46, 50], there is no doubt that such manipulations may contribute to increasing arsenic levels.

BROMINE

Little information is available on bromine metabolism. The element has not been conclusively shown to be involved in any essential function. The plasma or serum concentration can be determined by several analytical techniques. Neutron activation analysis is easily done in a purely instrumental way by use of the ^{82}Br isotope. Table 4 lists the mean values published by 10 groups. Most are satisfactorily consistent. Only the level found by Johnstone et al. [59, 60] is markedly higher than all the others. Behne and Jürgensen [42] disregarded 3 values (namely 21.6, 44.2 and 44.7 $\mu g\ ml^{-1}$) in calculating the mean.

The bromine level in plasma or serum has been shown to be largely dependent on the bromine supply. Sklavenitis and Comar [61] examined 50 subjects (including healthy individuals and patients with various diseases). In 33 a normal distribution was seen (mean ± s.d. = 3.2 ± 1.04 $\mu g\ ml^{-1}$; range = 1.5—5.5 $\mu g\ ml^{-1}$). In the others, higher levels were found, varying from 6 to 50 $\mu g\ ml^{-1}$. Most of these subjects appeared to take bromine-containing drugs. Bromides are available to the public without prescription in popular

TABLE 4

Plasma or serum bromine concentration

Authors and reference numbers	Analytical technique	Mean ($\mu g\ ml^{-1}$)	S.d. ($\mu g\ ml^{-1}$)	Range ($\mu g\ ml^{-1}$)	Number of subjects
Cabanis and Bonnemaire, 1970 [52]	Col.	2.13		0.62—5.2	29
Natelson et al., 1962 [53]	X.r.f.	2.520	0.208	2.15—2.82	15
Wester, 1973 [35]	N.a.a.	3.7	1.5		8
Duvaldestin, 1977 [54]	X.r.f.	3.93	0.73		10
Behne and Jürgensen, 1978 [42]	N.a.a.	4.5	2.2	2.5—	15
Cornelis et al., 1979 [55]	N.a.a.	4.87	2.02	1.28—7.48	10
Stump et al., 1977 [56]	X.r.f.	5.08	0.94	3.95—7.25	♂35
		5.14	0.46	3.42—7.45	♀38
Alfrey et al., 1975 [57]	X.r.f.	6.4	1.7		5
Goodwin, 1971 [58]	Col.	7.52	9.01	0—30.5	♂28
Johnstone et al., 1975 [59]	Unknown	30.4	8.0	8.8—99.9[a]	10

[a] Values reported by Johnstone et al., 1975 [60].

nostrums, nerve tonics, headache remedies, cough cures, and other proprietary preparations. Furthermore, the bromine level is said to be dependent on dietary habits [62, 63] and geographical or environmental factors [64, 65]. After oral intake of 1 g of KBr per kg of body weight, bromine is only slowly removed from the blood stream, the biological half-life varying from 10 to 12 days [61].

There are no reports of serious contamination problems during sampling. The reason for the high values found by Johnstone et al. [59] is not obvious. The subjects are said to be healthy laboratory technicians without known exposure to abnormal amounts of the element.

CAESIUM

Caesium has no known vital function. Its occurrence in biological samples has not evoked much interest among trace analysts. Table 5 summarizes the results of 7 studies, 6 being done by n.a.a. and 1 by e.s. The 5 lower mean values varying from 0.74 to 1.33 ng ml^{-1} are very similar, but the remaining 2 are substantially higher. The risk of caesium contamination during the collection of blood is probably minute. The element is not so ubiquitously present and is not a common component of collection and storage devices. But, as the caesium content of packed blood cells is about 6.5 times higher than that of serum [66], careless separation or hemolysis could seriously jeopardize the results.

Niedermeier and Griggs [4] used emission spectrometry, but preceded this with an elaborate sample preparation which probably resulted in a major

TABLE 5

Plasma or serum caesium concentration

Authors and reference numbers	Analytical technique	Mean (ng ml^{-1})	S.d. (ng ml^{-1})	Range (ng ml^{-1})	Number of subjects
Versieck et al., 1977 [66]	N.a.a.	0.74	0.20	0.45—1.18	36
Kasperek et al., 1979 [34]	N.a.a.	0.85	0.22		7
Wester, 1973 [35]	N.a.a.	1.0	0.9		8
Behne and Jürgensen, 1978 [42]	N.a.a.	1.10	0.32	0.67—2.06	25
Kasperek et al., 1972 [36]	N.a.a.	1.33	0.68		183
Yamagata and Iwashima, 1966 [67]	N.a.a.			10.5—166	4
Niedermeier and Griggs, 1971 [4]	E.s.	63	42	<40—240[a]	68

[a]Values reported by Niedermeier et al., 1971 [24].

systematic error. Furthermore, the analytical technique was inadequate as the element could be detected in only 60% of the specimens.

CHROMIUM

Much effort has been devoted to the determination of chromium in biological samples, mainly because of the presumed relation of the element to atherosclerosis [68—70] and diabetes [71, 72]. A large body of analytical data has accumulated but deep confusion remains as to the actual concentration in plasma or serum of healthy individuals. As shown in Table 6, widely divergent values have been reported, varying from 0.14 ng ml^{-1} [73] to 185 ng ml^{-1} [94].

The accurate determination of chromium in biological specimens presents a considerable challenge, as appears from the results of interlaboratory comparisons of reference materials [95]. The inconsistent chromium values obtained in NBS bovine liver (SRM 1577) (Fig. 1) unquestionably prove that most of the published values are in error. Two main causes have been postulated to explain the existing discrepancies: (1) volatilization during sample drying and/or dry ashing [107—112]; and (2) contamination during sample collecting and handling [74, 113]. Cumulative evidence indicates that the first explanation can no longer be sustained. Careful studies by Gorsuch [114], Jones et al. [115], Koirtyohann and Hopkins [116], and Kumpulainen [117] have proved that no perceptible losses occur. Moreover, a recent study by Rook and Wolf [118] also shows that less than 1% of the total chromium is lost at 300°C. Finally, experiments by Versieck et al. [119] indicate that there is no appreciable volatilization during dry ashing of Bowen's kale, NBS orchard leaves (SRM 1571), NBS bovine liver (SRM 1577), and NBS brewer's yeast (SRM 1569) at temperatures up to 450°C. In contrast, the second

TABLE 6

Plasma or serum chromium concentration

Authors and reference numbers	Analytical technique	Mean (ng ml^{-1})	S.d. (ng ml^{-1})	Range (ng ml^{-1})	Number of subjects
Kayne et al., 1978 [73]	A.a.s.	0.14			8
Versieck et al., 1978 [74]	N.a.a.	0.160	0.083	0.0382—0.351	20
Seeling et al., 1975 [1]	A.a.s.			<0.50	unknown
Kasperek et al., 1979 [34]	N.a.a.	0.45	0.15		7
Grafflage et al., 1974 [75]	A.a.s.	0.73		0.23—1.90	50
Pekarek et al., 1974 [76]	A.a.s.	1.62	0.31	0.20—	15
Liu and Morris, 1978 [77]	N.a.a.	1.67	0.45		♀15
van Kooten et al., 1967 [78]	N.a.a.			0.7—3.2	3
Hambidge, 1974 [79]	E.s.	3.1		1.0—	unknown
Davidson and Secrest, 1972 [80]	A.a.s.	5.07		3.10—7.19	7
Black and Sievers, 1976 [81]	G.c.—m.e.e.d.	6.96		3.57—9.92	5
Salvadeo et al., 1979 [17]	A.a.s.	8.2	2.4		12
Kasperek et al., 1972 [36]	N.a.a.	9.3	5.6		127
Behne and Diel, 1972 [37]	N.a.a.	10.3	6.2		♂4
Bierenbaum et al., 1975 [82]	A.a.s.	12	32		260[a]
Savory et al., 1972 [83]	G.c.—e.c.d.	13.5		2.7—24	21
Butt et al., 1964 [29]	E.s.	15.5			48
Feldman, 1969 [84]	A.a.s.	17.4		5.1—40	200
Panteliadis, 1975 [26]	E.s.	20.5			300
Koch et al., 1956 [85]	E.s.	22	12	7—52	17
Levine et al., 1968 [86]	A.a.s.	23.2	4		16
Paixao and Yoe, 1959 [87]	E.s.	25		16—39	39
Glinsmann et al., 1966 [88]	A.a.s.	28		23—34	♂5
Herring et al., 1960 [89]	E.s.	28		9—56	61
Niedermeier and Griggs, 1971 [4]	E.s.	28	48	<10—260[c]	68
Feldman et al., 1967 [90]	A.a.s.	30		11—66	132
Bierenbaum et al., 1975 [82]	A.a.s.	43	113		260[b]
Maxia et al., 1972 [91]	N.a.a.	45		14—77	3
Freund et al., 1979 [2]	Unknown			5—90	unknown
Niedermeier et al., 1962 [3]	E.s.	55		10—390	17
Li and Hercules, 1974 [92]	C.l.	150		41—251	11
Bala and Lifshits, 1966 [93]	E.s.	171[d]			unknown
Monacelli et al., 1956 [94]	E.s.	185		82—308	25

[a]Subjects from Kansas City, Kansas. [b]Subjects from Kansas City, Missouri. [c]Values mentioned by Niedermeier et al., 1971 [24]. [d]The mean value of Bala and Lifshits was recalculated assuming an haematocrit of 0.45.

explanation, viz. inadequacy of sample collecting and handling, is a major source of error; adequate blood collection has been proven to be of vital importance in ensuring reliable results. Investigations by Versieck et al. [113] have shown that huge extraneous additions result from blood being

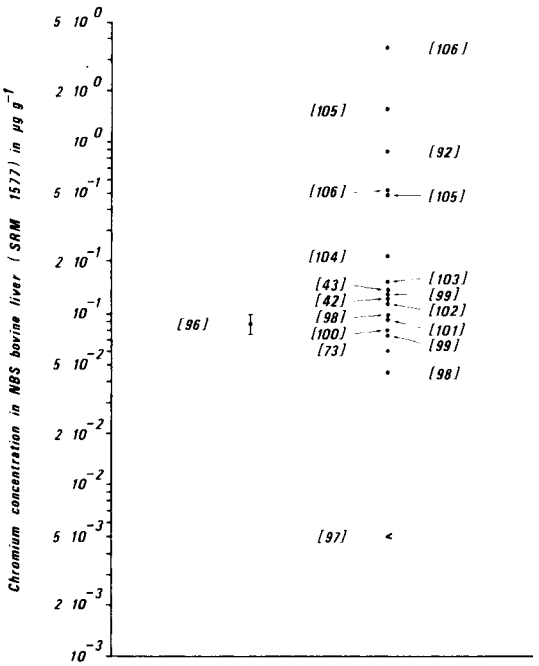

Fig. 1. Values for the Cr concentration in NBS bovine liver (SRM 1577) as reported by different investigators. The NBS certified value (mean ± s.d. = 0.088 ± 0.012 μg g^{-1}) [96] is indicated on the left.

drawn through a disposable steel needle (Terumo 18 G 1 1/2). In an in vitro experiment with an irradiated needle, the following additions were found in four successively collected 20-ml blood samples: 89.9, 12.7, 10.4, and 15.9 ng Cr ml^{-1}.

As shown in Table 6, the three lowest chromium levels reported are quite similar: a mean of 0.14 ng ml^{-1} by Kayne et al. using a.a.s. [73], a mean of 0.160 ng ml^{-1} by Versieck et al. employing n.a.a. [74], and an upper limit of 0.5 ng ml^{-1} by Seeling et al. also using a.a.s. [1]. Kayne et al. [73] digested their serum specimens with ultra-pure nitric acid and hydrogen peroxide in fused silica vials fitted with threaded teflon caps. After dilution with deionized distilled water, 20-μl fractions were injected into the graphite oven (with deuterium background corrector). Versieck et al. [74] ashed their lyophilized serum samples before irradiation in high-purity quartz tubes (Spectrosil) in a Simon—Müller oven at 100, 200, 350, and 450°C successively for 24 h. After irradiation, the ash was dissolved in a 1 : 1 mixture of perchloric acid (70%) and nitric acid (14 M). Chromium was selectively distilled as CrO_2Cl_2. A mean blank value of 0.0478 ng (range : 0.0262—0.0704 ng) was observed. Furthermore, it is interesting to mention that Kasperek and his associates have recently revised their values down from 9.3 ± 5.6 ng ml^{-1} of serum in 1972 [36] to 0.45 ± 0.15 ng ml^{-1} of plasma in 1979 [34].

Grafflage et al. [75] used a plastic catheter for blood collection and avoided glass vials. Application of high-sensitivity flameless a.a.s. on a 50-μl serum probe (without deuterium background correction) yielded a mean value of 0.73 ng ml^{-1}. Through application of a quite similar procedure (but with deuterium background correction) Pekarek et al. [76] found a mean value of 1.62 ng ml^{-1}. Their samples were allowed to clot in acid-cleaned glass test tubes. As borosilicate glass contains between 1 and 10 μg Cr g^{-1} [120], it remains open to question whether this has some bearing on the actual chromium content of the samples. At any rate, their reported chromium concentration is more than 10 times higher than the lowest value of 0.14 ng ml^{-1}. Liu and Morris [77] obtained a mean value of 1.67 ng ml^{-1} by n.a.a. Blood was collected in lead-free Vacutainers with the same siliconized needle as used for obtaining samples for insulin and blood glucose determinations.

Table 6 includes a long list of other chromium values, in steadily increasing order up to a mean value of 185 ng ml^{-1}. The recently reported values by Newman et al. [69] (6.09 ± 3.30 ng ml^{-1}) are not included as they were obtained in a control group (non-coronary artery disease patients) and not in apparently healthy individuals. Each group of researchers applied a particular sample collecting and processing procedure which they considered the most appropriate for the final detection method.

It cannot be said that the mean values from one particular technique agree satisfactorily. It is difficult to evaluate these divergent results, all obtained by well-established analytical techniques. The lowest values (0.14 and 0.16 ng ml^{-1}) are believed to be the most probable. In both studies, the accuracy of the applied technique was checked by analysing reference materials [73, 100, 119]. As far as the high figures are concerned, not the technique per se is at stake, but its application when unsuspected contamination is involved. The latter suspicion is supported by the different, generally progressively decreasing values published by the same authors on consecutive occasions. After reporting a mean value of 30 ng ml^{-1} in 1967 [90], Feldman mentioned a mean level of 17.4 ng ml^{-1} in 1969 [84]. Niedermeier and his associates mentioned 55 ng ml^{-1} and 28 ng ml^{-1} in 1962 and 1971, respectively [3, 4]. Determinations at the Pratt Trace Analysis Laboratory (University of Virginia) resulted in the following 3 mean values obtained by emission spectrometry : 185 ng ml^{-1} in 1956 [94], 25 ng ml^{-1} in 1959 [87], and a similar value of 28 ng ml^{-1} in 1960 [89]. Behne and co-workers mentioned a mean level of 10.3 ng ml^{-1} in 1972 [37] and reported an additional value of 1.44 ng ml^{-1} in 1978 [42] ; they have not yet given the mean concentration found in the 25 normal subjects studied.

Bierenbaum et al. [82], using a.a.s. found two substantially different mean values in the twin Kansas Cities on the opposite sides of the Missouri river, namely 12 ng ml^{-1} in subjects from Kansas City, Kansas, and 43 ng ml^{-1} in subjects from Kansas City, Missouri. From the foregoing discussion it will be evident that this observation should be interpreted with extreme caution. Both values are improbably high and the difference could be a mere

artefact. This statement is supported by other inconsistent values in the same publication, namely for Cu, Zn, and particularly for Co (see below).

The chromium response after a glucose load is also a matter of deep controversy [37, 77, 84, 86, 88, 121, 122]. It seems premature to draw any conclusions as long as the investigators have not established a reliable baseline value.

COBALT

The element serves its paramount, established biological function as a component of vitamin B_{12} where it is situated within a corrin ring. Its determination has also excited considerable interest. The results are set out in Table 7. Both the lowest (0.0 ng ml^{-1}) and the highest (146 ng ml^{-1}) mean values were obtained by Bierenbaum et al. [82], who claimed a geographical factor as the underlying cause for the observed difference. It is obvious, however, that these data should be disregarded. As a constituent of vitamin B_{12}, cobalt occurs in serum in amounts of about 0.010–0.025 ng ml^{-1}. The fact that no cobalt was detected in one population (in Kansas City, Kansas) proves that the method, as applied by the investigators, lacks sensitivity. The other value of 146 ± 419 ng ml^{-1} (mean ±s.d., the latter being recalculated from the standard error of the mean) seems most improbable as well. Such a

TABLE 7

Plasma or serum cobalt concentration

Authors and reference numbers	Analytical technique	Mean (ng ml^{-1})	S.d. (ng ml^{-1})	Range (ng ml^{-1})	Number of subjects
Bierenbaum et al., 1975 [82]	A.a.s.	0.0	0.0		260[a]
Lins and Pehrsson, 1976 [123]	N.a.a.			0.02—0.06	3
Thiers et al., 1955 [124]	E.s.			0.064–0.085	2
Versieck et al., 1978 [74]	N.a.a.	0.108	0.060	0.0394—0.271	20
Behne and Diel, 1972 [37]	N.a.a.	0.23	0.11		♂4
Parr and Taylor, 1964 [125]	N.a.a.	0.29	0.16	0.08—0.60	6
Kasperek et al., 1979 [34]	N.a.a.	0.33	0.22		7
Giovannetti et al., 1967 [38]	N.a.a.	0.46		0.20—1.30	12
Wester, 1973 [35]	N.a.a.	0.52	0.43		7
Samsahl et al., 1972 [126]	N.a.a.	0.8	0.6		♀30
Salvadeo et al., 1979 [17]	A.a.s.	1.2	0.4		12
Kasperek et al., 1972 [36]	N.a.a.	1.85	1.32		151
Alt and Massmann, 1976 [127]	A.a.s.			0.5—10	unknown
Muzzarelli and Rocchetti, 1975 [128]	A.a.s.	7.7	1.9	5.6—9.8	18
Koch et al., 1956 [85]	N.a.a.	12.2		0.38—72.8	25
Butt et al., 1964 [29]	E.s.	62			48
Kesteloot et al., 1968 [129]	Col.	72			unknown
Bierenbaum et al., 1975 [82]	A.a.s.	146	419		260[b]

[a] Subjects from Kansas City, Kansas. [b] Subjects from Kansas City, Missouri.

large standard deviation is highly suspect, indicating heavily contaminated samples.

The published plasma or serum cobalt levels are in better agreement than the existing chromium values. Several investigators, 5 using n.a.a. and 1 emission spectrometry, reported mean values lower than 0.35 ng ml^{-1}. Lins and Pehrsson [123] examined 3 normal individuals: 2 showed a level of 0.02 ng ml^{-1}, and the other 0.06 ng ml^{-1}. Thiers et al. [124] mention 2 values, namely 0.064 and 0.085 ng ml^{-1}. They used Pt—Ru alloy needles, mixed the blood with heparin, and applied an elaborate but careful separation before detecting the element by emission spectrometry. Versieck et al. [74] found a mean value of 0.108 ng ml^{-1} in 20 healthy individuals. Although high-purity quartz vials (Spectrosil) were used, a mean blank value of 0.0267 ng (range = 0.0167—0.0388 ng) was determined. In 1972, Behne and Diel [37] reported a mean value of 0.23 ng ml^{-1}. In an article dated 1978, Behne and Jürgensen [42] give one additional value of 0.36 ng ml^{-1} but they do not report the serum content of the 25 healthy persons investigated. Parr and Taylor [125] found 0.29 ng ml^{-1} of serum. Blood samples were collected with a Pt—Ir needle and processed in polythene vials. The recently revised value of Kasperek et al. [34] also agrees with previous figures. Moreover, the data published by Giovannetti et al. [38] and Wester [35] are only slightly higher. It is interesting to note that, whereas the chromium levels reported by the Pratt Trace Analysis Laboratory are highly questionable (see above), the cobalt values published in 1955 [124] turn out to be in excellent agreement with the most recent data.

Nevertheless, as for several other elements, high values have been published, namely by Muzzarelli and Rocchetti [128], Koch et al. [85], Butt et al. [29], and Kesteloot et al. [129]. As previous studies at Ghent University have proved that the risk of obtaining high values because of extraneous additions is also important in the case of cobalt [113], there are good reasons to suppose that these data result from analyses of improperly handled samples.

COPPER

Copper metabolism in man has been investigated for many years by numerous researchers. The element is being detected in a growing number of proteins and enzymes. It is involved in activities as diverse as haemoglobin synthesis, connective tissue development, and normal function of the central nervous system. A large number of studies has been published on plasma or serum concentrations. Table 8 illustrates the remarkably consistent results that have been obtained by the use of five different analytical techniques. The reported means vary from 0.54 to 1.7214 $\mu g\ ml^{-1}$, and 27 out of 36 values, i.e. 75%, lie between 0.8 and 1.20 $\mu g\ ml^{-1}$.

The lowest mean value of 0.54 $\mu g\ ml^{-1}$ as described by de la Cruz [130] is open to doubt. It is conspicuous that the mean value for patients with a high

TABLE 8

Plasma or serum copper concentration

Authors and reference numbers	Analytical technique	Mean ($\mu g\ ml^{-1}$)	S.d. ($\mu g\ ml^{-1}$)	Range ($\mu g\ ml^{-1}$)	Number of subjects
de la Cruz, 1973 [130]	N.a.a.	0.54	0.08	0.41—0.74	unknown
Olehy et al., 1966 [131]	N.a.a.	0.85	0.05		12
Aaseth et al., 1978 [132]	A.a.s.	0.89	0.19		30
Parr and Taylor,1964 [125]	N.a.a.	0.91	0.13	0.69—1.16	6
Hambidge and Droegemuller, 1974, [133]	E.s.	0.916			♂unknown
		1.074			♀unknown
Allain et al., 1977 [134]	A.a.s.	0.956	0.19		unknown
Niedermeier and Griggs, 1971 [4]	E.s.	0.970	0.321	0.46—2.18[a]	68
Samsahl et al., 1972 [126]	N.a.a.	0.97	0.23		♀30
Koch et al., 1956 [85]	Col.	0.98	0.12	0.65—1.35	58
Olatunbosun et al., 1976 [135]	A.a.s.	1.01	0.182	0.70—1.50	37
Wester, 1973 [35]	N.a.a.	1.01	0.33		8
Paixao and Yoe, 1959 [87]	E.s.	1.02		0.51—2.54	39
Salvadeo et al., 1979 [17]	A.a.s.	1.03	0.52		12
Kasperek et al., 1972 [36]	N.a.a.	1.040	0.145		15
Giovannetti et al., 1967 [38]	N.a.a.	1.05		0.65—1.50	11
Herring et al., 1960 [89]	E.s.	1.06		0.49—1.98	61
Versieck et al., 1974 [136]	N.a.a.	1.07	0.24	0.73—1.99	46
Lahey et al., 1953 [137]	Col.	1.09	0.17	0.68—1.43	63
Butt et al., 1964 [29]	E.s.	1.10	0.28		48
Danys and Kušleikaitė, 1971 [138]	E.s.	1.10	0.14		30
Bogden et al., 1977 [139]	A.a.s.	1.10	0.19		20
Alfrey et al., 1975 [57]	X.r.f.	1.120	0.220		5
Lafargue et al., 1976 [140]	A.a.s.	1.120	0.170		♂unknown
		1.210	0.180		♀unknown
Yunice et al., 1974 [141]	A.a.s.	1.128	0.189		♂180
		1.132	0.202		♀44
Funckes et al., 1976 [142]	A.a.s.	1.16	0.43		♀15
Stump et al., 1977 [56]	X.r.f.	1.20	0.22	0.90—1.58	♂32
		1.13	0.19	0.85—1.52	♀28
Muzzarelli and Rocchetti, 1975 [128]	A.a.s.	1.2	0.16	1.0—1.4	18
Zhernakova, 1967 [143]	E.s.	1.20	0.3345		♂unknown
		1.20	0.2786		♀unknown
Panteliadis, 1975 [26]	E.s.	1.23			300
Monacelli et al., 1956 [94]	E.s.	1.23		1.0—2.2	unknown
Niedermeier et al., 1962 [3]	E.s.	1.32		0.78—2.11	17
Hartoma, 1977 [144]	A.a.s.	1.3568	0.2592		♂391
		1.4711	0.3184		♀258
Bierenbaum et al., 1975 [82]	A.a.s.	1.4460	0.637		260[b]
Holtzman et al., 1966 [145]	A.a.s.	1.63	0.40		19
Kanabrocki et al., 1964 [146]	N.a.a.	1.64	0.41	1.025—2.875	♂30
Bierenbaum et al., 1975 [82]	A.a.s.	1.7214	0.768		260[c]

[a]Values reported by Niedermeier et al., 1971 [24]. [b]Subjects from Kansas City, Kansas. [c]Subjects from Kansas City, Missouri

risk of developing heart disease is 1.02 μg ml^{-1}, a value considered to be normal by most other researchers. Little comment from the analytical point of view can be given on the long list of results from 0.85 μg ml^{-1} to 1.35 μg ml^{-1}. Some values are slightly higher, including those of Holtzman et al. [145], and Kanabrocki et al. [146], as well as those of Novosel and Jelavić [147] which are not included in Table 8 (mean, 1.64 μg ml^{-1}).

There might be slight variations due to geographical factors, as observed by Hartoma [144] for different regions in Finland where men and women living in Oulu, an industrial town, were found to have higher copper levels than in other places (levels in men were 1.4254 ± 0.2771 μg ml^{-1}, and in women 1.5521 ± 0.3626 μg ml^{-1}). The two different values (1.4460 μg ml^{-1} and 1.7214 μg ml^{-1}) found by Bierenbaum et al. [82] should be interpreted with caution, both because of the other inconsistencies in this study and because of the particularly high levels in Kansas City, Missouri. Some investigators looked for differences in concentration between men and women [56, 125, 133, 136, 137, 140, 141, 143, 144]. Only Hartoma observed a statistically significant difference ($t = 4.84; p < 0.001$).

The good agreement between most results from different centres over the past 25 years indicates that there are no major methodological problems linked to the determination of copper in plasma or serum. This explains why many authors like Niedermeier et al. [3, 4], Salvadeo et al. [17], Panteliadis [26], Butt et al. [29], Koch et al. [85], Herring et al. [89], Monacelli et al. [94], and Muzzarelli and Rocchetti [128] obtain adequate copper values at the μg ml^{-1} level but erroneous chromium and cobalt values at the ng ml^{-1} level.

MANGANESE

Although considerable attention has been paid to the role of manganese, its specific biochemical actions in vivo remain largely unknown. Whereas metal–enzyme complexes that can be activated by the element are numerous, metalloenzymes with manganese incorporated firmly into the molecule are few. Knowledge of the intimate relationship between the element and various hormones and nucleic acids is just beginning to emerge.

The serum level has been a most controversial topic in trace metal research. As can be seen in Table 9, there is great variation in the mean values, namely from 0.54 to 34.3 ng ml^{-1}. Although high values are still being published [17, 127, 128, 152, 153], a consensus has arisen among investigators who have worked for a long time on the element, that the manganese levels in healthy subjects are normally distributed around a mean value of 0.5—0.6 ng ml^{-1}, with an upper limit of approximately 1.0—1.2 ng ml^{-1}. Fernandez et al. [148] were the first to suggest the very low range of 0.36—0.90 ng ml^{-1}. This was confirmed by the research of Cotzias et al. [8] who established a mean value of 0.587 ng ml^{-1}, followed by Damsgaard et al. [45] and Versieck et al. [136] who found mean levels of 0.54 ng ml^{-1} and 0.57 ng ml^{-1} respectively.

TABLE 9

Plasma or serum manganese concentration

Authors and reference numbers	Analytical technique	Mean (ng ml^{-1})	S.d. (ng ml^{-1})	Range (ng ml^{-1})	Number of subjects
Damsgaard et al., 1973 [45]	N.a.a.	0.54	0.16	0.36—0.78	11
Versieck et al., 1974 [136]	N.a.a.	0.57	0.13	0.38—1.04	46
Cotzias et al., 1966 [8]	N.a.a.	0.587	0.183		14
Fernandez et al., 1963 [148]	Spect.			0.36—0.90	12
Seeling et al., 1975 [149]	A.a.s.	0.97			unknown
D'Amico and Klawans, 1976 [150]	A.a.s.	1.02	0.19	0.74—1.25	19
Grafflage et al., 1974 [75]	A.a.s.	1.94		0.50—7.89	50
Papavasiliou and Cotzias, 1961 [151]	N.a.a.	2.50		2.05—2.97	16
Banta and Markesbery, 1977 [152]	A.a.s.			2.1—3.1	unknown
Olehy et al., 1966 [131]	N.a.a.	4.3	0.5		12
Sullivan et al., 1979 [153]	N.a.a.	6	4		37
Muzzarelli and Rocchetti, 1975 [128]	A.a.s.	9	4.3	5—16	9
Alt and Massmann, 1976 [127]	A.a.s.			5—20	unknown
Zhernakova, 1967 [143]	E.s.	10.5			♂unknown
		9.6	5.0		♀unknown
Butt et al., 1964 [29]	E.s.	13	7		48
Kanabrocki et al., 1964 [146]	N.a.a.	13	2		30
Niedermeier et al., 1962 [3]	E.s.	18.5		7.2—71.8	17
Panteliadis, 1975 [26]	E.s.	21			300
Salvadeo et al., 1979 [17]	A.a.s.	23.0	5.0		12
Niedermeier and Griggs, 1971 [4]	E.s.	24	33	<10—140[a]	68
Mahoney et al., 1969 [154]	A.a.s.	24	7	12—38	40
Danys and Kušleikaitė, 1971 [138]	E.s.	34.3	7.0		30

[a]Values mentioned by Niedermeier et al., 1971 [24].

The paramount importance of sample quality was fully understood for the first time by Cotzias and co-workers. In 1961, they published a mean value of 2.50 ng ml^{-1} [151] which they acknowledged to be unreliable in 1966 [8] as a careful search showed that systematic contamination with exogenous metal persisted in their first study. The extreme importance of stringent precautions to avoid extraneous additions was further emphasized by Heydorn and co-workers [46, 50, 155] and by Versieck et al. [136, 156]. Manganese contamination has turned out to be extremely difficult to control [51]. The most important measures that must be taken are: ultra-pure materials cleaned with utmost care [30, 136, 156, 157] and clean-room conditions [158—160]. Mutatis mutandis, an investigator working on manganese should observe the same stringent precautions to preserve chemical sterility as a surgeon does to preserve bacteriological sterility. Furthermore, as the

manganese content of packed blood cells is about 26 times greater than the serum level [136] the separation must be done with extreme care.

The values reported by Seeling et al. [149], D'Amico and Klawans [150], and Mazière et al. [161] (1.1 ± 0.2 ng ml^{-1}, not included in Table 9 because they were obtained in infants and children) are only slightly higher. Further studies are needed before deciding whether these values are attributable to some physiological variation or to minor contamination. Accumulated evidence suggests that all other values listed in Table 9 should be considered as more or less erroneously high because of having been obtained on inadequately collected and handled samples.

Apparently, the need for accuracy in manganese analysis is not accepted by all investigators, as exemplified by the remarkable statement of Muzzarelli and Rocchetti [162] that they do not attach excessive significance to absolute values but feel that concentration ratios are more important. A detailed discussion of the problem falls outside the scope of this publication. The reader is referred to the publications of Bowen [163, 164] and Cali [165].

MERCURY

Mercury has long been known as a toxic element. It is found in the environment in various chemical forms with different absorption, distribution, excretion, and accumulation patterns. Mercury has a long history as an occupational hazard but the increasing recent concern stems from the wide existence of mercury pollution in the environment and repeated outbreaks of methylmercury poisoning [166]. In some countries, notably Japan and Sweden, mercury is a major health hazard. The most serious problem is its high concentration in fish [167]: thus, fish-eating populations find themselves exposed to high levels of mainly organically bound mercury.

Table 10 lists the literature values with means ranging from 1.8 ng ml^{-1} up to 13.74 ng ml^{-1}, the four lowest values being comparable. Very heavy fish eaters from different parts of the Lake Vänern region in Sweden were found to have markedly higher plasma mercury levels (from 4.92 ± 1.03 ng ml^{-1} to 13.74 ± 2.98 ng ml^{-1}) than other Swedish subjects (2.33 ± 1.11 ng ml^{-1}). The values of Kubasik et al. [171] appear to be high, as the samples were collected from occupationally unexposed subjects in the U.S.A. In individuals from a local industry, who were known to be exposed to increased mercury hazards, a mean value of 21 ng ml^{-1} with a range from 0 to 94 ng ml^{-1} is said to have been observed [171].

The values obtained by Suzuki et al. [173] by mercury vapor photometry of maternal blood from spontaneous deliveries at the University of Tokyo Hospital are not mentioned in Table 10. The values found were 12.4 ± 7.3 ng ml^{-1}. None of the subjects is said to have had a particular exposure to the element.

From the analytical point of view, determinations of mercury have always

TABLE 10

Plasma or serum mercury concentration

Authors and reference numbers	Analytical technique	Mean (ng ml^{-1})	S.d. (ng ml^{-1})	Range (ng ml^{-1})	Number of subjects
Wester, 1973 [35]	N.a.a.	1.8	0.6		8
Magos and Clarkson, 1972 [168]	A.a.s.	2.2	0.9	1.0—4.3	10
Tejning, 1967 [169]	N.a.a.	2.33	1.11		83[a]
Birke et al., 1972 [170]	N.a.a.	3.28	0.51		13
Kubasik et al., 1972 [171]	A.a.s.	11		7—18	20
Tejning, 1967 [172]	N.a.a.	13.74	2.98		12[b]

[a]Normal Swedish population. [b]Heavy fish eaters from the lake Vänern region.

represented a challenge because of the high volatility of the element. As a consequence of radiolysis of plasma or serum, especially after long irradiations at high neutron fluxes, possible losses have to be reckoned with. Nevertheless, as very low concentrations of mercury are found in serum, the incidence of unsuspected contamination during blood collection and subsequent preparation should not be overlooked. Whereas n.a.a. is only suitable for determination of the total mercury content, some refinements preceding a.a.s. detection offer the possibility of distinguishing between organic and inorganic mercury.

MOLYBDENUM

Molybdenum is known to be an essential element as a constituent of xanthine oxidase and other flavin-dependent enzymes. As shown in Table 11, published mean values in human plasma or serum vary from 0.58 to 257 ng ml^{-1}, a factor of about 450. The lowest level is reported by Versieck et al. [174], confirming the upper limit previously determined by Baert et al. [175]. Both values were obtained by n.a.a. at Ghent University but completely different post-irradiation separation schemes were applied (extraction of ^{99}Mo with 0.05 M 8-quinolinol in chloroform at pH 1.1 [174] versus distillation of ^{99m}Tc, daughter isotope of ^{99}Mo [175]). More recently, Kasperek et al. [34] reported a practically identical value of 0.59 ± 0.23 ng ml^{-1} for plasma. It is notable that these values are in excellent agreement with the observations of Tjioe et al. [43] and Morgan and Holmes [177] who, respectively, found levels of 0.6 and 1 ng ml^{-1} in whole blood.

All other values are at least 10 times higher than the levels reported by Versieck et al. [174] and Kasperek et al. [34]. Niedermeier and Griggs [4] detected the element in only 42% of their normal controls, which illustrates the apparent lack of sensitivity of their analytical procedure. Not included in Table 11 is the value of ca. 7 ng ml^{-1} obtained by Christian and Patriarche [178] using a cathode-ray polarographic procedure.

TABLE 11

Plasma or serum molybdenum concentration

Authors and reference numbers	Analytical technique	Mean (ng ml^{-1})	S.d. (ng ml^{-1})	Range (ng ml^{-1})	Number of subjects
Versieck et al., 1978 [174]	N.a.a.	0.58	0.21	0.28—1.17	30
Kasperek et al., 1979 [34]	N.a.a.	0.59	0.23		7
Baert et al., 1976 [175]	N.a.a.			<1.1	6
Wester, 1973 [35]	N.a.a.	5.6	2.1		8
Danys and Kuśleikaité, 1971 [138]	E.s.	8.9	0.2		30
Panteliadis, 1975 [26]	E.s.	10			300
Walravens et al., 1978 [176]	A.a.s.			<5—34	24
Samsahl et al., 1972 [126]	N.a.a.	12	6		♀30
Bala and Lifshits, 1966 [93]	E.s.	13.1[a]			unknown
Butt et al., 1964 [29]	E.s.	34	14		48
Niedermeier and Griggs, 1971 [4]	E.s.	34	48	<20—190[b]	68
de la Cruz, 1973 [130]	N.a.a.	257	205	10—668	unknown

[a]The mean value of Bala and Lifshits was recalculated assuming an haematocrit of 0.45.
[b]Values reported by Niedermeier et al., 1971 [24].

At the sub-nanogram levels, at which molybdenum occurs in serum, contamination is likely to be such a major pitfall as completely to distort the original content. Molybdenum is a common constituent of stainless steel needles so that, whenever they are used in the blood collection process, they may contribute to the serum molybdenum content. Subsequent chemical treatments with impure reagents or manipulations with implements which are not perfectly clean, may also contribute to the existing, controversial literature values.

NICKEL

Nickel has been suspected of having a physiological role for decades, but direct evidence that the element is essential is a recent finding [179—181]. The precise function remains to be explored.

A survey of published levels (Table 12) shows an important spread of the mean values from 1.6 ng ml^{-1} to 220 ng ml^{-1}. The element has been determined by emission spectrometry and spectrophotometry but the most recent studies were done by furnace atomic absorption spectrometry.

Sunderman and co-workers have published a series of papers regarding the element. First, a spectrophotometric procedure was developed and a mean serum concentration of 22 ng ml^{-1} obtained [191]. At that time (1967), this value was lower than those reported by most other investigators using emission spectrometry [29, 85, 87, 89, 94]. In later studies, a.a.s. was found to be more convenient [184, 192]. Measurements by this technique showed a

TABLE 12

Plasma or serum nickel concentration

Authors and reference numbers	Analytical technique	Mean (ng ml^{-1})	S.d. (ng ml^{-1})	Range (ng ml^{-1})	Number of subjects
Spruit and Bongaarts, 1977 [182]	A.a.s.	1.6			♂10
		2.0			♀14
Høgetveit and Barton, 1977 [183]	A.a.s.	2.1			21
Sunderman et al., 1970 [184]	A.a.s.	2.6	0.8	1.1—4.6	40
McNeely et al., 1972 [185]	A.a.s.	2.6	1.0	0.8—5.2	26[a]
Salvadeo et al., 1979 [17]	A.a.s.	2.8	0.5		12
Mikac-Dević et al., 1977 [186]	A.a.s.	3.1	1.6	0.6—5.3	19
McNeely et al., 1972 [185]	A.a.s.	4.6	1.4	2.0—7.3	25[b]
Zachariasen et al., 1975 [187]	A.a.s.	4.7	1	2.0—6.5	8
Pekarek and Hauer, 1972 [188]	A.a.s.	15	5		20
Niedermeier et al., 1962 [3]	E.s.	21		9—56	17
Schaller et al., 1968 [189]	A.a.s.	21	9	6—37	♂26
Howard, 1970 [190]	E.s.	21		1—50	50
Sunderman, 1967 [191]	Spect.	22	18	1—77	23
Paixao and Yoe, 1959 [87]	E.s.	24		0.0—185	39
Koch et al., 1956 [85]	E.s.	30	19	10—85	unknown
Monacelli et al., 1956 [94]	E.s.	40		10—60	12
Niedermeier and Griggs, 1971 [4]	E.s.	41	51	<10—250[c]	68
Panteliadis, 1975 [26]	E.s.	51			300
Butt et al., 1964 [29]	E.s.	58			48
Herring et al., 1960 [89]	E.s.	62		0.0—277	61
Danys and Kušleikaitė, 1971 [138]	E.s.	220	60		30

[a]Subjects from Hartford, Connecticut. [b]Subjects from Sudbury, Ontario. [c]Values mentioned by Niedermeier et al., 1971 [24].

significantly lower mean value, i.e. 2.6 ng ml^{-1}. The most likely explanation was considered to be that the population of central Connecticut, sampled in the latter studies, has significantly lower levels of nickel than does the population of Florida, previously studied. To investigate the problem further, nickel was measured by a.a.s. in specimens from healthy inhabitants of Sudbury, Ontario, the site of the largest open-pit nickel mines in North America, and of Hartford, Connecticut, a city with relatively low environmental concentration of nickel [185]. The mean value in the Sudbury population appeared to be significantly higher than that in the Hartford population (4.6 ± 1.4 ng ml^{-1} versus 2.6 ± 1.0 ng ml^{-1}; $p < 0.001$). Nevertheless, as the values in the area with the high environmental exposure to nickel turned out to be considerably lower than the levels found in the first study (4.6 ± 1.4 ng ml^{-1} with a range of 2.0—7.3 ng ml^{-1} versus 22 ± 18 ng ml^{-1} with a range of 1—77 ng ml^{-1}), it remains open to doubt that purely methodological errors

affected the original observations [191]. This suspicion is further strengthened by the findings of Spruit and Bongaarts [182, 193] and Høgetveit and Barton [183] in exposed volunteers and in nickel refinery workers which show generally lower values than mentioned in the first study of Sunderman [191]. At present, there seem to be good reasons to presume that the previously reported mean values of more than 10 ng ml^{-1} in normal, unexposed individuals are due to methodological inaccuracies during sample collection and preparation, or during separation and preconcentration steps.

In view of the clinical concern about nickel toxicology [194, 195] reliable indices of exposure are needed. Consequently, further efforts should be directed at obtaining indisputable plasma or serum values in the general population to provide a solid basis for reliable conclusions.

RUBIDIUM

Biological interest in rubidium has been stimulated by its close physicochemical relationship to potassium. A growing body of experimental evidence indicates that the element possesses unique neurophysiological characteristics [196, 197].

Table 13 lists published values, showing means ranging from 0.0838 μg ml^{-1} up to 1.14 μg ml^{-1}. Roughly half the studies utilized n.a.a. The interlaboratory agreement is acceptable for most of the twelve research centres. The mean value of 0.25 μg ml^{-1} by Sutter et al. [201] is not included in

TABLE 13

Plasma or serum rubidium concentration

Authors and reference numbers	Analytical technique	Mean (μg ml^{-1})	S.d. (μg ml^{-1})	Range (μg ml^{-1})	Number of subjects
Yamagata and Iwashima, 1966 [67]	N.a.a.			<0.038—0.066	4
Alfrey et al., 1975 [57]	X.r.f.	0.0838	0.0202		5
Chechan et al., 1975 [198]	A.a.s.	0.12	0.037		♂20
		0.10	0.044		♀19
Kasperek et al., 1979 [34]	N.a.a.	0.150	0.020		7
Wood, 1970 [199]	A.a.s.	0.16	0.03	0.12—0.21	21
Versieck et al., 1977 [66]	N.a.a.	0.17	0.04	0.09—0.27	36
Kasperek et al., 1972 [36]	N.a.a.	0.174	0.092		183
Samsahl et al., 1972 [126]	N.a.a.	0.21	0.08		♀30
Behne and Jürgensen, 1978 [42]	N.a.a.	0.230	0.039	0.155—0.315	25
Wester, 1973 [35]	N.a.a.	0.27	0.19		8
Stump et al., 1977 [56]	X.r.f.	0.31	0.057	0.20—0.42	♂35
		0.28	0.086	0.13—0.42	♀38
Niedermeier et al., 1962 [3]	E.s.	0.39		0.06—0.96	17
Bertrand and Bertrand, 1951 [200]	E.s.	1.14		0.53—1.80	8

the table because it was not obtained in healthy individuals but in manic-depressive patients. The four values reported by Yamagata and Iwashima [67] seem to be improbably low in comparison with the other results. The data given by Niedermeier et al. [3] must also be considered critically, both because of the high mean (0.39 μg ml^{-1}) and the large spread (0.06—0.96 μg ml^{-1}) which are not confirmed by other researchers. Contamination of the samples during the elaborate procedure accompanying emission spectrometry may be the underlying cause of the high values. The mean value of 1.14 μg ml^{-1} obtained by Bertrand and Bertrand [200] must be interpreted in its historical context, as it was the first determination of rubidium in human plasma.

It is of interest to mention that a relatively large variability with time of the plasma rubidium concentration in healthy adults was noted by Wood [199]: results in a male varied from 0.09 to 0.20 μg ml^{-1} over a 3-month period.

SELENIUM

Selenium was known for its adverse effects long before it was recognized as an essential trace element. It has now been shown to be an essential constituent of glutathione peroxidase and there is a reasonable likelihood that it may be implicated in other enzymes as well. The biological effects of selenium are intimately related to vitamin E, both catalyzing alternative pathways of peroxide metabolism.

Table 14 gives a résumé of the existing data. The published means, varying from 0.042 μg ml^{-1} to 0.19 μg ml^{-1}, are fairly consistent, compared with the published levels for several other elements. The values found in infants and children by Mazière et al. [161] (0.0382 ± 0.0119 μg ml^{-1}), Burk et al. [211] (0.15 ± 0.05 μg ml^{-1}) and Lombeck et al. [212] (median value = 0.0512 μg ml^{-1}, range = 0.0185—0.112 μg ml^{-1}) are not included in Table 14.

N.a.a. is the most commonly applied procedure. Most investigators [34—37, 42, 66, 91, 161, 208, 212] measure the long-lived ^{75}Se isotope ($t_{1/2}$ = 121 d); others [45] determine the short-lived ^{81m}Se ($t_{1/2}$ = 56.8 min). Sullivan and co-workers [153, 209], Blotcky and co-workers [206, 207], and Dickson and Tomlinson [210] used a method based on a combination of pre-irradiation separation followed by a short irradiation and subsequent detection of the very short-lived ^{77m}Se ($t_{1/2}$ = 17.5 s).

Experimental evidence presented by Lombeck et al. [213] suggests that the selenium concentration in serum is age-dependent. The median value at birth is reported to be 0.050 μg ml^{-1}. After a decrease in early infancy to 0.034 μg ml^{-1}, it steadily increases to 0.058 μg ml^{-1} in the second half of the first year and to 0.092 μg ml^{-1} at the age of about 10 years. Furthermore, geographical differences appear to exist. New Zealand adults are reported to have a low selenium status [203, 204, 214]: this is primarily determined by a low dietary intake as a consequence of the low selenium content of

TABLE 14

Plasma or serum selenium concentration

Authors and reference numbers	Analytical technique	Mean ($\mu g\ ml^{-1}$)	S.d. ($\mu g\ ml^{-1}$)	Range ($\mu g\ ml^{-1}$)	Number of subjects
Westermarck et al., 1977 [202]	Fluor.	0.042	0.013		10[a]
Rea, 1976 [203]	Fluor.	0.051	0.009		10
Maxia et al., 1972 [91]	N.a.a.	0.0517		0.046—0.062	3
Behne and Diel, 1972 [37]	N.a.a.	0.061	0.016		♂4
Kasperek et al., 1979 [34]	N.a.a.	0.066	0.008		7
Damsgaard et al., 1973 [45]	N.a.a.	0.089	0.011	0.069—0.106	11
Kasperek et al., 1972 [36]	N.a.a.	0.098	0.018		184
Behne and Jürgensen, 1978 [42]	N.a.a.	0.105	0.0091	0.088—0.128	25
Rhead et al., 1972 [205]	Fluor.	0.105	0.018	0.071—0.128	7
Westermarck et al., 1977 [202]	Fluor.	0.108	0.033		23[b]
Broghamer et al., 1976 [206]	N.a.a.	0.118[c]	0.025[c]	0.080—0.182[c]	18
Sullivan et al., 1979 [153]	N.a.a.	0.12	0.01		37
Morss et al., 1972 [208]	N.a.a.	0.129	0.034	0.055—0.169	11
Aaseth et al., 1978 [132]	N.a.a.	0.129	0.009		10
Versieck et al., 1977 [66]	N.a.a.	0.13	0.02	0.09—0.18	36
Hahn et al., 1972 [209]	N.a.a.	0.131	0.007		♂8
		0.113	0.008		♀6
Dickson and Tomlinson, 1967 [210]	N.a.a.	0.144	0.0286		253
Wester, 1973 [35]	N.a.a.	0.19	0.06		8

[a]Subjects from Lappeenranta, Finland (south-eastern part of the country). [b]Subjects from Utsjoki, Finland (northern area). [c]Recalculated values, the original being given in $\mu g\ g^{-1}$ of dry serum (see McConnell et al. [207]).

New Zealand soils. Inhabitants of the central, eastern, and south-eastern districts of Finland were found to have lower selenium levels than other Finns [202].

In all probability however, some of the reported variation must be attributed to analytical errors. As selenium is a volatile element, the major problem is loss from volatilization during sample digestion. Thus, concentrations reported for Bowen's kale range from 174 ng g^{-1} down to 44 ng g^{-1} [215]. The quantitative character of dehydration procedures has also been questioned. Recently, de Goeij et al. [216] reported that measurable loss could not be detected during lyophilization but, according to Fourie and Peisach [217—219] there is an appreciable loss (some 15%) during oven drying at 120°C.

SILVER

There is no evidence that silver is essential for living organisms, nor that it should be classified among the more toxic trace elements.

TABLE 15

Plasma or serum silver concentration

Authors and reference numbers	Analytical technique	Mean (ng ml^{-1})	S.d. (ng ml^{-1})	Range (ng ml^{-1})	Number of subjects
Kasperek et al., 1979 [34]	N.a.a.	0.68	0.63		7
Wester, 1973 [35]	N.a.a.	0.90	0.40		8
Kasperek et al., 1972 [36]	N.a.a.	6.2	4.5		183
Butt et al., 1964 [29]	E.s.	13.5			48
Niedermeier et al., 1962 [3]	E.s.	25		3—113	17
Behne and Diel, 1972 [37]	N.a.a.	113	72		4

The 6 mean values in plasma or serum mentioned in Table 15 range from 0.68 up to 113 ng ml^{-1}. These few data do not allow definitive conclusions. In view of the poor agreement of different laboratories analysing biological reference materials such as Bowen's kale powder [163], it is likely that systematic errors are involved. As for several other elements, recently published values show a decline with time. After having found a level of 6.2 ± 4.5 ng ml^{-1} in 183 subjects [36], in a more recent study Kasperek et al. [34] determined a value of 2.10 ± 1.52 ng ml^{-1} in serum and 0.68 ± 0.63 ng ml^{-1} in plasma. Furthermore, when analysing serum samples to test the reproducibility of an instrumental neutron activation technique, Behne et al., who had previously found a concentration of 113 ± 72 ng ml^{1-} in 4 healthy individuals [37], observed a value of 0.19 ng ml^{-1} [42]. All the evidence indicates that contamination during sample handling is once again the main hazard.

TIN

Tin has chemical properties that offer possibilities for biological functions. The ability to form coordination complexes is considered to facilitate reactions with proteins and nucleic acids, thus contributing to the organization and stabilization of tertiary structures. In 1970 it was shown to be an essential element for animals [220].

Only three groups seem to have published data on tin levels in human plasma or serum. As shown in Table 16, the mean values are: 30, 37.2, and 103 ng ml^{-1}. It is not really possible to comment on these results from an analytical point of view. Tin is an element that cannot readily be determined by any method of analysis so that considerable efforts will be needed to obtain reasonably well documented information.

VANADIUM

Little is known about the metabolism and biological functions of vanadium. It appears likely that the element is involved in lipid metabolism but its site and mode of action are unknown. Evidence supporting the view that vana-

TABLE 16

Plasma or serum tin concentration

Authors and reference numbers	Analytical technique	Mean (ng ml^{-1})	S.d. (ng ml^{-1})	Range (ng ml^{-1})	Number of subjects
Niedermeier and Griggs, 1971 [4]	E.s.	30	49	<40—350[a]	68
Alfrey et al., 1975 [57]	X.r.f.	37.2	12.8		5
Panteliadis, 1975 [26]	E.s.	103			300

[a]Values reported by Niedermeier et al., 1971 [24].

dium is an essential element for animals was first published in 1971 [221, 222].

A list of values in human plasma or serum is given in Table 17. The ratio between the highest and the lowest mean values is about 10^4. The concentration of 4.6 ± 0.8 ng ml^{-1} found by Heydorn and Lukens [229] is not mentioned in the Table because it was determined in serum samples received from a hospital laboratory. The authors showed that serum samples ashed in porcelain crucibles are heavily contaminated with vanadium from the glaze of these vessels.

N.a.a. offers very good sensitivity, but because of the matrix activities, chemical separation is necessary. As the half-life of ^{52}V is short (3.76 min), either a very selective pre-irradiation separation, or a very fast post-irradiation procedure is needed. The values reported by Cornelis et al. [223, 224] were obtained by using a dry ashing procedure in ultra-pure quartz tubes before, and a very fast radiochemical separation after the irradiation. The serum

TABLE 17

Plasma or serum vanadium concentration

Authors and reference numbers	Analytical technique	Mean (ng ml^{-1})	S.d. (ng ml^{-1})	Range (ng ml^{-1})	Number of subjects
Cornelis et al., 1979 [223]	N.a.a.	0.047[a]	0.011[a]	0.035—0.260	♂9
		0.024	0.005	0.017—0.031	♀8
Cornelis et al., 1979 [224]	N.a.a.			0.029—0.939	♂22
		0.033[b]	0.012[b]	0.017—0.139	♀18
Damsgaard et al., 1972 [225]	N.a.a.	1			1
Sabbioni et al., 1979 [226]	N.a.a.	6.6[c]	3.0[c]	3.8—11.3[c]	5
Panteliadis, 1975 [26]	E.s.	21			300
Christian, 1971 [227]	Spect.	57	34	10—144	10
Schroeder et al., 1963 [228]	E.s.	420		350—480	13

[a]Three values were excluded for the calculation of the mean and the s.d., namely 0.138, 0.250, and 0.260 ng ml^{-1}. [b]One value was excluded for the calculation of the mean and the s.d., namely 0.139 ng ml^{-1}. [c]Recalculated values assuming an haematocrit of 0.45.

values for men vary over a relatively wide range, whereas those for women do not. The values given by Sabbioni et al. [226], obtained by a pre-irradiation separation are two orders of magnitude higher. The other results from Table 17 were obtained by emission spectrometry and a spectrophotometric method. It seems probable that they bear the burden of contamination inherent in those methodologies. Moreover, these methods have not sufficient sensitivity to detect subnanogram amounts.

ZINC

The biological importance of zinc was first recognized more than a century ago. The recent publication of a number of reviews and monographs on the metabolism and function of the element reflects the growing awareness of its importance in health and disease. Since the initial discovery of carbonic anhydrase in 1939, more than 70 zinc metalloenzymes have been isolated. In addition, the element has been shown to be related to both nucleic acid and protein metabolism.

The concentration in plasma or serum has been extensively investigated. Table 18 mentions the values obtained by six analytical methods in healthy subjects living in different countries of Europe (16 studies), the U.S.A. (16 studies), Canada (1 study), Nigeria (1 study), and the Philippines (1 study). The reported mean values vary from 0.84 $\mu g\ ml^{-1}$ to 4.28 $\mu g\ ml^{-1}$. However, it appears that about 75% of these values fall between 0.8 and 1.20 $\mu g\ ml^{-1}$. The concentration of zinc in serum has been said to be higher by 0.05 to 0.15 $\mu g\ ml^{-1}$ than in plasma because the element was believed to be released from disintegrating platelets during clot formation [239]. This has not been confirmed by other investigators. In a recent study [240], the plasma level was found to be higher [2.7%] than the serum concentration; haemolysis was thought to represent the major source of zinc contamination in either plasma or serum.

The most striking fact during the initial period of research on the plasma or serum zinc level in man is the downward revision by Vallee et al. of their normal value from 3.0 ± 1.6 $\mu g\ ml^{-1}$ [237] to 1.20 ± 0.19 $\mu g\ ml^{-1}$ [235], in contrast to the upward revision by the investigators from the Pratt Trace Analysis Laboratory from 1.33 $\mu g\ ml^{-1}$ (range 0.62—2.36 $\mu g\ ml^{-1}$) [94] to 2.77 $\mu g\ ml^{-1}$ (range 0.49—4.92 $\mu g\ ml^{-1}$) [87] and then to 3.09 $\mu g\ ml^{-1}$ (range 0.50—7.90 $\mu g\ ml^{-1}$) [89].

Three groups of investigators reporting plausible mean values, Stump et al. [56], Niedermeier and Griggs [4], and Monacelli et al. [94] mention unexpectedly high upper limits, namely 2.34, 2.90 and 2.36 $\mu g\ ml^{-1}$, respectively. Although one family with hereditary hyperzincemia (with serum zinc values from 2.50 to 4.35 $\mu g\ ml^{-1}$ in affected members) has been described by Smith et al. [241, 242], suspicion arises that sample contamination is more likely to have occurred.

The study of Davies and co-workers [231] seems to be one of the best

TABLE 18

Plasma or serum zinc concentration

Authors and reference numbers	Analytical technique	Mean ($\mu g\ ml^{-1}$)	S.d. ($\mu g\ ml^{-1}$)	Range ($\mu g\ ml^{-1}$)	Number of subjects
Giroux et al., 1976 [230]	A.a.s.	0.84	0.09		28
Samsahl et al., 1972 [126]	N.a.a.	0.86	0.26		♀30
Parr and Taylor, 1964 [125]	N.a.a.	0.87	0.07	0.82—1.02	6
Bogden et al., 1977 [139]	A.a.s.	0.87	0.12		20
Behne and Jürgensen, 1978 [42]	N.a.a.	0.905	0.120	0.555—1.130	25
Olehy et al., 1966 [131]	N.a.a.	0.93	0.05		12
Seeling et al., 1975 [149]	A.a.s.	0.935		0.804—1.209[a]	unknown
Versieck et al., 1974 [136]	N.a.a.	0.94	0.13	0.69—1.21	46
Wester, 1973 [35]	N.a.a.	0.95	0.44		8
Davies et al., 1968 [231]	A.a.s.	0.95	0.13	0.76—1.25	♂36
		0.96	0.105	0.76—1.25	♀31
Halsted and Smith, 1970 [232]	A.a.s.	0.96	0.12	0.72—1.15	89
Allain et al., 1977 [134]	A.a.s.	0.975	0.053		unknown
Giovannetti et al., 1967 [38]	N.a.a.	1.01		0.60—1.33	15
Pekarek et al., 1972 [233]	A.a.s.	1.02	0.17		♂99
Salvadeo et al., 1979 [17]	A.a.s.	1.02	0.48		12
Funckes et al., 1976 [142]	A.a.s.	1.03	0.15		♀15
Lafargue et al., 1976 [140]	A.a.s.	1.03	0.11		unknown
Stump et al., 1977 [56]	X.r.f.	1.04	0.17	0.63—1.40	♂35
		1.42	0.39	0.85—2.34	♀38
Olatunbosun et al., 1976 [135]	A.a.s.	1.07	0.12	0.80—1.30	37
de la Cruz, 1973 [130]	N.a.a.	1.08	0.31	0.68—1.85	unknown
Hartoma, 1977 [144]	A.a.s.	1.1277	0.2652		♂426
		1.0288	0.2217		♀287
Prasad et al., 1976 [234]	A.a.s.	1.13	0.136		70
Niedermeier and Griggs, 1971 [4]	E.s.	1.154	0.394	0.46—2.90[b]	68
Kasperek et al., 1972 [36]	N.a.a.	1.160	0.145		184
Vallee et al., 1956 [235]	Spect.	1.20	0.19		40
Koch et al., 1956 [85]	Col.	1.20	0.23	0.32—1.70	58
Butt et al., 1964 [29]	E.s.	1.30	0.42		48
Monacelli et al., 1956 [94]	E.s.	1.33		0.62—2.36	unknown
Panteliadis, 1975 [26]	E.s.	1.4			300
Bierenbaum et al., 1975 [82]	A.a.s.	1.49	0.81		260[c]
Karayalcin et al., 1974 [236]	A.a.s.	1.77	0.49	1.0—3.7	50
Paixao and Yoe, 1959 [87]	E.s.	2.77		0.49—4.92	39
Vallee and Gibson, 1948 [237]	Spect.	3.0	1.6	1.2—11.4	31
Danys and Kušleikaitė, 1971 [138]	E.s.	3.02	0.40		30
Herring et al., 1960 [89]	E.s.	3.09		0.50—7.90	61
Bierenbaum et al., 1975 [82]	A.a.s.	4.28	13.22		260[d]

[a]Values reported by Seeling et al., 1975 [238]. [b]Values reported by Niedermeier et al., 1971 [24]. [c]Subjects from Kansas City, Kansas. [d]Subjects from Kansas City, Missouri.

documented for plasma zinc. The results show that the level is one of the most uniform biochemical characteristics of blood but the determinations were proven to be of no value unless a few simple but stringent technical rules were observed. Two points were particularly stressed: first, zinc is an ubiquitous contaminant of glass, lead and rubber piping, water, and many chemicals even of the highest analytical grade; second, the zinc content of all cells (including blood platelets) is many times that of plasma. The inconsistencies observed during improper handling of the samples inevitably raise doubts about the reliability of many of the zinc studies reported in the literature. Nackowski et al. [243] examined the magnitude of potential trace metal contamination by various commercial evacuated blood collection tubes under experimental conditions. Whereas none gave rise to significant copper addition, leaching data clearly showed that all twenty types contributed unacceptable levels of zinc contamination under normal handling, shipping, and storing conditions. Reimold and Besch [244] also undertook a detailed examination of the routine practices and procedures involved in the analysis of serum. Some degree of contamination was found in almost all the steps. Their results suggest that the common practice of drawing blood into a Vacutainer tube (Becton—Dickinson) is unsuitable if the sample is to be analysed for zinc. The problem appears to be associated with a high and variable zinc content of the stopper [245]. Although the "low metal" Vacutainer tube (blue stopper) contributed much less contamination (varying from 0 to 0.0068 $\mu g\ ml^{-1}$), plasma from such tubes contained more zinc than from plastic acid-washed tubes. Possibly, these higher values are due to haemolysis during injection in the Vacutainers. It has thus been conclusively shown that the validity of plasma or serum zinc measurements depends primarily on the success of the investigator in avoiding extraneous additions.

Physiological variations are known to occur. Diurnal changes of plasma zinc concentrations have been described [246—249]. Hetland and Brubakk [248] found the following values in 13 adults: at 8 a.m., $1.04 \pm 0.12\ \mu g\ ml^{-1}$; at 11.30 a.m., $0.96 \pm 0.08\ \mu g\ ml^{-1}$; and at 3 p.m., $0.93 \pm 0.09\ \mu g\ ml^{-1}$. Furthermore, although some investigators were unable to demonstrate a food-intake effect [250], considerable evidence has accumulated that the fasting plasma zinc level is higher than the value approximately one hour after a meal [251—253]. Walker and his colleagues measured a mean concentration of $0.97\ \mu g\ ml^{-1}$ in 16 subjects after an overnight fast, and a level of $0.81\ \mu g\ ml^{-1}$ one hour after a usual midday meal [253]. Sex or age differences were observed by some investigators [66, 136, 144, 254—257] but not by others [231, 232]. The observed variations are generally rather small. Although they may explain some minor differences between the results of individual investigators, they can apparently not account for the marked inconsistencies.

Careful studies done by Björkstén et al. [255] and Hartoma [144] in Finland suggest that deviations attributable to geographical or environmental factors are also quite small, namely from $0.74 \pm 0.08\ \mu g\ ml^{-1}$ to 0.89 ± 0.13

$\mu g\ ml^{-1}$ [255] and from 0.64 ± 0.13 $\mu g\ ml^{-1}$ to 1.35 ± 0.16 $\mu g\ ml^{-1}$ [144]. The variations found by Bierenbaum et al. [82] in the two Kansas Cities, namely from 1.49 ± 0.81 $\mu g\ ml^{-1}$ to 4.28 ± 13.22 $\mu g\ ml^{-1}$ (the s.d. being recalculated from the reported standard error of the mean) is in violent contrast with these observations. Several values said to be found in Kansas City, Missouri, are apparently much higher than those reported for patients on zinc therapy [258—260], during a zinc tolerance test described by Sullivan et al. [261], or for patients with acute, iatrogenic zinc intoxication during parenteral nutrition [262] or haemodialysis [263].

GENERAL COMMENTS AND CONCLUSIONS

An overview of the Tables shows that numerous investigators determined several elements simultaneously. In the following paragraphs, the studies of these authors are examined more closely.

For copper, most results are reasonably consistent [4, 17, 26, 29, 35, 36, 38, 56, 57, 85, 89, 94, 125, 126, 128, 131, 132, 134—136, 138—140, 142, 143, 153]. One value is lower [130] and four are slightly higher [3, 82, 144, 146] than most others. For zinc, the situation is somewhat less satisfactory. Whereas most reported analyses agree well with one another [4, 17, 35, 38, 42, 56, 66, 85, 125, 130, 131, 134, 135, 139, 140, 142, 144, 149, 153], some give slightly higher [26, 29, 94] or markedly higher values [82, 87, 89, 138]. In view of the results of Davies et al. [231] and the observations of Nackowski et al. [243] and Reimold and Besch [244], contamination of the samples is the most likely cause of the existing differences. For bromine, rubidium and selenium, most workers also obtained fairly similar values [34—37, 42, 45, 55—57, 66, 91, 126, 132, 153]. There is one exception, namely Niedermeier et al. [3], who found a rather high mean and a definitely large spread of rubidium values.

For most other elements, striking disparities emerge when the results are examined critically. The data of Danys and Kuśleikaité [138], Herring et al. [89], Koch et al. [85], Monacelli et al. [94], Muzzarelli and Rocchetti [128], Olehy et al. [131], Paixao and Yoe [87], Panteliadis [26], Sullivan et al. [153], and Zhernakova [143] illustrate that a sampling procedure and a multi-element technique which permit the accurate determination of copper, may give erroneously high values for almost all other elements, particularly at the $ng\ ml^{-1}$ level or lower, such as aluminium [26], chromium [26, 85, 87, 89, 94], cobalt [85, 128], manganese [26, 128, 131, 138, 143, 153], molybdenum [26, 138], nickel [26, 85, 87, 89, 94, 138], and vanadium [26]. There are particularly solid reasons for assuming that the samples were heavily contaminated by several elements. The high values obtained by Alt and Massmann [127] for cobalt and manganese, and by Bala and Lifshits [93] for chromium and molybdenum also point to serious deficiencies in avoiding extraneous additions. The levels found by Grafflage et al. [75] for chromium and manganese approximate better the most recent values. Never-

theless, the published manganese levels leave no doubt that contamination occurred. The results of Butt et al. [29], and Niedermeier et al. [3, 4] strongly suggest the same conclusion. In addition, the applied technique obviously lacks sensitivity as several elements were not detected in a number of individuals.

The values published by Behne and Diel [37], Giovannetti et al. [38], Kasperek et al. [36], Salvadeo et al. [17], Samsahl et al. [126], and Wester [35] who succeeded in determining concentrations for one or more elements accurately at the ng ml^{-1} level but failed for others, illustrate the extreme difficulties in developing an adequate sampling method for multi-element analyses.

Obviously, not all disparities are attributable to contaminations. Analyses of biological intercomparison materials [95, 98, 163, 164, 215, 264, 265] have also revealed a number of inconsistencies caused by methodological inaccuracies. Bowen [164] states that about 40% of all reported analyses of reference kale powder are in error by more than ± 10%. The percentage of acceptable results for Al, Sb, Cr, and Mo turned out to be alarmingly low. Heinonen and Suschny [265] warn that the reliability of mercury determinations leaves much to be desired: a full third of all results were found to lie outside the limits of plus or minus 3 standard deviations from the overall mean. Parr [95] concluded that most of the results of chromium determinations in International Atomic Energy Agency (IAEA) intercomparison materials and non-IAEA reference materials must have been subject to significant sources of error. Thus, the chromium values published by Li and Hercules [92] may be rejected as the authors mention a tenfold too high value (0.87 ± 0.06 $\mu g\ g^{-1}$) for NBS bovine liver (SRM 1577). As very few investigators who have reported plasma or serum trace element levels, checked the accuracy of their analytical technique by analysing reference materials, doubt persists about the actual occurrence of systematic errors. Perusal of the data reported by Bierenbaum et al. [82] leads to deep concern as to the validity of the findings because of the very questionable results for all trace elements, including the copper and zinc values. Furthermore, the aberrant data for copper reported by de la Cruz [130] and Kanabrocki et al. [146] also raise suspicion. Circumstantial evidence however suggests that the real number of methodological inaccuracies must be considerably higher.

The results obtained at Ghent University may be summarized as follows. The concentrations found for Br, Cu, Rb, Se, and Zn [55, 66, 136, 156] are in close agreement with the values reported by most other investigators. The level found for manganese [136, 156] is low but nearly identical with the values published by three other workers who took extreme precautions to avoid sample contamination [8, 45, 148]. The concentrations of Al, Cs, Cr, Co, and Mo [15, 66, 74, 174, 175] are lower than reported by most other investigators, but in recent years similar values have been reported [34, 73, 123]; furthermore, the analytical methods used were repeatedly checked by analysing reference materials [74, 99, 119, 174]. Finally, the

concentration of vanadium [223, 224] is markedly lower than reported by other authors, but analyses of Bowen's kale, NBS orchard leaves (SRM 1571), NBS bovine liver (SRM 1577) and IAEA animal muscle (H-4) gave consistent results [223].

This review illustrates the serious inconsistencies in the reported concentrations of trace elements in plasma or serum of healthy individuals. Disparities of several orders of magnitude are not uncommon. Although some differences may reflect true biological variations, abundant experimental evidence points to analytical errors.

There is increasing awareness that specimen contamination is responsible for a considerable number of erroneous values. Sampling and sample handling are the Achilles' heel of trace element research. The most careful analysis of a contaminated sample remains a futile exercise that cannot but worsen the existing confusion. In our opinion, no program of low level trace element analysis should be started before adequate contamination control procedures as outlined by Zief and co-workers [157–160] have been developed (clean room facilities, container cleaning technique, sample collecting and handling devices).

Moreover, there is a growing consensus that some of the controversy may be due to systematic errors. Thus, a major trend should be to practice quality control by the regular use of reference materials [163, 164] and to apply statistical tests such as the analysis of precision [50] wherever possible.

In summary, much work remains to be done to establish the normal concentrations of trace elements in human blood plasma or serum. Hopefully, this survey of the existing discrepancies will be a challenging stimulus for further research.

The authors acknowledge with gratitude the invaluable help of Prof. Dr. J. Hoste and Prof. Dr. F. Barbier during the preparation of this review.

REFERENCES

1 W. Seeling, R. Dölp, F. W. Ahnefeld and W. Dick, Infusionstherapie, 2 (1975) 144.
2 H. Freund, S. Atamian and J. E. Fisher, J. Am. Med. Assoc., 241 (1979) 496.
3 W. Niedermeier, E. E. Creitz and H. L. Holley, Arthritis Rheum., 5 (1962) 439.
4 W. Niedermeier and J. H. Griggs, J. Chronic Dis., 23 (1971) 527.
5 F. J. M. J. Maessen, F. D. Posma and J. Balke, Anal. Chem., 46 (1974) 1445.
6 N. I. Ward and D. E. Ryan, Anal. Chim. Acta, 105 (1979) 185.
7 A. J. Bertinchamps, S. T. Miller and G. C. Cotzias, Am. J. Physiol., 211 (1966) 217.
8 G. C. Cotzias, S. T. Miller and J. Edwards, J. Lab. Clin. Med., 67 (1966) 836.
9 G. C. Cotzias and P. S. Papavasiliou, Nature, 201 (1964) 828.
10 P. S. Papavasiliou, S. T. Miller and G. C. Cotzias, Am. J. Physiol., 211 (1966) 211.
11 M. T. Kovalchik, W. D. Kaehny, A. P. Hegg, J. T. Jackson and A. C. Alfrey, J. Lab. Clin. Med., 92 (1978) 712.
12 F. J. Burger, in W. G. Hoekstra, J. W. Suttie, H. E. Ganther and W. Mertz (Eds.), Trace Element Metabolism in Animals, Vol. 2, University Park Press, Baltimore, 1974, p. 671.
13 D. P. Mertz, R. Koschnick, G. Wilk and K. Pfeilsticker, Z. Klin. Chem. Klin. Biochem., 6 (1968) 171.

14 J. Webb, K. A. Kirk, D. H. Jackson, W. Niedermeier, M. E. Turner, C. E. Rackley and R. O. Russell, Exp. Mol. Pathol., 25 (1976) 322.
15 N. De Baets, P. Lievens, J. Versieck and R. Cornelis, unpublished results (1978).
16 W. D. Kaehny, A. P. Hegg and A. C. Alfrey, N. Engl. J. Med., 296 (1977) 1389.
17 A. Salvadeo, C. Minoia, S. Segagni and G. Villa, Int. J. Artif. Organs, 2 (1979) 17.
18 H. Valentin, P. Preusser and K.-H. Schaller, Int. Arch. Occup. Environ. Health, 38 (1976) 1.
19 J. P. Clavel, M. C. Jaudon and A. Galli, Ann. Biol. Clin., 36 (1978) 33.
20 M. K. Ward, T. G. Feest, H. A. Ellis, I. S. Parkinson, D. N. S. Kerr, J. Herrington and G. L. Goode, Lancet, (1978) i, 841.
21 J. E. Gorsky and A. A. Dietz, Clin. Chem., 24 (1978) 1485.
22 C. Fuchs, M. Brasche, K. Paschen, H. Nordbeck and E. Quellhorst, Clin. Chim. Acta, 52 (1974) 71.
23 E. M. Clarkson, V. A. Luck, W. V. Hynson, R. R. Bailey, J. B. Eastwood, J. S. Woodhead, V. R. Clements, J. L. H. O'Riordan and H. E. De Wardener, Clin. Sci., 43 (1972) 519.
24 W. Niedermeier, J. H. Griggs and R. S. Johnson, Appl. Spectrosc., 25 (1971) 53.
25 M. Seibold, Klin. Wochenschr., 38 (1960) 117.
26 C. Panteliadis, in K. Betke and F. Bidlingmaier (Eds.), Spurenelemente in der Entwicklung von Mensch und Tier, Urban & Schwarzenberg, München, 1975, p. 103.
27 K. Julshamn, K.-J. Andersen, Y. Willassen and O. R. Braekkan, Anal. Biochem., 88 (1978) 552.
28 G. M. Berlyne, J. Ben-Ari, D. Pest, J. Weinberger, M. Stern, G. R. Gilmore and R. Levine, Lancet, (1970) ii, 494.
29 E. M. Butt, R. E. Nusbaum, T. C. Gilmour and S. L. Didio, Arch. Environ. Health, 8 (1964) 52.
30 A. Speecke, J. Hoste and J. Versieck, in P. D. LaFleur (Ed.), Accuracy in Trace Analysis: Sampling, Sample Handling, Analysis, Vol. 1, National Bureau of Standards, U.S. Government Printing Office, Washington, 1976, p. 299.
31 H. J. M. Bowen, Trace Elements in Biochemistry, Academic Press, London, 1966, p. 81.
32 H. L. Elliot, F. Dryburgh, G. S. Fell, S. Sabet and A. I. Macdougall, Br. Med. J., (1978) i, 1101.
33 G. S. Fell, personal communication (1979).
34 K. Kasperek, G. V. Iyengar, J. Kiem, H. Borberg and L. E. Feinendegen, Clin. Chem., 25 (1979) 711.
35 P. O. Wester, Acta Med. Scand., 194 (1973) 505.
36 K. Kasperek, H. Schicha, V. Siller, L. E. Feinendegen and A. Höck, in Nuclear Activation Techniques in the Life Sciences, International Atomic Energy Agency, Vienna, 1972, p. 517.
37 D. Behne and F. Diel, in Nuclear Activation Techniques in the Life Sciences, International Atomic Energy Agency, Vienna, 1972, p. 407.
38 S. Giovannetti, Q. Maggiore and R. Malvano, in Nuclear Activation Techniques in the Life Sciences, International Atomic Energy Agency, Vienna, 1967, p. 511.
39 M. Razeghi and B. Parsa, Radiochem. Radioanal. Lett., 13 (1973) 95.
40 D. E. Robertson, Anal. Chem., 40 (1968) 1067.
41 B. Mazière, A. Gaudry, J. Gros and D. Comar, in P. D. LaFleur (Ed.), Accuracy in Trace Analysis: Sampling, Sample Handling, and Analysis, National Bureau of Standards, U.S. Government Printing Office, Washington, 1976, p. 593.
42 D. Behne and H. Jürgensen, J. Radioanal. Chem., 42 (1978) 447.
43 P. S. Tjioe, J. J. M. de Goeij and J. P. W. Houtman, J. Radioanal. Chem., 37 (1977) 511.
44 G. V. Iyengar, H. Borberg, K. Kasperek, J. Kiem, M. Siegers, L. E. Feinendegen and R. Gross, Clin. Chem., 25 (1979) 699.
45 E. Damsgaard, K. Heydorn, N. A. Larsen and B. Nielsen, Simultaneous Determination

of Arsenic, Manganese and Selenium in Human Serum by Neutron Activation Analysis, Risø Report No. 271 (1973).
46 K. Heydorn, Clin. Chim. Acta, 28 (1970) 349.
47 G. R. Kingsley and R. R. Schaffert, Anal. Chem., 23 (1951) 914.
48 R. E. Gerhardt, J. B. Hudson, R. N. Rao and R. E. Sobel, Arch. Intern. Med., 138 (1978) 1267.
49 H. A. Schroeder and A. P. Nason, Clin. Chem., 17 (1971) 461.
50 K. Heydorn, in P. D. LaFleur (Ed.), Accuracy in Trace Analysis: Sampling, Sample Handling, Analysis, Vol. 1, National Bureau of Standards, U.S. Government Printing Office, Washington, 1976, p. 127.
51 K. Heydorn, E. Damsgaard, N. A. Larsen and B. Nielsen, in Nuclear Activation Techniques in the Life Sciences, International Atomic Energy Agency, Vienna, 1979, p. 129.
52 J. C. Cabanis and J. P. Bonnemaire, Trav. Soc. Pharm. Montpellier, 30 (1970) 61.
53 S. Natelson, B. Sheid and D. R. Leighton, Clin. Chem., 8 (1962) 630.
54 P. Duvaldestin, Anesthesiology, 46 (1977) 375.
55 R. Cornelis, G. Lemey, L. Mees and J. Versieck, unpublished results (1979).
56 I. G. Stump, J. Carruthers, J. M. D'Auria, D. A. Applegarth and A. G. F. Davidson, Clin. Biochem., 10 (1977) 127.
57 A. C. Alfrey, H. Rudolph and W. R. Smythe, Kidney Int., 7 Suppl. 2 (1975) 85.
58 J. F. Goodwin, Clin. Chem., 17 (1971) 544.
59 R. E. Johnstone, E. M. Kennell, M. G. Behar, W. Brummund, R. C. Ebersole and L. M. Shaw, Anesthesiology, 42 (1975) 598.
60 R. E. Johnstone, R. Andrews and W. Brummund, Anesthesiology, 43 (1975) 128.
61 H. Sklavenitis and D. Comar, in Nuclear Activation Techniques in the Life Sciences, International Atomic Energy Agency, Vienna, 1967, p. 435.
62 Z. Khalkhali and B. Parsa, in Nuclear Activation Techniques in the Life Sciences, International Atomic Energy Agency, Vienna, 1972, p. 461.
63 N. M. Spyrou, in Nuclear Activation Techniques in the Life Sciences, International Atomic Energy Agency, Vienna, 1972, p. 467.
64 L. O. Plantin, in Nuclear Activation Techniques in the Life Sciences, International Atomic Energy Agency, Vienna, 1967, p. 443.
65 L. O. Plantin, in Nuclear Activation Techniques in the Life Sciences, International Atomic Energy Agency, Vienna, 1972, p. 466.
66 J. Versieck, J. Hoste, F. Barbier, H. Michels and J. De Rudder, Clin. Chem., 23 (1977) 1301.
67 N. Yamagata and K. Iwashima, Nature, 211 (1966) 528.
68 S. Punsar, W. Wolf, W. Mertz and M. J. Karvonen, Ann. Clin. Res., 9 (1977) 79.
69 H. A. I. Newman, R. F. Leighton, R. R. Lanese and N. A. Freedland, Clin. Chem., 24 (1978) 541.
70 H. A. Schroeder, Med. Clin. North Am., 58 (1974) 381.
71 R. J. Doisy, D. H. P. Streeten, J. M. Freiberg and A. J. Schneider, in A. S. Prasad and D. Oberleas (Eds.), Trace Elements in Human Health and Disease, Vol. 2, Academic Press, New York, 1976, p. 79.
72 W. Mertz, E. W. Toepfer, E. E. Roginski and M. M. Polansky, Fed. Proc. Fed. Am. Soc. Exp. Biol., 33 (1974) 2275.
73 F. J. Kayne, G. Komar, H. Laboda and R. E. Vanderlinde, Clin. Chem., 24 (1978) 2151.
74 J. Versieck, J. Hoste, F. Barbier, H. Steyaert, J. De Rudder and H. Michels, Clin. Chem., 24 (1978) 303.
75 B. Grafflage, G. Buttgereit, W. Kübler and H.-M. Mertens, Z. Klin. Chem. Klin. Biochem., 12 (1974) 287.
76 R. S. Pekarek, E. C. Hauer, R. W. Wannemacher and W. R. Beisel, Anal. Biochem., 59 (1974) 283.

77 V. J. K. Liu and J. S. Morris, Am. J. Clin. Nutr., 31 (1978) 972.
78 W. J. van Kooten, J. W. H. Mali, J. J. M. de Goeij and J. P. W. Houtman, in Nuclear Activation Techniques in the Life Sciences, International Atomic Energy Agency, Vienna, 1967, p. 567.
79 K. M. Hambidge, Am. J. Clin. Nutr., 27 (1974) 505.
80 I. W. F. Davidson and W. L. Secrest, Anal. Chem., 44 (1972) 1808.
81 M. S. Black and R. E. Sievers, Anal. Chem., 48 (1976) 1872.
82 M. L. Bierenbaum, A. I. Fleischman, J. Dunn and J. Arnold, Lancet, (1975) i, 1008.
83 J. Savory, M. T. Glenn and J. A. Ahlstrom, J. Chromatogr. Sci., 10 (1972) 247.
84 F. J. Feldman, Bull. Pathol., 10 (1969) 42.
85 H. J. Koch, E. R. Smith, N. F. Shimp and J. Connor, Cancer, 9 (1956) 499.
86 R. A. Levine, D. H. P. Streeten and R. J. Doisy, Metabolism, 17 (1968) 114.
87 L. M. Paixao and J. H. Yoe, Clin. Chim. Acta, 4 (1959) 507.
88 W. H. Glinsmann, F. J. Feldman and W. Mertz, Science, 152 (1966) 1243.
89 W. B. Herring, B. S. Leavell, L. M. Paixao and J. H. Yoe, Am. J. Clin. Nutr., 8 (1960) 846.
90 F. J. Feldman, E. C. Knoblock and W. C. Purdy, Anal. Chim. Acta, 38 (1967) 489.
91 V. Maxia, S. Meloni, M. A. Rollier, A. Brandone, V. N. Patwardhan, C. I. Waslien and S. El Shami, in Nuclear Activation Techniques in the Life Sciences, International Atomic Energy Agency, Vienna, 1972, p. 527.
92 R. T. Li and D. M. Hercules, Anal. Chem., 46 (1974) 916.
93 Y. M. Bala and V. M. Lifshits, Fed. Proc. Fed. Am. Soc. Exp. Biol. Transl. Suppl., 25 (1966) 370.
94 R. Monacelli, H. Tanaka and J. H. Yoe, Clin. Chim. Acta, 1 (1956) 577.
95 R. M. Parr, J. Radioanal. Chem., 39 (1977) 421.
96 J. P. Cali, Certificate of Analysis, Standard Reference Material 1577, Bovine Liver, National Bureau of Standards, Washington, 1977.
97 K. Kasperek, H. Schicha and H. Weese, in Trace Elements in Relation to Cardiovascular Diseases, International Atomic Energy Agency, Vienna, 1973, p. 71.
98 J. O. Pierce, F. E. Lichte, C. R. Hastings Vogt, A. Abu-Samra, T. R. Ryan, S. R. Koirtyohann and J. R. Vogt, in Measurement, Detection, and Control of Environmental Pollutants, International Atomic Energy Agency, Vienna, 1976, p. 357.
99 P. Lievens, R. Cornelis and J. Hoste, Anal. Chim. Acta, 80 (1975) 97.
100 J. Versieck, J. De Rudder, J. Hoste, F. Barbier, G. Lemey and L. Vanballenberghe, in D. Shapcott and J. Hubert (Eds.), Chromium in Nutrition and Metabolism, Elsevier/North-Holland Biomedical Press, Amsterdam, 1979, p. 59.
101 L. P. Dunstan and E. L. Garner, in D. Hemphill (Ed.), Trace Substances in Environmental Health — XI, University of Missouri, Columbia, MO, 1977, p. 334.
102 L. O. Plantin, in Nuclear Activation Techniques in the Life Sciences, International Atomic Energy Agency, Vienna, 1979, p. 321.
103 I. Y. Donev and L. M. Marichkova, in P. D. LaFleur (Ed.), Accuracy in Trace Analysis: Sampling, Sample Handling, and Analysis, Vol. 2, National Bureau of Standards, U.S. Government Printing Office, Washington, 1976, p. 1293.
104 L. T. McClendon, J. Radioanal. Chem., 42 (1978) 85.
105 A. B. Brill, D. Page, N. Dyer, R. Boglan and W. S. Lyon, in Trace Elements in Relation to Cardiovascular Diseases, International Atomic Energy Agency, Vienna, 1973, p. 5.
106 R. A. Nadkarni and G. H. Morrison, J. Radioanal. Chem., 43 (1978) 347.
107 D. Behne, P. Brätter, H. Geszner, G. Hube, W. Mertz and U. Rosnick, Fresenius Z. Anal. Chem., 278 (1976) 269.
108 G. R. Doshi and B. Patel, Curr. Sci., 42 (1973) 307.
109 W. Mertz, R. A. Anderson, W. R. Wolf and E. E. Roginski, in M. Kirchgessner (Ed.), Trace Element Metabolism in Man and Animals, Vol. 3, Arbeitskreis für Tierernährungsforschung, Weihenstephan, 1978, p. 272.
110 D. Shapcott, H. Khoury, P. P. Demers, J. Vobecky and J. Vobecky, Clin. Biochem., 10 (1977) 178.

111 R. W. Tuman, J. T. Bilbo and R. J. Doisy, Diabetes, 27 (1978) 49.
112 W. Wolf, W. Mertz and R. Masironi, J. Agric. Food Chem., 22 (1974) 1037.
113 J. Versieck and A. Speecke, in Nuclear Activation Techniques in the Life Sciences, International Atomic Energy Agency, Vienna, 1972, p. 39.
114 T. T. Gorsuch, Analyst, 87 (1962) 112.
115 G. B. Jones, R. A. Buckley and C. S. Chandler, Anal. Chim. Acta, 80 (1975) 389.
116 S. R. Koirtyohann and C. A. Hopkins, Analyst, 101 (1976) 870.
117 J. Kumpulainen, Anal. Chim. Acta, 91 (1977) 403.
118 K. L. Rook and W. Wolf, in D. D. Hemphill (Ed.), Trace Substances in Environmental Health — XI, University of Missouri, Columbia, MO, 1977, p. 324.
119 J. Versieck, J. Hoste, J. De Rudder, F. Barbier and L. Vanballenberghe, Anal. Lett., 12 (1979) 555.
120 P. B. Adams, in M. Zief and R. Speights (Eds.), Ultrapurity, M. Dekker, New York, 1972, p. 293.
121 I. W. F. Davidson and R. L. Burt, Am. J. Obstet. Gynecol., 116 (1973) 601.
122 R. S. Pekarek, E. C. Hauer, E. J. Rayfield, R. W. Wannemacher and W. R. Beisel, Diabetes, 24 (1975) 350.
123 L. E. Lins and K. Pehrsson, Lancet, (1976) i, 1191.
124 R. E. Thiers, J. F. Williams and J. H. Yoe, Anal. Chem., 27 (1955) 1725.
125 R. M. Parr and D. M. Taylor, Biochem. J., 91 (1964) 424.
126 K. Samsahl, P. Schramel, R. Thieme and B.-J. Klose, Nuklearmedizin, 11 (1972) 79.
127 F. Alt and H. Massmann, Fresenius Z. Anal. Chem., 279 (1976) 100.
128 R. A. A. Muzzarelli and R. Rocchetti, Talanta, 22 (1975) 683.
129 H. Kesteloot, J. Roelandt, J. Willems, J. H. Claes and J. V. Joossens, Circulation, 37 (1968) 854.
130 B. de la Cruz, in Trace Elements in Relation to Cardiovascular Diseases, International Atomic Energy Agency, Vienna, 1973, p. 19.
131 D. A. Olehy, R. A. Schmitt and W. F. Bethard, J. Nucl. Med., 7 (1966) 917.
132 J. Aaseth, E. Munthe, Ø. Førre and E. Steinnes, Scand. J. Rheumatol., 7 (1978) 237.
133 K. M. Hambidge and W. Droegemueller, Obstet. Gynecol., 44 (1974) 666.
134 P. Allain, E. Foussard and J. Boyer, Clin. Chim. Acta, 78 (1977) 183.
135 D. A. Olatunbosun, J. O. Bolodeoku, T. O. Cole and B. K. Adadevoh, Bull. WHO, 53 (1976) 134.
136 J. Versieck, F. Barbier, A. Speecke and J. Hoste, Clin. Chem., 20 (1974) 1141.
137 M. E. Lahey, C. J. Gubler, G. E. Cartwright and M. M. Wintrobe, J. Clin. Invest., 32 (1953) 322.
138 J. Danys and M. Kušleikaitė, Z. Inn. Med., 26 (1971) 718.
139 J. D. Bogden, D. I. Lintz, M. M. Joselow, J. Charles and J. S. Salaki, Am. J. Clin. Pathol., 67 (1977) 251.
140 P. Lafargue, J.-C. Couture, R. Monteil, J. Guilbaud and L. Saliou, Clin. Chim. Acta, 66 (1976) 181.
141 A. A. Yunice, R. D. Lindeman, A. W. Czerwinski and M. Clark, J. Gerontol., 29 (1974) 277.
142 C. G. Funckes, M. Chvapil, R. W. Carrol and R. Bressler, Contraception, 14 (1976) 291.
143 T. V. Zhernakova, Biull. Eksp. Biol. Med., 63 (1967) 47.
144 T. R. Hartoma, Ann. Acad. Sci. Fenn. Ser. A5, 171 (1977) 1.
145 N. A. Holtzman, D. A. Elliot and R. H. Heller, N. Engl. J. Med., 275 (1966) 347.
146 E. L. Kanabrocki, T. Fields, C. F. Decker, L. F. Case, E. B. Miller, E. Kaplan and Y. T. Oester, Int. J. Appl. Radiat. Isot., 15 (1964) 175.
147 B. Novosel and N. Jelavić, Fresenius Z. Anal. Chem., 278 (1976) 287.
148 A. A. Fernandez, C. Sobel and S. L. Jacobs, Anal. Chem., 35 (1963) 1721.
149 W. Seeling, F. W. Ahnefeld, W. Dick, R. Dölp, L. Fodor, E. Schmitz and R. Hohage, in K. Betke and F. Bidlingmaier (Eds.), Spurenelemente in der Entwicklung von Mensch und Tier, Urban & Schwarzenberg, München, 1975, p. 159.
150 D. J. D'Amico and H. L. Klawans, Anal. Chem., 48 (1976) 1469.
151 P. S. Papavasiliou and G. C. Cotzias, J. Biol. Chem., 236 (1961) 2365.

152 R. G. Banta and W. R. Markesbery, Neurology, 27 (1977) 213.
153 J. F. Sullivan, A. J. Blotcky, M. J. Jetton, H. K. J. Hahn and R. E. Burch, J. Nutr., 109 (1979) 1432.
154 J. P. Mahoney, K. Sargent, M. Greland and W. Small, Clin. Chem., 15 (1969) 312.
155 K. Heydorn and K. Nørgård, J. Radioanal. Chem., 15 (1973) 683.
156 J. Versieck, A. Speecke, J. Hoste and F. Barbier, Z. Klin. Chem. Klin. Biochem., 11 (1973) 193.
157 M. Zief and F. W. Michelotti, Clin. Chem., 17 (1971) 833.
158 M. Zief and J. W. Mitchell, Contamination Control in Trace Element Analysis, J. Wiley, New York, 1976, p. 47.
159 M. Zief and A. G. Nesher, Environ. Sci. Technol., 8 (1974) 677.
160 M. Zief and A. G. Nesher, Clin. Chem., 18 (1972) 446.
161 B. Mazière, J. Gros, C. Ricour and D. Comar, in Nuclear Activation Techniques in the Life Sciences, International Atomic Energy Agency, Vienna, 1979, p. 227.
162 R. A. A. Muzzarelli and R. Rocchetti, Talanta, 24 (1977) 77.
163 H. J. M. Bowen, J. Radioanal. Chem., 19 (1974) 215.
164 H. J. M. Bowen, At. Energy Rev., 13 (1975) 451.
165 J. P. Cali and W. P. Reed, in P. D. LaFleur (Ed.), Accuracy in Trace Analysis: Sampling, Sample Handling, Analysis, Vol. 1, National Bureau of Standards, U.S. Government Printing Office, Washington, 1976, p. 41.
166 T. Suzuki, in A. Goyer and M. A. Mehlman (Eds.), Toxicology of Trace Elements, Advances in Modern Toxicology, Vol. 2, J. Wiley, New York, 1977, p. 1.
167 H. Ackefors, Proc. R. Soc. London Ser. B, 177 (1971) 365.
168 L. Magos and T. W. Clarkson, J. Assoc. Off. Anal. Chem., 55 (1972) 966.
169 S. Tejning, Rep. No. 67 02 06, Dept. Occupat. Med., University Hospital, Lund, Sweden, 1967, p. 3.
170 G. Birke, A. G. Johnels, L.-O. Plantin, B. Sjöstrand, S. Skerfving and T. Westermark, Arch. Environ. Health, 25 (1972) 77.
171 N. P. Kubasik, H. E. Sine and M. T. Volosin, Clin. Chem., 18 (1972) 1326.
172 S. Tejning, Rep. No. 67 08 31, Dept. Occupat. Med., University Hospital, Lund, Sweden, 1967, p. 30.
173 T. Suzuki, T. Miyama and H. Katsunuma, Bull. Environ. Contam. Toxicol., 5 (1971) 502.
174 J. Versieck, J. Hoste, F. Barbier, L. Vanballenberghe, J. De Rudder and R. Cornelis, Clin. Chim. Acta, 87 (1978) 135.
175 N. Baert, R. Cornelis and J. Hoste, Clin. Chim. Acta, 68 (1976) 355.
176 P. A. Walravens, R. Moure, C. C. Solomons, W. R. Chappell and G. Bentley, in M. Kirchgessner (Ed.), Trace Element Metabolism in Man and Animals, Vol. 3, Arbeitskreis für Tierernährungsforschung, Weihenstephan, 1978, p. 577.
177 A. Morgan and A. Holmes, Radiochem. Radioanal. Lett., 9 (1972) 329.
178 G. D. Christian and G. J. Patriarche, Analyst, 104 (1979) 680.
179 F. H. Nielsen and D. A. Ollerich, Fed. Proc. Fed. Am. Soc. Exp. Biol., 33 (1974) 1767.
180 A. Schnegg and M. Kirchgessner, Z. Tierphysiol., 36 (1975) 63.
181 F. W. Sunderman, S. Nomoto, R. Morang, M. W. Nechay, C. M. Burke and S. W. Nielsen, J. Nutr., 102 (1972) 259.
182 D. Spruit and P. J. M. Bongaarts, Dermatologica, 154 (1977) 291.
183 A. C. Høgetveit and R. T. Barton, in S. S. Brown (Ed.), Clinical Chemistry and Chemical Toxicology of Metals, Elsevier/North-Holland Biomedical Press, Amsterdam, 1977, p. 265.
184 F. W. Sunderman, S. Nomoto, A. M. Pradhan, H. Levine, S. H. Bernstein and R. Hirsch, N. Engl. J. Med., 283 (1970) 896.
185 M. D. McNeely, M. W. Nechay and F. W. Sunderman, Clin. Chem., 18 (1972) 992.
186 D. Mikac-Dević, F. W. Sunderman and S. Nomoto, Clin. Chem., 23 (1977) 948.
187 H. Zachariasen, I. Andersen, C. Kostøl and R. Barton, Clin. Chem., 21 (1975) 562.
188 R. S. Pekarek and E. C. Hauer, Fed. Proc. Fed. Am. Soc. Exp. Biol., 31 (1972) 700.
189 K. H. Schaller, A. Kühner and G. Lehnert, Blut, 27 (1968) 155.

190 J. M. H. Howard, unpublished observations, quoted by Sunderman et al. [184].
191 F. W. Sunderman, Clin. Chem., 13 (1967) 115.
192 S. Nomoto and F. W. Sunderman, Clin. Chem., 16 (1970) 477.
193 D. Spruit and P. J. M. Bongaarts, in S. S. Brown (Ed.), Clinical Chemistry and Chemical Toxicology of Metals, Elsevier/North-Holland Biomedical Press, Amsterdam, 1977, p. 261.
194 F. W. Sunderman, Ann. Clin. Lab. Sci., 7 (1977) 377.
195 F. W. Sunderman, in S. S. Brown (Ed.), Clinical Chemistry and Chemical Toxicology of Metals, Elsevier/North-Holland Biomedical Press, Amsterdam, 1977, p. 231.
196 R. R. Fieve, H. L. Meltzer and R. M. Taylor, Psychopharmacologia, 20 (1971) 307.
197 R. R. Fieve, H. L. Meltzer, D. L. Dunner, M. Levitt, J. Mendlewicz and A. Thomas, Am. J. Psychiatry, 130 (1973) 55.
198 C. Chechan, X. Marchandise and J. Lekieffre, C. R. Soc. Biol., 169 (1975) 991.
199 O. L. Wood, Biochem. Med., 3 (1970) 458.
200 G. Bertrand and D. Bertrand, C. R. Acad. Sci., 232 (1951) 131.
201 E. Sutter, S. R. Platman and R. R. Fieve, Clin. Chem., 16 (1970) 602.
202 T. Westermarck, P. Raunu, M. Kirjarinta and L. Lappalainen, Acta Pharmacol. Toxicol., 40 (1977) 465.
203 H. Rea, unpublished observations, quoted by J. M. McKenzie et al. [204].
204 J. M. McKenzie, H. Rea, A. M. Van Rij and M. F. Robinson, Proc. Univ. Otago Med. School, 54 (1976) 25.
205 W. J. Rhead, E. E. Cary, W. H. Allaway, S. L. Saltzstein and G. N. Schrauzer, Bioinorg. Chem., 1 (1972) 289.
206 W. L. Broghamer, K. P. McConnell and A. L. Blotcky, Cancer, 37 (1976) 1384.
207 K. P. McConnell, W. L. Broghamer, A. J. Blotcky and O. J. Hurt, J. Nutr., 105 (1975) 1026.
208 S. G. Morss, H. R. Ralston and H. S. Olcott, Anal. Biochem., 49 (1972) 598.
209 H. K. J. Hahn, R. V. Williams, R. E. Burch, J. F. Sullivan and E. A. Novak, J. Lab. Clin. Med., 80 (1972) 718.
210 R. C. Dickson and R. H. Tomlinson, Clin. Chim. Acta, 16 (1967) 311.
211 R. F. Burk, W. N. Pearson, R. P. Wood and F. Viteri, Am. J. Clin. Nutr., 20 (1967) 723.
212 I. Lombeck, K. Kasperek, L. E. Feinendegen and H. J. Bremer, Clin. Chim. Acta, 64 (1975) 57.
213 I. Lombeck, K. Kasperek, H. D. Harbisch, L. E. Feinendegen and H. J. Bremer, Eur. J. Pediatr., 125 (1977) 81.
214 M. F. Robinson, Proc. Nutr. Soc., 35 (1976) A34.
215 P. J. Peterson, C. A. Girling, D. W. Klumpp and M. J. Minski, in Nuclear Activation Techniques in the Life Sciences, International Atomic Energy Agency, Vienna, 1979, p. 103.
216 J. J. M. de Goeij, K. J. Volkers and P. S. Tjioe, Anal. Chim. Acta, 109 (1979) 139.
217 H. O. Fourie and M. Peisach, S. Afr. J. Sci., 72 (1976) 349.
218 H. O. Fourie and M. Peisach, Analyst, 102 (1977) 193.
219 H. O. Fourie and M. Peisach, Radiochem. Radioanal. Lett., 26 (1976) 277.
220 K. Schwarz, D. B. Milne and E. Vinyard, Biochem. Biophys. Res. Commun., 40 (1970) 22.
221 K. Schwarz and D. B. Milne, Science, 174 (1971) 426.
222 L. L. Hopkins and H. E. Mohr, in W. Mertz and W. E. Cornatzer (Eds.), Newer Trace Elements in Nutrition, M. Dekker, New York, 1971, p. 195.
223 R. Cornelis, L. Mees, J. Hoste, J. Ryckebusch, J. Versieck and F. Barbier, in Nuclear Activation Techniques in the Life Sciences, International Atomic Energy Agency, Vienna, 1979, p. 165.
224 R. Cornelis, J. Versieck, L. Mees, J. Hoste and F. Barbier, J. Radioanal. Chem., 55 (1980) 35.
225 E. Damsgaard, K. Heydorn and B. Rietz, in Nuclear Activation Techniques in the Life Sciences, International Atomic Energy Agency, Vienna, 1972, p. 119.

226 E. Sabbioni, E. Marafante, R. Pietra, L. Goetz, F. Girardi and E. Orvini, in Nuclear Activation Techniques in the Life Sciences, International Atomic Energy Agency, Vienna, 1979, p. 179.
227 G. D. Christian, Anal. Lett., 4 (1971) 187.
228 H. A. Schroeder, J. J. Balassa and I. H. Tipton, J. Chronic Dis., 16 (1963) 1047.
229 K. Heydorn and H. R. Lukens, Pre-irradiation Separation for the Determination of Vanadium in Blood Serum by Reactor Neutron Activation Analysis, Risö Report No. 138, 1966.
230 E. L. Giroux, M. Durieux and P. J. Schechter, Bioinorg. Chem., 5 (1976) 211.
231 I. J. T. Davies, M. Musa and T. L. Dormandy, J. Clin. Pathol., 21 (1968) 359.
232 J. A. Halsted and J. C. Smith, Lancet, (1970) i, 322.
233 R. S. Pekarek, W. R. Beisel, P. J. Bartelloni and K. A. Bostian, Am. J. Clin. Pathol., 57 (1972) 506.
234 A. S. Prasad, J. Ortega, G. J. Brewer, D. Oberleas and E. B. Schoomaker, J. Am. Med. Assoc., 235 (1976) 2396.
235 B. L. Vallee, W. E. C. Wacker, A. F. Bartholomay and E. D. Robin, N. Engl. J. Med., 255 (1956) 403.
236 G. Karayalcin, F. Rosner, K. Y. Kim and P. Chandra, Lancet, (1974) i, 217.
237 B. L. Vallee and J. G. Gibson, J. Biol. Chem., 176 (1948) 445.
238 W. Seeling, F. W. Ahnefeld, W. Dick and L. Fodor, Anaesthesist, 24 (1975) 329.
239 B. Foley, S. A. Johnson, B. Hackley, J. C. Smith and J. A. Halsted, Proc. Soc. Exp. Biol. Med., 128 (1968) 265.
240 D. J. Kosman and R. I. Henkin, Lancet, (1979) i, 1410.
241 J. C. Smith, J. A. Zeller and E. D. Brown, Science, 193 (1976) 496.
242 J. C. Smith, in G. J. Brewer and A. S. Prasad (Eds.), Zinc Metabolism: Current Aspects in Health and Disease, A. R. Liss, New York, 1977, p. 181.
243 S. B. Nackowski, R. D. Putman, D. A. Robbins, M. O. Varner, L. D. White and K. W. Nelson, Am. Ind. Hyg. Assoc. J., 38 (1977) 503.
244 E. W. Reimold and D. J. Besch, Clin. Chem., 24 (1978) 675.
245 R. W. Handy, Clin. Chem., 25 (1979) 197.
246 J. B. Dawson and B. E. Walker, Clin. Chim. Acta, 26 (1969) 465.
247 H. H. Hellwege, Klin. Wochenschr., 48 (1970) 1063.
248 Ö. Hetland and E. Brubakk, Scand. J. Clin. Lab. Invest., 32 (1973) 225.
249 M. D. Lifshits and R. T. Henkin, J. Appl. Physiol., 31 (1971) 88.
250 L. McBean and J. Halsted, J. Clin. Pathol., 22 (1969) 623.
251 K. Kasperek, H. Schicha, A. Höck, V. Siller and L. E. Feinendegen, Strahlentherapie, 145 (1973) 229.
252 M. Persigehl, A. Höck, K. Kasperek, E. Land and L. E. Feinendegen, Z. Klin. Chem. Klin. Biochem., 12 (1974) 171.
253 B. E. Walker, J. B. Dawson, J. Kelleher and M. S. Losowsky, Gut, 14 (1973) 943.
254 R. Berfenstam, Acta Paediatr., 41 (1952) Suppl. 87.
255 F. Björkstén, A. Arooma, P. Knekt and L. Malinen, Acta Med. Scand., 204 (1978) 67.
256 K. Kasperek, L. E. Feinendegen, I. Lombeck and H. J. Bremer, Eur. J. Pediatr., 126 (1977) 199.
257 R. D. Lindeman, M. L. Clark and J. P. Colmore, J. Gerontol., 26 (1971) 358.
258 M. W. Greaves and A. W. Skillen, Lancet, (1970) ii, 889.
259 T. Hallböök and E. Lanner, Lancet, (1972) ii, 780.
260 R. I. Henkin, P. J. Schechter, W. T. Friedewald, D. L. Demets and M. Raff, Am. J. Med. Sci., 272 (1976) 285.
261 J. F. Sullivan, M. M. Jetton and R. E. Burch, J. Lab. Clin. Med., 93 (1979) 485.
262 L. P. Bos, A. Van Vloten, A. F. D. Smith and M. Nubé, Neth. J. Med., 20 (1977) 263.
263 E. D. M. Gallery, J. Blomfield and S. R. Dixon, Br. Med. J., (1972) iv, 331.
264 J. Heinonen and O. Suschny, in Nuclear Activation Techniques in the Life Sciences, International Atomic Energy Agency, Vienna, 1972, p. 155.
265 J. Heinonen and O. Suschny, J. Radioanal. Chem., 20 (1974) 499.

Analytica Chimica Acta, 116 (1980) 255—274

STUDY OF THE COMPLEX FORMATION OF COPPER(II) BY HUMIC AND FULVIC SUBSTANCES

J. BUFFLE*, P. DELADOEY, F. L. GRETER and W. HAERDI

Department of Analytical and Inorganic Chemistry, University of Geneva, 1211-Geneva 4 (Switzerland)

(Received 12th November 1979)

SUMMARY

A study of the complexation of copper(II) by fulvic substances, based on ion-selective electrode measurements, is reported. The influences of the copper concentration (10^{-6} —10^{-4} M), fulvic acid concentration (2—100 mg l^{-1}), pH (3—8) and calcium concentration (10^{-4}—5×10^{-3} M) are given particular attention. The effects of statistical errors on the measurement of the values of the complex-formation parameters are considered. These parameters are measured for various surface-water samples, aqueous soil extracts, peat water and solutions of organic matter formed by in vitro decomposition of leaves. In general, these parameters vary little with actual source for a particular type of water.

The role of organic substances in establishing the behaviour of trace metals in natural waters has received increasing attention in recent years, as such substances may influence several of the properties of metals, and particularly their availability to organisms [1, 2]. Although numerous papers [e.g. 3—9] have been devoted to the measurement of the complex-formation properties of soil organic matter in the acidic pH ranges, little work [2, 10—12] has been done on the measurement of the complexing properties of the organic matter in natural waters in the "natural" pH range of 6—9. Knowledge of these properties is, however, very important in computing the chemical state of trace metals in waters. Despite the fact that these properties may play an important role in the speciation of some trace metal ions [11], there are wide variations in the stability constants of the complexes quoted in the literature. Such discrepancies may be due either to the methodology chosen or to the nature of the sample of organic matter used, both of which differ from author to author.

In this context, the aim of the work reported here was to compare the complexation properties of the organic matter in various types of natural water samples (lakes, rivers, peat, water extract of soils, solution produced by decomposition of leaves) and of fresh waters of various origins. In a second part [13], the present results and method will be compared with those described in the literature, in order to obtain a clearer idea about the main causes for the differences between the results of various authors.

Copper(II) was chosen as test ion; it provides an interesting case study because of its important role in biological activity, its relatively strong complexation by many organic substances, and its strong hydrolysing properties (compared with other first-row transition metals or heavy metals such as Pb(II) and Cd(II)), which may affect the measurement of the complexing properties of organic materials.

EXPERIMENTAL

Apparatus and reagents

The complex-formation properties were measured by potentiometric titrations by means of a copper(II)-selective electrode, as described previously [14]. Unless otherwise stated, the same experimental conditions were used here. However, the titrations were performed by means of a Tacussel automatic titrator (TT 100 and TT 300 modules, coupled to an Electroburex EBX1) modified in the following way. First, in order to obtain more accurate potential readings (± 0.1 mV), a Tacussel Aries 20 000 potentiometer was added to the system and modified so as to be controlled by the titrator. Secondly, the titrator was modified in such a way that it could be stopped automatically after a chosen volume of reactant had been delivered. This allowed the concentration of the titrant solution in the Electroburex to be changed three times during the titration. This modification made it possible to use a wide range of titrant concentration (e.g. 5×10^{-7} to 10^{-2} M copper(II)), and is useful because complexation measurements are made in solutions containing $[Cu(II)]_t < 10^{-4}$ M whereas the electrode parameters (slope and E°) are determined from the portion of the curve corresponding to $[Cu]_t > 10^{-3}$ M. Thirdly, the maximum waiting time between volume increments was increased from 100 s to 17 min, as the response time of the selective electrode is often several minutes for $[Cu]_t < 10^{-5}$ M. A Metrohm chart recorder (E478) was used for recording potential—time curves for each increment in order to check the attainment of equilibrium. Finally the Aries 20000 and Electroburex EBX1 were modified in such a way that the potential and titrant volume could be obtained in a suitable digitalized form for storage in a ticker tape (Module Ericsson type 34 and 3405-2) by means of a home-made interface [15].

The pH of the solution was controlled by means of a Tacussel PHIT-NX pH-stat, with module IM, coupled to two electric burettes (Metrohm E415). The concentrations of the stock solutions of acid and base were chosen in such a way that the total volume delivered by the pH-stat was negligible compared to that present in the titration cell.

The computations were done and graphs were produced by means of the Univac 1108 computer and Benson plotter of the University of Geneva.

All the commercial reagents were as described earlier [14]. The complex-formation measurements were made in 0.1 M sodium perchlorate.

Natural samples

A detailed description of the nature, chemical composition and pretreatment of the water samples containing the organic matter studied has already been given [16, 17].

The pretreatment of the natural waters (lakes, ponds, rivers) may be summarized as follows: after filtrations, the waters were concentrated 7—12 times by freezing concentration [16], acidified to pH 4 with perchloric acid to eliminate HCO_3^-, and filtered by the "concentration technique" [17] successively on three membranes (0.2 μm, 0.035 μm, Amicon PM10). The filtrate was then filtered through Amicon UMO5 membrane by using the "washing technique" with distilled water. The same treatment (except for the freezing concentration) was applied to the water extracts from soils. In all these cases, the material retained in the last filtration represented the major portion of the total organic content of the waters (about 70% for fresh waters and 50% for soil extracts) and these fractions were used for complex-formation measurements.

The same technique was applied to the aqueous solutions resulting from decomposition of leaves, except that the washing technique was used with a 0.035-μm membrane, as about 65% of organic matter was found to be retained between 0.2 and 0.035 μm. For peat water, the concentrate obtained from freezing concentration was divided into two portions; one was treated in the same way as the fresh waters and the other as the "leaf extracts". For all the samples, the last filtration before complexation was done by using the washing technique, in order to remove as much of the "non-humic" low-molecular-weight compounds (such as Ca^{2+} or amino acids) as possible.

Procedures

For valid comparison of the complexing properties of various water samples, as well as the parameters determined by various workers in this field, it is essential to determine (a) the role of the most important variables of the system, and (b) the true error made in the measured parameters.

The three most important variables, (i.e. total copper concentration, $[Cu]_t$, total concentration of organic matter, $\{L\}_t$, and pH) were studied by titrating each sample in three different ways as described earlier [14]. In the following, all the values of $\{L\}_t$ are given in mg of organic matter per litre. These values are taken as equal to twice the values of total organic carbon, as it was observed that the fractions of carbon in our samples were very often close to 50% [16].

Titration of L by Cu(II) (T_{Cu}). $\{L\}_t$ was kept constant (50—80 mg l^{-1}), $[Cu]_t$ was varied between 5×10^{-7} M and 10^{-2} M, and pH was maintained at 6.0 up to 10^{-3} M $[Cu]_t$, above which the solution was acidified to about pH 4. The portion of the titration curve for which $[Cu]_t > 10^{-3}$ M was used for the determination of the E^0 and slope (S) of the copper(II)-selective electrode.

Titration of Cu(II) by L (T_L). $[Cu]_t$ (3×10^{-6} M) and pH (6.0) were kept constant, and $\{L\}_t$ was varied by diluting the initial solution having a concentration of about 100 mg l^{-1}, to about 2 mg l^{-1}, with a solution containing 0.1 M $NaClO_4$ and 3×10^{-6} M copper ions.

Titration of L + Cu(II) by H^+ (T_H). $[Cu]_t$ (5×10^{-6} M) and $\{L\}_t$ (40—60 mg l^{-1}) were kept constant and the pH was varied. The solution, initially acidified to pH 2—3, was titrated with sodium hydroxide up to pH 8. The resulting solution was back-titrated with perchloric acid to test the reversibility of the system.

As indicated before, all the samples were freed from HCO_3^- by acidification and degassing and all the subsequent operations (filtrations and titrations) were done under a nitrogen atmosphere. Sodium hydroxide solutions were prepared with carefully degassed distilled water.

Computation of the complexation parameters and the errors on these parameters

Computer programs were written in FORTRAN V to decode the ticker-tape data recorded in the binary mode, and to use these data to compute and plot the following functions:

$$E = f(\log[Cu]_t);\ \log \alpha = f(\log[Cu]_t);\ Y = (\{L\}_t/[Cu]_t) \times (\alpha/\alpha - 1) = f(\alpha/[Cu]_t);$$

$$\log \alpha = f(\log\{L\}_t);\ (\alpha - 1)/\{L\}_t = f(\{L\}_t);\ E = f(\mathrm{pH});$$

$$\log(\alpha - 1) = f(\mathrm{pH});\ Z = f(\mathrm{pH})$$

Here E is the measured potential of the selective electrode. Z is a function of $[Cu]_t$, $\{L\}_t$ and α, as defined earlier [14]. $\alpha = \alpha_m - \delta_{OH}$, where α_m is the degree of complexation defined as $\alpha_m = [Cu]_t/[Cu^{2+}]$ where $[Cu^{2+}]$ is the concentration of hydrated copper(II) ion in solution, measured with the selective electrode. $\delta_{OH} = \Sigma_{i=1}^{4}\ \beta_i^{OH}\ [OH]^i$ and is a correction term used to eliminate any possible contribution from $CuOH^+$, $Cu(OH)_2^0$, $Cu(OH)_3^-$ and $Cu(OH)_4^{2-}$.

Graphical methods [14] were used to obtain the following complexation parameters (for full definitions of symbols, see [14]):

(a) M_{eq} and β_1' from the graph $Y = f(\alpha/[Cu]_t)$ (T_{Cu}^g method in Table 1);

(b) β_1' and β_2' from the $(\alpha - 1)/\{L\}_t = f(\{L\}_t)$ plot (T_L^g method in Table 1);

(c) β_1' and x from the graph $Z = f(\mathrm{pH})$ (T_H method in Table 2).

Here M_{eq} is the equivalent weight of a complexing site on the organic molecules (M_{eq} is equal to the molecular weight if there is only one site per molecule); β_1' and β_2' are the overall stability constants of the complexes CuL and CuL_2 at a given pH, respectively, and x is as defined earlier [14]. The values of these parameters are listed in Table 1.

In addition, attempts were made to estimate the extent to which the mode of computation of the complexation parameters affected the final results. This was done by comparing the results of the graphical methods with

those obtained by means of a curve-fitting computer program which also made it possible to estimate the order of magnitude of the "true" errors on the parameters. The program written for this purpose was based on the following steps.

(a) First estimates of the values of β'_1, β'_2 and M_{eq} were obtained by trial and error as described earlier [14].

(b) Equation 14 [14] was rewritten as:

$$\alpha^3 - \alpha^2 [(1 + \{L\}_t\beta'_1/M_{eq} + \{L\}_t^2\beta'_2/M_{eq}^2) - 4\{L\}_t\beta'_2[Cu]_t/M_{eq} + 4\beta'_2[Cu]_t^2] + \alpha[(\{L\}_t\beta'^2_1/M_{eq}^2 - 4\{L\}_t\beta'_2/M_{eq}) \cdot [Cu]_t + (8\beta'_2 - \beta'^2_1)[Cu]_t^2] + [\beta'^2_1 -]_t^2 = 0 \quad (1)$$

By using the above values of the complexation parameters, the theoretical value of α, α_{theor}, was computed for each couple ($\{L\}_t$, $[Cu]_t$) and a first estimate of the error, ϵ, (for 92% probability) of the experimental values of log α, was computed from the variability of the points around the theoretical curve log $\alpha_{theor} = f(\log[Cu]_t)$ (or log $\alpha_{theor} = f(\log\{L\}_t)$).

(c) Then, by using eqn. (1) and the estimated value of ϵ, better estimates of β'_1, β'_2 and M_{eq} were computed by the trial and error method, by applying the minimizing function:

$$F(\alpha) = \sum_i (\log \alpha_{theor,i} - \log \alpha_i)^2/2\epsilon^2 \quad (2)$$

where α_i is the experimental value of α for the i^{th} couple ($\{L\}_t$, $[Cu]_t$). The minimization function was computed by means of the Computer Centre library program MINUIT [18]. In this program, the optimum values of parameters are determined by utilizing Monte Carlo and simplex methods [19] and a variable metric step method [20] successively. The methods used to estimate the complexation parameters by this curve-fitting technique are denoted by T^c_{Cu} and T^c_L, depending on whether the parameters are computed from the T_{Cu} or the T_L titration curves. They are listed in Table 1.

(d) By using the best values of β'_1, β'_2 and M_{eq}, a better value of the error, ϵ_α (for 92% probability), was computed as before. The "true" negative error in log β'_1 (for 92% probability) is then computed by keeping log β'_2 and M_{eq} constant and decreasing log β'_1 until the variability around the curve log α = $f([Cu]_t)$ (or log $\alpha = f(\{L\}_t)$) is increased by an amount corresponding to ϵ_α. The "true" positive error on log β'_1 is computed in the same way by gradually increasing the value of log β'_1. The "true" error ϵ_1 given in Table 1 is the mean value of the negative and positive errors. The errors ϵ_2 and ϵ_M in β'_2 and M_{eq} were computed analogously.

(e) Finally, the MINUIT program also verifies whether the function $F(\alpha)$ has a normal distribution profile around the minimum, and plots log β'_1 vs. log β'_2 contours for $F(\alpha)$ = constant. Such plots make it possible to check, by simple inspection, whether the minimization procedure is satisfied by only one well-characterized set of values of complexation parameters.

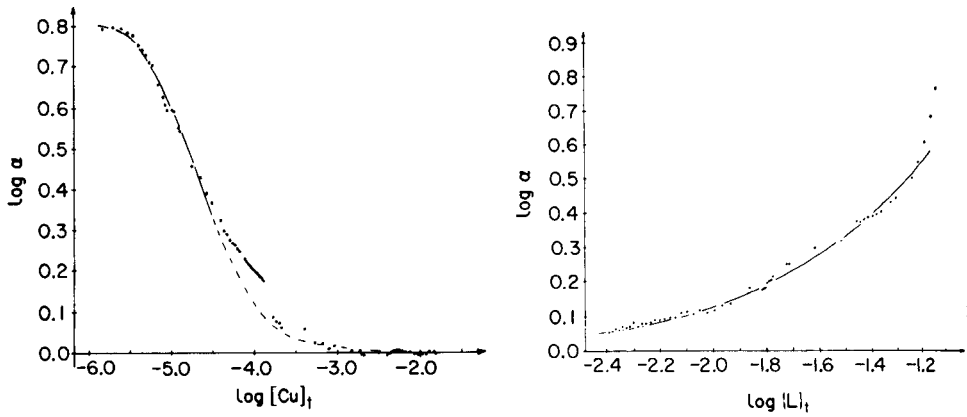

Fig. 1. Titration of fulvic acids with Cu^{2+} (T_{Cu}): experimental points and adjusted curve. Sample 21, pH 6, $\{L\}_t$ = 51 mg l^{-1}, 0.1 M $NaClO_4$, $[Cu]_t$ as mol l^{-1}.

Fig. 2. Dilution (T_L) titration : experimental points and adjusted curve. Sample 21, pH 6, $[Cu]_t$ = constant = 3×10^{-6} M, 0.1 M $NaClO_4$, $\{L\}_t$ as g l^{-1}.

RESULTS

The values of the complex-formation parameters and their errors measured at pH 6 for a number of aqueous samples, are given in Table 1, while the parameters obtained from T_H titrations are given in Table 2. These tables make it possible to obtain an idea of (i) the accuracy of the measured parameters, (ii) the validity of the corresponding model of complex formation, and (iii) the behaviour of organic matter of different origins.

Accuracy of the complex-formation parameters

The validity of the computed parameters were always checked in two ways. First the adjusted and experimental curves were compared; typical examples are shown in Figs. 1 and 2. Secondly, the corresponding contours of the function $F(\alpha)$ were examined. The adjustment was considered as valid only if a well defined minimum was observed.

Although the values obtained for M_{eq} by T^c_{Cu} and T^c_L titrations are similar, the accuracy of the latter is poor. For this reason the value of M_{eq} obtained by T^c_{Cu} was imposed in the evaluation of β'_1 and β'_2 by the T^c_L method.

The following remarks may be made about these results. A mean value of $\bar{\epsilon}_\alpha = 0.07$ (Table 1) implies that only the values of α exceeding 1.2 may be considered significant. By using the mean values $\beta_1 = 10^5$ and $M_{eq} = 1000$, the calculations show that, at pH 6, significant change in the measured potential will be observed only when $\{L\}_t > 2$ mg l^{-1}. This condition was used in the T_L titration. Although the errors, ϵ_α, on the measured parameter, log α, are relatively low, the absolute error on log β'_1 is not better than ± 0.2. This has to be taken into consideration in comparing the properties of

TABLE 1

Values of the complex-formation parameters β_1', β_2' and M_{eq} and the corresponding errors ($\epsilon_1 = \Delta \log \beta_1'$, $\epsilon_2 = \Delta \log \beta_2'$, $\epsilon_M = \Delta M_{eq}/M_{eq}$ (%)) of various aqueous samples of organic matter. These parameters were determined by means of different titration methods. ϵ_α ($= \Delta \log \alpha$) is the variability around the curve $\log \alpha = f(\log[Cu]_t)$

Sample no.	Nature of the sample[a]	Method	M_{eq}	ϵ_M (%)	$\log \beta_1'$	ϵ_1	$\log \beta_2'$	ϵ_2	ϵ_α
21	S_1	T^c_{Cu}	1460	6	4.8	0.10	9.5	0.10	0.03
		T^g_{Cu}	1350		4.9				
		T^c_L			4.8	0.10	—	—	0.04
		T^g_L			4.7		—		
22	S_1	T^c_{Cu}	510	3	4.9	0.14	9.2	0.13	0.06
		T^g_{Cu}	470		4.9				
		T^c_L			4.7	0.31	9.2	0.28	0.10
		T^g_L			4.6		9.2		
1a	S_r	T^c_{Cu}	2040	16	5.6	0.20	11.0	0.31	0.2
		T^g_{Cu}	1000		4.8				
1b	S_r	T^c_{Cu}	1450	9	5.1	0.10	10.1	0.16	0.08
		T^g_{Cu}	1090		5.0				
2	S_r	T^c_{Cu}	2000	6	5.1	0.06	10.4	0.16	0.02
		T^g_{Cu}	2070		5.2				
3	S_r	T^c_{Cu}	1920	—	5.8	0.28	10.9	0.34	0.26
		T^g_{Cu}	2100		5.9				
4	S_r	T^c_{Cu}	1330	8	4.5	0.11	9.3	0.10	0.03
		T^g_{Cu}	1500		4.7				
11	S_r	T^c_{Cu}	2370	11	5.3	0.18	10.2	0.17	0.08
		T^g_{Cu}	1700		5.1				
		T^c_L			5.6	0.05	9.8	0.26	0.03
		T^g_L			5.4		10.0		
10	S_m	T^c_{Cu}	1460	12	5.3	0.15	10.0	0.15	0.08
		T^g_{Cu}	1220		5.2				
		T^c_L			5.2	0.21	9.4	0.51	0.13
		T^g_L			5.0		9.5		
50a(1)[b]	S_m	T^c_{Cu}	2730	17	5.2	0.23	10.2	0.39	0.13
		T^g_{Cu}	1550		4.9				
		T^c_L			5.4	0.46	9.2	0.49	0.01
		T^g_L			5.2		9.4		
50a(2)	S_m	T^c_{Cu}	1800	14	5.3	0.19	9.9	0.23	0.11
		T^g_{Cu}	1160		5.0				
		T^c_L			5.7	0.11	10.0	0.43	0.09
		T^g_L			5.5		10.1		

TABLE 1 (continued)

Sample no.	Nature of the sample[a]	Method	M_{eq}	ϵ_M (%)	$\log \beta_1'$	ϵ_1	$\log \beta_2'$	ϵ_2	ϵ_α
24	S_m-T	T^c_{Cu}	2020	7	5.2	0.17	9.8	0.18	0.07
		T^g_{Cu}	1570		5.0				
		T^c_L			5.3	0.27	9.7	0.8	
		T^g_L			4.9		9.8		
41a	T	T^c_{Cu}	610	15	4.9	0.25	9.3	0.26	0.15
		T^g_{Cu}	820		5.3				
		T^c_L			5.3	0.04	9.4	0.10	0.02
		T^g_L			5.1		9.5		
F1	F	T^c_{Cu}	500	5	3.7	0.24	8.1	0.18	0.02
	(holm-oak)	T^g_{Cu}	490		3.8				
		T^c_L			3.8	0.14	7.3		0.03
		T^g_L			3.7				
F2	F	T^c_{Cu}	570	50	4.4	0.17	8.4	0.19	0.05
	(beech)	T^g_{Cu}	530		4.5				
		T^c_L			4.2	0.18	7.7	0.8	0.05
		T^g_L			4.0		8.2		
F3	F	T^c_{Cu}	440	21	4.2	0.21	8.2	0.21	0.12
	(larch)	T^g_{Cu}	480		4.3				
		T^c_L			4.0	0.06	8.0	0.17	0.02
		T^g_L			4.6		7.7		
F4	F	T^c_{Cu}	1040	3	4.9	0.09	9.2	0.09	0.05
	(chestnut)	T^g_{Cu}	980		4.9				
		T^c_L			4.9	0.21	8.8	0.52	0.05
		T^g_L			4.9		8.7		
S2	So	T^c_{Cu}	1910	5	4.9	0.20	10.0	0.17	0.06
	(6.0)	T^g_{Cu}	2910		4.5				
		T^c_L			5.2	0.17	10.0	0.24	0.05
		T^g_L			4.6		9.4		
S1	So	T^c_{Cu}	1710	3	4.8	0.30	9.5	0.25	0.06
	(17.6)	T^g_{Cu}	1890		5.0				
		T^c_L			5.2	0.51	10.0	0.51	0.14
		T^g_L			4.9		10.0		
S0	So	T^c_{Cu}	1420	12	4.9	0.08	9.2	0.36	0.06
	(18.1)	T^g_{Cu}	1700		5.2				
		T^c_L			4.9	0.21	9.3	0.58	0.06
		T^g_L			4.8		9.3		
S4	So	T^c_{Cu}	1430	31	4.8	0.3	9.2	0.2	0.02
	(57.2)	T^g_{Cu}	1800		5.1				

[a]The nature of the samples is described in the discussion of different water samples. For the F and So samples, the nature of the leaves and the initial content of humus in the soil (in %) are indicated. [b]This sample was filtered on 0.2-μm filters only, before measurements were made.

TABLE 2

Values of the slopes, S_α and S_Z, of the curves log $(\alpha - 1) = f(\text{pH})$ and $Z = f(\text{pH})$, respectively, at various pH and for different water samples. The values of log β_1' given in this table are approximate values computed from T_H titration curves from eqn. (9)

Sample no.	Nature of the sample	S_α		S_Z		log β_1' (pH 6)
		$3.5 \leqslant \text{pH} \leqslant 6$	pH 8	$5 \leqslant \text{pH} \leqslant 7$	pH 8	
21	S_l	0.59	0.97	0.51	0.61	4.7
22	S_l	0.46	1.02	0.50	0.50	4.9
11	S_r	0.48	0.91	0.40	0.60	5.5
10	S_m	0.60	0.95	0.55	0.55	4.9
50a(1)	S_m	0.53	0.78	0.53	0.53	5.6
50a(2)	S_m	0.54	1.04	0.52	0.64	5.2
24	S_m-T	0.54	1.09	0.60	0.62	5.2
41a	T	0.74	0.90	0.54	0.48	5.3
F1	F	0.55	1.45	0.46	0.76	4.1
F2	F	1.04	1.08	0.64	0.50	4.9
F3	F	1.50	1.50	—	—	4.1
F4	F	0.73	0.66	0.60	0.45	4.8
S0	So	0.59	0.68	0.45	0.45	5.1
S1	So	0.50	0.45	0.27	0.25	5.6
S2	So	0.50	0.78	0.42	0.42	5.3
S4	So	0.50	1.04	—	—	4.9

various waters or the results of various methods. The main reason for the relatively large values of ϵ_1 and ϵ_2 is probably that log β_1' and log β_2' are actually mean values for the mixture under study, obtained from measurements over a wide range of concentrations of Cu(II) and L. Finally, it must be noted that both the graphical and computer methods yielded similar values for log β_1' within experimental errors for the titration of T_{Cu} or T_L at pH 6, which confirms the validity of the computed values of the errors. Indeed, the differences in the results observed between graphical and computer methods represent the order of magnitude of the error that arises from the method of computation; because of mathematical manipulation, the weighting factors and possible systematic errors affect the results of the two methods differently.

Nature of the complexes

The fact that the results obtained from the titrations with different reagents (T_{Cu}, T_L (Table 1) and T_H (Table 2)) all yield similar values for log β_1' and log β_2' indicates that the model of complex formation used is applicable over a relatively wide range of experimental conditions. However, the model has the following limitations.

T_{Cu} titrations. Although the curve log $\alpha = f([\text{Cu}]_t)$ levels off at $[\text{Cu}]_t < 5 \times 10^{-6}$ M, the applicability of the model should be tested for lower con-

centrations. This is made difficult, when the copper(II)-selective electrode is used, because of its high sensitivity limit ($>2-3 \times 10^{-6}$ M).

A good theoretical fit to the experimental data was possible (according to the criteria mentioned in the above discussion of accuracy) only for a portion of the curve corresponding to $3 \times 10^{-6} < [Cu]_t < [Cu]_t^{max}$. $[Cu]_t^{max}$, above which the fit was poor, was found experimentally from the fitting procedure. For high values of $[Cu]_t$, the value of α, calculated by using the values of constants obtained in the concentration range $[Cu]_t < [Cu]_t^{max}$, was less than that found experimentally. The fact that the adjustment is not possible for high values of $[Cu]_t$ may be due (a) to the formation of $Cu_\nu L$ ($\nu > 1$) complexes, as has been assumed by some authors, or (b) to the hydrolysis of copper(II) with resultant formation of mixed complexes with L and OH^- or polynuclear hydrolysed complexes of copper(II) or a precipitate of copper hydroxide. The first hypothesis is supported by the fact that the ratio $r = [Cu]_t^{max}/[L]_t$ (Table 3) ($[L]_t$ in mol l^{-1}) is 0.5—1.0, irrespective of the nature of the water sample, and also by the observation that, by modifying the curve-fitting program (see below), it was possible to adjust the theoretical values on the whole experimental curve (10^{-6} M $< [Cu]_t < 6 \times 10^{-4}$ M) by taking into account the formation of CuL (β'_1), CuL_2 (β'_2) and Cu_2L (β'_{12}) complexes. However, because of the large number of adjustable parameters, the significance of β'_{12} is questionable. The formation of polynuclear hydrolysed complexes or copper hydroxide precipitates seems unlikely under the present conditions, as the solubility product of CuO, the less soluble hydrolysed compound of copper(II), ($\log K_{So}^{CuO} = -19.66$ at 25°C and $\mu = 0.1$ and for the molar surface $S \to 0$ [21, 22]) is never overcome for $[Cu]_t = [Cu]_t^{max}$, even by neglecting the complexation of copper (Table 3). The problem of hydrolysis of copper(II) is discussed in more detail in the consideration of pH effects (see below). Anyway, it must be emphasized that, for most natural waters, the condition $[Cu]_t/[L]_t < 0.5$ is fulfilled. Hence this part of the titration curve was not studied in more detail.

T_L titrations. The fact that for all the water samples the plot of $\log \alpha = f(\log\{L\}_t)$ yields a continuous curve with the slope increasing with $\{L\}_t$ shows clearly that the complexation properties of L cannot be explained in terms of only 1:1 complexes as has been assumed by many authors. A discussion of the importance of this last assumption for the interpretation of the data will be given elsewhere [13].

To take into account the above observations, CuL_2 complexes were assumed to be formed earlier [14] as well as by other authors [8], without any assumption being made on the nature of the bonding of copper(II) with the two ligand molecules. However, complexes of the "classical" CuL_2 type (where copper is bound to two molecules of L) may be formed with compounds whose molecular weights are less than some thousands (as for samples 10—24, 50, S0—S3 [17]), but this seems unlikely to occur with compounds having molecular sizes greater than 0.035 μm (e.g., samples 41a, F1—F4 [17]). Moreover, although only few titrations were performed with

TABLE 3

Values of dimerization constant, $K_2'^{L}$, of the ratio $r = [Cu]_t/[L]_t$ corresponding to the concentration $[Cu]_t^{max}$ below which the model used here for interpreting the data is valid, and of the product $[Cu]_t^{max}[OH^-]^2$. The values given under log $K_2'^{L}$ were computed by means of eqn. (4) from the mean values, $\overline{\log \beta_1'}$ and $\overline{\log \beta_2'}$ of the constants of the 1:1 and 1:2 complexes obtained from T_{Cu}^{c}, T_{Cu}^{g}, T_{L}^{c} and T_{L}^{g} titrations (see Table 1)

Sample no.	Nature of the sample	$\overline{\log \beta_1'}$	$\overline{\log \beta_2'}$	log $K_2'^{L}$	r	$-\log([Cu]_t^{max}[OH^-]^2)$
21	S_l	4.8	9.5	4.7	0.30	20.11
22	S_l	4.8	9.2	4.4	0.45	19.96
1a	S_r	5.2	11.0	5.8	0.67	20.16
1b	S_r	5.1	10.1	5.0	0.61	20.46
2	S_r	5.1	10.4	5.2	0.75	20.08
3	S_r	5.9	10.9	5.0	0.53	20.21
4	S_r	4.6	9.3	4.7	0.84	19.96
11	S_r	5.3	10.0	4.7	0.51	20.26
10	S_m	5.2	9.6	4.4	0.43	20.06
50a(1)	S_m	5.2	9.6	4.4	0.73	20.36
50a(2)	S_m	5.4	10.0	4.6	0.52	20.11
24	S_m-T	5.1	9.7	4.6	0.62	20.04
41a	T	5.2	9.4	4.3	0.59	19.76
F1	F	3.7	7.7	4.0	1.43	19.56
F2	F	4.3	8.1	3.8	0.53	19.86
F3	F	4.2	8.1	3.9	1.1	19.66
F4	F	4.9	8.9	4.0	0.57	19.86
S0	So	4.9	9.3	4.4	1.0	19.66
S1	So	5.0	9.8	4.8	0.46	20.01
S2	So	4.8	9.8	5.0	0.84	19.76
S4	So	4.9	9.2	4.3	1.30	19.81

$\{L\}_t > 100$ mg l^{-1}, it was observed that, in several cases, the slope of the plot $(\alpha - 1)/\{L\}_t = f(\{L\}_t)$ increased abruptly for $\{L\}_t \geqslant 80$ mg l^{-1} (e.g. see Fig. 3). This phenomenon seems to indicate the formation of CuL_n $(n > 2)$ complexes. The possible formation of such complexes is in accordance with the finding that the curvature of the experimental $\log \alpha = f(\log\{L\}_t)$ curves is always more pronounced than the theoretical one for high values of $\{L\}_t$ (Fig. 2), and this may be a reason why higher values for ϵ_2 are obtained from T_L titration curves than from T_{Cu} curves.

The mean number of ligands bound to a metal ion can be estimated from the ratio of $d \log \alpha / d \log\{L\}_t$ given in Table 4 and was found to vary roughly between 0 and 3 for $\{L\}_t = 0$—100 mg l^{-1}.

Far more probable than the formation of "classical" complexes is the formation of CuL_n $(n > 1)$ complexes where the complexation of Cu^{2+} by one complexing site of an aggregate of L occurs as follows:

$$nL \rightleftarrows L_n; \quad Cu^{2+} + L_n \underset{K_{(n)}'^{Cu}}{\rightleftarrows} Cu(L_n) \qquad (3)$$

TABLE 4

Values of the slopes of the experimental plots $\log \alpha = f(\log\{L\}_t)$, for different values of $\{L\}_t$ and various water samples

Sample No.	Nature of the sample	$d(\log \alpha)/d \log(\{L\}_t)$			$\{L\}_t^{max}$ (m
		$\{L\}_t = 10$ mg l^{-1}	$\{L\}_t = 50$ mg l^{-1}	$\{L\}_t = \{L\}_t^{max}$[a]	
21	S_l	0.24	1.86	2.76	87
22	S_l	0.32	1.48	2.43	74
11	S_r	0.70	1.20	1.52	63
10	S_m	0.56	1.23	1.8	130
50a(1)	S_m	0.46	0.95	1.17	94
50a(2)	S_m	0.85	1.45	1.63	90
24	S_m-T	0.48	1.40	3.40	100
41a	T	0.85	1.50	—	42
F1	F	0.08	0.70	—	50
F2	F	0.24	0.78	0.82	68
F3	F	0.49	0.75	1.35	97
F4	F	0.57	1.03	1.52	135
S0	So	0.21	0.79	1.16	150
S1	So	0.53	1.28	1.41	128
S2	So	0.30	1.10	1.33	180

[a]The values of the slopes corresponding to the maximum value of $\{L\}_t = \{L\}_t^{max}$ used in the titration.

where the protons liberated by the complexation of copper(II) are omitted. The method used here does not allow these $Cu(L_n)$ complexes and the "classical" CuL_n complexes to be distinguished. However, it must be emphasized that the aggregation of humic substances has been postulated by some authors [23, 24]. Also fluorescence measurements [16] seem to support the suggestion that aggregation phenomena become important (or measurable by fluorescence parameters) for $\{L\}_t > 100$ mg l^{-1}.

If reaction (3) is valid and if $K'^{Cu}_{(n)}$ is taken, as a first approximation, as $K'^{Cu}_{(n)} \approx \beta'_1$, then, for $n = 2$:

$$\beta'_2 = [Cu(L_2)]/[Cu]\,[L]^2 = [Cu(L_2)]\,[L_2]/[Cu]\,[L_2]\,[L]^2 = K'^{Cu}_{(2)} K'^{L}_2 = \beta'_1 K'^{L}_2 \quad (4)$$

Mean values of $\log K'^{L}_2$ were computed for each sample, (Table 3), by substituting the mean values of $\log \beta'_1$ and $\log \beta'_2$ in eqn. (4). It must be noted that the value of $\log K'^{L}_2$ obtained in this way is only a rough approximation, as the existence of $(LH_x)_2$ was not taken into account in the mass-balance equation of $\{L\}_t$ which was used for the computation of $\log \beta'_1$ and $\log \beta'_2$. However, a more rigorous computation is of little use because of the increased uncertainties on the parameters obtained (see below). By using mean values of 4.7 for $\log K'^{L}_2$ (Table 3) and 1580 for M_{eq}, for fresh waters, one may compute that 23%, 46% and 63% of L would be dimerized, for $\{L\}_t = 7.5$ mg l^{-1}, 30 mg l^{-1} and 90 mg l^{-1}, respectively.

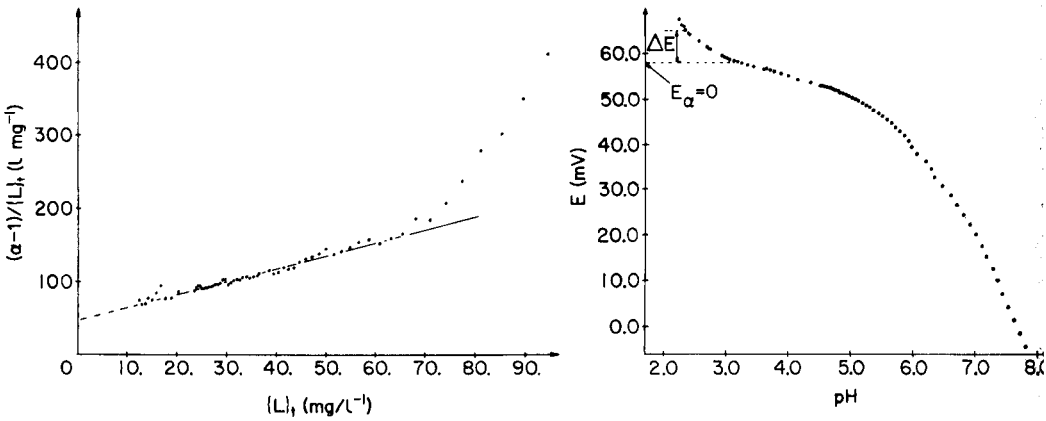

Fig. 3. Graphical method for the determination of β'_1 and β'_2 from T_L titration. Formation of CuL_n ($n > 2$) complexes for $\{L\}_t > 70$ mg l^{-1}. Sample 24, pH 6, $[Cu]_t = 3 \times 10^{-6}$ M, 0.1 M $NaClO_4$.

Fig. 4. Change in the potential E of the copper-selective electrode with pH. Sample 24, $\{L\}_t = 54$ mg l^{-1}, $[Cu]_t = 4.7 \times 10^{-6}$ M, 0.1 M $NaClO_4$. $E_{\alpha=0}$ is the potential of the electrode in a solution containing $[Cu]_t = 4.7 \times 10^{-6}$ M, $\{L\}_t = 0$, at pH 5.

In the subsequent discussion, L—Cu—L will be used for the "classical" type of CuL_2 complex, $Cu(L_2)$ will be used for the complex formation of copper with one site of the dimerized form of L, and CuL_2 will be used as a general formula for these copper complexes.

A general computer program based on MINUIT, and on the same principle as that described above, was written to include the possibility of adjusting the experimental curves by taking into account other reactions than those of the program described under Experimental. The two following combinations of parameters were tested: (M_{eq}, β'_1, K'^{L}_2 with $\beta'_2 = \beta'_1 \cdot K'^{L}_2$), and ($M_{eq}$, β'_1, β'_2, $\beta'_{1,2}$). The latter was used in order to try to adjust that part of the T_{Cu} curve for which $r > 0.5$ (see T_{Cu} titrations above), by taking into account the formation of Cu_2L complexes. However, in both cases, because of the increased number of species considered compared to the "simple" model used initially, the errors incurred in the calculated constants become so large that it is difficult to tell whether or not they have any significance.

Influence of pH

A typical T_H titration curve is shown in Fig. 4. $E_{\alpha=0}$ represents the potential of the electrode in copper(II) solution in the absence of fulvic acid. It can be seen that a positive shift in potential, ΔE, is observed for pH less than 3. In this region the electrode responds to H^+, and, indeed, ΔE was found to be roughly proportional to pH in this domain. From Fig. 4 it can be also seen that copper(II) is very weakly complexed below pH 4, whereas the tendency to complex formation increases above pH 6.

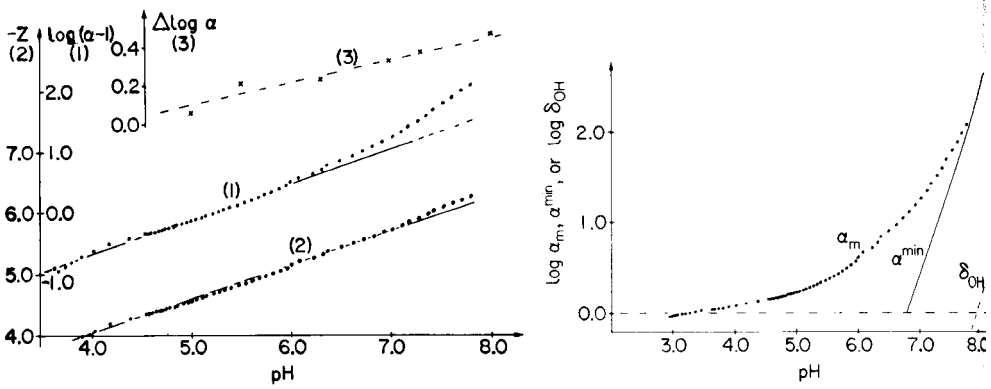

Fig. 5. Log(α − 1) (curve 1) and Z (curve 2) functions computed from results of Fig. 4. Curve 3: influence of the pH on the drift in potential with time at constant pH. $\Delta \log \alpha = \log \alpha_{fin} - \log \alpha_{in}$, where $\log \alpha_{fin}$ and $\log \alpha_{in}$ are the values of $\log \alpha$ at times t = 6 h and t = 0, respectively. Sample 50a, $\{L\}_t$ = 50 mg l^{-1}, $[Cu]_t = 8 \times 10^{-6}$ M, 0.1 M $NaClO_4$.

Fig. 6. Change in $\log \alpha_m$, $\log \alpha^{min}$ and $\log \delta_{OH}$ with pH. See text for the definition of the parameters and the values of the constants used for the computation of α^{min} and δ_{OH}. The experimental curve $\log \alpha_m = f(pH)$ was computed from the results of Fig. 4.

It was assumed earlier [14] that the influence of pH on the complexation of copper(II) is due to the reactions:

$$Cu^{2+} + LH_x \rightleftarrows CuL + xH^+ \quad (5)$$

and $$Cu^{2+} + 2LH_x \rightleftarrows L{-}Cu{-}L + 2xH^+ \quad (6)$$

However, in view of the results of the preceding section, it appears that other reactions could occur:

(a) complexation of Cu^{2+} by aggregates of LH_x. In that case, reaction (6) could also be written as

$$Cu^{2+} + (LH_x)_2 \rightleftarrows Cu{-}(L{-}LH_x) + xH^+ \quad (7)$$

(b) formation of mixed ligand complexes with OH^-:

$$Cu^{2+} + LH_x + H_2O \rightleftarrows L{-}Cu{-}OH + (1 + x)H^+ \quad (8)$$

(c) the hydrolysis of copper(II) leading to precipitation or formation of polynuclear complexes.

Hence, from the $E = f(pH)$ plots, the curves $\log(\alpha - 1) = f(pH)$ and $Z = f(pH)$ were constructed for the various samples (Fig. 5). The slope S_α of the $\log(\alpha - 1) = f(pH)$ curve at a given pH represents the global influence of pH on all the complexes present in the solution while the slope, S_Z, of the $Z = f(pH)$ function is equal to x when only reactions (5) and (6) occur (eqn. 15 in [14]). The experimental values of S_α and S_Z at about pH 6 and at pH 8 are given in Table 2.

The stability of the potential readings was also tested at various pH values, by means of "individual measurements"; the results are also plotted in Fig. 5.

For each individual measurement, a solution containing copper(II) ions (8×10^{-6} M), LH_x (50 mg l^{-1}) and 0.1 M $NaClO_4$, at a pH of approximately 4.5, was neutralized to the desired pH by adding the base gradually but fairly quickly (during 15 min). The potential vs. time was then recorded by keeping the pH constant by means of a pH-stat. Fresh solutions were used for each pH measurement. A negative drift in the potential was observed for most of the pH range. The potential stabilized only after 5—6 h. The drift in log α, $\Delta\log\alpha$, was computed from the final and initial values of the potential (Fig. 5). It can be seen that $\Delta\log\alpha$ decreases with pH. It must be pointed out that the drift in the potential was slow (ca. 0.03 mV min^{-1}) and therefore would not be observed during the brief potential—time recordings commonly involved in titrations.

Results for pH ⩽ 6. It may be seen from Table 2 that in the case of the organic matter of fresh-water samples, S_α and S_Z values were found to be similar and close to 0.5. The values of log α found by "individual measurements" (see above) were similar to those of the titration method. In the former case the variation in log α was less than 0.2 for a period of 6 h. Finally, the value of x was checked by computing the values of log β'_1 at various pH values (5.3 — 6.3) from the T_{Cu} titration for sample 50a[25], and determining the slope of the plot log $\beta'_1 = f(\text{pH})$. A value of 0.5 was found for x (see also Fig. 7). All these observations seem to indicate that reactions (6) and (8) are probably not very important for pH < 6, in the conditions used here, particularly for the concentration of LH_x. In such a case, the values of S_α and S_Z obtained from the functions $\log(\alpha - 1)$ and Z are both fixed by reactions (5) and (7) and therefore should be similar and equal to x. With this condition, an approximate value of log β'_1 (at pH 6) can be computed from the value of x and of $\alpha - 1$ at pH 5 (where reactions (6) and (8) may be considered negligible):

$$\log\beta'_1 = \log(\alpha - 1) + x - \log([LH_x]) \qquad (9)$$

where $[LH_x]$ is the free concentration (in mol l^{-1}) of LH_x at pH 5 ($[LH_x] = [L]_t - [Cu]_t(\alpha - 1)/\alpha$). Neglecting reaction (6) is not valid in all cases, and it can be seen that discrepancies between the values of log β'_1 of Tables 2 and 3 correspond usually to samples having large values of log K'^{L}_2. However, Table 2 shows that, in most cases, the values of log β'_1 obtained from eqn. (9) are in reasonable agreement with those obtained from T_{Cu} and T_L titrations (Table 3). The differences obtained in log β'_1 by the three methods give an order of magnitude of the influence of the technique used on the final values of the constants.

The foregoing observations seem to confirm that for fresh-water samples, the complex-formation parameters measured for pH < 6 may be considered as fairly reliable. This is further supported by the fact that in this pH range the results observed by various authors are in fairly good agreement. In the case of other types of organic matter (particularly those produced by decomposition of leaves) the values of S_α and S_Z differ significantly, and

consequently the values of log β'_1 computed from eqn. (9) are not in very good agreement with those obtained from T_{Cu} and T_L titrations. Moreover, it must be noted that the latter type of organic matter seemed to adsorb on the electrode surface and that there was a correlation between these adsorption effects and the importance of the discrepancy between the results of T_H and T_L or T_{Cu} titrations.

Results for pH > 6. If the complexing groups of LH_x are assumed to be mainly carboxylic acid groups which dissociate fully at pH > 5.5 and phenolic groups which are undissociated below pH 9, then it is reasonable to expect x to remain relatively constant over the pH range 5.5—8. Then the increase in S_α with pH can be explained only by taking into account reaction (6) or (8) or the formation of a more strongly hydrolysed product of copper(II).

The rough constancy of x obtained from the Z function (Table 2) up to pH 8 seems to favour the predominance of reaction (6). However, the slow change in potential with time observed in the "individual measurements" cannot be explained by these reactions. Previous reports [14] also show that no hysteresis is observed for back (acid) titration when compared with direct (base) titration, if the whole titration is carried out within a few hours. But if the back-titration with acid is carried out after the base-titrated solution has been left at pH 8 overnight (ca. 15 h), then the solutions exhibit greater complexing properties. Considering that these phenomena are observed at pH values above 6—6.5 and that the profile of the log $\alpha = f(\text{pH})$ curve, as well as the degree of shift in the potential—time curve, depend on the way in which the solution is neutralized, it seems probable that slow hydrolysis of copper(II) plays a role in the global complexation of copper at pH > 6.

Figure 6 shows a comparison of the overall degree of complexation, α_m, measured experimentally, with the hydrolysis parameters. Because of the lack of available stability constants for polynuclear complexes, only the mononuclear hydroxo complexes of copper(II) were considered for δ_{OH} calculations, although the existence of polynuclear complexes cannot be ruled out, as significant amounts of these may be formed even at low concentrations of copper(II) [26]. The values of β_i^{OH} (i = 1—4) cited in the literature are themselves relatively uncertain [22]. However, the most probable values of these constants at 25°C [21, 22] were chosen and corrected [22] for 0.1 M ionic strength (log β_1^{OH} = 5.51; log β_2^{OH} = 11.92; log β_3^{OH} = 13.72; log β_4^{OH} = 16.2). It is apparent from Fig. 6 that under the present conditions: $\delta_{OH} \ll \alpha_m$ for pH < 9. Figure 6 also shows the α^{min} curve, where α^{min} is the minimum degree of complexation required to prevent the formation of a precipitate of the less-soluble hydrolysed compounds of copper(II), e.g. CuO; α^{min} was computed from $\alpha^{min} = [Cu]_t[OH^-]^2/K_{So}^{CuO}$ using experimental values of copper(II) concentration ($[Cu]_t = 5 \times 10^{-6}$ M) and log $K_{So}^{CuO} = -19.66$ (μ = 0.1; T = 25°C [21, 22]). It must be mentioned that the influence of the small particle size of the precipitate on the value of K_{So}^{CuO} [22] could not be taken into account as nothing is known about the influence of organic matter on the surface tension of these particles.

Although it was seen above that δ_{OH} is not an important factor, this might no longer be true in the case of precipitation reactions. Indeed, in the present case, for pH $\geqslant$ 7.5, α_m is not much larger than α^{min}. The exact nature of the hydrolysed species formed in such reactions is unknown, although some information was obtained from the solutions used for "individual measurements". After being left to stand for 6 h, these solutions were filtered through Amicon PM10 membranes. The results showed that neither copper nor the organic ligand were retained by the membrane. Thus the molecular weight of the hydrolysed species formed during the first 6 h at pH $\leqslant$ 8 is less than 10,000. Hence these substances are either very small nuclei of copper hydroxide or, more likely, mixed ligand complexes with hydroxide and L. The particular case of the formation of L—Cu—OH will be discussed in detail in a later paper [13]. It will be shown that such a complex could play an important role in the pH range 6—8.

In conclusion, it is not possible to obtain a better insight into the relative importance of reactions (6) and (8) but it is likely that reaction (8) will predominate for natural waters where $\{L\}_t$ is relatively small. Moreover, it is apparent from Fig. 6 that correct interpretation of the complex-formation data is made very difficult for pH > 8, because of possible precipitation reactions. It must be noted also that this limiting pH value of 8 is generally valid when $\{L\}_t \geqslant 50$ mg l^{-1}, but it decreases when $\{L\}_t$ decreases.

Competition between copper(II) and calcium(II) for organic ligands

In order to predict the complexation of copper(II) by organic ligands in natural waters, the competitive nature of these two metal ions for the organic ligands must be known. As fulvic acids have been reported [27] to poison calcium-selective electrodes, the competitive reaction between copper(II) and calcium(II) was studied here by means of the copper(II)-selective electrode. For this purpose, a solution containing copper(II) ($[Cu]_t = 10^{-5}$ M) and L ($\{L\}_T = 35$ mg l^{-1}) was titrated with calcium(II) solution and the corresponding potentials were recorded after each addition. These measurements were repeated for various pH values below 6.5. Sample 50a which contained low initial amounts of Ca^{2+} (ca. 2×10^{-4} M) was used.

The high $[Cu]_T/[L]_t$ ratio chosen for these measurements made it possible to neglect the formation of CuL_2. Under these conditions the following mass-balance equations may be written:

$$[L]_t = [LH_x] + [CuL] + [CaL] \tag{10}$$

$$[Ca]_t = [Ca^{2+}] + [CaL] \tag{11}$$

The stability constants of L with copper(II) and calcium ions at constant pH are

$$\beta'_1 = \beta_1^L/[H^+]^x = [CuL]/([Cu^{2+}]\ [LH_x]) \tag{12}$$

$$\beta'_{Ca} = \beta_{Ca}/[H^+]^y = [CaLH_{x-y}]/([Ca^{2+}]\ [LH_x]) \tag{13}$$

where y is the number of protons liberated by the complexation of calcium ions. Since $[Ca]_t$ is generally much greater than $[L]_t$, $[Ca]_t \approx [Ca^{2+}]$. Combining these equations gives

$$\left\{\frac{[L]_t}{\alpha - 1} - \frac{[Cu]_t}{\alpha}\right\} = \frac{1}{\beta'_1} + \frac{\beta'_{Ca}}{\beta'_1} \cdot [Ca]_t \qquad (14)$$

Figure 7 shows the plots of the left-hand side of eqn. (14) against $[Ca]_t$ at pH 5.0, 5.5, 6.0 and 6.5. Log β'_{Ca} obtained at these pH values was found to be 2.44, 2.39, 2.39 and 2.39, respectively; log β'_1 was 4.57, 4.83, 5.12 and 5.46, respectively. The latter values agree quite well with those given in Tables 1 and 2. A value of 0.6 for x was obtained by plotting these values against pH, which is also in good agreement with that given in Table 2.

The fact that log β'_{Ca} was found to be independent of pH probably indicates that calcium ions are bound to fulvic acid through carboxylate groups which are almost fully deprotonated in the pH range studied and not through phenolic groups. The mean value of log β'_{Ca} is also in good agreement with those obtained for outer-sphere complexes of calcium(II) with carboxylate groups.

In practice, Fig. 7 shows that for pH > 6 and $[Ca]_t < 5 \times 10^{-3}$ M (i.e., the conditions for most fresh waters) the competitive effect of calcium(II) is negligible.

COMPARISON OF THE COMPLEX-FORMATION PROPERTIES OF DIFFERENT WATER SAMPLES

The water samples studied may be divided into the following categories: type F, which are aqueous solutions formed by in vitro decomposition of leaves under controlled conditions [16]; type T, which are interstitial waters of peats produced by leaching peat bog with rain water; type So, which are water extracts of soils; type S, which are surface waters from marshes (S_m), ponds (S_p), rivers (S_r) and lakes (S_l).

With samples F and to a lesser extent with samples T and So, the electrode response was found to be slightly affected by some ill-controlled phenomena probably related to some kind of adsorption process at the electrode surface. These have to be considered in making a comparison of data. It must also be noted that the So extracts initially had fairly large amounts of aluminium, iron and silicon ions, which could affect the value of the complex-formation parameters, in spite of the sample being purified in the preliminary ultrafiltration step.

However, Tables 1 and 2 show that, in most cases, the values of the complex-formation parameters are similar, within experimental error, for samples belonging to a given group. From the values of M_{eq} these groups may be classified as: S $\simeq$ So > T $\simeq$ F. A comparison of the M_{eq} values corresponding to these groups with earlier results [14, 17] shows that the order of magnitude of M_{eq} is similar to the molecular weight M_w of the organic matter for the S and So groups but is much lower than the M_w for T and F. This tends to suggest that the latter compounds may fix much larger numbers of copper(II) ions on one molecule than the organic matter of the S and So groups.

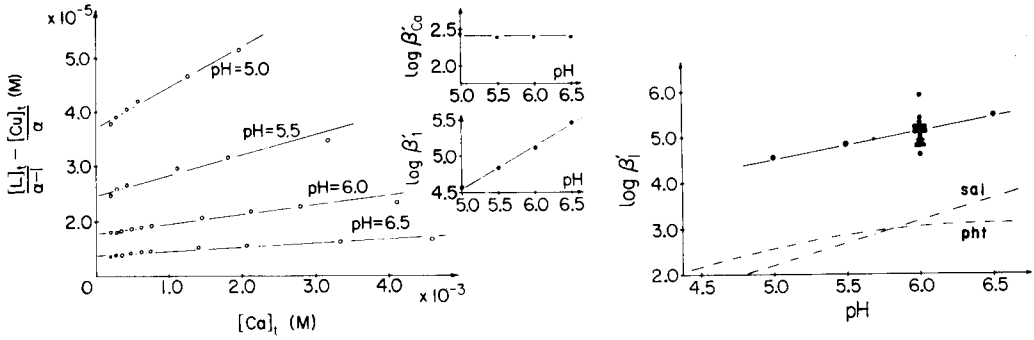

Fig. 7. Influence of $[Ca^{2+}]$ on the complexation of Cu^{2+} by fulvic acid. Sample 50a filtered on 0.2-μm membrane. The pH values are indicated on each curve. $\{L\}_t$ = 35 mg l^{-1}, $[Cu]_t = 10^{-5}$ M, 0.1 M $NaClO_4$. A value of M_{eq} = 2000 was used for the computation of $[L]_t$. The influence of pH on the values of β'_{Ca} and β'_1 computed from the straight lines, is shown in the insets.

Fig. 8. Change in the conditional stability constants of 1:1 copper salicylate (sal) and copper phthalate (pht) complexes with pH. The points are the values reported for β'_1 in this paper (Table 3) for all the surface and soil water samples. The dispersion of most of the points, near pH 6, is due only to the requirements of drawing: except for pH 5.0, 5.5 and 6.5, all the measurements were done at pH 6.0. The slope of the straight line passing through the points is equal to the mean value of x (= 0.53) found for all the surface and soil water samples, from S_α measurements at pH 6.

The values of log β'_1 decrease in the order: $S_r \approx S_m \approx T \geqslant S_1 \approx So > F$. In fact, considering the value of ϵ_1, it is difficult to say whether the values of log β'_1 for So are significantly different from those of S. Similarly, the values of log β'_1 for the lakes (samples 21, 22) seems to be slightly lower than those for other S samples and rather close to those of So samples. If similar results were observed for a number of lakes, this could indicate that a relatively important part of the organic matter comes from the leaching of the surrounding land by rain water. All other S samples (even those from rivers in Zaire) had a relatively high content of dissolved organic matter (TOC > 4 mg l^{-1}) and contained a large proportion of plant debris. However, the low values of log β'_1 for the F samples (except for sample F4) as well as the large difference in molecular weights between F and S samples [17] indicates that, in most cases, an important degradation process is needed to transform F- into S-type substances.

A mean value of S_α = 0.5 was observed for most of the S, So and T samples. These results confirm the earlier findings [14] as well as the discussion given in that paper on the nature of the complexing groups. The values of log β'_1 found for the Cu—fulvic acid complexes are higher than those for either copper salicylate or copper phthalate at pH 6 (Fig. 8), indicating that the presence of such groups alone does not explain satisfactorily the complexing properties of fulvic acids [28].

In conclusion, the results show that the complex-formation parameters are essentially independent of source for the same type of water, particularly for surface waters. Hence, the discrepancies sometimes observed in the values quoted by different authors are, at least partly, due to the methods of measurement. The results obtained by different authors will be compared in a further paper, in order to ascertain the most important factors governing the reactions of copper(II) with fulvic substances in the pH range 6—9.

This work is part of project 2587-076 of the Swiss National Foundation, the support of which is gratefully acknowledged. The authors thank M. P. Vuagnat for advice on the computation of statistical errors, J. P. Cerez and F. Bujard for assembling the automatic titration apparatus, Dr. H. Häni and Dr. P. Blaser for providing soils and leaf extracts, J. Mallevialle for assistance with concentration of waters, and M. Auriel for providing concentrated water samples of rivers in Zaïre (Nos. 1—4).

REFERENCES

1 M. Whitfield and D. Turner, in E. A. Jenne (Ed.), Chemical Modeling in Aqueous Systems, ACS Series No. 93 (1979), Ch. 29, p. 657.
2 P. Baccini and U. Suter, Schw. Z. Hydrol., in press.
3 M. Schnitzer and L. Skinner, Soil Sci., 102 (1966) 361.
4 M. Schnitzer and L. Skinner, Soil Sci., 103 (1967) 247.
5 M. Schnitzer and E. H. Hansen, Soil Sci., 109 (1970) 333.
6 A. M. Elgala, A. H. El-Damaly and T. Abdel-Alif, Z. Pflanzern. Bodenk., 3 (1976) 293.
7 F. J. Stevenson, Soil Sci., 123 (1977) 10.
8 F. J. Stevenson, S. A. Krastanov and M. S. Ardakani, Geoderma, 9 (1973) 129.
9 V. Cheam and D. S. Gamble, Can. J. Soil Sci., 54 (1974) 413.
10 R. F. C. Mantoura and J. P. Riley, Anal. Chim. Acta, 78 (1975) 193.
11 R. F. C. Mantoura, A. Dickson and J. P. Riley, Estuarine and Coastal Marine Science, 6 (1978) 387.
12 C. M. G. van den Berg and J. R. Kramer, Anal. Chim. Acta, 106 (1979) 113.
13 J. Buffle, Anal. Chim. Acta, submitted.
14 J. Buffle, F. L. Greter and W. Haerdi, Anal. Chem., 49 (1977) 216.
15 J. Buffle, P. Deladoey and W. Haerdi, Application d'un système de titration automatique à la mesure de la complexation du cuivre par les substances fulviques et humiques et interprétation des résultats, Report 2.587-076, Swiss National Foundation (1978).
16 J. Buffle, P. Deladoey and W. Haerdi, Etude comparative des propriétés physico-chimiques de différents types de matières organiques naturelles et de leurs complexes avec Cu(II), Report 2.587-076, Swiss National Foundation (1978).
17 J. Buffle, P. Deladoey and W. Haerdi, Anal. Chim. Acta, 101 (1978) 339.
18 F. James and M. Roos, CERN/DD Internal Report 75/20.
19 J. A. Neldes and R. Mead, Comput. J., 7 (1965) 308.
20 R. Fletcher, Comput. J., 13 (1970) 317.
21 R. M. Smith and A. E. Martell, Critical Stability Constants, Vol. 4, Plenum, New York, 1976.
22 C. F. Baes and R. E. Mesmer, Hydrolysis of Cations, J. Wiley, New York, 1976.
23 R. L. Wershaw and D. J. Pinckney, J. Res. U.S. Geol. Surv., 1 (6) (1973) 701.
24 M. Schnitzer and S. U. Kahn, Humic Substances in the Environment, M. Dekker, New York, 1972.
25 F. L. Greter, Thèse, Université de Genève (1978).
26 D. D. Perrin, J. Chem. Soc., (1960) 3189.
27 E. S. Kobus, Desalination, 12 (1973) 333.
28 J. Buffle, Techniques et Sciences Municipales; 3—10 (Janvier, 1977).

Analytica Chimica Acta, 116 (1980) 275—287

A CONTINUOUS-FLOW, ISOTOPE-DILUTION METHOD FOR STUDIES OF ADSORPTION BEHAVIOUR OF METAL IONS

E. HARTMANN

Department of Chemistry, University of Birmingham, P.O. Box 363, Birmingham B15 2TT (Gt. Britain)

K. RANDLE*

Birmingham Radiation Centre, University of Birmingham, P.O. Box 363, Birmingham B15 2TT (Gt. Britain)

(Received 3rd December 1979)

SUMMARY

A method is described for studying adsorption from liquids based on a continuous-flow system. The major innovation is the use of radioisotope dilution to determine the change in the eluate concentration. The metal under study is radioactively labelled and the activity of the eluate leaving the cell is monitored with a well-shielded NaI(Tl) detector. From the known flow rate and initial activity, the activity of the eluate can be related to the adsorbate concentration. The counts accumulated over a set period of time are automatically stored in successive memory locations of a computer. These data are also displayed, allowing continuous monitoring of the developing wash-in curve as well as on-line data manipulation. Modifications to the ultrafiltration cell used and to the method of pumping solutions through the cell are described. The method is worked out for the mercury—humic acid system via ^{203}Hg; applications to other systems are indicated.

Continuous-flow techniques for studying adsorption mechanisms have been known for some time. The continuous-flow stirred-cell method was first introduced by Blatt et al. [1] to study binding of calcium ions and methyl orange to human serum albumin. The method is based on the dia-filtration technique in which an adsorbate solution of known fixed concentration is introduced under nitrogen pressure into a continuously-stirred ultrafiltration cell. A suspension or solution of the adsorbent is held in the cell by an anisotropic ultrafiltration membrane, which is permeable to the adsorbate but not to the adsorbent. Several known volumes of the eluate are collected by using a fraction collector. The effluent samples are subsequently analyzed for the element or compound of interest by an appropriate analytical technique. The eluate concentration can be predicted as a function of cumulative filtration volume — or time, if the flow rate is known — by performing a differential material balance around the cell [1].

Although this method has been applied in studies of the binding behaviours of steroid to protein [2], phenoltetrabromosulphonphthalein (sodium salt) to human serum albumin [3], and organic chemicals to soils and soil colloid

systems [4—8], so far there has been only one report on the possibility of studying metal ion interactions with solid organic matter by this technique [9].

In this paper, the practicability of combining isotope dilution and the continuous-flow stirred-cell method is explored, and an on-line analysis procedure for studying metal ion—soil organic matter binding mechanisms is described. The basic principle of this method is that the count rate of a radioactively-labelled metal ion solution is directly proportional to its metal ion concentration. Therefore measuring the activity of a small volume of liquid leaving the ultrafiltration cell and comparing it with the activity of the reservoir solution containing a known concentration of the metal ion, gives a direct measure of the metal ion concentration in the effluent. The major practical problem involved is the shielding of the γ-ray detector from all activity other than that arising from a very short section of the exit tube viewed by the detector.

Theory

A general mathematical representation for the continuous-flow stirred-cell method was presented by Blatt et al. [1], relating eluate concentration to eluate volume. Their approach included the treatment of parameters that are inherent in the method such as (a) variations in the cell volume, (b) binding or rejection of adsorbate by the membrane, and (c) fluctuations in the void volume. In contrast, Ryan and Hanna [2] used a more empirical approach in which the experimental conditions were adjusted either to determine the effect of varying these parameters or to eliminate their influence altogether. Burchill and Hayes [7] adopted a similar procedure and derived a set of equations to describe the adsorption behaviour in the cell. These equations were derived from a consideration of the mass balance around the cell, the fundamental mass-balance equation being

$$C_{max}\,dv - C_i dv = dn_i \tag{1}$$

where C_{max} is the adsorbate concentration of the reservoir, dv is the eluate volume increment, C_i is the eluate concentration (which is also equal to the concentration within the cell), and n_i is the total amount of solute i bound in the cell, both adsorbed (n_i^{σ}) and in solution (VC_i).

From eqn. (1), the following two equations can be derived:

$$C_i = C_{max}\,(1 - \exp\,(-v_i/V)) \tag{2}$$

$$C_i = C_{max}\,\exp\,(-v_i/V) \tag{3}$$

where V is the cell volume and v_i is the eluate volume. Equation (2) represents the theoretical "wash-in" dilution curve obtained with no adsorbent in the cell. Equation (3) represents the equivalent "wash-out" curve obtained when distilled water (or some other desorbent) replaces the eluate after C_i has reached C_{max}, i.e. the adsorbate concentration in the cell equals the reservoir

concentration. These two curves, together with the curves obtained when adsorbent is present in the cell, are presented in Fig. 1.

In the case of an adsorbent present in the cell, the adsorption equation derived takes the form:

$$n_i^{\sigma} = C_{max} v_i - C_i V - \int_0^{v_i} C_i dv \quad (4)$$

The value of the integral is obtained from the area under the wash curves for the appropriate C_i and v_i. The plot of n_i^{σ} against C_i represents the adsorption isotherm for the particular adsorbent under study. The form of eqn. (4) implies that it will be strictly applicable only to small volume increments of eluate entering the cell. Such small increments also permit higher definition of the wash curves and consequently increased accuracy of the adsorption isotherms.

EXPERIMENTAL

Isolation of humic acid materials

An air-dried histosol (500 g, 80% organic) was first saturated with hydrogen ion by rolling for 1 h with 1 l of 1.0 M hydrochloric acid, and then filtered on a Buchner funnel. This procedure was repeated twice. The retained soil was washed with deionised water until chloride-free, and then the soil residue was air-dried.

Humic acid (HA) was isolated from the soil by extraction for 6 h with 1 l of 0.5 M sodium hydroxide under a nitrogen atmosphere, and then centrifuged at 10,000 g for 20 min. The supernatant liquid was adjusted to pH 1.0 with dilute hydrochloric acid; then the precipitate formed was separated

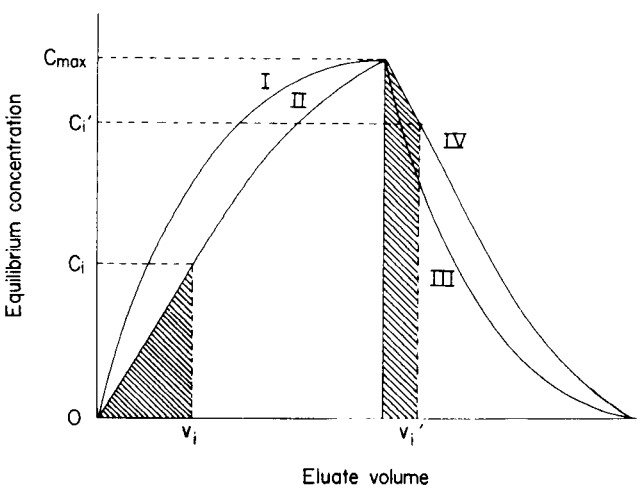

Fig. 1. Sample wash-in (I and II) and wash-out (III and IV) curves in the absence (I and III) and presence (II and IV) of adsorbent.

by centrifugation, dialysed against deionised water until chloride-free, and freeze-dried.

A stock solution (1000 μg ml^{-1}) was prepared from the freeze-dried HA in deionised water.

Radioisotopes and preparation of labelled metal ion solutions

Solutions of the appropriate radioisotopes were obtained from the Radiochemical Centre (Amersham, England). Almost all the work described here involved the use of ^{203}Hg obtained in the form of mercury(II) chloride in hydrochloric acid solution at pH 1—2. This isotope decays by β^--emission, followed by the emission of a single γ-ray of 279-keV energy. The half-life is 46.9 days.

A standard solution of the metal under consideration is required. The compound chosen should be such that the metal ion will be rapidly and completely exchanged with the radioactive metal isotope used, and if possible contain the same anion. The metal ion solution was mixed with a radioisotope of known specific activity, and then the total metal ion concentration adjusted to the required value. It was found that about 1 mCi of activity in a total volume of 30 ml was sufficient for the measurements. The highest specific activity of ^{203}Hg available was ca. 1.7 mCi mg^{-1} Hg, and the total concentration of mercury was adjusted to 25 μg ml^{-1} with mercury(II) chloride from the stock standard (100 μg Hg ml^{-1}). Obviously, in some cases the specific activity of an isotope determined the lowest concentration of metal ion that could be used. ^{203}Hg, however, has one of the lowest specific activities available, and it is expected that this problem would not be encountered with other metal isotopes.

Equipment

The complete experimental arrangement of the cell and associated equipment is shown in Fig. 2.

Cell assembly. A detailed diagram of the ultrafiltration cell used is shown in Fig. 3. The tips of the peristaltic tubing were reinforced with stainless steel hypodermic needles to prevent the walls from collapsing when connected to the teflon tubing. The cell volume, calculated from the difference in weights between the cell empty and filled to capacity with deionised water, was found to be about 8.2 ml.

Three types of ultrafilters were used: Amicon membranes XM-50 and PM-10 (Amicon Ltd., Woking, Surrey) with molecular weight cut-off at ca. 50,000 and 10,000, respectively, and Millipore Pellicon PSAC-10 ultrafilter (Millipore Corporation, Bedford, Massachusetts) with a nominal molecular weight cut-off at ca. 1000.

Proportionating pump. The labelled metal ion solution was introduced into the ultrafiltration cell by a Technicon AutoAnalyzer 2-speed proportionating pump (Technicon Instruments Corp.) operated at the normal speed. Solvaflex and Accurate Flow peristaltic tubing with designated flow rates of 0.60 ml min^{-1} and 0.25 ml min^{-1} were used.

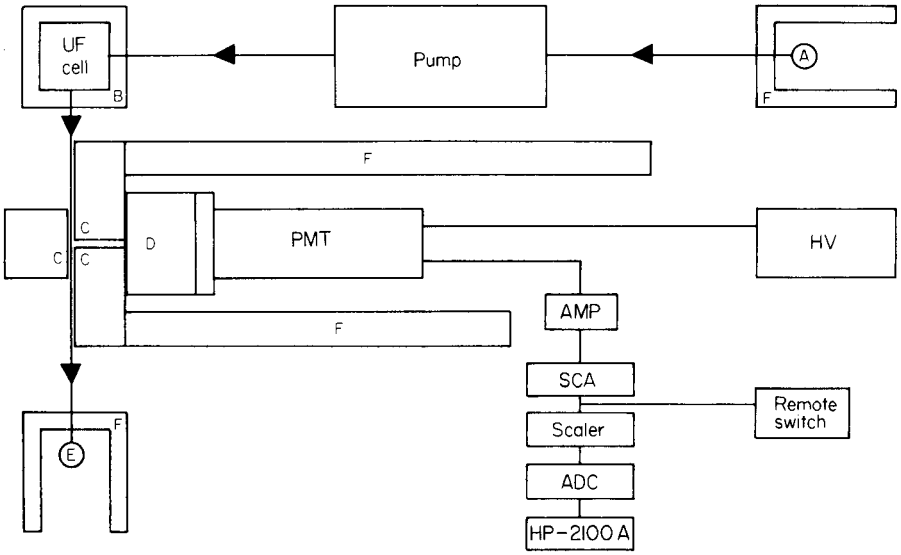

Fig. 2. Schematic representation of ultrafiltration cell and associated equipment. A, Radioactive metal ion reservoir; B, magnetic stirrer; C, collimating lead block; D, 7.6 × 7.6-cm NaI (Tl) detector; E, waste effluent reservoir; F, 10-cm lead shielding. The associated electronics are described in the text.

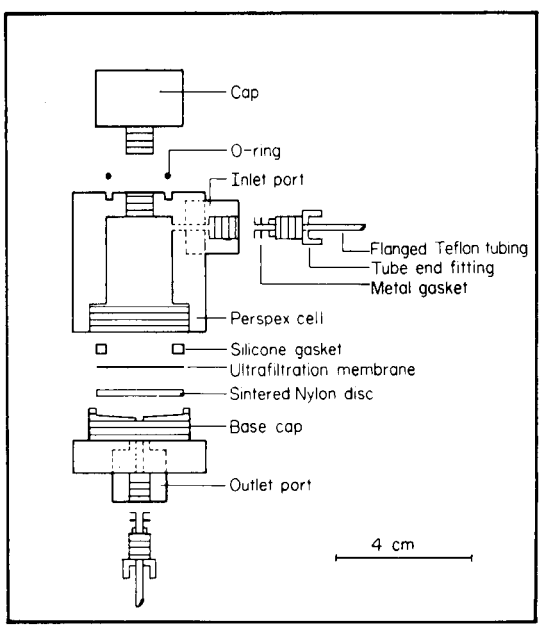

Fig. 3. Detailed diagram of the ultrafiltration cell.

Shielding material and collimator. It was necessary to construct a collimator system as illustrated in Fig. 4. It consisted of a lead block (10-cm thick) in which a slit, SL (5-mm wide), was cut through the face. The output tubing from the cell rested in a 3-mm groove, GR, aligned centrally to the detector; the latter was thus shielded from the rest of output tubing by 10 cm of lead.

There were still, however, heavy demands on shielding particularly from the reservoir which at the start of the experiment contained the maximum activity (ca. 1.0 mCi), and from the waste effluent reservoir which contained the majority of activity at the final stages of the experiment. Shielding requirements for these reservoirs can be considerably reduced by placing them some distance away from the detector region. However, during the course of the experiment, the ultrafiltration cell acquired a significant proportion of the total initial activity and therefore had to be adequately shielded because it had to be as close as possible to the detector if "void" volume was to be minimised. In practice, it was found that 15—18 cm of lead provided sufficient shielding against the range of γ-ray energies used (279—662 keV).

The detector was housed inside a counting "castle" which consisted of two layers of interlocking, 5-cm thick lead bricks (Graviner Manufacturing Co. Ltd., Gosport, Hants.) giving a total thickness of 10 cm, and was roofed with 5-cm thick lead blocks. The two reservoirs were completely surrounded by 5 cm of lead, increased to 15 cm on those sides closest to the detector. Entrance and exit tubings of the cell were channelled through V-shaped lead bricks as far as possible.

Attention had also to be paid to shielding the detector from that portion of exit tubing extending from the cell to the collimating slit. Experiments carried out with ^{137}Cs (emitting 662-keV γ-rays) emphasised the effects of the activity in this portion of tubing on the count rate. With ^{203}Hg, however, 10 cm of lead appeared to provide adequate shielding.

Shielding efficiency was checked by placing solutions containing the maximum reservoir activity first at the reservoir, then at the other relevant positions and measuring a background count for each case. These were subsequently compared with a background count measured without activity

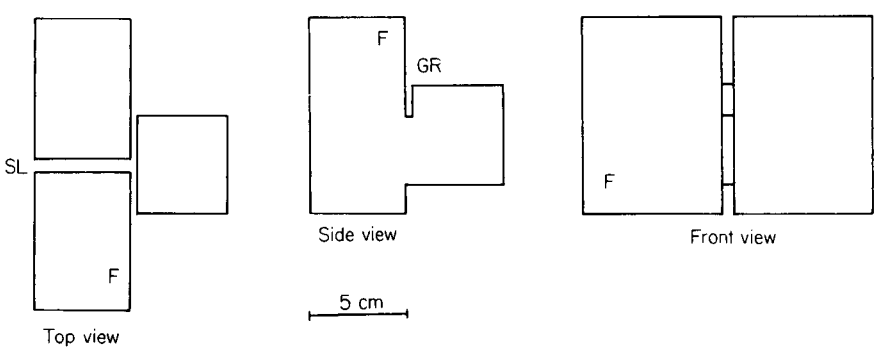

Fig. 4. Collimating lead block.

present in the vicinity of the detector. Shielding was assumed adequate only if the counts were the same or within statistical fluctuations of the general background count.

Counting equipment. Gamma-rays emitted by the ^{203}Hg isotope were counted with an NE12AX12/DM1-3, 7.6 × 7.6-cm NaI(Tl) detector (Nuclear Enterprises Ltd.) with the associated electronics shown in Fig. 2. The PMT was operated at 850 V using an ORTEC 456 HV source. A preamplifier was incorporated in the base of the PMT and is not shown separately. Pulses from the preamplifier were fed to an ORTEC 472A Spectroscopy amplifier (AMP). Shaped and amplified signals then passed to an NE4602 analyser (SCA; Nuclear Enterprises Ltd.) set to discriminate against all pulses except those in a narrow window with amplitudes corresponding to the γ-rays from ^{203}Hg. This produced a low background count and high signal-to-noise ratio. Logic output pulses from the analyser were fed into a scaler where they were counted. It was possible to accumulate a scaler count for a set period of time, T_a, ranging from 1 μs to 999999 s. The accumulated count was stored via a Hewlett-Packard 5416B analog/digital converter (ADC) into a given memory location (channel number) of a Hewlett-Packard 2100A computer. The scaler was then automatically reset to zero, the computer memory location was advanced by one, and the whole counting procedure was repeated. Thus the computer was essentially behaving as a multiscaler, in which counts accumulated over a given time period, T_a, were in successive memory locations. Each stored count was displayed as a single dot on a CRT and is referred to as a "record". The vertical position of each dot corresponded to the total count accumulated, and the horizontal position represented the total time elapsed from the start of counting (channel number × T_a). The computer in use was capable of storing up to 6144 records.

Procedure

Initially, it was necessary to determine the count rate resulting from the radioactive solution contained in reservoir A. This was achieved by injecting an aliquot portion of the solution into a suitable length of clear acrylic tubing identical to that used for the output line, and sealing the ends. The tube was inserted in the groove, GR, of the collimating block facing the detector and repeatedly counted for a fixed time period, T_a. T_a was chosen such that when multiplied by the flow rate, the resultant volume would be sufficiently small to allow very close monitoring of eluate concentrations. A value for T_a of 8 s was chosen initially, and increased to 40 s later.

The reservoir liquid was counted for 100 records (each T_a seconds long) and the mean of these represented the reservoir count (CTMAX). A background count (BACKGD) was measured similarly, the radioactive liquid being replaced by deionised water in a fresh length of tubing.

The cell, containing a suitable ultrafiltration membrane and a star-head magnetic follower, was filled to capacity with humic acid stock solution by pumping the slurry via the inlet port. Air bubbles were carefully removed

and the lid securely fitted. This method of filling was found to minimise entrainment of air bubbles within the cell. After thoroughly washing the peristaltic tubing by pumping deionised water through at the higher pump speed, the end was inserted in reservoir A. Radioactive liquid was drawn to the flanged tip and the pump switched off. The tube end was securely fitted in place and the cell assembly placed in an inverted position inside a polythene box (5-cm deep) to protect the equipment against any leakage that might occur.

Keeping the cell in the inverted position allows a maximum residence time for metal cations inside the cell, thus increasing the contact between metal and reactive humic acid sites. This arrangement also minimises the possibility of humic acid depositing on the membrane, hence ensuring a steady flow rate across the cell.

The magnetic stirrer and pump were then switched on. Counting was initiated via a remote-control switch as soon as the eluate solution was in front of the collimator slit. The accumulated count, T_a seconds after start, was stored in the initial memory location and represented record one. After automatic clearing and resetting of scaler and timer, and incrementing the memory location by one, the counting sequence was repeated as more liquid passed the detector. Since each record was displayed on a CRT, it was possible to view the resultant curve as it progressed. Experiments were terminated when count rates reached a plateau value corresponding to CTMAX, or within statistical deviations of that value.

Measurement of flow rate

Since flow rate has a direct control on the magnitude of eluate volume leaving the cell, it was necessary to determine this from a set of blank experiments carried out under conditions identical to those previously discussed but without the radioactive tracer. The cell was filled with humic acid suspension, and then a mercury solution (25 μg ml^{-1}, acidified with 300 μl of concentrated hydrochloric acid) was pumped through via the inlet port. Thirty eluate fractions were collected every 3 min into accurately weighed polythene vials. After 90 min, the vials were weighed and flow rates calculated from the difference in weights. This procedure was repeated for the Amicon PM-10, XM-50 and Pellicon PSAC-10 membranes. Flow rate profiles for the three membranes are shown in Fig. 5.

It is evident that, initially, flow rates of the Amicon membranes were far from constant. Pellicon PSAC-10 membranes, however, showed very steady flow rates throughout the duration of the experiment; these also matched the flow rates specified by the manufacturer for peristaltic tubings employed. Consequently, these membranes were preferred for all later experiments. Although the aberrant behaviour reported here may not be typical, the flow rates should be carefully measured when a fresh batch of membranes is used.

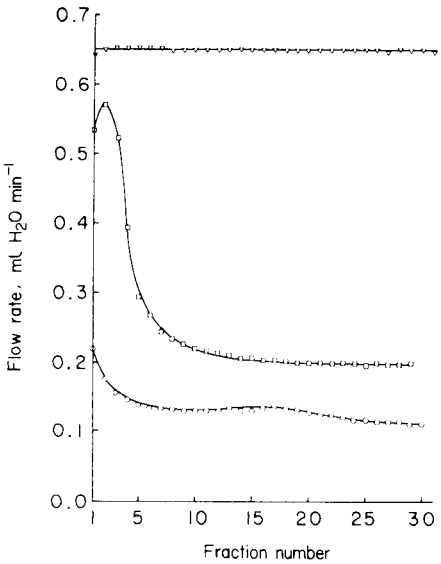

Fig. 5. Variation in flow rate through different ultrafilters. (▽) Pellicon PSAC 2510; (□) Amicon XM-50; (○) Amicon PM-10.

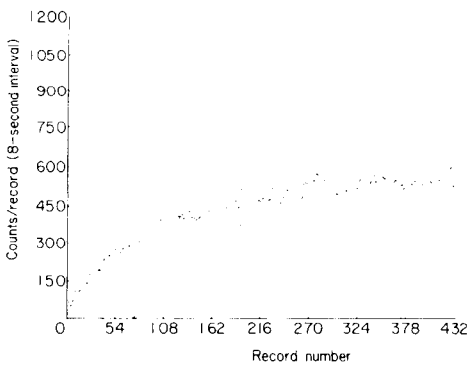

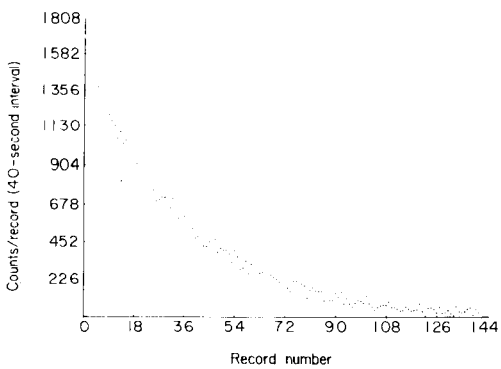

Fig. 6. Typical wash-in curve obtained with ^{203}Hg.

Fig. 7. Typical wash-out curve obtained with ^{137}Cs.

RESULTS AND DISCUSSION

A wash-in curve for ^{203}Hg and a wash-out curve for ^{137}Cs are shown in Figs. 6 and 7, respectively. These curves have been corrected for the background count for each record.

The primary aim was to establish whether the technique was capable of producing results similar to the theoretical wash curves described by eqns. (2) and (3). Trial experiments were conducted with ^{203}Hg, counted in

8-s records, but counting statistics were poor (Fig. 6); more precise results were achieved with time intervals of 40 s (Fig. 7). Typical values for both an 8-s and a 40-s background and reservoir count are given in Table 1. A smaller amount of isotope was used for the 40-s counts. Even for the highest flow rates used (0.6 ml min^{-1}), 40 s represented a volume increment of only 0.4 ml.

The presence of "spikes" in the wash-in curve (Fig. 6) is due to sudden increases in the metal ion concentration of the eluate, which lasted for a few records before the original slope was restored. This behaviour can probably be ascribed to solubilisation of part of the metal–humate complexes. This soluble fraction would be washed out in a few volume increments during which period there would be an increase in the eluate count rate. That this anomalous behaviour is not due to defects in the ultrafiltration membrane is supported be eventual restoration of the original slope of the curve. The waste effluent reservoir was frequently found to have a pale straw-yellow colouration indicative of the presence of soluble humate.

The wash curves obtained from these experiments are similar to those observed for other metal–HA systems where fraction-collecting has been employed [9]. No wash curves for mercury–HA have been previously reported, presumably because of difficulties in analysing for mercury.

The requirement for an improved continuous-flow stirred-cell technique arises from the three main disadvantages inherent to the existing method. First, the use of nitrogen gas-pressure to provide liquid flow through the cell results in less precise control of flow rates. Secondly, eluate from the cell needs to be collected in large enough fractions for the analytical technique which is to be used (1–2 ml); such volumes may mask the fine structure of wash curves. Also, the differential equation (eqn. 1) describing the mass balance around the cell implies the use of very small volume increments [1]. Thirdly, fraction-collecting requires continuous monitoring and special care has to be exercised to reduce effects from evaporation [8]. The fractions must then be removed for analysis and the data are not readily available for processing by computer.

In the modified technique reported here, these problems were either reduced or totally eliminated. Thus, problems encountered with a gas-driven system were entirely eliminated by the use of an appropriate proportionating

TABLE 1

Typical background and reservoir counts for ^{203}Hg and ^{137}Cs

Isotope	Counting period (s)	Background count (cpm)	Reservoir count (cpm)
^{203}Hg	8	126 ± 11	687 ± 23
^{203}Hg	40	563 ± 25	1968 ± 51
^{137}Cs	40	300 ± 18	1287 ± 38

pump and a range of constant-flow peristaltic tubing. It should also be added that a pump-driven system is inherently much safer should a leak occur, since in the gas system pressure release may spray liquid over a wide area, which would be extremely hazardous when dealing with radioactive liquids.

Undoubtedly the size of volume increments was considerably reduced in this technique. It has already been shown that the largest volume increment involved only 0.4 ml of solution which is ca. 5% of the cell volume. By use of much higher specific or total activity, the volume necessary for an accurate analysis by this isotope dilution method could be reduced even further. There are, however, a number of problems associated with the use of higher activities. In the first place, the available specific activity of many isotopes is strictly limited. Secondly, the use of higher activities would increase both hazards and costs, and the shielding problems would become very much greater. It should also be remembered that simply increasing the total activity of an isotope of a given specific activity would also increase the concentration of the element or compound, often to unacceptable amounts. In general, shielding problems prevent the use of much more than 1.2 mCi of total activity.

Finally, the use of fraction-collecting was entirely eliminated in this modified technique. Indeed, it is the major advantage of this method that wash curves generated and displayed as the experiment proceeds can be continually monitored. The conversion of counts to concentrations, and of record numbers to volumes, and the calculation of adsorption isotherms can all be done on-line, with suitable programming, and within minutes after the completion of a given run.

Probably the limiting factor to the usefulness of this method is the problem of shielding the detector from γ-rays emitted from parts of the apparatus other than the tubing immediately in front of the collimator. There are two points to bear in mind. The first is that adsorption of γ-rays is given by $I = I_0 \exp(-\mu x)$, where I_0 is the initial γ-ray activity, I is the activity of γ-rays after passing through a thickness x of shielding material, and μ is the total linear adsorption coefficient for the absorption of a γ-ray of given energy. Thus absorption for a given γ-ray energy increases rapidly as the thickness of shielding material increases. However, since μ decreases rapidly with increasing γ-ray energy, a given thickness of shielding becomes much more "transparent" as the γ-ray energy increases.

The exponential nature of the variation of intensity with thickness for a given γ-ray energy means that however thick the shielding, a certain fraction of γ-rays will penetrate it, and this imposes a considerable restraint. For low-energy γ-rays, i.e. below about 800 keV in energy, this fraction can be kept small enough that extraneous γ-ray activity does not contribute significantly to the counting rate under all the conditions of the experiment, providing the total activity is below a certain value. Experiments have shown that for γ-rays not exceeding 300-keV energy the total activity can be about 1.4 mCi. For energies above 600 keV, however, this figure must be reduced to less

than 0.8 mCi. This leads to the conclusion that the method is not practicable for isotopes emitting γ-rays with energies in excess of 800 keV. A list of potentially useful isotopes of several elements is given in Table 2, which includes only those isotopes which emit γ-rays of less than 800 keV, which have half-lives greater than 12 h and which are commercially available. A γ-ray energy enclosed in brackets indicates that this γ-ray is emitted but that its intensity is so low that it is not expected to have any significant effect on the determination.

An interesting application of the technique would be in the study of competitive adsorption of two or more elements. Providing the isotopes used emit γ-rays sufficiently different in energy to be resolved by the NaI(Tl) detector, then the counts from the different isotopes could be used to follow the simultaneous adsorption of the elements concerned.

Shielding problems are much less severe with isotopes that emit β-particles only. Such activity is completely adsorbed by only a few millimetres of lead even for the most energetic β-emitters. Consequently, experiments have just started on the use of such isotopes. The NaI(Tl) detector was replaced by an end-window Geiger—Müller tube to detect the β-particles. There are, however, limitations to the application of such isotopes because there are relatively few pure β-emitters. Investigations of multi-element systems with such isotopes would, of course, be impossible with a Geiger—Müller tube.

The technique described shows potential as a rapid and accurate method for study of adsorption behaviour. One possible major advantage over existing methods is the potential for study of systems containing more than one adsorbate, particularly as wash curves are produced directly for each element as the experiment proceeds.

TABLE 2

Isotopes emitting γ-rays of less than 800-keV energy

Isotope	Energy of principal γ-rays (keV)	Half-life	Isotope	Energy of principal γ-rays (keV)	Half-li
^{47}Sc	160	3.4 d	^{125m}Te	109	58 d
^{51}Cr	320	27.8 d	^{133}Ba	81, 276, 303, 356, 384	7.5 y
^{57}Co	122, 136	270 d	^{139}Ce	166	140 d
^{64}Cu	511, (1346)	12.8 h	^{153}Sm	70, 103, 173	47.1 h
^{69m}Zn	439	13.8 h	^{153}Gd	70, 98, 103	236 d
^{74}As	511, 596, 635, (1204)	17.5 d	$^{175+181}$Hf	90, 133, 230, 344, 346, 433, 482	70 d
^{75}Se	97, 121, 136, 265, 280, 401	121 d	^{185}W	126	70 d
^{85}Sr	514	64 d	^{195m}Pt	99	4.1 d
^{109}Cd	88	470 d	^{199}Au	158, 208	3.2 d
^{113}Sn	255	115 d	^{210}Pb	47	22 y

The authors thank Dr. M. H. B. Hayes for valuable help and discussions during the course of this work. One of the authors (E. H.) is greatly indebted to Eboroil (UK) Ltd., for the provision of a studentship.

REFERENCES

1 W. F. Blatt, S. M. Robinson and H. J. Bixler, Anal. Biochem., 26 (1968) 151.
2 M. T. Ryan and N. S. Hanna, Anal. Biochem., 40 (1971) 364.
3 J. S. Crawford, R. L. Jones, J. M. Thompson and W. D. E. Wells, Br. J. Pharmacol., 44 (1972) 80.
4 R. E. Grice and M. H. B. Hayes, Proc. 11th Br. Weed Control Conf., 2 (1972) 784.
5 R. E. Grice, M. H. B. Hayes, P. R. Lundie and M. H. Cardew, Chem. Ind., (1973) 223.
6 I. G. Burns, M. H. B. Hayes and M. Stacey, Pestic. Sci., 4 (1973) 629.
7 S. Burchill and M. H. B. Hayes, Proc. Int. Congr. Soil Sci., Symposium, Jerusalem, 1976, in press.
8 R. J. Smedley, Ph.D. Thesis, University of Birmingham (1978).
9 E. Hartmann, M.Sc. Thesis, University of Birmingham (1978).

Analytica Chimica Acta, 116 (1980) 289—296

A DIELECTRIC CONSTANT DETECTOR FOR THE DETERMINATION OF TRI-n-BUTYLPHOSPHATE IN MIXTURES WITH HYDROCARBONS

LEON N. KLATT

Analytical Chemistry Division, Oak Ridge National Laboratory, Oak Ridge, Tennessee 37830 (U.S.A.)*

(Received 12th November 1979)

SUMMARY

An instrument based on the measurement of dielectric constant is described for determining the tri-n-butylphosphate (TBP) content of TBP—n-dodecane solutions is described. The system utilizes a phase-locked-loop feedback network to measure the resonant frequency of a parallel inductor-capacitor circuit in which the sample is the dielectric material of the capacitor. The shape of the frequency vs. volume percent TBP response curve is explained by the dimerization of TBP. Values of 3.09 and 8.23 for the dielectric constant of TBP monomer and TBP dimer, respectively, were calculated. Standard mixtures containing 4—30% (v/v) TBP were analyzed and an average error of —0.08% TBP was obtained; average precision is 0.02% TBP. Total time required to process a sample, including chemical pretreatment, is approximately 5 min.

The recovery of various elements from irradiated nuclear fuel involves a solvent extraction step to separate the fissionable material from the fission products. Tri-n-butylphosphate (TBP) dissolved in dodecane or kerosene is commonly used as the extracting medium. Because the composition of the medium is an important parameter in defining the efficiency of this separation, a simple and rapid procedure for determining its composition is required. This report describes an instrument developed to determine the TBP content of TBP—dodecane mixtures. It measures the dielectric constant of the solution, and is based upon the circuit concept utilized in a dielectric constant liquid-chromatographic detector developed by Klatt [1]. The instrument is designed for laboratory use; however, it could be readily modified to operate as an in-line monitor. Although the discussion herein is focused on the determination of TBP, the instrument can be utilized in any situation where the measurement of dielectric constant can form the basis for analyses of binary mixtures.

DESCRIPTION OF THE INSTRUMENT

Dielectric constant is determined by measuring the capacitance of a cell in which the dielectric medium separating the capacitor plates is the material of

*Operated for the U.S. Department of Energy by Union Carbide Corporation under contract W-7405-eng-26.

interest. The observed capacitance, C, is related to the dielectric constant, ϵ, by $C = k\epsilon$, where k is the cell constant and is a function of the cell geometry. If one considers materials of reasonably low dielectric constant, the dielectric constant of a binary mixture, ϵ_{12}, can be related to the volume fraction, V_2, of the solute and the volume fraction of the solvent, V_1, by

$$\epsilon_{12} = V_1\epsilon_1 + V_2\epsilon_2 \tag{1}$$

where ϵ_1 and ϵ_2 correspond to the dielectric constant of the solvent and solute, respectively.

The resonant circuit is shown in Fig. 1. R_s and C_s are the solution resistance and the capacitance due to the dielectric properties of the solution, respectively. The circuit impedance is a maximum when

$$\omega C_s - 1/\omega L = 0 \tag{2}$$

and is the sum of the resistances R and R_s. ω is the frequency in radians per second. The phase angle between the voltages at points V_R and V_X, as given by

$$\phi = \arctan\left[(R/\omega L)\,(1 - \omega^2/\omega_0{}^2)/(1 + R/R_s)\right] \tag{3}$$

is a monotonic function of frequency and is zero at the resonant frequency, ω_0, independent of the resistive elements in the circuit. This condition of zero phase angle provides the unique information necessary to determine whether the resonant frequency is applied to the network and is the basis for the operation of the detector.

The instrument consists of five basic elements and is shown in block diagram form in Fig. 2. The voltage-controlled oscillator (v.c.o.) phase detector, low-pass filter, and d.c. gain amplifier comprise a phase-locked-loop circuit and operates with zero phase angle between the voltages V_R and V_X. The implementation of the phase-locked-loop circuit is essentially identical to that described by Klatt [1], except that an instrumentation

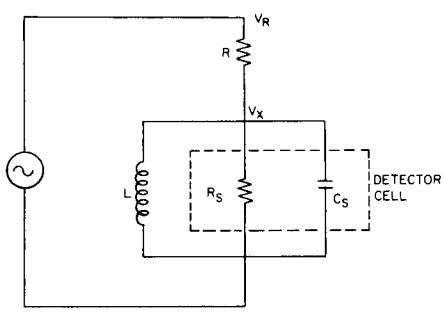

Fig. 1. Resonant network of the dielectric constant detector.

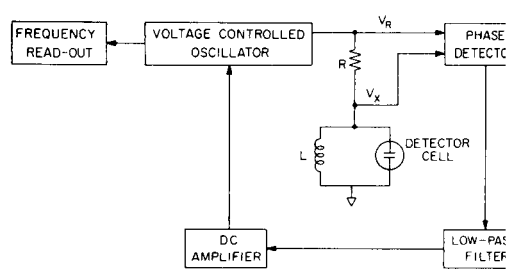

Fig. 2. Block diagram of the dielectric constant detector.

amplifier replaces both a subtractor and X640 gain amplifier employed in the original design; logic to generate an out-of-lock signal has been added. The coarse v.c.o. tuning switch required for the liquid chromatographic application was eliminated because the current instrument operates over a narrower frequency range, well within the tuning range of a single voltage-variable-capacitance diode. The fifth circuit element is the digital display of the v.c.o. frequency and is implemented with a universal counter chip (Intersil, Inc., Cupertino, CA model 7216A). The out-of-lock signal is used to blank the digital display whenever the phase-locked-loop fails to operate at the zero phase angle condition.

The detector cell is a dip design and utilizes a parallel plate geometry. The detector cell and the sample support assembly are shown in Fig. 3. The capacitance cell was constructed from a variable air capacitor (Cardwell Condenser Corporation, Lindenhurst, NY, Mfg. No. HF-140). The two plate

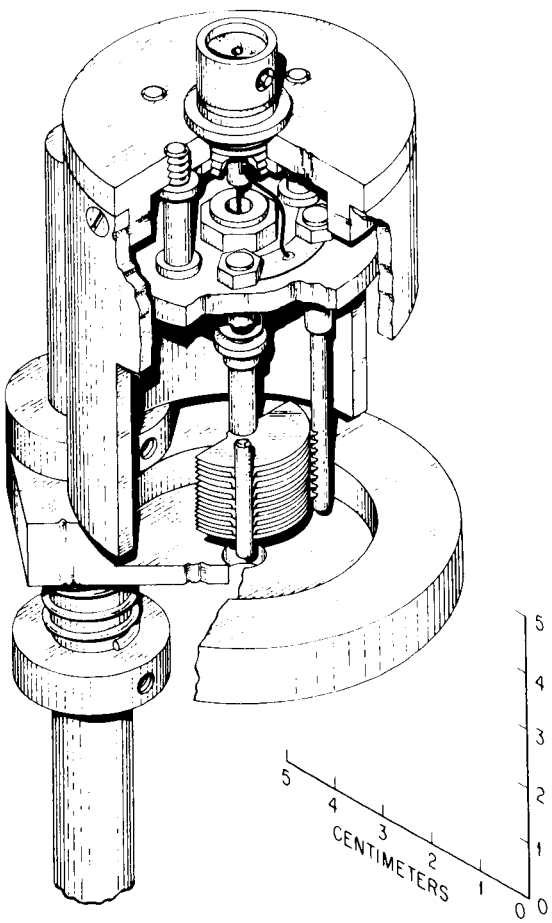

Fig. 3. Detector and sample cell support assembly.

assemblies were removed from the ceramic insulator and all of the original mounting hardware discarded. The upper nine plates were removed from each assembly and the lower posts shortened to leave approximately 0.05 in. between the bottom plate and the end of the post. The two assemblies were then soldered to brass adapters mounted on a fiber-glass board which provided mechanical support for the capacitance cell as well as providing a simple means of making electrical contact between the capacitor plates and the BNC connector. The capacitor plates are positioned for maximum overlap, and the measured capacitance with air as the dielectric medium is approximately 78 pF. The cell is connected to the phase-locked-loop circuit with 15 in. of RG62 coaxial cable. The sample support assembly is constructed from aluminium and uses an indexing notch and a circular recessed area in the cell support platform to locate the sample cell reproducibly with respect to the capacitor plates. Temperature control of the sample cell or detector assembly is not provided. Details of the instrument may be obtained from the Technology Utilization Office, Oak Ridge National Laboratory, Oak Ridge, TN 37830, reference Q-5716, TBP Dielectric Constant Detector.

INSTRUMENT PERFORMANCE

According to eqn. (2), the product $\omega C_s^{1/2}$ should be independent of the capacitance. The response observed with standard capacitors replacing the sample cell is shown in Fig. 4. Theoretical response is observed at low frequency, i.e. $f < 2$ MHz ($C > 250$ pF). The deviation from the theoretical response at high frequency is due to stray capacitance, which is in parallel with the capacitance of the detector cell. This stray capacitance is composed of two components; about 23 pF is due to the coaxial cable and its connectors and about 19 pF is due to the circuit board and the bulkhead BNC connector mounted on the circuit board. The solid curve in Fig. 4 is the response calculated when these stray capacitances are added to the model circuit shown in Fig. 1. The range of capacitance values between the two

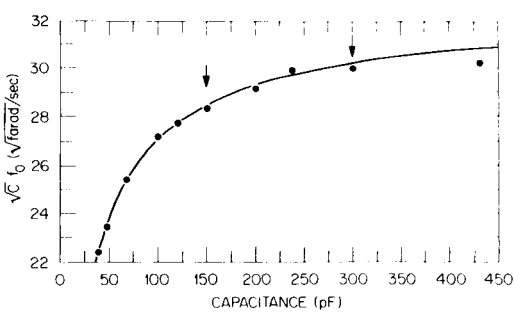

Fig. 4. Normalized response of the instrument as a function of the capacitance. Points are experimental data obtained with known capacitors, and the line is the calculated response $C^{1/2}f_0 = C^{1/2}/2\pi\ [2.43 \times 10^{-5}(C + 4.23 \times 10^{-11})]^{1/2}$

arrows corresponds to capacitance changes observed for typical samples of TBP dissolved in n-dodecane.

The response of the phase-locked-loop to a step change in capacitance is shown in Fig. 5. This response curve was obtained by placing a 100 pF standard capacitor in parallel with a voltage-variable-capacitance diode. The bias of the voltage-variable-capacitance diode was changed in a step manner, producing a change in v.c.o. frequency of 0.3 MHz, and the response of the control voltage at the v.c.o. was monitored. The response is a damped harmonic oscillation typified by an underdamped feedback control system.

Noise on the v.c.o. control signal is approximately 0.1 mV, which in the linear tuning region of the v.c.o. transfer function corresponds to a frequency noise of approximately 48 Hz. Substituting this frequency noise into eqn. (3), and assuming that $R_s \gg R = 1K$, the precision of phase angle control at a nominal operating frequency of 2 MHz is approximately 0.01 degrees. The accuracy of the phase angle control under normal operating conditions is a function of the difference in propagation times of the signals V_R and V_X from resistor R to the phase detector and of the voltage offsets originating in the low pass filter and d.c. amplifier. Measurement of the difference in propagation times yielded 0.3 degrees as an upper bound for the phase angle

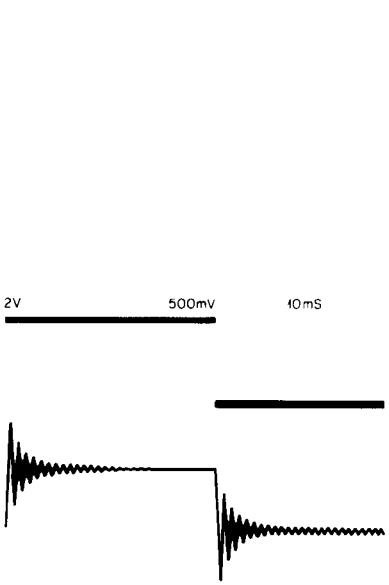

Fig. 5. Response of v.c.o. control voltage to a step change in cell capacitance. Upper trace is the step change in bias of the voltage-variable-capacitance diode, and the lower trace is the v.c.o. control voltage.

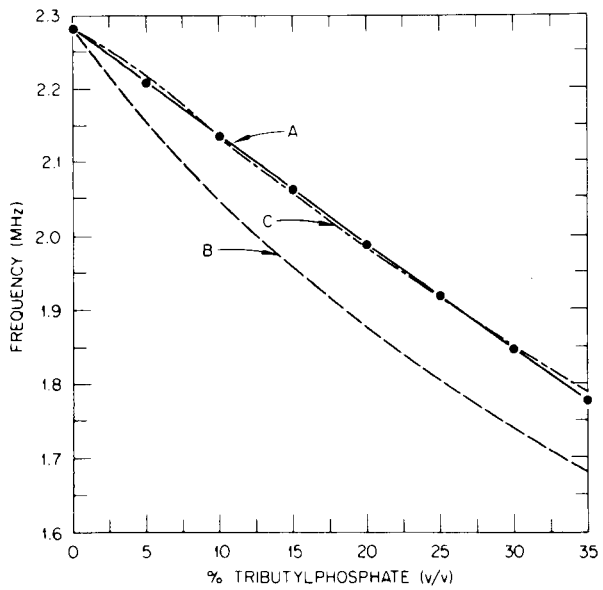

Fig. 6. The frequency vs. % TBP response curve. Points are observed data for standard mixtures. Curve A: eqn. (4), see text. Curve B: simple model of a binary mixture of TBP dissolved in n-dodecane with $\epsilon = 8.143$. Curve C: model with dimerization of TBP.

error. Based on a simplified system analysis of the phase-locked-loop circuit, voltage offsets as large as 10 mV introduce a phase angle error of only 0.02 degrees, which is significantly less than the error resulting from differences in signal propagation times. The phase angle variance and phase angle error can be expressed in times of an analysis variance and an analysis error via eqn. (3) and the calibration equation (see below). At the midpoint of the calibration equation (f_0 = 2 MHz), a phase angle variance of 0.01 degrees corresponds to a TBP variance of 0.004% TBP. Similarly, a phase angle error of 0.3 degrees yields an error of 0.1% TBP.

Standard mixtures of TBP in n-dodecane were utilized to evaluate the performance of the instrument with respect to its analytical application. An extraction procedure was used to minimize interferences from dibutylphosphoric, monobutylphosphoric and phosphoric acids [2, 3], which result from hydrolytic and radiolytic decomposition of TBP.

Samples of known TBP content were prepared by pipetting a specified volume of TBP into a 100-ml volumetric flask and diluting to volume with n-dodecane. A 30-ml portion was equilibrated for 1 min with an aqueous 1% (w/v) sodium carbonate solution followed by two 1-min equilibrations with distilled water. After the final equilibration the organic phase was centrifuged for 1 min to provide a complete separation between the two phases. The organic phase was transferred to the sample cell and the frequency reading recorded.

The observed frequency as a function of the volume percent TBP in n-dodecane is shown in Fig. 6, curve A. The smooth curve is the quadratic equation

$$f_0 = 2282 - 15V_2 + 0.0176V_2^2 \quad (4)$$

obtained from a least-squares regression analysis of the experimental data, with frequency in kHz. A theoretical response curve based on eqns. (1) and (2) and the equation for C is also shown in Fig. 6, curve B. In calculating the latter curve, the stray capacitance (see above) were taken into account; however, the presence of dissolved water in the samples was neglected. It should be noted that accounting for the water content of these samples would shift the calculated curve to lower frequencies. The principal implication of the difference between the observed response curve and the simple model embodied in this calculation is that solute–solute interactions are significant in this system. Petkovic [4] reported a value of 2.6 l mol^{-1} for the dimerization constant of TBP in n-dodecane. Including the effect of this dimerization equilibrium in the response model, dielectric constant values of 3.093 and 8.234 for the monomeric and the dimeric forms of TBP, respectively, were obtained from a least-squares fit of the experimental data to the model. The densities of TBP monomer and TBP dimer were assumed equal to the density of neat TBP. The calculated response curve is shown in Fig. 6, curve C; the agreement between the experimental data and the model is excellent. Assuming that the dimerization constant for TBP dissolved in n-dodecane is valid for

neat TBP and substituting the dielectric constant values for the monomer and dimer into eqn. (1), a value of 7.18 for the dielectric constant of neat TBP is calculated. This compares with literature values of 8.143 [5] and 8.05 [6]. Considering the assumptions required to perform the calculation, the differences between the calculated and literature values are acceptable.

Typical precisions obtained for triplicate readings of representative samples are shown in Table 1. Data in the second and third columns refer to the situation where the sample cell was removed from the detector assembly and the detector plates washed with acetone and blown dry between each reading. Data in the last two columns were obtained by simply removing the sample cell from the detector assembly and then repositioning the cell in the detector without washing the detector between readings. The variances obtained with the latter procedure reflect sample cell positioning errors, while the former procedure reflects total sample reading errors. These frequency variances are significantly larger than the electronic noise of the instrument and indicate that the precision of the analyses is determined by the sample handling procedure and not by the instrument. The difference in observed resonant frequency is due to temperature changes arising from the evaporative cooling of the detector plates and sample caused by the acetone wash. Based upon the temperature coefficient of the dielectric constant for n-dodecane, this observed frequency difference corresponds to a temperature change of 1°C.

The accuracy of the instrument and sample treatment procedure were determined by preparing two sets of samples, each containing three different percentages of TBP and representing expected samples near the ends of the calibration curve. Results are summarized in Table 2. The average error is −0.08% TBP. Samples D—F were prepared with a second lot of n-dodecane and were analyzed 24 h after preparation of the calibration curve; the results were calculated without re-establishing the calibration curve. The negative bias observed for this sample set is probably due to the n-dodecane, because similar variations were observed with the liquid chromatographic detector [1]. The temperature change required to yield the average error for samples D—F is about 5°C, which is too large a variation for an air-conditioned laboratory. Verifying the calibration curve with a single standard sample while analyzing a series of unknowns and applying a correction factor would minimize errors from the diluent. For example, when sample E was used as

TABLE 1

Precision of measurement

TBP (%)	Detector washed		Cell repositioned	
	f_0 (kHz)	s (kHz)[a]	f_0 (kHz)	s (kHz)[a]
30	1846.7	0.4	1848.2	0.2
5.0	2206.8	0.6	2209.3	<0.1

[a]The variances are calculated from triplicate readings.

TABLE 2

Accuracy of measurement

Sample No.	TBP taken (% v/v)	TBP found (% v/v)[a]
A	29.00	28.99 ± 0.03
B	30.00	29.97 ± 0.02
C	31.00	30.93 ± 0.02
D	4.00	3.93 ± 0.02
E	5.00	4.87 ± 0.02
F	6.00	5.86 ± 0.02

[a]Error limits are the 95% confidence limits based on triplicate readings with an acetone wash of the detector plates between each sample.

the standard and the correction factor of 0.13% TBP was applied to samples D and F, the error was reduced to 0.04% TBP.

In conclusion, the instrument developed is suitable for determining the TBP content of TBP—hydrocarbon mixtures. Since a bulk property of the solution is measured, chemical pretreatment of the sample is required to minimize the effects of interferences. The sensitivity, accuracy, and precision of the instrument are excellent. The instrument design is sufficiently general that it can be applied to the analysis of different types of binary mixtures. Modifications required to use it as an in-line monitor are relatively simple.

REFERENCES

1 L. N. Klatt, Anal. Chem., 48 (1976) 1845.
2 R. K. Klopfenstein, J. H. Krekeler, N. R. Leist, C. T. Hicks, D. E. Richards and J. R. Nelli, USAEC Report NLCO-815 (1960).
3 Y. Lee and G. Ting, Anal. Chim. Acta, 106 (1979) 373.
4 D. M. Petkovic, J. Inorg. Nucl. Chem., 30 (1968) 603.
5 D. M. Petkovic, B. A. Kezele and D. R. Rajic, J. Phys. Chem., 77 (1973) 922
6 G. K. Estok and W. W. Wendlandt. J. Am. Chem. Soc., 77 (1955) 4767.

Analytica Chimica Acta, 116 (1980) 297—305

A TRANSIENT CURRENT MONITORING AND ELECTRODE CHARACTERIZATION SYSTEM FOR A PULSED OXYGEN ELECTRODE

K. D. WISE

Department of Electrical and Computer Engineering, The University of Michigan, Ann Arbor, Michigan 48109 (U.S.A.)

R. B. SMART*[a] and K. H. MANCY

The Environmental Chemistry Laboratory, School of Public Health, The University of Michigan, Ann Arbor, Michigan 48109 (U.S.A.)

(Received 24th September 1979)

SUMMARY

Non-steady state voltammetry has been applied to membrane electrodes to provide improved sensitivity as well as independence of stirring. This paper describes a new instrumentation system based on complementary metal oxide—silicon technology for the characterization of a pulsed oxygen electrode. The system provides the necessary timing, analog-to-digital conversion, and digital display of the transient current.

Dissolved oxygen voltammetric membrane electrodes have found wide use for in-situ determination of oxygen in natural and waste water, biological fluids, cells, tissues, and non-aqueous media [1—3]. Most of the systems presently available are based on steady-state measurements. The use of a membrane electrode under continuous polarization, however, has the disadvantage of being operated with the lowest possible sensitivity. Under these conditions the sensitivity is dependent on the membrane thickness and permeability, as shown by Mancy et al. [2]. The highest sensitivity should be obtained with very thin membranes, but practical considerations limit the membrane thickness to about 2.54×10^{-3} cm. The cathode area can be increased, but larger electrodes tend to become bulky and generally exhibit excessive residual currents. The use of membranes with higher permeability coefficients can also increase the steady-state response. After several years of laboratory and field experience, the main limitations of steady-state electrode systems have been largely due to: (a) lack of long term sensitivity, (b) low sensitivity, and (c) the need to maintain a certain amount of mixing at the electrode surface.

[a]Present address: Department of Chemistry, West Virginia University, Morgantown, West Virginia 26506, U.S.A.

The application of a very brief potential pulse to the electrode should make the sensitivity independent of the membrane thickness [2]. The non-steady state voltammetric technique has been reported by Schmid and Mancy [4], Mancy [5], Lilley et al. [6], and Fowler and Oldham [7]. The use of pulsed potential polarization will increase the electrode sensitivity as well as eliminate the need for constant stirring. A problem associated with the pulsed potential technique is the operational need for more sophisticated and cumbersome electronic equipment than that required for steady-state measurements. The current measurement is often done milliseconds after the pulse application, therefore the measurement must be made with a storage oscilloscope or other fast recording device. The application of the pulse is accompanied by an instantaneous rise of current followed by a decay to the steady-state value. The means for providing accurately timed voltage pulses must also be provided. The instrumentation system described below was developed to provide an accurate technique for electrode characterization by using the pulsed potential method; it also provides higher sensitivity in a portable system for field measurements.

EXPERIMENTAL

Apparatus

A YSI (Yellow Springs Instrument Co., Yellow Springs, Ohio) Model 4004 Oxygen Electrode filled with 3.5 M KCl saturated with AgCl was used throughout. The membrane was 1-mil FEP teflon. The area of the platinum cathode was experimentally determined as 9.2×10^{-2} cm^2 [8]. A Tektronix Type 564 storage oscilloscope (Tektronix, Inc., Beaverton, Oregon) was used to record the transient currents. The electrode was calibrated by using the standard Winkler method [9].

Instrumentation

The design of the transient current monitoring system was based on the need for independent control over the pulse amplitude, duration, and frequency (interpulse interval). Complementary metal oxide—silicon (CMOS) technology was selected for this application because it provides low power dissipation, relatively high speed, and a high insensitivity to variations in power supply voltage and ambient temperature. The system consists of several sections, as shown in Fig. 1. The voltage to be applied to the electrode is selected by a potentiometer and is continuously variable between zero and ±1.2 V. This electrode voltage is buffered and applied to the working electrode through a series electronic switch. For three-electrode systems, the reference electrode potential is added to the selected electrode voltage to eliminate the effects of polarization at the anode. An FET-input operational amplifier is used as a non-inverting buffer, to ensure a reference electrode current of less than 20 pA. A second FET-input amplifier senses the current passed by the working electrode and converts it to a voltage with an output

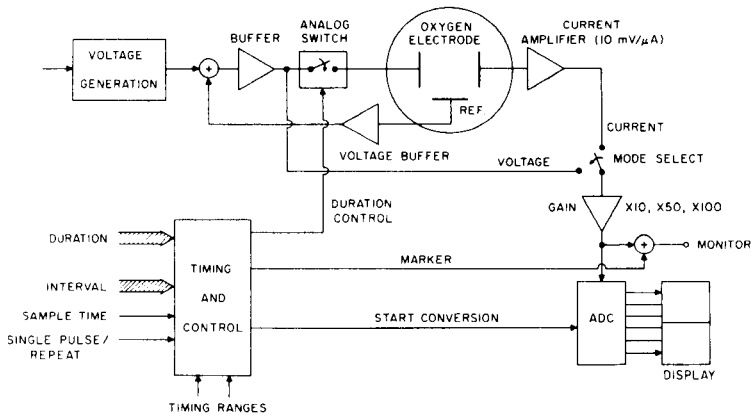

Fig. 1. Schematic of transient current monitoring electrode characterization system.

of 10 mV μA^{-1}. Subsequent amplifiers allow the user to select overall amplifications of 0.1 V μA^{-1}, 0.5 V μA^{-1}, or 1 V μA^{-1}. The resulting signal is available for display on an oscilloscope via a connector on the back of the chassis. The amplification section has a frequency response from d.c. to about 10 kHz.

The pulse duration and interpulse interval are determined by the timing and control section. These parameters are selected by sixteen toggle switches on the front panel, eight of which are used for each parameter. These switches are binarily weighted and are used to preset eight-bit binary counters which are driven by a crystal-generated clock signal. The clock can be adjusted at 1 ms or 10 ms for pulse duration and at 10 ms or 100 ms for pulse interval. The resulting parameter ranges are selectable from 1 ms to 2.55 s for duration and 10 ms to 25.5 s for interval. The pulses may be applied repetitively or individually (single pulse) via front panel switches. These timing intervals are accurate to within 0.3% or better and are stable to within ±20 ppm over the ambient temperature range from 10°C to 40°C.

The sample time on the present system is continuously variable between 5 ms and about 1.5 s in two overlapping ranges which are automatically switched with pulse duration. The sample time is the time at which electrode current is measured. It can be accurately set by using the pulse duration switches to establish first the end of the pulse at the desired sample point, adjusting the variable sample time control to the pulse edge, and then subsequently setting the desired duration. An alternative being considered for future versions of this system is to enter all three timing intervals digitally via a single set of panel switches, storing the desired settings in internal latches, and allowing sample time to be established more easily and with greater stability. A marking pulse is introduced into the electrode current waveform available for display to identify the sample point. Figure 2 shows the current waveforms as well as the marking pulse produced by this system operating with an oxygen electrode.

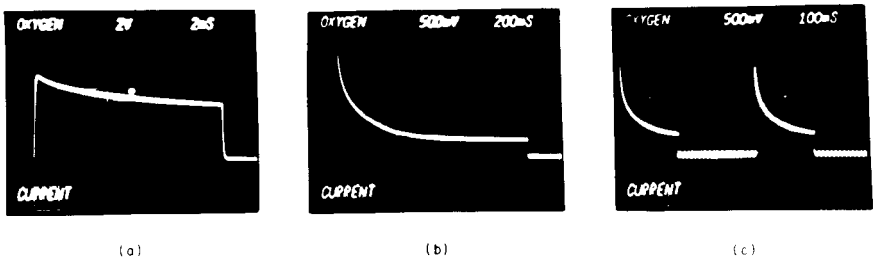

(a) (b) (c)

Fig. 2. Typical current waveforms (V vs. time) for an oxygen electrode. $E = -0.8$ V vs. Ag/AgCl; marking pulse defines time of current sampling; (a) pulse duration = 15 ms; (b) pulse duration = 1.55 s; (c) pulse duration = 250 ms. Pulse interval = 300 ms.

In order to quantify the electrode current at the desired sample time, the amplified current waveform is presented to an eight-bit CMOS successive-approximation analog-to-digital converter (ADC). A start signal is generated by the timing section to initiate the conversion at the desired sample time. The conversion time is about 75 μs for eight-bits as used, although the converter (an Analog/Devices AD7570JD) could perform the conversion in as little as 20 μs if required. The output of the converter is an eight-bit binary representation of the current amplitude at the sample time and this information is displayed on two hexadecimal LED displays. Decimal displays could also be used with additional decoding logic.

The eight-bit converter quantizes a 10-V reference voltage into 256 equal intervals, allowing electrode current to be determined with an accuracy of 20 nA or better. For the present electrodes, this corresponds to an error of 20 $\mu g\ l^{-1}$ or less in the measured oxygen concentration. Clock noise, thermal noise, and system stability appear consistent with the use of a 10-bit converter, which would increase the accuracy and resolution of the system by an additional factor of four while maintaining the same dynamic range. A panel switch allows the present converter to display the electrode voltage as an alternative to electrode current so that the required level can be accurately adjusted in the field.

This monitoring system has been realized by using commercial integrated circuits on a standard 30-in^2 wire-wrap board. Power dissipation, excluding the displays (which dissipate approximately 1.2 W at 6 V), is less than 0.5 W. The system requires +6 and ±12 V supplies. Both a.c.- and d.c.-powered versions have been realized, the latter operating from rechargeable Gel-cell batteries. Table 1 summarizes the operating characteristics of the system. The small size of the system makes it easily portable for field measurements.

MODEL FOR A PULSED OXYGEN ELECTRODE

The theory of two-layer diffusion current for a membrane electrode has been described in detail by Mancy et al. [2]. The steady-state current is given by:

$$i_{ss} = nFA\ P_m\ C/b \quad (1)$$

where i_{ss} is the steady-state current (A); n is the number of electron equivalents per mole of oxygen; F is the Faraday constant; A is the electrode area (cm^2); P_m is the membrane permeability coefficient ($cm^2\ s^{-1}$); b is the membrane thickness (cm); and C is the bulk oxygen concentration (mol cm^{-3}). Upon application of a very short potential pulse, the current may be described by:

$$i_t = nFA\ (P_m/\pi t)^{1/2}\ C \quad (2)$$

where i_t is the current (A) at time t (s). Equation (2) will be valid only if sufficient time is provided between pulses to re-equilibrate the membrane and electrolyte.

Morris and Faulkner [10] have investigated normal pulse voltammetry, using an open circuit interval and a platinum disc electrode. Equilibration of the diffusion layer during the pulse interval was inhibited by coulostatic discharge of the double layer. At time $t = 0$, a potential step was made to E (see Fig. 4) where subsequent electrolysis is diffusion-limited. This potential was applied for a specific duration and the electrode was then open-circuited. Electrolysis proceeded coulostatically until the potential fell to $E_{1/2}$. The time it took for E to fall back to $E_{1/2}$ was designated as the effective pulse width. At that time the surface flux and hence the electrolysis rate may be regarded as zero. The effective pulse width was described as follows:

$$(t_p)_{eff}^{1/2} = [\pi^{1/2}\ C_d\ (E_{1/2} - E)/2\ nFD^{1/2}\ C^*] + t_p^{1/2} \quad (3)$$

where t_p is the pulse duration (s); $(t_p)_{eff}$ is the effective pulse width (s); C_d is the differential double layer capacitance (farads); $E_{1/2}$ is the half-wave potential (V); E is the applied potential (V); D is the diffusion coefficient ($cm^2\ s^{-1}$); F is the Faraday constant; C^* is the bulk concentration of the reactant (mol cm^{-3}); and n is the number of electrons. The dependence of $(t_p)_{eff}$ on the solution concentration is evident from eqn. (3). Table 2 gives the calculated values for $(t_p)_{eff}$ for a typical oxygen electrode at various t_p and oxygen concentrations.

The thickness of the diffusion gradient, x, caused by oxygen reduction at the electrode surface can be calculated [11] for any pulse duration by

$$C(x,t) = C\{2/\pi^{1/2} \int_0^{x(2Dt)^{-1/2}} e^{-y^2}\,dy\} \quad (4)$$

Examining the point where the bulk oxygen concentration is only 1% different than the concentration at the electrode surface, eqn. (4) can be solved to give $x\ (2\ Dt)^{-1/2} = 1.8$. At $t = 1$ ms and $D_f = 2.4 \times 10^{-5}\ cm^2\ s^{-1}$, the diffusion gradient thickness is calculated as 5.6 μm. This is the approximate thickness of the electrolyte layer for the test electrode. At times greater than 1 ms, it is therefore necessary to consider diffusion in the membrane and the membrane diffusion coefficient, D_m, must be used to solve eqn. (4).

TABLE 1

Characteristics of the transient current monitoring system

Electrode voltage	Continuously adjustable 0 to ±1.2 V; two- or three-electrode operation
Operating modes	Single-pulse or repetitive pulse train
Pulse duration	1 ms to 2.55 s in two overlapping ranges
Pulse interval	10 ms to 25.5 s in two overlapping ranges
Timing accuracy	Less than 0.3% error; temperature drift less than 20 ppm
Current amplification	Selectable: 0.1 V μA^{-1}; 0.5 V μA^{-1}; 1 V μA^{-1}
Sample time	Continuously adjustable, 5 ms to 1.5 s in two overlapping ranges
Display modes	Electrode voltage (±2 mV in high gain position); electrode current (±20 nA in high gain position)
Power dissipation	20 mA at ±12 V; 200 mA at +6 V: 1.7 W total, including displays
Size	240 $in.^3$ (3 × 8 × 10 in.)

The theoretical current given by eqn. (2) is based on the absence of capacitance current; however, the contribution of capacitance current to the total observed experimental current in pulsed electrode voltammetry is well known [12]. The pulse capacitance current is given by

$$i_c = (\Delta E/R) \exp(-t/RC) \quad (5)$$

where i_c is the capacitance current (A); E is the potential change (V); R is the electrode-solution resistance (ohms); C is the electrode capacitance (farads); and t is the pulse duration (s).

RESULTS AND DISCUSSION

The instrumentation system was originally designed to hold the electrode at 0 V during the pulse interval and step to −0.8 V for the pulse duration. Under these conditions, very little current difference was observed for large differences in oxygen concentration. In addition to the expected cathodic faradaic current observed during the pulse duration, an anodic discharge current was also observed upon pulse termination. This condition is illustrated in Fig. 3. The anodic current arises in part from the discharge of the electrical double layer when the electrode is forced back to 0 V. Also, when operating in the pulse mode, sufficient time must be given between pulses for the electrode to become depolarized. If this does not happen, a thick diffusion layer similar to that resulting from steady-state operation will build up, reducing electrode response.

In the light of these results, the instrument was modified to allow the electrode to float at open-circuit potential during the pulse interval as shown in Fig. 4. The open-circuit interval condition prevented the electrode double layer from completely discharging and thus reducing the charging current on the subsequent pulse. This modification greatly improved the system per-

TABLE 2

Calculated effective pulse widths for various oxygen concentrations and pulse durations

$[O_2]$ (mg l^{-1})	$(t_p)_{eff}$ (ms)			$[O_2]$ (mg l^{-1})	$(t_p)_{eff}$ (ms)		
	t_p = 50 ms	t_p = 100 ms	t_p = 500 ms		t_p = 50 ms	t_p = 100 ms	t_p = 500 ms
8	64	119	542	4	80	140	585
7	66	122	548	3	91	154	615
6	69	125	555	2	116	187	677
5	73	132	569	1	208	300	882

formance, allowing the electrode characteristics to be examined. The open-circuit potential, while variable, was found to be considerably more negative than 0 V.

Current versus oxygen concentration for various pulse durations and an interval of 2 s was recorded using the instrument described, and these data are given as the open points in Fig. 5. The sample time was just prior to pulse termination in all cases. Theoretically, the relationship between current and concentration should have been linear according to eqn. (2), but breaks were observed at 100-ms and 150-ms pulse durations. A series of similar experiments was done with the potential and timing controlled by the instrument

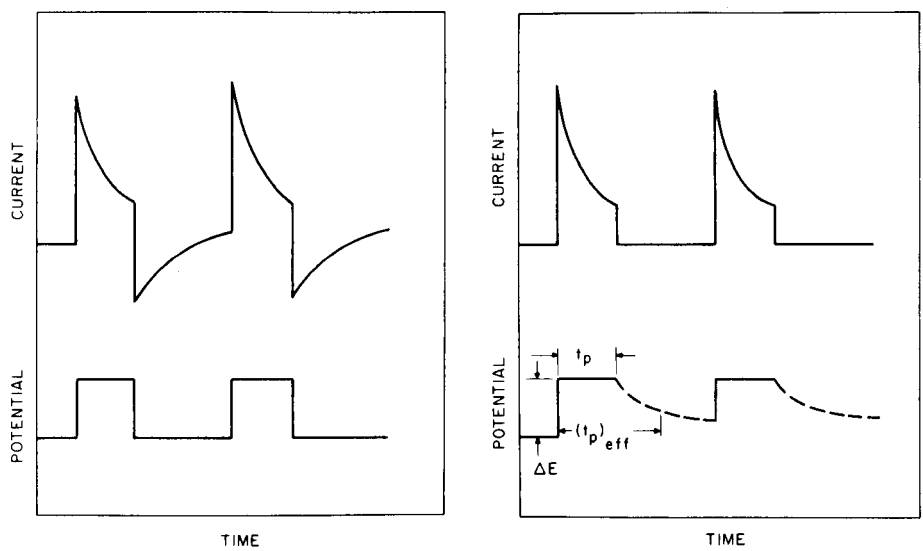

Fig. 3. Current—potential waveform for pulse potential voltammetry with closed-circuit interval.

Fig. 4. Current—potential waveform for pulse potential voltammetry with open-circuit interval. ΔE, applied potential; t_p, pulse duration; $(t_p)_{eff}$, effective pulse duration.

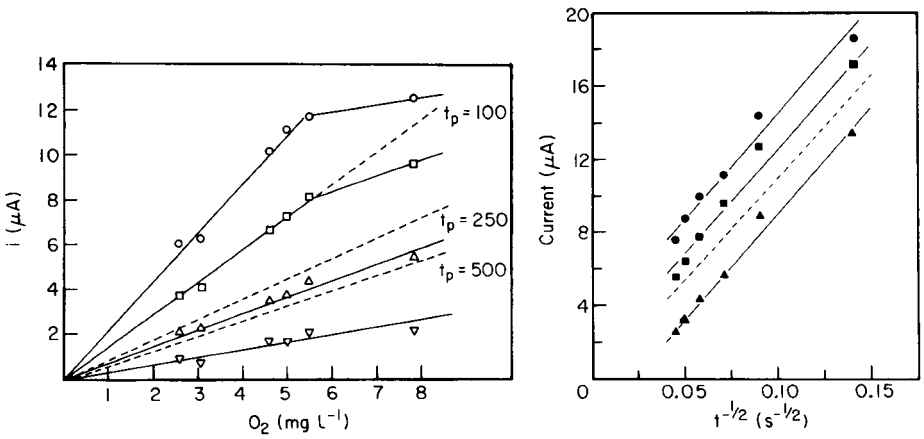

Fig. 5. Calibration curves for the pulsed oxygen electrode. Dashed lines are theoretical for indicated t_p; (○) 100 ms; (□) 150 ms; (△) 250 ms; (▽) 500 ms pulse duration; pulse interval, 5 s.

Fig. 6. Electrode response at various pulse durations and intervals. Dashed line is theoretical current.

but with current levels determined by photographing the current at a 500-ms pulse duration and then reading the reduction currents at shorter pulse durations from the photograph. The data exhibited the expected linear relationship at all pulse durations and the effect of pulse duration on electrode sensitivity, ϕ, is evident from Table 3. The sensitivity for the 50-ms pulse is six times higher than steady state.

The breaks shown in Fig. 5 can be explained by examination of the effective pulse widths and oxygen concentrations at these times. With a t_p of 100 ms and an oxygen concentration of 8 mg l^{-1}, the $(t_p)_{eff}$ obtained from Table 2 is 119 ms. In this case the currents observed by both methods should be similar; however, as Fig. 5 shows, the currents differ experimentally by several μA. By means of eqn. (5), the charging current at 100 ms is calculated to be 6.1 μA (C = 25 F cm^{-2}, R = 30 K, E = —0.8 V). This might explain the difference in the two sets of data at this time and concentration. At lower oxygen concentrations the effect of $(t_p)_{eff}$ is much greater (Table 2) and the observed current must be less than expected. Apparently, a point is gradually reached where the oxygen concentration is no longer sufficient to remove E to $E_{1/2}$ before the subsequent pulse. With a t_p of 500 ms and an oxygen concentration of 8 mg l^{-1}, $(t_p)_{eff}$ is 542 ms and the two sets of data

TABLE 3

Effect of pulse duration on the pulsed voltammetric membrane oxygen electrode for a pulse interval of 2 s

Pulse duration (ms)	50	100	150	250	500	ss
ϕ(μA mg^{-1} l)	1.51	1.09	0.81	0.66	0.34	0.25

should again be similar; in this case, they are, because the charging current is negligible. At the same t_p but with an oxygen concentration of only 1 mg l^{-1}, $(t_p)_{eff}$ is about 1.5 t_p; however, the difference in current at this pulse time is also negligible.

Data obtained by applying a 500-ms pulse duration and sampling the current at shorter times were taken for different oxygen concentrations at pulse intervals of 3 and 5 s. The theoretical current for an oxygen concentration of 8 mg l^{-1} at different pulse durations was calculated from eqn. (2) and is plotted as the dashed line in Fig. 6 versus the reciprocal square root of the pulse duration. The experimental currents were also plotted for the different time intervals. The agreement between the slopes is excellent. Experimental currents were higher than predicted by eqn. (2) possibly because of an error in the selection of a permeability coefficient (known to change from batch to batch) and/or the electrode area determination.

Conclusions

The transient current monitoring instrumentation system has been shown to be a very useful device for pulsed electrode characterization. It has eliminated the need for using an oscilloscope to record transient current, making it portable and suitable for field measurements. In order to achieve still greater flexibility in investigating transient electrode phenomena, an all-CMOS microcomputer-controlled instrumentation system has also been developed. This system should allow correction for the effects of secondary parameters, such as temperature, which can also influence electrode response and will be reported in a separate paper.

The authors gratefully acknowledge the many contributions of K. Holloway, N. Ho, and J. C. Huang in the construction and testing of the instrumentation system. This work was supported by U.S. Environmental Protection Agency Grant No. R804834-01-1.

REFERENCES

1 K. H. Mancy and T. Jaffe, Analysis of Dissolved Oxygen in Natural and Waste Waters, U.S. Dept. HEW, Public Health Service, Publ. No. 999-WP-37, April 1966.
2 K. H. Mancy, D. A. Okun, and C. N. Reilly, J. Electroanal. Chem., 4 (1962) 65.
3 I. Fatt, Polarographic Oxygen Sensors, CRC Press, Cleveland, OH, 1976.
4 M. Schmid and K. H. Mancy, Schweitzerische für Hydrologie, 32 (1970) 328.
5 K. H. Mancy, in W. A. Adams (Ed.), Chemistry and Physics of Aqueous Gas Solutions, The Electrochemical Society, Princeton, NJ, 1976.
6 M. Lilley, J. Story, and R. Raible, J. Electroanal. Chem., 23 (1969) 425.
7 J. K. Fowler and K. B. Oldham, in W. A. Adams (Ed.), Chemistry and Physics of Aqueous Gas Solutions, The Electrochemical Society, Princeton, NJ, 1976.
8 R. Adams, Electrochemistry at Solid Electrodes, M. Dekker, New York, 1969.
9 Standard Method for the Examination of Water and Wastewater, 14th edn., Am. Public Health Assoc., 1976.
10 J. L. Morris and L. R. Faulkner, Anal. Chem., 49 (1977) 489.
11 J. Crank, The Mathematics of Diffusion, Clarendon Press, Oxford, 1956.
12 P. Delahay, New Instrumental Methods in Electrochemistry, Interscience, New York, 1954.

Analytica Chimica Acta, 116 (1980) 307—314

IMPROVED ENZYME SENSOR FOR GLUCOSE WITH AN ULTRA-FILTRATION MEMBRANE AND IMMOBILIZED GLUCOSE OXIDASE

MASAO KOYAMA* and YUICHI SATO

Chemicals Laboratory, Toshiba Research and Development Center, Toshiba Corporation 1, Komukai Toshiba, Saiwai, Kawasaki 210 (Japan)

MASUO AIZAWA and SHUICHI SUZUKI

Research Laboratory of Resources Utilization, Tokyo Institute of Technology, 4259, Nagatsuta, Midori, Yokohama 227 (Japan)

(Received 30th October 1979)

SUMMARY

A specific enzyme sensor for glucose was constructed by covering an immobilized glucose oxidase membrane on an oxygen electrode with an asymmetric ultra-filtration membrane. The response time is only 10 s, the calibration graph is linear for 3×10^{-6} — 2×10^{-3} M glucose, and the sensor can be used repeatedly at room temperature for at least 100 days with little deterioration in response.

Many biosensors, including enzyme sensors [1, 2], immunosensors [3—6], enzyme immunosensors [7—9] and microbial sensors [10, 11], have been developed. Those enzyme sensors for glucose that have been evaluated for practical use are listed in Table 1. There remains, however, the need to develop an enzyme membrane which has a rapid response, long-term stability and high reproducibility. This paper describes a novel enzyme membrane particularly for use in enzyme sensors. The membrane enables the sensor to respond within 10 s. Because of the fragility of the membrane, the sensor is protected with an asymmetric ultra-filtration membrane.

EXPERIMENTAL

Materials

Glucose oxidase (β-D-glucose: oxygen 1-oxidoreductase; EC 1.1.3.4; Amano Pharmaceutical Co., Nagoya) was used. Cellulose triacetate (acetyl content 43.2%), cellulose diacetate (acetyl content 39.8%), 1,8-diamino-4-amino-methyloctane, and 50% glutaraldehyde were obtained from Eastman Kodak Co. (Rochester, N.Y.), Asahi Kasei Co. (Tokyo), and Tokyo Kasei Kogyo Co. (Tokyo), respectively. Controlled human serum Consera (Nissui Pharmaceutical Co., Tokyo) and standard human serum (Toshiba Kagaku Kogyo Co., Tokyo) were used as standards. Deionized water was used throughout.

TABLE 1

Enzyme sensors for glucose [12—19]

Electrode	Enzyme (membrane material)	Response time (min)	Linear range (mM)
O_2 (Pt: −0.65 V vs. Ag/AgCl)	Glucose oxidase (polyacrylamide)	0.5—3 (steady state)	0.56—2.9
H_2O_2 (Pt:0.4 V vs. SCE)	Glucose oxidase (nylon screen + cellophane)	3—10 (steady state)	2—20
H_2O_2 (Pt: 0.6 V vs. SCE)	Glucose oxidase (polyacrylamide)	4—12 s (kinetic)	0.05—15
	(polyacrylic acid derivative)	1 (steady state)	0.05—20
Iodide	Glucose oxidase + peroxidase (polyacrylamide / polyacrylic acid derivative)	1—4 (flow system)	0.1—1
O_2 (Pt: −0.6 V vs. SCE)	Glucose oxidase (albumin)	1 (steady state)	0.005—1.28
O_2 (Pt:KOH : Pb)	Glucose oxidase (collagen)	1.5	0.5—5
H_2O_2 (Pt: 0.65 V vs. Ag/AgCl)	Glucose oxidase (collagen)	2—3 (steady state) 30—50 s (kinetic)	10^{-4}—1
O_2 (Pt: −0.6 V vs. Ag/AgCl)	Glucose oxidase + catalase (polyacrylamide)	2—10 (steady state)	0—14

Glucose oxidase membrane preparation. With stirring, 250 mg of cellulose triacetate was dissolved in 5 ml of dichloromethane, and 0.2 ml of 50% glutaraldehyde was added followed by 1 ml of 1,8-diamino-4-aminomethyloctane. This solution was cast on a glass plate and evaporated at room temperature to form a thin membrane (0.02—0.03 mm thick in the wet state). After 3 days, the membrane was removed from the glass plate and immersed in a glutaraldehyde solution (1% in phosphate buffer, pH 7.7) at 35°C for 1 h. The membrane was washed with water, immersed in a pH 7.7 phosphate buffer solution containing glucose oxidase (1 mg ml^{-1}) at 35°C for 2—3 h, and then reduced with sodium tetrahydroborate (0.5 cm^{-2} membrane). The membrane was washed with water and stored in pH 7.0 phosphate buffer at 4—10°C.

The amount of glucose oxidase immobilized was found to be 0.05—0.06 mg cm^{-2} of membrane, by spectrophotometric assay of the mother liquor. The membrane-bound glucose oxidase apparently retained 9% of the activity of original enzyme.

Ultrafiltration membrane preparation. The membrane was prepared as described previously [20—23]. Cellulose diacetate (20 g) was dissolved in 35 g of formamide and 45 g of acetone. After this solution was cast on a glass plate, the solvents were evaporated for 10—30 s at room temperature, to give a membrane 0.03 mm thick in the wet state. The membrane attached to the glass surface was soaked in ice-water (0—4°C) for 1 h.

Enzyme sensor

This was constructed as shown in Fig. 1. The platinum cathode of the galvanic oxygen sensor is covered with a teflon membrane over which the glucose oxidase and ultrafiltration membranes are placed. The smoother side of the ultrafiltration membrane is fixed to face the sample solution. The oxygen sensor has a lead anode and potassium hydroxide electrolyte. Figure 1 also shows the electrical circuitry from which the response is displayed as a current (I) and as a rate of change of current (dI/dt). Because the response time of the amplifier was <10 ms and the maximum recording pen speed was 15 $\mu A\ s^{-1}$, there was no delay in recording the signal from the enzyme sensor.

Procedure

A glass measuring cell (20.5-mm inner diameter) was filled with 5 ml of air-saturated 0.066 M phosphate buffer solution at 37 ± 0.1°C. The solution was stirred magnetically with a 20-mm teflon bar during measurement. When the output of the sensor had reached a steady state, 100 μl of sample solution was injected into the buffer solution while stirring. The decrease in current was directly displayed along with the dI/dt signal.

RESULTS

Enzyme sensor response

Figure 2 shows a typical response for the enzyme sensor coupled with an ultrafiltration membrane to 0.196 mM (final concentration) glucose at 37°C and pH 6.0. The buffer solution, stored in a measuring cell, was initially saturated with oxygen by air bubbling. The sensor gave a constant response to the dissolved oxygen. When 100 μl of a sample solution containing 0.01 M

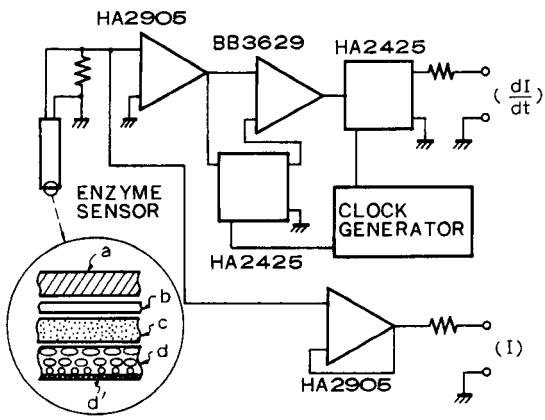

Fig. 1. Block diagram of enzyme sensor construction and circuitry. For the magnified construction of the sensor: (a) platinum cathode; (b) teflon membrane; (c) immobilized enzyme membrane; (d) porous layer of ultrafiltration membrane; (d') semipermeable layer of ultrafiltration membrane.

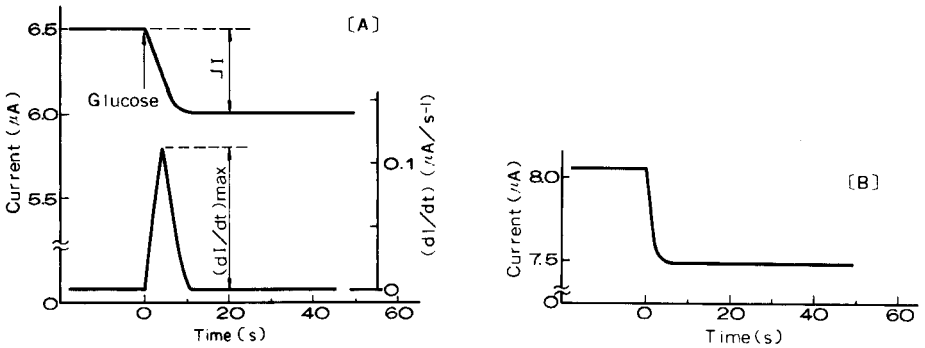

Fig. 2. Enzyme sensor response to 0.196 mM glucose: (A) with ultrafiltration membrane; (B) without ultrafiltration membrane.

glucose was injected, the concentration of dissolved oxygen around the sensor decreased because of oxidation of the glucose by the membrane-bound glucose oxidase action. The sensor output current decreased rapidly, reaching a steady state within 10 s. Figure 2 also shows that the greatest rate of change of current was obtained in 4—5 s. The effect of the ultrafiltration membrane can also be seen in Fig. 2. A steady current was obtained within 5 s after injecting the sample solution. However, the delay caused by the ultrafiltration membrane was small, and the 10-s response time was considered sufficient for practical purposes.

The effects of pH and temperature on the sensor response were investigated for a 0.196 mM glucose solution. Solutions of 0.066 M KH_2PO_4—Na_2HPO_4 buffers were used in the pH range 4.0--9.0. The sensor output current was hardly affected by pH in the range 4.7—8.0 but was markedly decreased in more strongly acidic and alkaline media. The output current increased linearly with temperature over the range 20—40°C, at 14 nA per degree. This value corresponded to about 6% of the output at 20°C and 3% at 37°C.

The reproducibility for determining glucose in aqueous solution or human serum was obtained at various concentrations (Table 2). The relative standard deviations were $\leqslant$2.6% for all samples. The calibration graph was linear from 3 μM to 2.0 mM final concentration of glucose and reached a plateau at 4 mM. Below 3 μM the relative standard deviation increased above 50%. The final concentration range 3 μM—2.0 mM corresponds to a sample concentration range of 0.15—100 mM (2.8—1800 mg dl^{-1}). The plot of dI/dt vs. glucose concentration was linear below 1.0 mM.

Sensor stability

The sensors with and without an ultrafiltration membrane were used repeatedly to confirm their stability over a long period. Measurements were made at a final concentration of 0.196 mM glucose and pH 6.0 or 7.7. The sensor was kept in the buffer solution at room temperature (15—28°C) when not in use. Figure 3A shows the response of the sensor without an ultrafiltration membrane, at pH 7.7. Each plot is the average of 5—15 measurements.

TABLE 2

Reproducibility of steady-state measurements of glucose solutions and human serum at pH 6.0 and 37°C, expressed as mean, standard deviations (s), and relative standard deviation (s_r) for N measurements

	Glucose (M)[a]			Human serum (mg dl^{-1})	
	0.10	0.05	0.01	110	290 ± 17
N	26	20	24	26	29
Mean	4.42	2.37	0.488	113.6	283.6
s	0.0238	0.0369	0.0102	2.95	6.30
s_r (%)	0.54	1.6	2.1	2.6	2.2

[a]Mean and standard deviation given in μA.

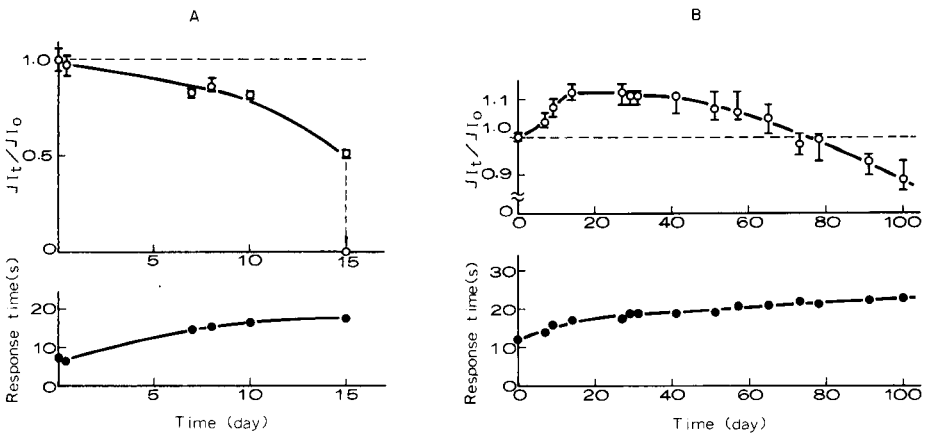

Fig. 3. Long-term stability of sensors: (A) without an ultrafiltration membrane (pH 7.7); (B) with an ultrafiltration membrane (pH 6.0).

The response, expressed as the current relative to the initial response current ($\Delta I_t/\Delta I_0$), decreased gradually, followed by a sudden break-down after 15 days. The response time at each measurement increased during the experiment from 6 to 17 s (Fig. 3A). The glucose oxidase membranes tested were mechanically in bad condition after 5—14 days. The long-term stability was also tested for a sensor coupled with an ultrafiltration membrane (Fig. 3B). The relative output increased gradually over 15 days in pH 6.0 buffer solution and then remained stable for up to 40 days; it decreased slightly over the period 40—100 days. The response time gradually increased from 12 to 22 s after 100 days. Similar results were obtained at pH 7.7. It should be noted that the output current was quite stable for 12 h during which period measurements were repeatedly carried out. The response of the sensor was also maintained for many glucose measurements in human serum. The sensor stability might arise from the ultrafiltration membrane, which prevents large molecules from reaching the glucose oxidase membrane.

DISCUSSION

The combined use of the novel glucose oxidase membrane and the asymmetric ultrafiltration membrane leads to considerable improvement in response time and long-term reproducibility for the glucose sensor. Since the platinum cathode is covered with three membranes, the sensor functions via the following processes: (1) diffusion of glucose through the ultrafiltration membrane; (2) diffusion of glucose into the glucose oxidase membrane; (3) oxidation of glucose by immobilized glucose oxidase; (4) diffusion of oxygen from the glucose oxidase membrane through the teflon membrane; (5) electrochemical reduction of oxygen at the cathode. Of these processes, (1), (2) and (4) depend primarily on membrane permeability and thickness. The ultrafiltration membrane has an asymmetric structure, in which the porosity varies from one surface to the other. In order to test the ability of this membrane to exclude molecules the membrane pore size was varied from 0.01 to 10 μm, and permeability tests were performed on substances of different molecular weights. Figure 4 shows the rejection (%) vs. molecular weight curves obtained. Glucose (m.w. 180) permeated through the membrane easily. The membrane rejected molecules of molecular weight larger than 10,000. These results indicate that the asymmetric ultrafiltration membrane has no appreciable resistance against glucose diffusion. However, the attachment of the ultrafiltration membrane resulted in a little delay in response, so it might be reasonable to take the membrane thickness into account.

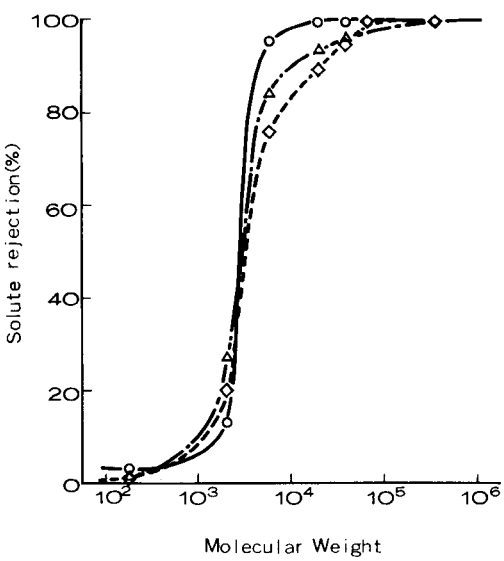

Fig. 4. Permeability of the ultrafiltration membrane at 4 kg cm^{-2} and 30°C. Feed solution flow rate, 0.4—1 m s^{-1}. Rejection = (1 — permeated conc./feed conc.) × 100. Solvent evaporation time during membrane preparation (○) 30 s; (△) 20 s; (◇) 10 s.

The glucose oxidase membrane was found to be very porous and hydrophilic. According to permeation tests carried out as above, even a macromolecule such as catalase (m.w. = 240,000), can permeate through the membrane. Glucose and oxygen, of course, diffuse easily through the membrane. The amount of membrane-bound glucose oxidase was estimated as 50—60 μg cm^{-2} of membrane. The membrane thus provided good conditions for processes (2) and (3).

Since the teflon membrane was 12.5 μm thick, it had no serious effects on oxygen diffusion. The diffused oxygen was almost instantly reduced at the electrode surface, because a sharp concentration gradient develops across the teflon membrane. Therefore process (5) cannot be rate-determining.

The combination of the two membranes, therefore, has facilitated processes (1)—(4), which has resulted in considerable improvement in the response time for the sensor. The conventional sensor requires at least 30 s to respond to glucose, in contrast to the 10-s response time of the present sensor.

The ultrafiltration membrane has other roles in the improved sensor performance. Not only does it protect the fragile glucose-oxidase membrane from mechanical stress, but it prevents contamination of the immobilized enzyme by blood constituents. These protective effects stabilize the sensor very considerably. Furthermore, the ultrafiltration membrane functions as a noise filter, cutting down mechanical vibration. Thus the noise on the output current was reduced to 0.005—0.01 μA, which allowed reliable glucose determinations to be made above 3×10^{-6} M.

REFERENCES

1 G. G. Guilbault, Handbook of Enzymatic Methods of Analysis, Dekker, New York, 1976.
2 T. M. S. Chang (Ed.), Biomedical Applications of Immobilized Enzymes and Proteins, Plenum Press, New York, 1977.
3 M. Aizawa, S. Kato and S. Suzuki, J. Membr. Sci., 2 (1977) 125.
4 M. Aizawa, S. Suzuki, Y. Nagamura, R. Shinohara and I. Ishiguro, Chem. Lett., (1977) 779.
5 M. Aizawa, S. Kato, S. Suzuki, Y. Nagamura and I. Ishiguro, Kobunshi Ronbunshu, 34 (1977) 813.
6 M. Aizawa, S. Suzuki, Y. Nagamura and I. Ishiguro, J. Solid-Phase Biochem., 4 (1979) 25.
7 M. Aizawa, A. Morioka, H. Matsuoka, S. Suzuki, Y. Nagamura, R. Shinohara and I. Ishiguro, J. Solid-Phase Biochem., 1 (1976) 319.
8 M. Aizawa, A. Morioka and S. Suzuki, J. Membr. Sci., 4 (1978) 221.
9 M. Aizawa, A. Morioka and S. Suzuki, Anal. Biochem., 94 (1979) 22.
10 I. Karube, T. Matsunaga, S. Mitsuda and S. Suzuki, Biotechnol. Bioeng., 19 (1977) 1535.
11 K. Matsumoto, H. Seijo, T. Watanabe, I. Karube and S. Suzuki, Anal. Chim. Acta, 105 (1979) 429.
12 S. J. Updike and G. P. Hicks, Nature (London), 214 (1967) 986.
13 D. L. Williams, A. R. Doig, Jr. and A. Korosi, Anal. Chem., 42 (1970) 118.
14 G. G. Guilbault and G. L. Lubrano, Anal. Chim. Acta, 60 (1972) 254; ibid., 64 (1973) 439.
15 G. Nagy, L. H. von Storp and G. G. Guilbault, Anal. Chim. Acta, 66 (1973) 443.

16 M. Nanjo and G. G. Guilbault, Anal. Chim. Acta, 73 (1974) 367.
17 M. Aizawa and S. Suzuki, Denki Kagaku, 44 (1976) 279.
18 D. R. Thévenot, R. Sternberg, P. R. Coulet, J. Laurent and D. C. Gautheron, Anal. Chem., 51 (1979) 96.
19 S. Ikeda, K. Ito, K. Ito and T. Kondo, Denki Kagaku, 46 (1978) 667.
20 S. Manjikian, Ind. Eng. Chem. Prod. Res. Dev., 6 (1967) 23.
21 G. J. Gittens, P. A. Hitchcock and G. E. Wakley, Desalination, 12 (1973) 315.
22 G. Boari, C. Merli, G. Mossa and R. Passino, Desalination, 16 (1975) 271.
23 M. C. Chan and J. W. McCutchan, Desalination, 17 (1975) 353.

Analytica Chimica Acta, 116 (1980) 315—322

PULSED ROTATION VOLTAMMETRY IN A FLOW-THROUGH CELL

W. J. BLAEDEL* and J. WANG

Department of Chemistry, University of Wisconsin-Madison, Madison, Wisconsin 53706 (U.S.A.)

(Received 16th October 1979)

SUMMARY

A flow cell with a rotating glassy carbon disk electrode has been exploited for voltammetric and amperometric determinations. The high analytical currents due to the efficient mass-transport are coupled with a new hydrodynamic modulation technique that discriminates against the major background currents, resulting in high sensitivity and low detection limits. For a rotated disk electrode immersed in a stream at a constant flow rate, the current difference is measured with the rotation switched on and off. Well defined current—potential curves are obtainable. Mass-transport properties, sensitivity, precision and linearity of response are reported. Modulation rates range from 0.1 to 1 Hz. Cell performance is demonstrated by the anodic oxidations of micromolar concentration levels of ascorbic acid, NADH, and hexacyanoferrate(II).

Increasing attention and effort are being directed toward the adaptation of electrochemical detectors for a variety of analytical flowing systems. Forced convective solid electrodes, operated in the amperometric mode, are frequently used because of their high sensitivity. Various electroanalytical flow cells have been designed for these purposes. These include cells in which the solution flows through an open tubular electrode [1], through a thin layer channel [2], onto a wall-jet electrode [3], and through various porous electrode materials [4]. The characteristic common to all of these configurations is that a solution flows past a stationary electrode. Since the response (i.e. the measured current) of the electrochemical detector is dependent on the rate of mass transport at the electrode surface, the sensitivity is usually increased by increasing the solution flow rate.

Recently the rotating disk electrode (RDE) has been adapted to a flow-through cell in connection with on-line anodic stripping voltammetry [5]. The efficient mass-transport of the rotating disk has been exploited to shorten the deposition time, while low solution flow rates are used. In the present work, the advantages of the RDE flow cell permit the amperometric quantification of low concentrations of non-amalgam forming electroactive species. The use of very low flow rates without sacrificing the sensitivity is an important advantage of detectors in analytical flow systems (e.g. liquid chromatography or the AutoAnalyzer type), which are frequently restricted to low flow rates. The virtual independence of response upon flow rate

permits uncritical control of the flow rate. Proper design of the cell can give a low dead volume of about 100 μl.

The electroanalytical monitoring of very low concentrations is limited by the signal-to-background ratio of the detector. The high signal arising from the efficient mass-transport may be coupled with sensitive techniques designed to discriminate against the background currents. Potential pulse techniques do not offer enhanced sensitivity when employed at solid electrode flow cells [6, 7]. The use of a d.c. offset compensation is not always possible because of changes in background level (caused by variations in solvent composition, flow rate, etc.). Tenfold changes in detectability have been reported by simply changing the magnitude of the background currents at different applied potentials [7]. Efficient background current compensation at a solid electrode may be achieved by using hydrodynamic modulation techniques, in which a difference current is measured between two rates of convective transport. This difference current is purely convective, thereby eliminating the major components of the background current which arise from non-convective sources. The concept of a pulsing or oscillating convective flux to an electrode surface is not new [8, 9]. It has been exploited for continuous flow analysis using the pulsed-flow technique at open tubular [10, 11] and at various porous [12, 13] electrodes. The RDE flow cell permits the development of a new hydrodynamic modulation approach, based on pulsing the rotational speed of the electrode, while maintaining a constant low flow rate. The characteristics and advantages of such a modulation technique are elucidated in this paper.

EXPERIMENTAL

Apparatus

A schematic diagram of the cell is shown in Fig. 1. The body consisted of two plexiglas blocks, one 1 in. thick and the other 1.25 in. thick, held together with four stainless steel bolts (not shown). The silver—silver chloride reference electrode was wound around a plexiglas post (0.225 in. long and 0.55-in. diameter) which extended from the upper block into a cavity (1.125-in. diameter, 0.222 in. deep) in the lower block. Bolting the two blocks together exerted pressure on three cation-exchange membrane washers (0.01-in. thick, 0.3-in. i.d., 1.0-in. o.d., Nafion XR-170, E. I. du Pont de Nemours & Co., Wilmington, DE) located in the cavity of the lower block. This provided a leak-free solution bridge between the working and reference electrodes. A solution flow channel was drilled through the plexiglass body. It consisted of a 2-mm solution inlet, widened to 7,8-mm to accept the working electrode rotated shaft. Solution outflow was maintained through a 2-mm channel branching off from the rotational channel at a right angle. The rotated shaft is a plexiglas sleeve (2.8-in. long, 0.24-in. o.d., 0.1-in. i.d.), on the end of which a glassy carbon rod (2.5-mm o.d.) was set with a low-temperature setting epoxy resin (Hardman Inc., Belleville, NJ). Electrical contact to the

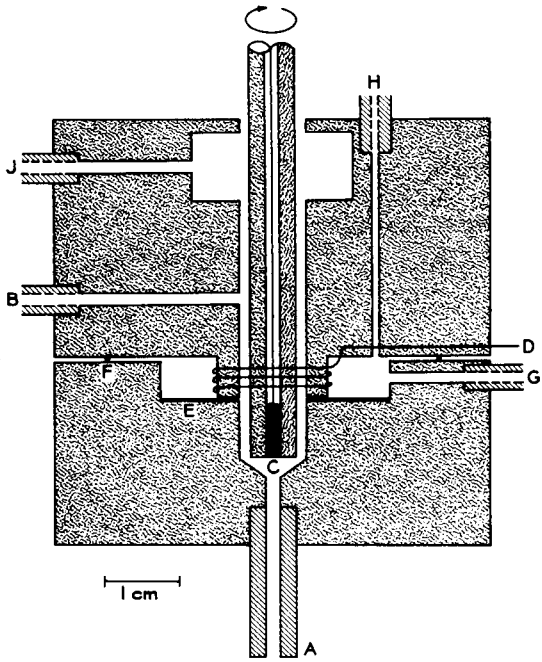

Fig. 1. Flow-through cell with an RDE. (A) Sample solution inlet; (B) sample solution outlet; (C) working electrode; (D) lead to reference electrode; (E) cation-exchange membranes; (F) O-ring; (G) reference solution inlet; (H) reference solution outlet; (J) nitrogen inlet.

glassy carbon rod was made by filling a portion of the plexiglas sleeve with mercury and dipping a stainless steel lead into it. The glassy carbon disk was first roughly polished with silicon carbide papers (No. 400 and 600), followed by a 0.1-μm alumina slurry, until a mirror-like surface was obtained. The glassy carbon disk face was centered in the flow channel, which formed a working electrode compartment with a very low working volume (about 100 μl). The plexiglas shaft did not come in contact with the plexiglas body during its rotation.

Sample solutions were stored above the cell in a 0.5-l glass vessel, containing a fritted glass bubbler for sparging with water-saturated nitrogen. In addition, nitrogen was used to flush the cell cavity at which the rotation shaft entered. Solution flowed from the glass storage vessel to the cell by gravity via 2-mm i.d. glass tubing, the flow rate being measured with a calibrated rotameter (No. 9143, Fischer and Porter, Warminster, PA) placed upstream from the cell. Flow rates were controlled by adjusting a clamp located on a short length of tygon tubing that connected the glass tube and the rotameter. Plexiglas tubes (4-cm long, 6-mm o.d., 2-mm i.d.), cemented to the plexiglas body, were used for some inlets and outlets. The remaining

inlets and outlets were drilled to receive tygon tubing, press-fitted, and sealed with cyclohexanone.

The reference electrode cavity was slowly flushed with 0.1 M KCl saturated with AgCl. All potentials in this paper are given with respect to this reference electrode. The resistance of the cell with the supporting electrolyte solution flowing through was 250 ohms. Such a resistance caused negligible distortion in current—potential curves, and did not affect the amperometric measurements taken at potentials on the plateau, where the limiting current is independent of applied potential. All measurements were made with a Sargent model FS polarograph. The rotation assembly and the rotation counting system were similar to those described previously [9], with the exception that another motor speed controller (model GT-21, G. K. Heller Corp., Bellrose, NY) was used.

Reagents

All solutions were prepared from deionized water (Continental Water System; charcoal bed filter, mixed bed deionizer, 0.2 μm Gelman filter). All chemicals were analytical-reagent grade. Stock solutions (10^{-3} M) of ascorbic acid, NADH, and potassium hexacyanoferrate(II) were made up fresh each day. Boiled deionized water containing 0.5 g l^{-1} $Na_2EDTA \cdot 2H_2O$ was used in the preparation of ascorbic acid solutions to minimize air-oxidation, which is catalyzed by heavy metal ions [14]. The NADH solutions were stored refrigerated at 4°C, and the hexacyanoferrate(II) solutions were stored in the dark. The supporting electrolyte was 0.1 M phosphate buffer (pH 7.4) prepared from a (1 + 4) mixture of KH_2PO_4 and K_2HPO_4 solutions. Aliquots of the stock solution were added to the supporting electrolyte to give the desired concentration.

Procedure

A 250-ml aliquot of the buffer was deaerated with nitrogen for 20 min. During deaeration the working electrode was pretreated (without rotation) while passing the buffer solution through slowly (at 0.5 ml min^{-1}). The pretreatment consisted of applying a potential of +1.35 V for 10 min, then cycling the applied potential between —1.35 V and +1.35 V for an additional 12 min, allowing 3 min at each potential. This was followed by a 1-min period at zero applied potential before use. The pretreatment served to put the glassy carbon surface into a clean and reproducible state prior to the experiment. Following pretreatment, the desired working potential was applied. Steady-state measurements were made after the transient currents decayed, with steady state usually being reached within 15 to 30 min. Pulsed rotation experiments were performed only a short time (15 s to 3 min) after the working potential was applied. Pulsing was achieved by switching manually between a high and low (usually zero rpm) rate, while maintaining a constant flow.

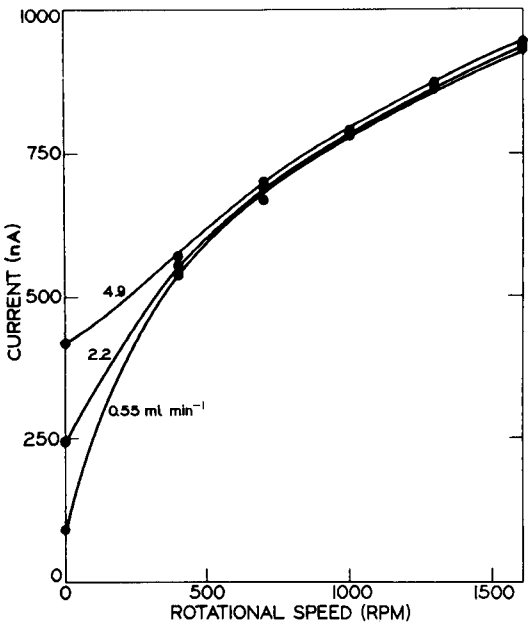

Fig. 2. Dependence of current upon rotation speed for various flow rates. 50 μM $K_4Fe(CN)_6$ in 0.1 M phosphate buffer; applied potential, +0.8V.

RESULTS AND DISCUSSION

Mass transport

The dependences of the steady-state limiting current on the rotation speed for various flow rates are given in Fig. 2. The dependence of the limiting current on flow rate decreases as the rotation speed increases. Above 1000 rpm only a slight increase (of about 1%) in current is observed over a ten-fold range of flow rates. Mass transport at the rotating electrode is 3—10 times more efficient than at the stationary electrode. These characteristics would be advantageous for making measurements in flowing systems with poorly controlled flow rates, or where low flow rates are employed. These data are in accord with studies reported for the anodic stripping RDE flow cell, which employed a different configuration with a much larger dead volume [5]. However, the existence of a flow rate-dependent current was not recognized for that cell. When replotted on a log—log scale, the data of Fig. 2 yield three straight lines for rotation speeds greater than 400 rpm. The slopes of these plots correspond to 0.36, 0.38, and 0.42 for flow rates of 4.9, 2.2, and 0.55 ml min^{-1}, respectively, and appear to approach a value of 0.5, as expected for a well-behaved RDE [15].

Hydrodynamic modulation

Current—time responses of various pulsed-rotation procedures at the RDE flow cell are shown in Fig. 3. The difference current is measured under

constant flow, by switching the rotation speed on and off (traces A,B,D), or by pulsing the rotation speed between two values (trace C). In contrast to previously reported hydrodynamic modulation modes employed in flow cells, these new approaches do not involve any change in the solution flow rate. The choice of the two rates of convective transport for achieving a larger current difference is based on the steady-state data, as discussed in the previous section. Minimum attenuation of the steady-state signal is obtained for a current measurement between a very low flow rate (without rotation) and a high rotation speed at the same flow rate (Fig. 3A). Further study of Fig. 3. indicates that the attenuation of the difference current increases as: the flow rate is increased (B); pulsing between two rotational speeds is applied (C); or the period is decreased (D). It is noteworthy that a 12-fold reduction in the cycling period results in a current diminution of only around 60% (compare A and D, Fig. 3). A detailed study of rapid flow modulation techniques, with sub-second cycling times, has been completed recently for various forms of tubular electrodes [16].

Current—potential curves

Figure 4 shows a pulsed-rotation current—potential curve for the oxidation of 22.5 μM ascorbic acid, along with the corresponding background current. The curves were taken pointwise by making 50-mV changes in applied potential, and waiting about 20 s before applying the rotation pulse. In this way current—potential data were taken within 12 min, compared to more than an hour for steady-state voltammetry [17]. The wave and plateau regions are well-defined, and the background is very low, indicating good correction for currents arising from electrode surface reactions and solvent decomposition. The low background also indicates the absence of electroactive contaminants. The pulsed-rotation half-wave potential is —0.025 V. It should be noted that the shape and the half-wave potential of the hydrodynamic modulation voltammograms should not be expected to be identical

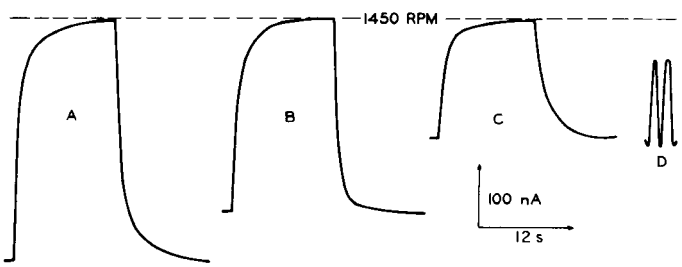

Fig. 3. Current—time curves for the hydrodynamically-modulated RDE. (A and B) Pulsed rotation between 0 and 1450 rpm; (C) pulsed rotation between 500 and 1450 rpm; (D) rapid pulsed rotation between 0 and 1450 rpm. 20 μM $K_4Fe(CN)_6$ in 0.1 M phosphate buffer. Constant flow rate of 1 ml min^{-1} (A,C,D) and 3.4 ml min^{-1} (B); pulsing period, 12 s (A,B,C), 1 s (D); applied potential, +0.75 V.

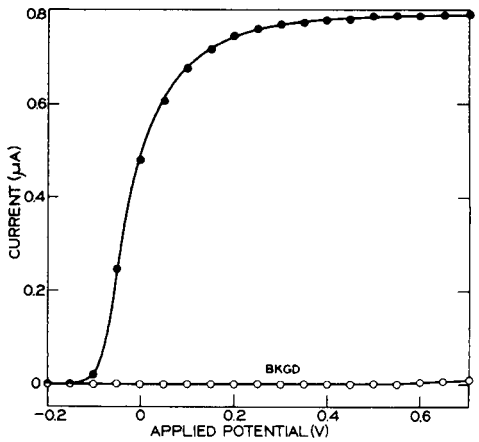

Fig. 4. Hydrodynamic voltammogram for 22.5 μM ascorbic acid. Pulsed rotation between 0 and 1200 rpm; supporting electrolyte, 0.1 M phosphate buffer; flow rate, 0.5 ml min^{-1}.

with those obtained in conventional voltammetry, since convective transport affects both the shape and half-wave potential [18].

Sensitivity and precision

Quantitative evaluation of the RDE flow-cell is based on the linear correlation between the pulsed-rotation current amplitude and the analyte concentration. Six concentration increments from 10 to 80 μM of added hexacyanoferrate(II) yield a linear plot (conditions: rotation on (1200 rpm) and off; continuous flow at 1 ml min^{-1}; +0.8 V applied potential; 0.1 M phosphate buffer). A least-squares analysis of the standard addition data yields a slope of 15.8 ± 0.3 nA μM^{-1} (90% confidence limits).

Figure 5 is a reproduction of a pulsed-rotation chart-record for 1 μM ascorbic acid in 0.1 M phosphate buffer. The blank pulsed-rotation current amounted to 1 nA (too low to be shown in Fig. 5), corresponding to a concentration around 0.04 μM. The non-convective component of the background current that is eliminated by the pulsed rotation technique is about 45 nA. The noise level is very low, about 1% of the total current difference at this level of operation. If the limit of detection is taken to be equal to the noise level, a value around 0.01 μM is obtained.

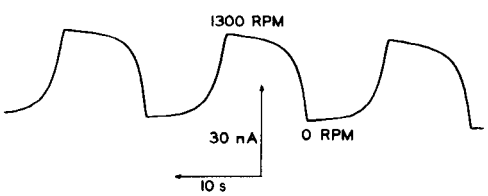

Fig. 5. Pulsed-rotation response for 1 μM ascorbic acid. Solution flow rate, 1 ml min^{-1}; applied potential, +0.65 V; supporting electrolyte, 0.1 M phosphate buffer.

The precision of results was estimated by 22 repeated pulsed-rotation measurements of 10 μM NADH (conditions as in Fig. 5, except that the rotational speed was 0 and 1200 rpm). The pulses were a little sharper than those of Fig. 5. The mean current difference found was 95 nA with a range of 92—97 nA. The relative standard deviation over the complete series was 1.3%.

The same electrode was employed throughout this study. It functioned properly without the need for wiping or polishing between measurements. It seems probable that the daily pretreatment, with fairly high anodic and cathodic potentials, provides adequate cleaning of the electrode surface. More extreme potentials (±1.6 V) were required for surface renewal after the NADH study, probably because of adsorption of its oxidation product [17].

This work was funded in part by the University Sea Grant Program under a grant from the Office of Sea Grant, National Oceanic and Atmospheric Administration, U.S. Department of Commerce, and by the State of Wisconsin.

REFERENCES

1 W. J. Blaedel, C. L. Olson and L. R. Sharma, Anal. Chem., 35 (1963) 2100.
2 P. T. Kissinger, C. Refshauge, R. Dreiling and R. N. Adams, Anal. Lett., 6 (1973) 465.
3 J. Yamada and H. Matsuda, J. Electroanal. Chem., 44 (1973) 189.
4 D. C. Johnson and J. Larochelle, Talanta, 20 (1973) 959.
5 J. Wang and M. Ariel, Anal. Chim. Acta, 99 (1978) 89.
6 D. G. Swartzfager, Anal. Chem., 48 (1976) 2189.
7 W. Lund, M. Hannisdal and T. Greibrokk, J. Chromatogr., 173 (1979) 249.
8 B. Miller, M. Bellavance and S. Bruckenstein, Anal. Chem., 44 (1972) 1983.
9 W. J. Blaedel and R. C. Engstrom, Anal. Chem., 50 (1978) 476.
10 W. J. Blaedel and S. L. Boyer, Anal. Chem., 43 (1971) 1538.
11 W. J. Blaedel and D. Iverson, Anal. Chem., 49 (1977) 1563.
12 W. J. Blaedel and S. L. Boyer, Anal. Chem., 45 (1973) 258.
13 W. J. Blaedel and J. Wang, Anal. Chem., 51 (1979) 799.
14 L. Erdey and G. Svehla, Ascorbinometric Titrations, Akademiai Kiado, Budapest, 1972.
15 V. G. Levich, Physico-Chemical Hydrodynamics, Prentice-Hall, Englewood Cliffs, NJ, 1962.
16 W. J. Blaedel and Z. Yim, Anal. Chem., 52 (1980) 564.
17 W. J. Blaedel and R. A. Jenkins, Anal. Chem., 47 (1975) 1337.
18 J. Jordan and R. A. Javick, Electrochim. Acta, 6 (1962) 23.

Analytica Chimica Acta, 116 (1980) 323—333

THE DIFFERENTIAL PULSE POLAROGRAPHIC DETERMINATION OF MOLYBDENUM IN NITRATE MEDIA

T. E. EDMONDS

Department of Soil Fertility, The Macaulay Institute for Soil Research, Craigiebuckler, Aberdeen AB9 2QJ (Gt. Britain)

(Received 12th November 1979)

SUMMARY

The differential pulse polarographic determination of molybdenum in nitrate media is described. The effects of pH, nitrate concentration, temperature, and cationic and anionic interferents on the peak current are reported. The detection limit is 0.45 $\mu g\ l^{-1}$ for a single scan. Signal averaging can be used to achieve a detection limit of 0.2 $\mu g\ l^{-1}$, and a linear calibration graph over three orders of magnitude. The kinetics and mechanism of the catalytic current are discussed within the framework of a series of equations which describe the relationship between peak current, pulse height, time of measurement and concentration of both analyte and background electrolyte. The key species appears to be electrochemically generated Mo(IV) which is oxidized to Mo(V) by nitrate.

The electrochemical reduction of molybdenum(VI) at the dropping mercury electrode (DME) has been described by many authors [1—36]. Some [20—36] have reported on the catalytic currents that may be obtained when anions such as nitrate, chlorate and perchlorate are present in the background electrolyte. Polarographic methods based on these catalytic currents yield sensitivities of 1×10^{-5}—5×10^{-3} M, and linear calibration graphs are achieved over about two orders of magnitude. Most authors have reported the presence of three polarographic waves. Catalytic phenomena are observed on the second wave. There are several conflicting interpretations of the polarographic behaviour of molybdenum both in the presence and in the absence of oxidative anions. This study investigates the use of the nitrate-mediated catalytic current for the differential pulse polarographic determination of molybdenum. In addition, an attempt is made to elucidate the mechanism of this reduction.

EXPERIMENTAL

The apparatus used has been described previously [36]. A PAR 303 SMDE static mercury drop electrode was used in place of the conventional DME. The SMDE forms a mercury drop which rapidly attains its maximum size. This is achieved by forcing a controlled volume of mercury, from a solenoid-actuated valve, through a short length (12.7 cm) of wide-bore

capillary tubing (0.015 cm). The drop size is static during the measurement cycle, effectively reducing to zero the charging current from drop growth. The improvement in signal-to-noise ratio permits more sensitive analyses. Three drop sizes may be selected, small, medium and large, corresponding to mercury flow rates of 1.14, 2.28, 4.56 mg s^{-1} for a drop time of 1 s. Unless otherwise indicated, a large 1-s drop and a 100-mV pulse at 5 mV s^{-1} were used. Data were acquired on a single-scan basis and were filtered by using a 15-point window. The polarographic cell was thermostatted at 17 ± 0.2°C. All solutions were purged with oxygen-free nitrogen prior to analysis, and were blanketed with nitrogen during the analysis. Aristar (BDH) nitric acid and Ultrapure (Alfa Products) potassium nitrate were used to prepare the electrolytes, otherwise all chemicals were reagent grade. A molybdenum solution (1000 mg l^{-1}) was prepared from $(NH_4)_6Mo_7O_{24}$, and working concentrations were obtained by serial dilution.

RESULTS AND DISCUSSION

Background electrolyte

Violanda and Cooke [29] indicated that by increasing the concentration of the nitric acid background electrolyte, larger signals could be obtained for molybdenum by d.c. polarography. In Fig. 1A, the peak current i_p is plotted against nitric acid concentration from 0.04 M to 1.43 M, for each of the three drop sizes of the SMDE 303. The three drop sizes were selected to gauge the performance of the SMDE: the dashed lines in Fig. 1A indicate how closely this conforms to theory with respect to drop area. After an initial steep rise in i_p, the molybdenum signal follows a linear relationship with nitric acid concentration. The variation in the peak potential E_p for these conditions is shown in Fig. 1B. Higher acidities were not used because dissolution of the mercury drop increased the background currents. The separate effects of pH and nitrate concentration on i_p are shown in Fig. 2.

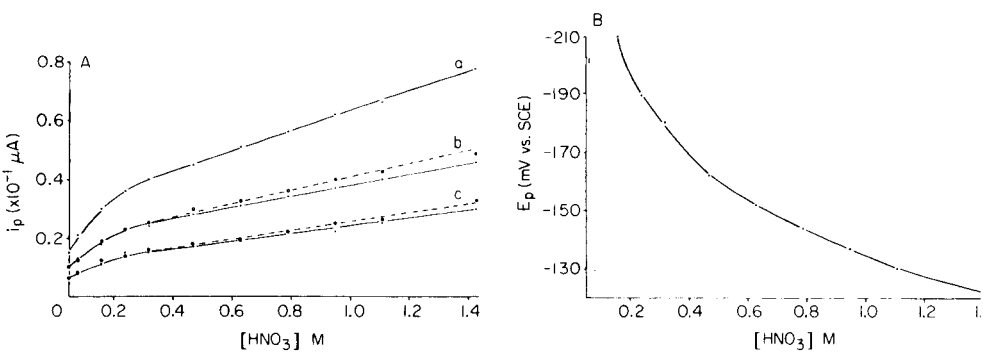

Fig. 1. Variation with nitric acid concentration of: (A) i_p for (a) large, (b) medium, (c) small drop size; (B) E_p vs. SCE. 50 × 10^{-3} μg Mo ml^{-1}. Dashed lines represent calculated currents based on drop areas.

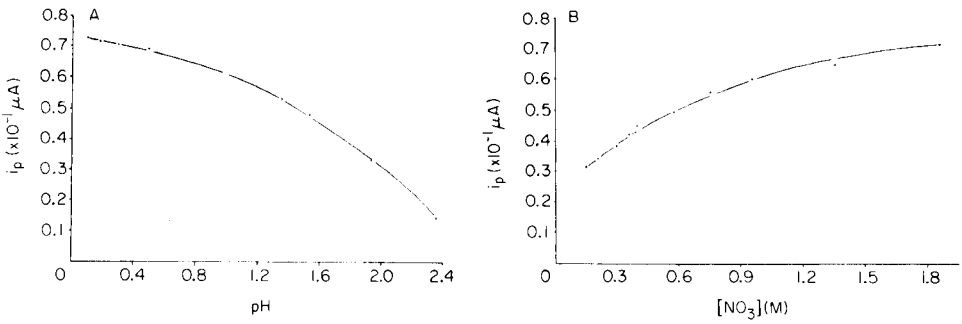

Fig. 2. Variation of i_p with: (A) pH at a total nitrate concentration of 1.5 M; (B) nitrate concentration at pH 0.9. 50 × 10^{-3} μg Mo ml^{-1}.

Clearly both pH and nitrate concentration are important factors for maximizing i_p, but neither shows a linear relationship with the molybdenum signal, so that the linearity of Fig. 1A would appear to be fortuitous. Violanda and Cooke [29] demonstrated a linear relationship between i_d, the diffusion current, and nitric acid concentration for d.c. polarography, but did not examine pH and nitrate concentration effects separately.

Temperature effects

The temperature coefficient of the molybdenum peak current, i_p, in 0.5 M nitric acid was determined over the range 15—27°C. Temperature increments of 2°C were used, and the coefficient calculated at each increment by the method described by Meites [37]. The seven results were averaged to give a value of 3.6% K^{-1}. This is less than half the value obtained by Violanda and Cooke [29], but these authors gave no clear indication of the method used to determine the coefficient.

Sensitivity and detection limits

The calibration graphs for molybdenum in 0.5 M nitric acid are shown in Fig. 3. A linear range of 3 orders of magnitude, from 2 × 10^{-4} to 2 × 10^{-1} mg l^{-1} was obtained. The data points were achieved by signal-averaging five scans. The detection limit of this method was discussed earlier [36]. The improved signal-to-noise ratio of the SMDE enabled this detection limit to be lowered to 0.45 μg Mo l^{-1} for a single scan. The SMDE did not always provide better detection limits. When the large drop size was used with a rapid drop time (0.5 s), erratic signals were obtained. Bond and Grabaric [38] reported disturbances in the faradaic current at drop times between 0.2 s and 0.4 s for a pressurized mercury electrode. Here, the cause was thought to be turbulence in the solution, arising from the very rapid growth of the drop. At short drop times, there was insufficient time for this turbulence to decay, thus disturbing the diffusion patterns around the drop and giving rise to irreproducible signals.

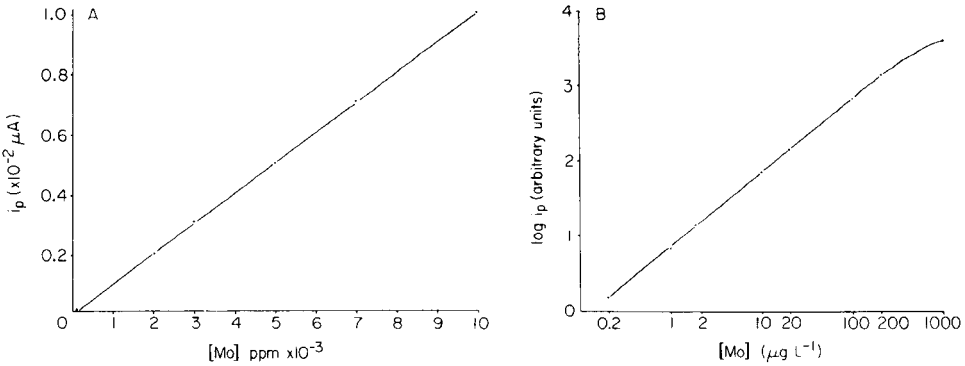

Fig. 3. Calibration curves for (A) 0.2—10 μg Mo l^{-1}; (B) 0.2—1000 μg Mo l^{-1}. 0.6 M nitric acid.

Interferences

Interferences on the molybdenum peak were of two kinds: those that decreased the height of the peak by changing the rate of chemical reaction, and those that provided closely overlapping peaks. Several interfering species were investigated; the results are summarized in Table 1. The interferences from overlapping peaks may be ameliorated by changing the conditions of the determination. Thus, in 0.6 M nitric acid and with a pulse amplitude of 100 mV and scanning at 5 mV s^{-1}, 5×10^{-2} mg Cu l^{-1} is the maximum tolerable concentration for accurate determination of 20 μg Mo l^{-1}. In 0.16 M HNO_3—1 M KNO_3, at 2 mV s^{-1} and with a 50-mV pulse, 3×10^{-1} mg Cu l^{-1} may be tolerated. Moderate interferences affecting peak height can generally be overcome by applying the method of standard additions.

For electrolytes containing the same nitrate concentration, decrease in pH within the range 2.4—0.1 gives increased peak currents. However, in the more strongly acidic media the molybdenum signal shifts to more anodic potentials and begins to merge with the mercury dissolution peak; also the hydrogen peak becomes more pronounced and may even merge with the cathodic tail of the molybdenum peak. At about pH 0.8, the molybdenum peak is much better separated and may be measured more precisely.

Although this determination of molybdenum is sensitive and relatively free from interferences, close control of the composition of the background electrolyte is necessary because of the effect on both i_p and E_p, unless standard additions are used. The variability of E_p with background electrolyte concentration can be advantageous in that judicious selection of the electrolyte may help to overcome interference problems.

Mechanism and kinetics

To understand the mechanism of the catalytic wave of molybdenum in nitrate media it is necessary to relate i_p to the various instrumental and chemical parameters of the d.p.p. system.

TABLE 1

Interferences on the molybdenum determination

Interferent	Max. tolerable concentration (mg l^{-1})	Interferent	Max. tolerable concentration (mg l^{-1})
Effect on 30 μg Mo l^{-1}		*Effect on 20 μg Mo l^{-1}*	
Cl^-	35[a]	Cu(II)	0.05[b]
SO_4^{2-}	1700[a]	Pb(II)	20[c]
PO_4^{3-}	95[a]	W(VI)	2[c]
SO_3^{2-}	80[a]	As(III)	2[c]
Mn(VII)	5.5[a]	Sn(IV)	0.5[c]
Se(IV)	0.2[a]	Tl(III)	0.5[c]
		Ti(IV)	3[c]

[a]Significant decrease in i_p above these values. [b]More anodic peak. [c]More cathodic peak.

Catalytic waves in polarography arise from the following mechanisms:

$$O + ne \rightleftharpoons R\ ;\ R + X \xrightarrow{k_f} O + Z \tag{1}$$

$$O + ne \xrightarrow{{}^1k_f} R\ ;\ R + X \xrightarrow{k_f} O + Z \tag{2}$$

where O and R are the oxidized and reduced forms of the analyte species, respectively, and X is a species that is not reducible at the potential at which O is reduced. X is chemically reduced by R to yield Z and O, thus replenishing the supply of O at the electrode, and causing a greater current to flow than could be obtained by diffusion of O to the electrode alone.

Nicholson and Shain [39] have shown that for voltammetry at a stationary electrode, the relationship between the applied potential (E) and the current (i) for mechanisms (1) and (2) may be given by

$$i = nFA\,(Dk_f)^{1/2}\,C_o/[1 + \exp\,(nF(E - E_{1/2})/RT)] \tag{3}$$

for reversible reactions, and

$$i = nFA\,(Dl_f)^{1/2}\,C_o \Big/ \left\{1 + \exp\left[\frac{\alpha nF}{RT}\left((E - E_0) + \frac{RT}{\alpha n_a F}\ln\left(\frac{(\Pi Db)^{1/2}}{k_s}\right)\right.\right.\right.$$

$$\left.\left.\left. + \frac{RT}{\alpha n_a F}\ln\left(\frac{k_f}{\Pi a}\right)^{1/2}\right)\right]\right\} \tag{4}$$

for irreversible reactions. Here n is the number of electrons in the electrochemical reduction, n_a the number of electrons in the rate-determining step, k_f the rate constant of the chemical redox reaction, ${}^1k_f$ the rate constant of the irreversible reduction; $l_f = k_f + {}^1k_f$; k_s is the rate constant of the O—R couple at $E = E_0$; $b = \alpha n_a Fv/RT$; $a = nFv/RT$; v is the sweep rate, α the transfer coefficient, C_o the bulk concentration of O, D the diffusion coefficient of O, and A the area of the electrode; F, R, T, E_0 and $E_{1/2}$ have their usual meaning.

Galus [40] includes the term $(C_x)^{1/2}$ in the numerator of both eqns. (3) and (4), as well as incorporating it into the denominator of eqn. (4):

$$i = nFAC_o\,(Dl_fC_x)^{1/2}\Big/\left\{1 + \exp\left[\frac{\alpha n_a F}{RT}\left((E - E_0) + \frac{RT}{\alpha n_a F}\ln\left(\frac{(Db\Pi)^{1/2}}{k_s}\right)\right.\right.\right.$$

$$\left.\left.\left. + \frac{RT}{\alpha n_a F}\ln\left(\frac{k_f C_x}{\Pi a}\right)^{1/2}\right)\right]\right\} \qquad (5)$$

where C_x is the bulk concentration of X. The exponential term of eqn. (5) may be rewritten as:

$$\exp\left[(\alpha n_a F\,(E - E_0)/RT) + \ln\,(Dk_f\alpha n_a C_x/k_s^2 n)^{1/2}\right]$$

If $k_f \gg {}^1k_f$ then $n_a = n$, and eqn. (5) becomes

$$i = nFAC_o\,(Dk_fC_x)^{1/2}/\{1 + \exp\,[(\alpha nF\,(E - E_0)/RT) + H]\} \qquad (6)$$

where $H = \ln\,(Dk_f\alpha C_x/k_s^2)^{1/2}$.

In the limiting case, where $E_0 \gg E$, or $E_{1/2} \gg E$ (i.e. at more cathodic potentials), the exponential function in eqns. (3) and (6) will tend to zero. In this case the limiting current, i_{lim} is given by

$$i_{lim} = nFA\,C_o\,(Dk_fC_x)^{1/2} \qquad (7)$$

Thus eqns. (3) and (6) may be rewritten as:

$$i = i_{lim}\,\{1 + \exp\,[nF\,(E - E_{1/2})/RT]\}^{-1} \qquad (8)$$

$$i = i_{lim}\,\{1 + \exp\,[(\alpha nF\,(E - E_0)/RT) + H]\}^{-1} \qquad (9)$$

Equation (8) resembles the equation for a reversible O—R couple without subsequent catalytic reactions. Hence, by the same arguments as used by Parry and Osteryoung [41], it can be shown that in d.p.p., for a pulse amplitude ΔE, the peak current, (i_p), is given by

$$i_p = i_{lim}\,(\sigma - 1)/(\sigma + 1) \qquad (10)$$

where $\sigma = \exp\,(\Delta E\,nF/2RT)$ and $\Delta E = E_2 - E_1$. It can also be shown that $E_p = E_{1/2} - (\Delta E/2)$.

To develop eqn. (9) in a similar manner, the following expressions are useful:

$$P = \exp\,\{[((E_1 + E_2)/2) - E_0]\,(\alpha nF/RT) + H\}$$

$${}^1\sigma = \exp\,[(E_2 - E_1)\,\alpha nF/2RT]$$

Thus from eqn. (9)

$$\Delta i = i_{lim}\,(P\,{}^1\sigma^2 - P)/({}^1\sigma + P + P\,{}^1\sigma^2 + P\,{}^1\sigma)$$

where Δi is the change in current on moving from potential E_1 to E_2. To obtain i_p, let $P \to 1$. Thus $i_p = i_{lim}\,[({}^1\sigma - 1)/({}^1\sigma + 1)]$ and

$$E_p = E_0 - (\Delta E/2) - HRT/\alpha nF \quad (11)$$

That is, in d.p.p., for an irreversible reduction followed by a catalytic reaction, $E_p \propto \ln (C_x)^{1/2}$.

Table 2 shows the change in E_p (ΔE_p) calculated for values of C_x from 0.1 M to 2.0 M. Common values of D, α, n, k_s and k_f were substituted in eqn. (11) in order to give an indication of the direction and magnitude of the shift in E_p. Several experiments were carried out in which molybdenum was determined by d.p.p. in electrolytes with nitrate concentrations in the range 0.15—1.86 M. A systematic shift in E_p was not observed in any of these experiments. This indicates that the electrochemical reduction preceding the chemical reaction is reversible, in which case i_p should obey eqn. (10). In Fig. 4A the experimental curves for i_p vs. ΔE, the pulse height, are compared with theoretical curves from eqn. (10) in which a 1e reduction is assumed. At each nitrate concentration, the experimental point at 100-mV pulse amplitude was used to calculate an effective i_{lim}, because eqn. (7) takes no account of the change in i_{lim} with the time (t) that has elapsed between pulse application and signal measurement. The theoretical points were calculated on the basis of the effective i_{lim} values. The agreement between the theoretical curves and the experimental curves is excellent: theoretical curves for $n = 2$ showed no such agreement.

For a catalytic reaction following an electrochemical reduction, the decay in i_{lim} with time t for a flat, stationary electrode, following a voltage step, has been shown by Delahay and Stiehl [42] to be given by:

$$i = nFAD^{1/2} C_o [(k_f C_x)^{1/2} \text{ erf } (k_f C_x t)^{1/2} + \exp(-k_f C_x t)/(\Pi t)^{1/2}] \quad (12)$$

where erf $(k_f C_x t)^{1/2} = 2\Pi^{-1/2} \int_0^{(k_f C_x t)^{1/2}} \exp(-u^2) du$. Thus eqn. (10) may be rewritten, by substituting eqn. (12) for i_{lim}

$$i_p = nFAD^{1/2} C_o [(k_f C_x)^{1/2} \text{ erf } (k_f C_x t)^{1/2} + \exp(-k_f C_x t)/(\Pi t)^{1/2}]$$
$$[(\sigma - 1)/(\sigma + 1)] (7/3)^{1/2} \quad (13)$$

The factor $(7/3)^{1/2}$ is included to account for the spherical nature of the mercury drop, in the same manner as Ilkovic [43].

To calculate k_f from experimental data, it would be necessary to evaluate the error function erf $(k_f C_x t)^{1/2}$ for each value of C_x over a range of expected k_f values. The corresponding error function values and k_f estimates could then be introduced into eqn. (13), and the calculated i_p compared with the experimental i_p, to determine which was the best k_f value. From previous work, it was expected that $k_f \approx 1.2 \times 10^3$ l mol^{-1} s^{-1}. Over the concentration

TABLE 2

Variation of ΔE_p with C_x, where $\Delta E_p = HRT/\alpha nF$

C_x (M)	0.1	0.3	0.7	1.3	2.0
ΔE_p (mV)	298	326	346	364	375

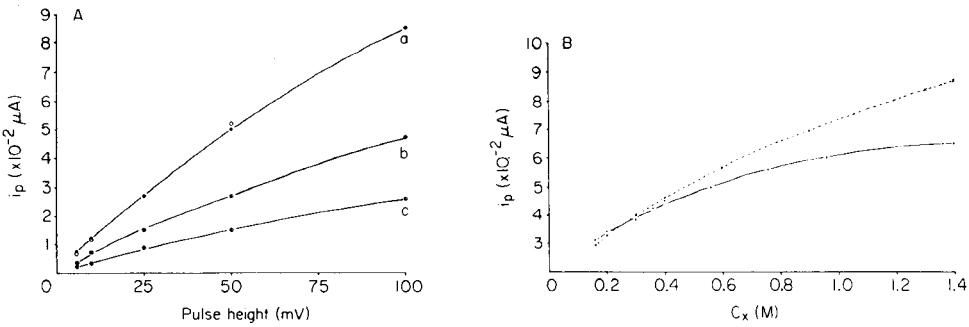

Fig. 4. (A) Variation of i_p with pulse height: (•) experimental points for 0.1 mg Mo l^{-1}, with a medium drop for (a) 1.43 M HNO_3, (b) 0.3 M HNO_3, (c) 0.16 M HNO_3; (○) theoretical results calculated from eqn. (10) for n = 1. (B) Variation of i_p with C_x: (•) experimental results for 0.05 mg Mo l^{-1}; (×) theoretical results from eqn. (13).

range 0.16—1.86 M and with t = 0.0485 s, this gives a value for the error function which approaches unity. Also, the exponential function in eqn. (13) tends to zero, thus calculation of k_f is rendered much easier.

Figure 4B shows the graph of i_p vs. C_x plotted for a series of experimental points, along with the theoretical points calculated from eqn. (13). The values of F and D came from the literature; A, C_o, C_x, t, σ were derived from the experimental conditions. A k_f value was calculated from eqn. (13) for each of the first five experimental points, and an average taken of these values. The agreement between the two curves is reasonable up to C_x values of 0.4 M, but above this, the experimental values fall short of the predicted results. Delahay and Stiehl [42] found reasonable agreement between the theoretical and experimental results for C_x concentrations up to 0.36 M, in the d.c. polarographic determination of the iron(II)/hydrogen peroxide catalytic wave but higher values of C_x were not tested. Haight [23] found a linear relationship between i and $[NO_3]^{1/2}$ over 0.025—0.3 M nitrate in a d.c. polarographic study of the Mo/nitrate system; again, higher C_x values were not listed.

The value of k_f, calculated from the present work is 1.26 (±0.1) × 10^3 l mol^{-1} s^{-1} at 25°C. Kolthoff and Hodara [26] calculated a k_f value of 2.3 × 10^2 l mol^{-1} s^{-1}, for the Mo/NO_3^- catalytic wave in 1 M H_2SO_4 on the basis of a 2e reduction prior to the chemical step. For a 1e reduction in a nitrate medium, in which the current is about 25% greater, recalculation of their result yields k_f = 1.44 × 10^3 l mol^{-1} s^{-1} at 25°C. Haight [23] arrived at $k_f = 2700/n^2$ l mol^{-1} s^{-1} at 25°C, using a spherical correction factor of 2.25 instead of $(7/3)^{1/2}$, and a higher value for D in eqn. (13). His value may be recalculated with the constants used here to give k_f = 0.9 × 10^3 l mol^{-1} s^{-1} at 25°C. In a later paper, Bergh and Haight [44] assigned a value of 2 for n. The three k_f values are remarkably close, bearing in mind the different techniques with which the values were measured. The shortfall in the experimental results with respect to theoretical data above 0.4 M nitrate may be due to several causes.

The derivation of the i—t relationship for catalytic waves [42] makes no allowance for the consumption of X at the electrode surface; for moderate values of k_f this is of little consequence. In cases where k_f is large there could be an initial rapid depletion of X at the electrode, with a concomitant decrease in i. X can obviously be supplied by diffusion from the bulk solution, but if this initial rate of replenishment does not match the rate of consumption of X, i will drop below the value predicted by eqn. (13). This effect will be most noticeable at small values of t. For larger t values, the rate of X consumption decreases because of depletion of O at the electrode surface, and i will return to the predicted value as C_x(electrode) tends to C_x(bulk solution). Thus, Christian et al. [35] reported limited sensitivity for molybdenum in 2 M KNO_3 at pH 1.6 (2 μg Mo l^{-1}), and no catalytic signal for 0.2 mg Mo l^{-1} in 1 M nitric acid. These authors used d.p.p. with a pulse duration of 19 ms. In the present work, the delay between pulse application and current measurement was 48.5 ms; Kolthoff and Hodara used t = 4.96 s [26].

The diffusion coefficient of an electroactive species is a function of the viscosity of the solution in which the measurements are made [37]. Generally, i is proportional to $\eta^{-1/2}$, where η is the viscosity of the solution. The wide range of nitrate concentrations used here covers a range of relative viscosities from 0.994 to 0.974. On this basis, the value of i_p would be expected to decrease by about 1% over the full range of nitrate concentrations.

The solutions used to obtain the experimental data for Fig. 4 were at about pH 0.9. It can be seen from Fig. 2 that in decreasing the pH from 0.9 to 0.1 for a solution 1.5 M in nitrate, i_p increases by 17%. An experimental value of 0.65 μA was obtained for i_p in 1.5 M nitrate at pH 0.9; the calculated value for i_p under these conditions is some 35% greater than the experimental result. Hence it appears that decreasing the pH could make up some of the shortfall in the experimental i_p values with respect to the theoretical values. It is unlikely that the hydrogen ion is directly involved in the catalytic reaction. The effect is probably due to alterations in the equilibria between the various forms of polymeric molybdenum(VI) species in solution [45].

The principal difference between the treatment of Kolthoff and Hodara [26] and this study lies in the interpretation of the electrochemical step preceding the catalytic reaction. Kolthoff and Hodara considered the mechanism to be a 2e reduction involving Mo(V) → Mo(III), whence nitrate ion may oxidize the Mo(III) to Mo(V). Haight and Bergh [23, 44] proposed a 2e reduction involving Mo(VI) → Mo(IV), with nitrate reoxidizing Mo(IV) to Mo(VI).

Neither mechanism agrees with the evidence of this work, that a 1e transition precedes the catalytic reaction. It is possible that the second reduction wave of molybdenum in nitrate media involves Mo(VI) → Mo(V) as reported by Carritt [3] for hydrochloric acid media (0.8 M) and Kolthoff and Hodara [11] for sulphuric acid media (2.5 M). Guymon and Spence [46] have shown that in bulk solution Mo(V) is oxidized to Mo(VI) by nitrate in a

tartrate buffer. The key species appeared to be complexed monomeric Mo(V), and although the rate constant was rather low (2.14×10^{-3} (mol $l^{-1})^{-1/2}$ min^{-1}) the authors indicated that in situ generation of Mo(V) gave much larger values for k. The Mo(V) monomer was shown [47] to have a finite lifetime in acidic aqueous media, and to be generated by electrochemical reduction at a mercury cathode. The dimerization rate constant of this species in a tartrate buffer was 2.9×10^3 l mol^{-1} min^{-1}. However, in acidic chloride media, this reaction was reported to be much faster.

Haight and Sager [48] have shown that in bulk solution molybdenum(IV) is an active reducing agent, whereas, under similar circumstances, Souchay [13] found that Mo(V) and Mo(III) could not reduce nitrate. Haight [23] proposed the following scheme as a possibility for the second molybdenum wave: Mo(V) + e → Mo(IV) and 2Mo(IV) → Mo(V) + Mo(III). The disproportionation of Mo(IV) proceeds at a sufficient rate to render the second polarographic wave a kinetically-controlled, apparently 2e, wave. Thus, an alternative explanation for the 1e step could be that in the presence of nitrate, the Mo(IV) is oxidized to Mo(V), not Mo(VI) as proposed [23, 44].

On balance, the latter alternative mechanism seems more probable. There is no firm evidence that the second reduction wave of molybdenum is reversible. Should this wave be due to reduction of a different species of Mo(VI) to Mo(V), then this process must be reversible to satisfy the data presented in this paper. In fact, even the first reduction wave of molybdenum, which is certainly due to Mo(VI) → Mo(V), is not reversible, hence a second more cathodic wave is almost bound to be irreversible. The work of Guymon and Spence [46] indicates that the active form of Mo(V) is the monomer, but in nitrate media the dimerization rate will be rapid. Direct figures are not available; Ojo et al. [49] reported a rate constant of $1.71 \pm 0.1 \times 10^5$ l mol^{-1} s^{-1} for the dimerization of $[HMoO_3]^+$ in 0.2—3.0 M perchloric acid solution at 25°C. Hence the Mo(V) monomer generated at the DME would be likely to experience fierce competition between dimerization and oxidation by nitrate.

Conclusion

The d.p.p. determination of molybdenum in nitrate media is both sensitive and selective. The sequence of reactions that gives rise to the Mo/nitrate wave may be written thus:

$$Mo(VI) + e \rightarrow Mo(V) \quad (A); \quad Mo(V) + e \rightleftharpoons Mo(IV) \quad (B)$$
$$Mo(IV) + NO_3 \rightarrow Mo(V) + Z \quad (C); \quad 2Mo(IV) \rightarrow Mo(V) + Mo(III) \quad (D)$$

Reaction (A) is the initial reduction wave of a typical molybdenum polarogram. Reaction (B) is a fast reversible reduction occurring at the potentials of the second molybdenum wave. In the presence of nitrate, reaction (C) occurs, replenishing the supply of Mo(V) at the electrode at a rate well in excess of Mo(VI) diffusion. In the absence of nitrate, (D) takes place, giving the wave from (B) a kinetic character. Z represents the reduction products of nitrate.

REFERENCES

1 R. von Stackelberg, P. Klinger, W. Koch and E. Krath, Tech. Mitt. Krupp. Forsch., 2 (1939) 59.
2 R. Holtje and R. Geyer, Z. Anorg. Allg. Chem., 246 (1941) 58.
3 D. E. Carritt, Ph.D. Thesis, Harvard, 1947.
4 G. Jongh, Ph.D. Thesis, Amsterdam, 1950.
5 I. M. Kolthoff and E. P. Parry, J. Am. Chem. Soc., 73 (1951) 5315.
6 L. Meites, Anal. Chem., 25 (1953) 1752.
7 E. P. Parry and M. G. Yakubik, Anal. Chem., 26 (1954) 1294.
8 R. L. Pecsok and R. M. Parkhurst, Anal. Chem., 27 (1955) 1920.
9 L. Guibe and P. Souchay, J. Chim. Phys., 54 (1957) 684.
10 K. Grasshof and H. Hahn, Fresenius Z. Anal. Chem., 186 (1962) 132.
11 I. M. Kolthoff and I. Hodara, J. Electroanal. Chem., 4 (1962) 369.
12 R. Ripan and N. Calu, Bull. Soc. Chim. Fr., 11 (1964) 2902.
13 P. Souchay, Talanta, 12 (1965) 1187.
14 J. J. Wittick and G. A. Rechnitz, Anal. Chem., 37 (1965) 816.
15 A. Cumakov and P. Lutonska, Rostl. Vyroba, 12 (1966) 525.
16 M. Cadiot and M. Lamache-Duhameaux, C.R. Acad. Sci., Ser. C, 264 (1967) 1282.
17 J. P. G. Farr and G. O. A. Laditan, J. Less-Common Met., 36 (1974) 151.
18 P. Jost, P. Lagrange, M. Wolff and J. Schwing, J. Less-common Met., 36 (1974) 169.
19 K. S. Pakhamova and L. P. Volkova, Zh. Anal. Khim., 31 (1976) 952.
20 F. A. Uhl, Fresenius Z. Anal. Chem., 110 (1937) 102.
21 G. P. Haight, Anal. Chem., 23 (1951) 1505.
22 M. G. Johnson and R. J. Robinson, Anal. Chem., 24 (1952) 366.
23 G. P. Haight, Acta Chem. Scand., 15 (1961) 2012.
24 W. Jakob and J. Chojnacka, Rocz. Chem., 35 (1961) 13.
25 Hsiao-Hsia Kao and Tien-Chiu Shih, K'o Hsueh T'ung Pao, 7 (1963) 53.
26 I. M. Kolthoff and I. Hodara, J. Electroanal. Chem., 5 (1963) 2.
27 R. V. Bikbulatova and S. I. Sinyakova, Zh. Anal. Khim., 19 (1964) 1434.
28 V. A. Bolshakov and G. P. Stoilov, Pochvovedenie, 5 (1964) 95.
29 A. T. Violanda and W. D. Cooke, Anal. Chem., 36 (1964) 2287.
30 E. G. Chikryzova and L. G. Kiriyak, Zh. Anal. Khim., 27 (1972) 1747.
31 F. Pottkamp, F. Umland and H. Reimann, Fresenius Z. Anal. Chem., 26 (1972) 102.
32 E. G. Chikryzova and S. M. Bardina, Zh. Anal. Khim., 29 (1974) 2414.
33 A. A. Kaplin, V. F. Slipchenko and N. N. Zubrovd, Izv. Tomsk. Politekh. Inst. Im. S. M. Kirova., 272 (1972) 41.
34 B. Stack and K. Schoene, Mikrochim. Acta, 2 (1977) 565.
35 G. D. Christian, J. L. Vandenbalck and G. J. Patriarche, Anal. Chim. Acta, 108 (1979) 149.
36 T. E. Edmonds, Anal. Chim. Acta, 108 (1979) 155.
37 L. Meites, Polarographic Techniques, J. Wiley, New York, 1965.
38 A. M. Bond and B. S. Grabaric, Anal. Chim. Acta, 88 (1977) 227.
39 R. S. Nicholson and I. Shain, Anal. Chem., 36 (1964) 706.
40 Z. Galus, Fundamentals of Electrochemical Analysis, Ellis Horwood, Chichester, 1976.
41 E. P. Parry and R. A. Osteryoung, Anal. Chem., 37 (1965) 1634.
42 P. Delahay and G. L. Stiehl, J. Am. Chem. Soc., 74 (1952) 3500.
43 D. Ilkovic, Collect. Czech. Chem. Commun., 6 (1934) 498.
44 A. A. Bergh and G. P. Haight, Inorg. Chem., 1 (1962) 688.
45 L. Krumenacker, Ann. Chim., 7 (1972) 425.
46 E. P. Guymon and J. T. Spence, J. Phys. Chem., 70 (1966) 1964.
47 J. T. Spence and M. Heydanek, Inorg. Chem., 6 (1967) 1489.
48 G. P. Haight and W. F. Sager, J. Am. Chem. Soc., 74 (1952) 6056.
49 J. F. Ojo, R. S. Taylor and A. G. Sykes, J. Chem. Soc. Dalton Trans., 6 (1975) 500.

Analytica Chimica Acta, 116 (1980) 335—343

COULOMETRIC DETERMINATION OF TOTAL SULFUR IN ORGANIC AND INORGANIC MATERIALS AFTER A TUNGSTEN TRIOXIDE—QUARTZ TUBE DECOMPOSITION METHOD

M. C. VAN GRONDELLE* and P. J. ZEEN
Koninklijke/Shell-Laboratorium (Shell Research B.V.), Amsterdam (The Netherlands)
(Received 19th October 1979)

SUMMARY

A method is described for the determination of total sulfur in samples that differ widely in nature and origin, such as aqueous solutions, coal, catalysts and other organic and inorganic materials. The samples are introduced into the heated part of a quartz tube, where the presence of tungsten trioxide in combination with an oxygen stream ensures complete decomposition of inorganic sulfur compounds. The sulfur dioxide formed is titrated microcoulometrically. Concentrations ranging from 1 mg kg^{-1} to several percent can be determined with a standard deviation of 1.5% relative.

Owing to the tighter specifications imposed on products and effluents, the determination of total sulfur in a wide variety of materials such as residual fuels, coal, catalysts, waste water, polymers, deposits, etc. is required to an increasing extent. Quite often the samples concerned contain metals or mixtures of organic and inorganic sulfur compounds. In such cases the well-known direct combustion in a quartz tube, followed, for example, by microcoulometric titration of the sulfur dioxide formed [1—3], gives low results if stable involatile sulfur compounds are retained, e.g. in the combustion residue. The existing methods for analysis of these samples frequently involve time-consuming decomposition techniques, such as fusion procedures, acid digestion or oxygen flask combustion, followed by ion exchange and a titrimetric finish. In many cases high blank values originating from reagents are introduced, resulting in relatively high detection limits.

It was therefore considered worthwhile to look for a combustion/decomposition system that converts both organic and inorganic compounds to gaseous products directly in the quartz tube. A suitable system was obtained upon addition of tungsten trioxide — a compound capable of converting inorganic sulfur compounds quantitatively to gaseous SO_2/SO_3 — to the sample boat in the quartz tube. This speeded up the analysis considerably and also resulted in a much lower limit of detection.

EXPERIMENTAL

Apparatus

The apparatus consists of a combustion section, followed by scrubbers to

remove interfering compounds, and a titration cell controlled by a Dohrmann microcoulometer (Fig. 1). The sample (5 mg maximum for organic products) is weighed on, or injected into, a small platinum boat, which contains a layer of tungsten trioxide. The boat is moved into the hot part of the quartz tube by means of a ladle and magnet. Sample combustion and decomposition take place in pure oxygen; gaseous sulfur oxides are formed. Under the conditions used, the equilibrium $2SO_2 + O_2 \rightleftharpoons 2SO_3$ gives about 80% SO_2 [2]. The gases are dried in a small scrubber containing phosphoric acid, and passed first through a gas splitter system and then through a silver wool scrubber to remove interfering halogen compounds [3]. Finally, the sulfur dioxide is titrated with electrolytically generated iodine, the read-out appearing as a peak. Calibration is done by analysing a standard solution.

Details of the quartz tube and sample inlet system used are depicted in Fig. 2. The secondary oxygen stream, which is introduced through a capillary extending about one third of the way inside the heated part of the quartz tube, ensures complete (flash-type) combustion of organic products. Typical gas flows are 125 ml min^{-1} for the primary and 225 ml min^{-1} for the secondary oxygen stream. The scrubbers (B and E in Fig. 1) have been described previously [2, 3]. Initially 75% sulfuric acid was used in scrubber E, but this was later replaced by concentrated phosphoric acid, as the sulfuric acid sometimes led to peak broadening; the effect was far less pronounced with 88% orthophosphoric acid.

Choice of decomposition aid and conditions

For a material to be acceptable as an aid for the conversion of sulfur from stable inorganic compounds to SO_2/SO_3, it should fulfill at least three conditions. First, it must liberate the sulfur quantitatively within about one minute at a temperature no higher than 1100°C (the maximum obtainable

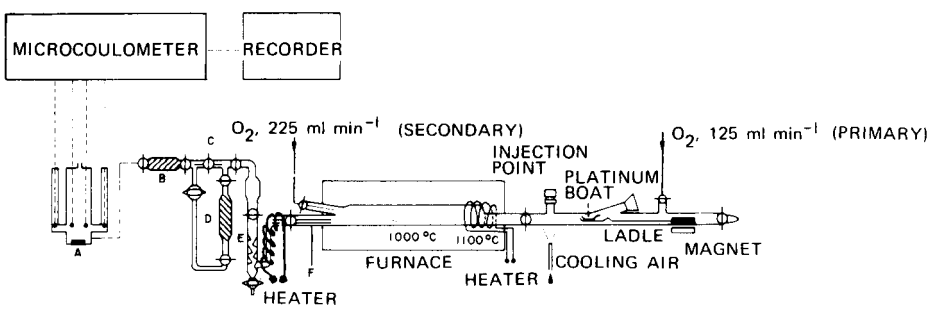

Fig. 1. Diagram of apparatus (A) titration cell and stirrer; (B) scrubber with silver wool; (C) capillary; (D) scrubber with K_2CO_3 on active carbon; (E) scrubber with conc. H_3PO_4; (F) outlet tube.

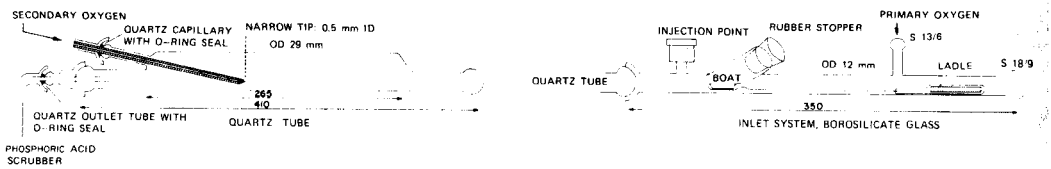

Fig. 2. Quartz tube and sample inlet system.

temperature with standard laboratory furnaces). Secondly, it must not retain sulfur in the colder parts of the quartz tube outlet. Thirdly, it must not act as a catalyst for the oxidation of sulfur dioxide to sulfur trioxide in these colder parts of the quartz tube. Only acidic compounds can be considered for use, because the expected gases, SO_2 and SO_3, are acidic. Many of the possible sintering agents or fluxes mentioned in the literature are employed at extremely high temperatures, e.g. vanadium pentoxide is used at 1400°C or higher for the determination of sulfur in glasses [4] steel [5] and geological materials [6], and iron(III) phosphate [7] at 1200°C for the determination of sulfur in coal. Reagents reported for pyrohydrolysis at 900–1200°C are tungsten and uranium oxides [8, 9]. In the work described here, several materials were tested for the analysis of an aqueous solution of sodium sulfate containing 500 mg S kg^{-1}. The peak shape and SO_2 recovery were compared with those obtained for pure organic standards. The results are given in Table 1; boron trioxide was tested but gave zero recovery whereas molybdenum trioxide volatilizes.

Vanadium pentoxide, although frequently mentioned in the literature [5], gave low recoveries, probably because it catalyses the oxidation of SO_2 to SO_3. Tungsten trioxide proved most satisfactory of the reagents tested. Moreover, the sample mixture in the platinum boat did not melt but remained as a loose powder, as has been noted by many workers since the initial introduction of tungsten trioxide as a combustion aid in elemental analysis [10]. Tungsten trioxide was therefore used in all further work.

Initially, a furnace temperature of about 1000°C was adopted, but as a result of the temperature gradient the temperature of the inlet part of the furnace did not exceed about 950°C. At this temperature certain solid inorganic samples (e.g., coal ash) gave rise to tailing peaks. Raising the inlet temperature to 1100°C, by means of a supplementary heating coil, improved the results. With these solid samples, the "sintering" of sample and tungsten trioxide is the rate-determining step and is therefore highly temperature-dependent [9].

The amount of tungsten trioxide used in the boat is not critical, but should be large enough to maintain an acidic environment. Normally a boat of about 10 × 4 × 4 mm is used, half-filled with tungsten trioxide. Sintered sample residues can easily be removed. When aqueous solutions or virtually ash-free organic materials are analysed, the tungsten trioxide can be used many times before addition or replacement becomes necessary.

TABLE 1

Comparison of various decomposition aids
(Test sample used: Na_2SO_4 in water, 500 mg S kg^{-1}. Furnace temperature: 1000°C.)

	None	WO_3	Cr_2O_3	V_2O_5	Fe_2O_3	Co_3O_4	$FePO_4$	UO_2	TiO_2
Recovery within 5 min	Very low	Good	Good	Low	Slightly low	Slightly low	Low	Low	Slightly low
Peak shape	Bad tailing	Excellent	Good	Tailing[a]	Tailing	Tailing	Poor[b]	Tailing	Tailing

[a]Reagent melts. [b]Compound reacts too slowly.

Optimization of the coulometric titration

The iodimetric titration is essentially the same as that described previously [2, 3]. The electrolyte used here contained 0.002% KI, 2% KBr, 0.05% acetic acid and a few milligrams of Thyodene, a commercial water-soluble starch preparation. The well-known problem of the oxidation of iodide by oxygen, which is catalyzed by light, nitrogen oxides and metals, was minimized by choosing a mixed bromide/iodide electrolyte [2] with the iodide concentration kept as low as possible, and by making the titration cell of amber glass. A high bromide concentration was used to ensure that the titration efficiency remained 100% even at the relatively high current densities applied for titrating large amounts of sulfur dioxide.

In the analysis of certain metal-containing samples, traces of volatile metals may accumulate in the titration cell, resulting in negative signals (metal-induced oxidation of the iodide). This effect can be suppressed by adding Thyodene to the electrolyte. About 20 mg was employed; the amount is not critical, but too much gives a positive baseline shift, which decreases slowly.

The correct choice of bias potential is essential for good performance of the titration cell. The bias potential is related to the free iodine concentration in the electrolyte [1]. The optimum bias is governed by two contradictory effects: the iodine concentration should be high enough to prevent SO_2 escaping from the electrolyte but it should be as low as possible for optimum stability, because of the volatility of iodine. In practice, two separate bias settings are used: one for high and the other for low sulfur contents. The maximum amount of sulfur that can be titrated with the standard cell is 1.5 μg. A cell with a volume four times that of the standard cell is therefore preferred for the titration of larger amounts of sulfur. Typical operating conditions are given in Table 2. The optimum bias can vary from cell to cell and must be determined. It can be found by measuring the baseline shift caused by the continuous evaporation of iodine when gas is passed through the cell [2].

For samples with sulfur contents in the percent range, which cannot be dissolved and diluted, a chemical gas splitter was developed. Details of its construction are shown in Fig. 3. With the stopcock open, about 95% of the gas passes through the scrubber containing potassium carbonate on active carbon, where the SO_2 is replaced by carbon dioxide. The main components of the combustion gases, carbon dioxide and oxygen (water vapor is removed in the phosphoric acid scrubber), are not absorbed. The split ratio is governed by the ratio of the resistance of the capillary to that of the scrubber and can be altered by changing the resistance of the capillary. The split ratio is not affected by pressure changes brought about by sample introduction as all the gas eventually enters the cell.

RESULTS AND DISCUSSION

Recovery of sulfur from various types of compounds

The recovery of sulfur as sulfur dioxide found when tungsten trioxide is used, is the same for organic and inorganic compounds and is independent of concentration (Table 3). The recovery is about 80%, which is close to the

TABLE 2

Typical operating conditions of the titration cell

Amount of S to be titrated (ng)		Bias (mV)	Baseline shift[c] (mV)
Standard cell[a]	Large cell[b]		
1—300	10—1200	$x + 20$[d]	0.8
Up to 1500	Up to 6000	x	4

[a]Cell containing 15 ml of electrolyte. [b]Cell containing 60 ml of electrolyte. [c]Measured at a 999 Ω setting and a gas flow of 350 ml min^{-1}. [d]x mV is the optimum bias found for a particular cell.

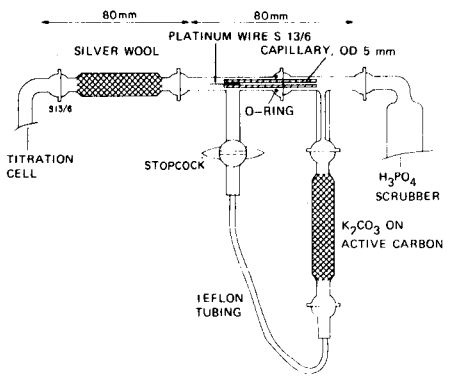

Fig. 3. Detail of the stream splitter.

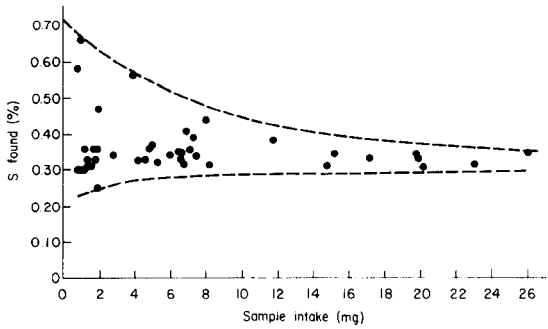

Fig. 4. Effect of amount of intake on precision of repeated analyses of African coal ground to <250 μm (ash content 14%).

theoretical value calculated for the SO_2/SO_3 equilibrium at 1000°C when oxygen only is used. The recovery must remain constant and must not be influenced by accumulation of metals in the system. Small amounts of volatile metals or metal oxides tend to collect on the cooler parts of the outlet tube, which is, therefore, the most critical part of the apparatus, particularly as SO_2 may be oxidized to SO_3 in these cooler parts of the outlet section. Fortunately, when tungsten trioxide is used, an inert layer is constantly formed in the quartz outlet tube, thereby suppressing the catalytic action of other metals and obviating these problems. The outlet tube is cleaned or replaced when appreciable deposits become visible, usually once every two weeks. In analysis of samples containing large amounts of relatively volatile metals such as silver, more frequent replacement is necessary. The outlet tube is kept in position with an O-ring seal (Fig. 2) and is easy to replace.

To assess the applicability of the procedure to samples containing various metals, some pure inorganic compounds were analyzed (Table 4). Small sample sizes between 0.1 and 1 mg were used, in combination with a gas split ratio of about 0.02. Of the compounds tested only calcium sulfate gave rise to problems, because it does not react with tungsten trioxide at 1100°C; the results were improved when powdered graphite was added to the sample boat as its combustion resulted in a much higher temperature. Most other sulfur-containing salts are less stable and should be easily decomposed at temperatures over 950°C. Examples of the determination of sulfur in various

TABLE 3

Recovery for organic and inorganic solutions

Sodium sulfate in water	(mg kg^{-1})	5.64		140	765		765	14000
Dibenzyl disulfide in gas oil	(mg kg^{-1})		100			1000		
Recovery (%)		80	79	79	77	80	2.18[a]	2.16[a]

[a]Gas splitter used.

TABLE 4

Determination of sulfur in pure inorganic compounds

Compound		Ag_2SO_4	$BaSO_4$	$PbSO_4$	$HgSO_4$	$MgSO_4$	$CaSO_4$
S found	(%w)	10.2	13.8	10.7	10.6	26.6	<3[a]; 23[b]
S calculated	(%w)	10.3	13.7	10.6	10.8	26.8	26.6

[a]Tungsten trioxide only. [b]Tungsten trioxide and graphite added.

sulfates and sulfides have been given by Budesinsky and Krumlova [11], who analyzed salts of Cu, Mn, Th, U and Ni.

Applications

The method has been used for analyzing a variety of products; aqueous solutions, solid catalysts, doped oil products, coal, etc. Table 5 compares some results with those obtained by other methods such as hydroiodic acid reduction [3], gravimetry, peroxide fusion, high-temperature combustion [7], etc. Good agreement is found in both the percentage and the parts per million ranges.

The results for some oil-contaminated waters and ethylene oxide catalysts are slightly higher than those expected from the results obtained with the hydroiodic acid reduction method [3]. This discrepancy is caused by the presence of organic sulfur compounds which are not completely co-determined in the reduction method, in contrast to the new method, which determines both organic and inorganic compounds. The presence of relatively large amounts of silver in the solid catalysts did not present any difficulties and sample sizes up to 20 mg could be used. However, it is important that a large excess of tungsten trioxide should be maintained in the boat.

Blank effects play an important role in determining the limit of detection. The tungsten trioxide itself can be made completely sulfur-free by heating it to 1000°C. When samples with low sulfur contents must be analyzed after a series with very high ones, it is sometimes necessary to wash the ladle and inlet system with water and acetone in order to restore low blank values. When the weighing-boat procedure is used, e.g., with solid catalysts, relatively large signals can be generated by boat and flux alone. To minimize these blank effects, the clean boat should not be exposed to the atmosphere for periods longer than are absolutely necessary for weighing. In practice the limit of detection is about 1 mg kg^{-1} for samples of about 5 mg.

The initial results obtained with coal samples, particularly those having a very high ash content, showed very poor repeatability. As the sample size strongly influenced the precision (see Fig. 4), it was thought that the samples had not been ground to a sufficiently small particle size. Calculations made in our laboratory and based on the assumption that particles of pyritic sulfur were present (worst possible case), showed that the whole sample

TABLE 5

Determination of total sulfur in various samples

Sample type			Found (mg kg^{-1})	Expected (mg kg^{-1})
Oil-contaminated groundwater,		A	14.3	3.4
		B	2.3	1.6
		C	12	3.6
		D	5.3	2.4
Caustic solution, 20% NaOH, 0.04% Ca			280	275
Caustic solution, 20% NaOH, 0.04% Ca			158	151
Ethylene oxide catalyst, 7% Ag		A	0.5	0.5
		B	60	55
		C	130	112
			(%)	(%)
Acceptor catalyst	5% Cu,	35% Al	3.69	3.52
Catalyst dust	13% Fe,	39% Al	0.046	0.06
Fly ash	50% SiO_2,	25% Al	0.36	0.4
Doped oil	6% Ca		0.34	0.34
Doped oil	12% Ca		0.054	0.057
Mixture of calcium salts (60%) and organic materials			0.54[a]	0.58
Japanese coal,	<88 μm	15% ash	1.81	1.75
Oklahoma coal,	<88 μm	5% ash	0.57	0.54
Belgian coal,	<88 μm	28% ash	0.95	0.95

[a]Graphite added.

had to be ground until all of it passed through a 88-μm sieve. In this case a standard deviation of better than 0.035% absolute might be expected for a sample size of 10 mg. This was confirmed by analysis of various sample fractions. For instance, a Belgian coal, containing 1% S and having an ash content of 28%, gave a standard deviation of 0.067% for a fraction of particle size <250 μm, compared to 0.025% for a fraction of <88 μm.

Table 5 shows that the average sulfur contents found for various coal samples are in good agreement with those obtained by other methods.

Conclusions

The tungsten trioxide—quartz tube—coulometric method is now frequently and successfully used in this laboratory for almost all sample types. The essential element is the tungsten trioxide/quartz tube combination as this guarantees a proper decomposition of the sample. As to the method of detection, techniques other than microcoulometry, e.g., mass spectrometry [13], can also be considered for application. The microcoulometric finish is, however, extremely sensitive and therefore has the advantage that it requires only small sample sizes; thus the sample/tungsten trioxide ratio is low and contamination of the quartz tube is limited.

REFERENCES

1 F. C. A. Killer in R. Belcher (Ed.), Instrumental Organic Elemental Analysis, Academic Press, London, 1977.
2 M. C. van Grondelle, P. J. Zeen and F. van de Craats, Anal. Chim. Acta, 100 (1978) 439.
3 M. C. van Grondelle, F. van de Craats and J. D. van der Laarse, Anal. Chim. Acta, 92 (1977) 267.
4 W. J. Beesly and B. R. Chamberlain, Talanta, 21 (1973) 318.
5 K. E. Burke, Anal. Chem., 39 (1967) 1727.
6 J. Lange and H. Brumsack, Fresenius Z. Anal. Chem., 286 (1977) 361.
7 W. Lädrach and J. D. van der Laarse, Anal. Chim. Acta, 94 (1977) 213.
8 G. Tölg, Talanta, 19 (1972) 1489.
9 Z. Šulcek, P. Povondre and J. Doležal, Anal. Chem., 6 (1977) 255.
10 R. Belcher, J. E. Fildes and A. J. Nutten, Anal. Chim. Acta, 13 (1955) 431.
11 B. Buděšínský and L. Krumlová, Anal. Chim. Acta, 39 (1967) 375.
12 H. C. E. van Leuven, Fresenius Z. Anal. Chem., 264 (1973) 220.

Analytica Chimica Acta, 116 (1980) 345—351

SEPARATION OF DIXANTHOGEN AND SULPHUR XANTHATES BY H.P.L.C.
Disproportionation of Sulphur Dixanthates

R. T. HONEYMAN and R. R. SCHRIEKE*

Department of Chemistry, Ballarat College of Advanced Education, Mount Helen, Victoria 3350 (Australia)

G. WINTER

Division of Mineral Chemistry, CSIRO Chemical Research Laboratories, P.O. Box 124, Port Melbourne, Victoria 3207 (Australia)

(Received 10th October 1979)

SUMMARY

High-performance liquid chromatography on C_{18} reverse-phase or silica gel columns, with methanol—water (85:15) or n-hexane, respectively, as mobile phase, is used to separate dixanthogens and sulphur xanthates with different alkyl groups. Detection limits are as low as 1 ng (0.05 ppm) with u.v. detectors. When molecular emission cavity analysis is used for the detector, detection limits are reduced to ca. 0.25 ng (0.013 ppm). In aqueous methanol, alkyl sulphur dixanthates, $(ROCS_2)_2S$, disproportionate to yield mixtures of the corresponding dixanthogen, $(ROCS_2)_2$, alkyl sulphur monoxanthates, $(ROCS_2)_2S_2$, and dixanthates.

Since the successful application in 1925 by Keller [1] of xanthates for the froth flotation separation of sulphide minerals from gangues in their ores and from each other, several theories have been proposed to explain the mechanism whereby certain particles are rendered hydrophobic and thus floatable. There is general agreement [2—8] that the principal process taking place at the surface of sulphide minerals during flotation with xanthate collectors is oxidation of the xanthate to dixanthogen. Evidence has also been presented [9] for the formation of metal xanthates so that a mixed electrochemical mechanism may be operating. Winter has suggested a further possibility that sulphur xanthates may also be formed as part of the overall mechanism [10].

In an attempt to determine the possible role of dixanthogen and sulphur xanthates in the flotation of sulphide minerals, methods were investigated for separating, detecting and analysing xanthates, dixanthogen and sulphur xanthates at very low concentrations. The two techniques investigated were molecular emission cavity analysis (m.e.c.a.) [11] and high-performance liquid chromatography (h.p.l.c.) [12—14]. M.e.c.a. is a sensitive analytical technique for sulphur compounds [15, 16]. It is selective for the less volatile inorganic species and also provides a rapid and sensitive means of determining

sulphur-containing organic compounds such as drugs, amino acids and proteins [17]. Separation by h.p.l.c. is said to be successful for mixtures of symmetrical and asymmetrical dixanthogens alone and with xanthic esters and xanthates [13, 14, 18]. Although Bond et al. [19] described a polarographic technique for determining such compounds, it does not lend itself to the analysis of complex mixtures.

This paper describes studies on the h.p.l.c. separation of xanthate species likely to be formed during the flotation of sulphide minerals, including ethyldixanthogen and ethyl sulphur xanthates, as well as methyldixanthogen and methyl sulphur xanthates.

EXPERIMENTAL

Chemicals and syntheses

The solvents used for the synthetic work (benzene, petroleum ether and diethyl ether) were all analytical-reagent grade and were not purified further. The solvents used for h.p.l.c. were water, methanol and n-hexane. Deionised-distilled water was filtered and degassed immediately before use. The methanol (Ajax Chemicals, Unichrom reagent, purified for h.p.l.c.) and n-hexane (Ajax Chemicals, Spectrosol) were filtered (0.45-μm Millipore filter) and degassed immediately before use.

Reagent-grade materials were used in all preparations, except for sulphur dichloride, SCl_2, which was distilled from phosphorus trichloride immediately before use.

Alkali xanthates and dixanthogens were prepared by known methods [10, 20]. Sulphur xanthates were prepared by the method described by Winter [10]. The dixanthogens were recrystallised from petroleum ether (40—60°C). Except for methyl sulphur dixanthate, which was recrystallised several times from petroleum ether, all sulphur xanthates were obtained as oils which could not be crystallised.

Instrumentation

All h.p.l.c. experiments were done with an Altex Model 100A solvent metering system, an Altex Model 153 analytical u.v. single-wave-length (254 nm) detector (10-mm path length, 8-μl cell), and a Rikadenki Model B140 chart recorder. Injections (20 μl) were made onto two columns. Column (a) had a 250 mm × 4.6 mm C_{18} reverse-phase (5-μm particle size) packing and the mobile phase was methanol—water (85:15) with a flow rate of 0.5 cm^3 min^{-1} at 720 psi and 20°C. Column (b) had a 250 mm × 4.6 mm silica gel (5-μm particle size) packing and the mobile phase was n-hexane, with a flow rate of 0.5 cm^3 min^{-1} at 240 psi and 20°C.

The m.e.c.a. spectrophotometer used in this work [21] was constructed from a modified Beckman Model B flame emission spectrometer, in which the electrical system was replaced with a Varian-Techtron Model 1200 a.c. amplifier, chopper and photomultiplier. The burner was of the pre-mix type,

with a 1.25-cm diameter head containing 19 evenly spaced holes. For aqueous solutions, a carbon cavity (6 mm diam., 4 mm depth) was used, and for hexane solutions an aluminium cavity (6 mm × 4 mm). A hydrogen—nitrogen flame with flow rates of 3.2 l min^{-1} and 7.0 l min^{-1}, respectively, was always used.

General procedure

A sample (5 μl) of each fraction of eluent collected from the column was manually injected into the cavity in the vertical position. The cavity was rotated into a horizontal position 10 mm into the flame and with the centre of the cavity 18 mm above the burner top. The cavity was air-cooled to room temperature prior to each injection. The S_2 emission at 384 nm was measured as a function of time. Peak heights were measured. Calibration curves were obtained by using standard solutions of dixanthogen. Detection limits were determined by progressive dilution until a signal-to-noise ratio of 2:1 was obtained.

RESULTS AND DISCUSSION

Since it has been shown [15—17] that different sulphur-containing compounds can be estimated satisfactorily in mixtures by m.e.c.a., it was hoped that this technique could be applied to the direct measurement of mixtures of dixanthogen and sulphur xanthates. Although emission profiles showed minor differences for these compounds (see Fig. 1,a—c), separation was not possible because t_m values [11] were almost indistinguishable. However, the sensitivity was very high and detection limits of ca. 0.25 ng of sulphur were obtained.

The log—log calibration curves were linear over the range 2.2—10 ppm S, and had the equation $\log I = 1.34 \log [S] + 0.81$, where I is the emission intensity.

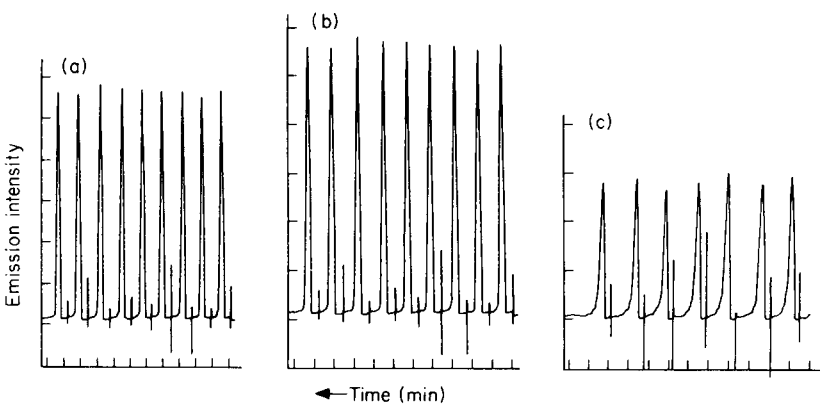

Fig. 1. Repeated m.e.c.a. emissions (hexane solvent; aluminium cavity, H_2/N_2 flame) from (a) ethyl dixanthogen (4 ppm); (b) ethyl sulphur dixanthate (1.07 ppm); (c) ethyl sulphur monoxanthate (7.05 ppm).

The solvent was not evaporated before the introduction of the cavity into the flame, as this technique resulted in irreproducible, instantaneous S_2 emissions.

To achieve a separation of dixanthogen and sulphur xanthates, various chromatographic techniques were investigated. Gas—liquid chromatography proved unsuitable since extensive decomposition of these compounds occurred at the minimum operating temperatures of the columns. The technique of h.p.l.c. was then investigated, because this can be operated at room temperature. Two different solvent systems were investigated.

Methanol—water solvents

For the separation of dixanthogens with different alkyl chains, Hasty [13] successfully used water—methanol mixtures. This was confirmed, and it was found that separation according to chain length can be effected for the alkyl sulphur mono- and di-xanthates by using a C_{18} reverse-phase column. With methanol alone, separation on the column was not achieved, but with methanol—water mixtures, good separation was observed although the m.e.c.a. detection proved unsatisfactory. When aluminium was used as the cavity material, single sharp emissions were obtained with sulphur compounds in pure methanol. However, the presence of water in this solvent resulted in a splitting of the S_2 emission, and the extent of splitting and peak intensities depended on the methanol—water ratio. In contrast, aqueous solutions gave reproducible sharp signals in a graphite cavity, but the presence of methanol (or other organic solvents) delayed and depressed the S_2 emissions. This is illustrated in Table 1. U.v. absorption was therefore used as a detection technique for methanol—water mixtures.

The degree of separation was directly related to the proportion of water in the mobile phase. For each alkyl series of sulphur xanthates and corresponding dixanthogen, good separation with minimum analysis time was achieved when the proportion of methanol to water in the mobile phase was 85:15 (v/v), as shown in Fig. 2 for ethyl xanthates.

TABLE 1

Some m.e.c.a. responses in different cavity materials and solvent systems

Compound	Mobile phase	Cavity material	t_m (s)	Peak height (mV)	Peak width (s)[a]
$(C_2H_5OCS_2)_2$	Methanol	Al	8	120	1
$(C_2H_5OCS_2)_2$	MeOH—water (85:15)	Al	5, 10	80, 46	1, 1.5
$(C_2H_5OCS_2)_2$	Hexane	Al	5.7	142	1.2
$K(C_2H_5OCS_2)$	H_2O	C	7.5	75	3.0
$(C_2H_5OCS_2)_2$	MeOH—water (85:15)	C	12	50	10
$(C_2H_5OCS_2)_2$	Methanol	C	15	28	12.5

[a]Measured at half peak height.

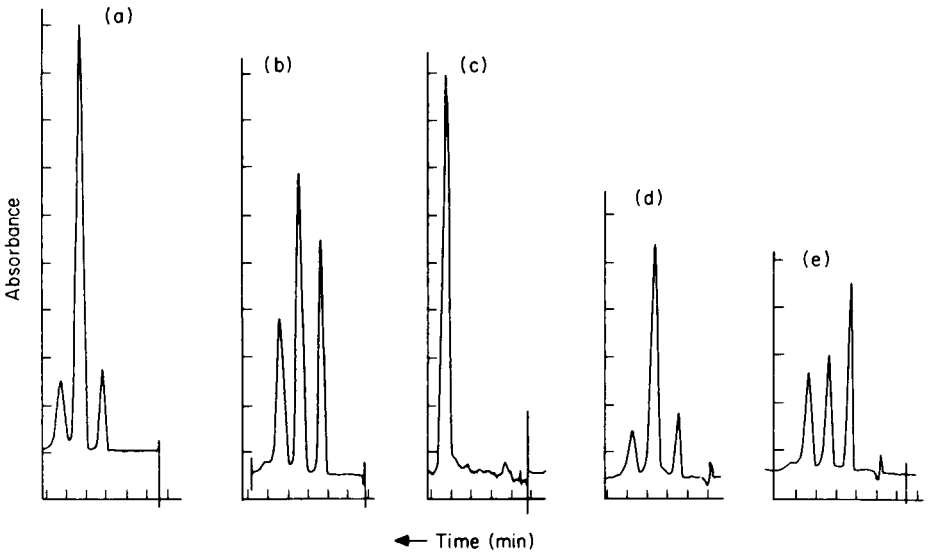

Fig. 2. H.p.l.c. traces for ethyl sulphur dixanthate C_{18} column, 85:15 methanol—water, 1 cm^3 min^{-1}, 1130—1150 psi, u.v.-detection): (a) freshly prepared sample; (b) sample (a) after standing for 20 h; (c) fraction (ii) from (a) run immediately; (d) fraction (ii) from (a) run after standing for 1 h; (e) fraction (ii) from (a) after standing for 23 h.

Ethyl dixanthogen gave a single peak which was used as a reference (R_t = 1.00) for calculating relative retention times (R_t). Methyl dixanthogen also gave a single peak with R_t = 0.802. Freshly prepared samples of ethyl sulphur dixanthate gave three peaks with relative retention times of 1.00, 1.42 and 1.82. The corresponding fractions were collected and identified by their characteristic u.v. spectra [10] as the dixanthogen, sulphur dixanthate and sulphur monoxanthate, respectively. When the major fraction, ethyl sulphur dixanthate, was collected and rechromatographed, these same fractions were invariably obtained (Fig. 2. c—e). This same phenomenon was observed with the methyl analogue. It appears that, in this solvent, sulphur dixanthates undergo disproportionation:

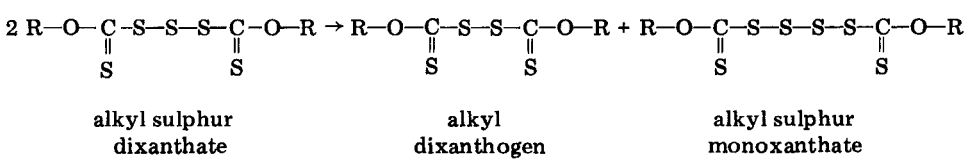

When the alkyl sulphur monoxanthate fractions were rechromatographed, they did not show any breakdown.

n-Hexane solvent

It has been shown previously [10] that sulphur xanthates are stable in n-hexane and this was chosen as an alternative mobile phase. A polar support is

TABLE 2

Relative retention times for some dixanthogens and sulphur xanthates
(For columns (a) and (b), see Experimental.)

Compound	R_t (Column a)	R_t (Column b)	Compound	R_t (Column a)	R_t (Column b)
$(C_2H_5OCS_2)_2$	1.00	1.00	$(CH_3OCS_2)_2$	0.80	1.06
$(C_2H_5OCS_2)_2S$	1.42	0.89	$(CH_3OCS_2)_2S$	1.03	0.95
$(C_2H_5OCS_2)_2S_2$	1.82	0.79	$(CH_3OCS_2)_2S_2$	1.29	0.86

required for this non-polar solvent, and silica gel was found to be satisfactory. The methods of detection were u.v. absorption and m.e.c.a. Although hexane was less flexible than the mixed solvent system in that retention times could not be varied by gradient elution, effective separation of the xanthates was achieved. This system also proved less effective for separating given sulphur xanthates with different alkyl groups, since these have similar relative retention times (see Table 2). However, alkyl sulphur dixanthates did not disproportionate on standing in hexane or on the column.

The alkyl sulphur dixanthates were purified to give satisfactory sulphur analyses and u.v. and i.r. spectra that corresponded closely with those reported by Winter [10]. Their chromatography in the hexane—silica gel system invariably showed the presence of both the corresponding dixanthogen and sulphur monoxanthate. Collection and further chromatography of the main fraction gave a single sharp peak, showing that adsorption from hexane can be used for the purification of sulphur xanthates.

Elution, detection limits and application

In the C_{18}—methanol—water system, the order of elution followed increasing molecular weight. This order was reversed in the silica gel–hexane system (see Table 2). Eckhardt et al. [18] obtained u.v. detection limits of

TABLE 3

Detection limits after h.p.l.c. separation
[Systems A and B involve columns (a) and (b), respectively with u.v. detection. System C involves column (b) with m.e.c.a. detection.]

Compound	log ϵ (at 254 nm)	Detection limit (ng)		
		System A	System B	System C
$(C_2H_5OCS_2)_2$	4.2	4	1	0.25
$(C_2H_5OCS_2)_2S$	4.1	6	1.8	0.4
$(C_2H_5OCS_2)_2S_2$	4.2	5	2	0.5
$(CH_3OCS_2)_2$	4.1	4	0.8	0.25
$(CH_3OCS_2)_2S$	4.0	—	—	0.3
$(CH_3OCS_2)_2S_2$	4.1	6	1.8	0.4

10 ng for dixanthogens in a C_{18}—methanol—water system. This compares with ca. 4 ng for all species in the present investigation, as shown in Table 3. With the silica gel—hexane system, detection limits as low as 1 ng were obtained for dixanthogens with a u.v. detector and ca. 0.25 ng with a m.e.c.a. detector.

The method was applied to simulated flotation liquors represented by aqueous dispersions of dixanthogen and sulphur xanthates. These were extracted with hexane and the extracts analysed on a silica gel column. All the species introduced were readily detected at concentrations as low as 0.05 ppm in the emulsions.

The authors thank Mr. P. Brady, Chemistry Department, Royal Melbourne Institute of Technology, for helpful discussions on h.p.l.c.

REFERENCES

1 C. H. Keller, U.S. Patent 1,554,216,1925.
2 R. Tolun and J. Kitchner, Trans. Inst. Min. Metall., 73 (1963) 313.
3 S. G. Salamy and J. C. Nixon, Aust. J. Chem., 7 (1954) 146.
4 R. J. Gardner and R. Woods, Aust. J. Chem., 26 (1973) 1635; 27 (1974), 2139; 30 (1977) 981.
5 I. N. Plaskin and R.Sh. Shafeen, Inst. Min. Metall. Bull., 72 (1963) 715.
6 R. Woods, J. Phys. Chem., 75 (1971) 354; Proc. Aust. Inst. Min. Metall., 241 (1972) 53. Aust. J. Chem., 25 (1972) 2329.
7 M. C. Fuerstenau, M. C., Kuhn and D. A. Elgillani, Trans. AIME, 241 (1968) 148.
8 A. Granville, N. P. Finkelstein and S. A. Allison, Inst. Min. Metall., Trans., Sect. C, 81 (1972) 1.
9 Q. Taggart, G. Delguidice and O. Ziehl, Trans. AIME, 112 (1934) 267.
10 G. Winter, Inorg. Nucl. Chem. Lett., 11 (1975) 113.
11 R. Belcher, S. L. Bogdanski and A. Townshend, Anal. Chim. Acta, 67 (1973) 1.
12 K. Tsui and W. Morozowich (eds.), GLC and HPLC Determination of Therapeutic Agents, Part I, Dekker, New York, 1978.
13 R. A. Hasty, Analyst, 101 (1976) 828.
14 R. A. Hasty, Analyst, 102 (1977) 519.
15 R. Belcher, S. L. Bogdanski, D. J. Knowles and A. Townshend, Anal. Chim. Acta, 79 (1975) 292.
16 M. Q. Al-Abachi, R. Belcher, S. L. Bogdanski and A. Townshend, Anal. Chim. Acta, 86 (1976) 139.
17 M. Q. Al-Abachi, Proc. Anal. Div. Chem. Soc., (1977) 251.
18 J. G. Eckhardt, K. Stetsenbach, M. F. Burke and J. L. Moyers, J. Chromatogr. Sci., 16 (1978) 510.
19 A. M. Bond, Z. Sztajer and G. Winter, Anal. Chim. Acta, 84 (1976) 37.
20 S. R. Rao and C. C. Patel, Soc. Mining Engr., (1963) 243.
21 K. J. Cowell, M.App. Sci. Thesis, Ballarat College of Advanced Education, 1979.

Analytica Chimica Acta, 116 (1980) 353—357

APPLICATIONS OF ELECTRON SPIN RESONANCE IN THE ANALYTICAL CHEMISTRY OF TRANSITION METAL IONS
Part 3. Determination of Chromium(III) in Aqueous Solution [1]

WARREN G. BRYSON

Hugh Adam Cancer Biology Research Unit, Department of Surgery, University of Otago, P.O. Box 913, Dunedin (New Zealand)

DAVID P. HUBBARD (the late), BARRIE M. PEAKE* and J. SIMPSON

Department of Chemistry, University of Otago, P.O. Box 56, Dunedin (New Zealand)

(Received 5th December 1979)

SUMMARY

Chromium(III) can be determined in aqueous solution at pH 1.5—2.5 by electron spin resonance techniques. The analytical range is 2.0×10^{-1}—2.0×10^{-6} mol dm^{-3}; the precision is ±0.3%. The effects of instrumental variables are discussed. Few commonly occurring species up to a concentration of 1.0×10^{-1} mol dm^{-3} interfered with the determination. The characteristic g value of 1.98 for chromium(III) suggests that the method may also be used to identify chromium(III).

Chromium(III) is paramagnetic and in aqueous solutions gives rise to a single line electron spin resonance (e.s.r.) spectrum with a characteristic g value of 1.98. The typical peak-to-peak linewidth (ΔB_{pp}) of about 165 G accounts for the lack of any resolved hyperfine structure from ^{53}Cr which is present in 9.55% natural abundance and is the only chromium isotope to have a non-zero nuclear spin value (3/2).

There have been several reports [2—6] of the use of e.s.r. to determine chromium(III) in aqueous solution. In the course of a survey of the applications of e.s.r. for the determination of transition metal ions [1, 7, 8], some of this earlier work has been carefully examined and extended. In this paper, improved values are reported for the limit of detection, precision and sensitivity; the effects of interference from a number of common species and of instrumental variables and pH are also described.

EXPERIMENTAL

A Varian E-4 spectrometer was used with a standard Suprasil sample cell (Scanco S-812). The interference measurements were made with this cell modified to allow samples to be changed by a flow method, without removing the cell or detuning the spectrometer [9].

Standard chromium(III) solutions were prepared by dissolving "Baker Analyzed" $Cr(NO_3)_3 \cdot 9H_2O$ in deoxygenated, triple glass-distilled water. Chromium(III) sulphate was unsuitable because it required several days to dissolve completely. Chromium(III) chloride dissolved readily to form a bright-green solution which changed colour slowly over a period of a week to give the characteristic violet colour associated with the hexaaquochromium-(III) cation. The e.s.r. signal amplitude of a freshly prepared solution of chromium chloride showed a time dependence; after a week it reached the same value as that for the nitrate. This behaviour has been observed previously and has been attributed to reactions leading to a variety of chromium(III) chloro and aquo complexes [10].

Chemicals used in the pH and interference studies were of analytical-reagent grade.

The spectrometer was tuned and operated as described in Part 1 [7].

RESULTS AND DISCUSSIONS

Effect of instrumental parameters and pH on signal intensity

As observed in the previous studies in this series [1, 7], the peak-to-peak first derivative signal amplitude (A) was found to vary linearly with receiver gain (G) for a range of chromium(III) concentrations. A plot of the ratio A/G vs. modulation amplitude (M) is shown in Fig. 1 and can be seen to be linear when M is less than 8 gauss. The deviation from linearity for larger M values is predominantly due to the effect of thermal instability of the Varian E-231 cavity [11]. Hence M was kept less than or equal to 5 gauss during the determination of analytical curves.

Ten solutions containing chromium(III) concentrations in the range 1.0×10^{-4} —1.0×10^{-1} mol dm^{-3} were used to evaluate the effect of micro-

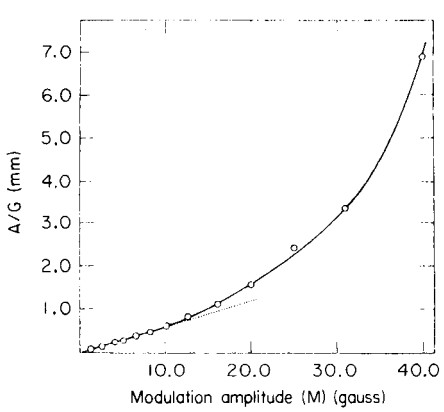

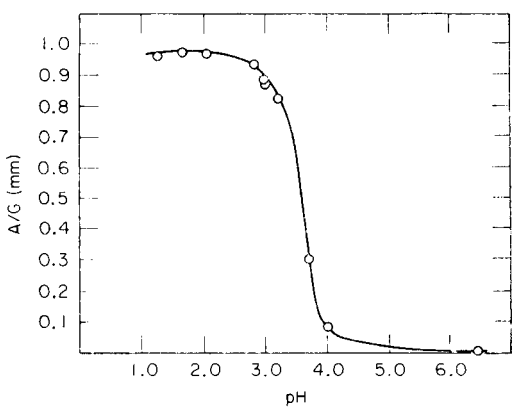

Fig. 1. Variation of signal amplitude to gain ratio (A/G) with modulation amplitude (M); 1.0×10^{-2} mol Cr(III) dm^{-3}.

Fig. 2. Variation of A/G with pH for a 1.0×10^{-2} mol Cr(III) dm^{-3} solution.

wave power (P) by the procedure outlined in Part 1 [7]. P was varied from 2.0 to 100.0 mW for each solution. The amplitude A increased linearly as a function of P^k where k was calculated to have a value of 0.53 ± 0.01. When P was varied the normalised signal A/GMP^k was found to remain constant for a given chromium(III) concentration.

The variation in signal intensity expressed as A/GM (constant P) as a function of pH for 1.0×10^{-2} mol Cr(III) dm^{-3} is shown in Fig. 2, which indicates that the signal intensity is constant within the pH range 1.5—2.5. Solutions within this range were clear violet, indicating the presence of hexaaquochromium(III) ions. At pH values exceeding 3.0, the solutions were green and the signal intensity decreased very rapidly with increasing pH. Green precipitates formed on standing, because of hydrolysis and associated reactions of the chromium(III) species to form colloidal polymers and chromium(III) hydroxides [12]. These results suggest that the pH should be adjusted to within the range 1.5—2.5 for optimum determination of chromium(III) in aqueous solution. All standard chromium(III) solutions used in the other studies were adjusted to pH 2.0.

Analytical curve and limits of detection

The conditions outlined above were used to determine the analytical curve. The plot of normalised signal intensity (log A/GMP^k) vs. the logarithm of the chromium(III) concentration was linear over the range 2.0×10^{-1}—2.0×10^{-6} mol dm^{-3}; the corresponding logarithmic signal intensity ranged from −0.5 to −5.0. The precision, defined as the relative standard deviation of the gradient over the linear range was calculated to be ±0.3% [7]. The logarithmic A/GMP^k signal no longer increases linearly at concentrations greater than 2.0×10^{-1} mol dm^{-3} because relaxation mechanisms broaden the chromium(III) linewidth and thereby reduce A. Levanon et al. [13] have suggested that the dominant relaxation mechanism for $[Cr(H_2O)_6]^{3+}$ arises from modulation of the zero-field splitting interaction resulting from collisions of the hydrated complex with the solvent molecules. Concentration effects such as ion-pairing and viscosity changes also affect the efficiency of this relaxation mechanism, causing an increase in linewidth.

The highest concentration of chromium(III) measured was 1.0 mol dm^{-3}. This value can be regarded as the upper limit of determination since it is impractical to prepare solutions of higher concentration. A limit of detection of 2.6×10^{-6} mol dm^{-3} for M = 5.0 gauss and P = 20.0 mW was calculated by the standard deviation method described earlier [7]. This was improved to a value of 1.3×10^{-6} mol dm^{-3} by increasing P to 100 mW.

Interferences

It is important to establish the maximum concentrations of other species which will not interfere with the e.s.r. determination of chromium(III). The mechanisms of such interferences include changes in relaxation effects leading to line-broadening or narrowing, and chemical effects such as ligand

substitution at chromium, precipitation, and redox reactions.

In the present study, some ions were selected which are commonly encountered in aqueous solutions and biological materials, in addition to some paramagnetic ions and some water-soluble complexing agents. Their effects on the determination of 1.0×10^{-3} mol Cr(III) dm^{-3} in aqueous solution were evaluated over the concentration range 1.0×10^{-5}—1.0×10^{-1} mol dm^{-3}. The results are shown in Table 1. The values quoted are the maximum concentration which caused not more than a 5% change in the chromium(III) signal. It was generally found that interfering substances decreased the signal amplitude. However, in the case of iron(III) nitrate and vanadyl sulphate, their e.s.r. signals overlapped with that from chromium(III) to enhance the signal of the latter. In the case of manganese(II) such an overlap led to a cancellation and hence an apparent decrease in the chromium(III) intensity.

A comparison of these results with the composition of common biological materials indicates that interferences might arise from the presence of sulphate and iron(III). For example, these are present in human whole blood in typical amounts of 0.87—2.02×10^{-4} and 8×10^{-3} mol dm^{-3}, respectively [14]. In such situations, procedures such as precipitation of sulphate with barium, or selective reduction of iron(III), may be necessary before the determination of chromium(III).

Conclusions

The analytical range for the e.s.r. determination of chromium(III) in aqueous solution is 2.0×10^{-1}—5.0×10^{-6} mol dm^{-3} with a relative standard deviation of ±0.3%. These values have been achieved by careful control of instrumental variables and pH and represent an improvement on previous

TABLE 1

Effect of other salts and complexing agents[a]

Chemical	Conc. for 5% amplitude change	Chemical	Min. conc. for 5% amplitude change
Inorganic salts		*Organic salts*	
Na_2SO_4	5.4×10^{-4}	$CH_3COONa \cdot 3H_2O$	5.4×10^{-3}
$Na_3PO_4 \cdot 12H_2O$	2.0×10^{-3}	$Na_2C_4H_4O_6 \cdot 2H_2O$ (tartrate)	1.2×10^{-3}
		$Na_3C_6H_5O_7 \cdot 2H_2O$ (citrate)	1.0×10^{-3}
Paramagnetic salts		$Na_2C_2O_4$	4.2×10^{-4}
$VOSO_4 \cdot 5H_2O$	2.7×10^{-5}		
$MnCl_2 \cdot 4H_2O$	$<1.0 \times 10^{-5}$	*Complexing agents*	
$MnSO_4 \cdot 4H_2O$	$<1.0 \times 10^{-5}$	$NH_2CH_2CH_2NH_2$	3.0×10^{-3}
$Fe(NO_3)_3 \cdot 9H_2O$	4.9×10^{-3}	EDTA	7.8×10^{-4}
$Cu(NO_3)_2 \cdot 3H_2O$	2.1×10^{-3}	Quinoline sulphate	3.6×10^{-4}

[a]The following salts had no effect at concentrations up to 0.1 mol dm^{-3}: $NaClO_4$, $NaNO_3$, NaCl, KNO_3, KCl, KI, NH_4NO_3, $Mg(NO_3)_2 \cdot 6H_2O$, $Ca(NO_3)_2 \cdot 4H_2O$, $Zn(NO_3)_2 \cdot 3H_2O$, $Co(NO_3)_2 \cdot 6H_2O$, $Ni(NO_3)_2 \cdot 6H_2O$.

work. Moyer and McCarthy [4] reported a usable range of three concentration decades with a lower limit of 3.7×10^{-5} mol dm^{-3}, while Meisel and Guilbault [5] reported a range of 1.0×10^{-1}—8.0×10^{-5} mol dm^{-3} with a precision of ±0.4%. The present limit of detection (1.3×10^{-6} mol dm^{-3} at P = 100 mW) compares favourably with those found for other techniques such as flame atomic absorption (1×10^{-7} mol dm^{-3}) [15], atomic emission (1×10^{-7} mol dm^{-3}) [15], and spectrophotometric determination with EDTA (2×10^{-5} mol dm^{-3}) [16].

The e.s.r. technique has the added advantage that it is specific for the trivalent oxidation state of chromium. This allows an estimate to be made of the concentration of this species alone, to the exclusion of other diamagnetic chromium species. Other advantages are that e.s.r. is non-destructive and requires as little as 0.1 cm^3 of sample, and that the chromium(III) resonance signal appears at a magnetic field position corresponding to a distinctive g value of 1.98. Most other paramagnetic species have g values very much closer to the free electron value of 2.0023. This advantage has also been recently noted by Swartz and co-workers [17] in e.s.r. studies of chromium-(III) in tissue samples.

We thank the Mellor Fund, the New Zealand Universities Grants Committee, the New Zealand Cancer Society, and the Cancer Research Trust Fund for financial support. We also thank Ms. Jacqui Smith for assistance in making the interference measurements.

REFERENCES

1 W. G. Bryson, D. P. Hubbard, B. M. Peake and J. Simpson, Anal. Chim. Acta, 96 (1978) 99.
2 G. G. Guilbault and E. S. Moyer, Anal. Chem., 42 (1970) 441.
3 E. S. Moyer, Ph.D. Dissertation, West Virginia, U.S.A. (1970).
4 E. S. Moyer and W. J. McCarthy, Anal. Chim. Acta, 48 (1969) 79.
5 T. Meisel and G. G. Guilbault, Anal. Chim. Acta, 50 (1970) 143.
6 G. G. Guilbault and T. Meisel, Anal. Chim. Acta, 50 (1970) 151.
7 W. G. Bryson, D. P. Hubbard, B. M. Peake and J. Simpson, Anal. Chim. Acta, 77 (1975) 107.
8 W. G. Bryson, M.Sc. Thesis, University of Otago, Dunedin, New Zealand (1975).
9 W. G. Bryson, A. Huffadine and B. M. Peake, unpublished work.
10 B. R. McGarvey, J. Phys. Chem., 61 (1957) 1232.
11 Technical Manual E-4 EPR Spectrometer System, 87-125-502 B1271, Varian Analytical Instruments Div., U.S.A., 1973.
12 J. C. Bailar, H. J. Emeléus, R. S. Nyholm and A. D. Trotman-Dickenson, Comprehensive Inorganic Chemistry, Vol. 3, 1st edn., Pergamon, Oxford, 1973, p. 676.
13 H. Levanon, S. Charbinsky and Z. Luz, J. Chem. Phys., 53 (1970) 3056.
14 G. V. Iyengar, W. E. Kollmen and H. J. M. Bowen, The Elemental Composition of Human Tissues and Body Fluids, Verlag Chemie, Weinheim, 1978.
15 J. D. Winefordner, S. G. Schulman and T. C. O'Haver, Luminescence Spectrometry in Analytical Chemistry, Wiley—Interscience, New York, 1972, p. 248.
16 K. Burger, Organic Reagents in Metal Analysis, Pergamon, Oxford, 1975, p. 190.
17 P. L. Gutierrez, T. Sarna and H. M. Swartz, Phys. Med. Biol., 21 (1976) 949.

Analytica Chimica Acta, 116 (1980) 359—364

LABELING THE MANGANESE IN GEOCHEMICAL MATRICES BY NEUTRON ACTIVATION

A. RUSSELL FLEGAL*

Oregon State University, School of Oceanography, Corvallis, Oregon 97331 (U.S.A.)

(Received 12th November 1979)

SUMMARY

A method of tracing the phase transformations of particulate manganese in estuarine zones by neutron activation of the element in geochemical matrices was evaluated. Data indicate that this procedure provides a sensitive and accurate method of following the labile forms of particulate manganese, despite the potential for isotopic disequilibria produced by the Szilard—Chalmers effect. Consequently, two radioisotopes, ^{56}Mn and ^{54}Mn, may be employed simultaneously to study fluxes from and to particulate phases in the estuarine zone.

Numerous studies have indicated that manganese is involved in a complex series of phase transformations in the estuarine zone [1]. Measurements of those transformations have been made with both stable manganese and its artificial radioisotope, ^{54}Mn. However, the former measurements are limited by problems of contamination [2]; and the latter may be limited by problems of isotopic disequilibria, especially in systems containing several chemical species of the element. While the disequilibria problem may be partially resolved by allowing the added radiotracer to equilibrate with the more exchangeable forms of manganese [3], the resultant distribution of labeled species may still differ from the original distribution of stable species because of the kinetics of phase transformations among the stable forms.

In order to circumvent these problems, some of the manganese originally present in a geochemical matrix may be labeled as the radioisotope ^{56}Mn by neutron activation. Since the ^{55}Mn (n, γ) ^{56}Mn reaction is independent of the form or position of the atoms in a matrix, the different species of manganese are activated in proportion to their relative concentration; and because the required period of irradiation is relatively short (1 min), the potential for time-dependent phase transformations is limited. Additionally, this radiotracer technique capitalizes on the well-known [4] analytical advantages of determining manganese concentrations by neutron activation analysis (n.a.a.).

However, there are some qualifications associated with this technique, including unknowns in the hot-atom chemistry of the activation products

*Present Address: Division of Geological and Planetary Sciences, California Institute of Technology, Pasadena, CA 91125, U.S.A.

and in other forms of radiation damage. The principal of these concerns is the extent of bond rupture and resultant isotopic disequilibria, which is associated with n.a.a. and is referred to as the Szilard–Chalmers effect [5]. This effect occurs because the recoil energy of an atom after thermal neutron capture is characteristically greater than most chemical bond energies, and recoiling nuclei may therefore rupture one or more of their original bonds and form different ones [6].

Consequently, the applicability of this radiotracer technique is contingent on the proposition that the separation efficiency of ^{56}Mn due to the Szilard–Chalmers effect is negligible with respect to the required accuracy of the radiotracer measurements. This must be empirically determined for each matrix and each treatment because the magnitude of this effect is highly variable [7].

In this paper, the magnitude of the Szilard–Chalmers effect is reported for three geochemical matrices containing non-labile (i.e., not solubilized by cation exchange) forms of manganese. The fraction of labile manganese in another geochemical matrix containing measurable fractions of both labile and non-labile forms of manganese is also reported and compared to the fraction determined by an alternative, stable element technique. Additionally, the cationic form of the labile ^{56}Mn in the latter matrix is confirmed by data on its elution through a chelating resin.

EXPERIMENTAL

Materials

Three geochemical matrices containing non-labile forms of manganese were used: synthetic manganese dioxide (MnO_2), rhodonite ($MnSiO_3$) and a manganese nodule (MnOOH and MnO_2). These materials were powdered with a glass mortar and pestle in order to maximize their surface area-to-volume ratio and thereby optimize the potential for observing the Szilard–Chalmers effect, as well as to make them comparable in size to the more reactive particulates in the environment. An intra-laboratory standard (YBC) of fine-grained sediment from Young's Bay, Oregon (containing both labile and non-labile forms of manganese) was also used to compare the fraction of labile manganese determined with the n.a.a. radiotracer method with the fraction found with a stable element determination. (In the latter determination, the labile manganese was determined by a 0.05 M copper(II) sulfate elution and the total manganese was determined by hydrofluoric acid bomb digestion.) Deionized, distilled water was used throughout.

Procedure

Five aliquots (0.5 mg) of each of the matrices, as well as operational blanks and N.B.S. standards, were weighed in acid-cleaned (reagent-grade nitric acid) lab-grade activation polyvials with 1 ml of deionized, distilled water. The heat-sealed, double encapsulated vials were irradiated for 1 min

with a thermal neutron flux of about 9×10^{12} n cm^{-2} s^{-1} in the pneumatic terminal position of the Oregon State University TRIGA research reactor. Separate irradiations of iron standards were made to determine the relative production of ^{56}Mn from ^{56}Fe by fission spectrum neutrons (cadmium ratio), and from these it was found that this form of contamination accounted for <0.1% of the ^{56}Mn produced in each of the matrices.

Each of the activated matrices was leached with 50 ml of sea water, which preliminary 5-ml cumulative leachings had indicated would extract >99.9% of the labile ^{56}Mn. (Separate 0.05 M transition metal salt solutions, 0.05 M NaCl, 0.2 M NaCl and 0.05 M acetic acid extractions had previously [8] been found to elute comparable fractions of ^{56}Mn from an irradiated matrix.) The eluates were separated from the particulates by passing them through Nuclepore filters (47-mm diameter, 0.4-μm pore size). Filters containing the particulates and 5-ml aliquots of the eluates were transferred to clean activation vials and counted in the well position of a 3 × 3-in. NaI(Tl) scintillation detector in order to attain optimum counting geometry ($\approx 4\pi$) and efficiency.

The form of the labile ^{56}Mn in the YBC sediment was further characterized by its affinity to a chelating resin [9]. The sea-water solutions were passed through polyethylene ion-exchange columns with 5 ml of the ammonium form of Chelex-100 resin (100—200 mesh; BioRad Laboratories). The flow rate was approximately 2.5 ml min^{-1}. The resin columns were then purged of interstitial ^{56}Mn with two 15-ml rinses of deionized-distilled water and the ^{56}Mn which was extracted by the resin was eluted with 15 ml of 2 M nitric acid. Aliquots (5 ml) of the sea-water and deionized-distilled water rinses, the nitric acid elution, and the resin were placed in clean activation vials and counted in the well position of the NaI(Tl) detector. This procedure is illustrated in Fig. 1.

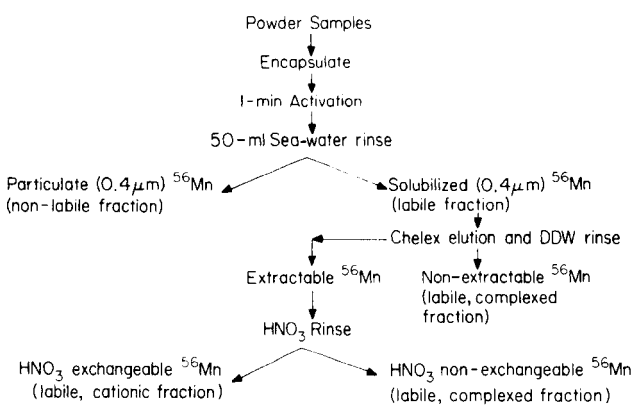

Fig. 1. Flow diagram for radiotracer studies of particulate manganese labeled by neutron activation.

RESULTS AND DISCUSSION

Non-labile and labile forms of manganese

The non-labile forms of manganese in the geochemical matrices were observed to remain non-labile (>99%) in spite of the Szilard—Chalmers effect (Table 1). This is probably because a recoiling nucleus is usually displaced only a short distance (1—3 Å) [10] and is then believed to be trapped in a cavity where "due to the extremely high local temperature, we shall expect that the stablest combination involving the radioactive atom and the ions in the coordination sphere will be formed" [11]. Therefore, most of the activated manganese within a geochemical matrix is not involved in cation-exchange reactions on the surface of the sample.

The magnitude of the Szilard—Chalmers effect on the YBC sediment was also observed to be negligible. The fraction of labile manganese determined by the n.a.a. radiotracer technique and by the stable element determination were the same (Table 2), and the chelating resin extractions (Table 3) indicated that >98% of the labile ^{56}Mn was in an exchangeable form. These observations are consistent with those of other studies of some systems which have shown that cationic ^{56}Mn does not stabilize in higher oxidation states [12, 13]. It is also consistent with the results of another study on the leachability of activated elements in fly ash [14].

Radiation damage to the matrix

The radiation dosage of the samples in this activation process is less than 3×10^4 rads. This amount of radiation will denature many enzymes, lyse cells and kill most organisms, but it will not cause much chemical damage [10]. For example, the calculated ratio of altered molecules to the total number of molecules would be less than 9×10^{-7}, assuming an overestimated radiation yield (G value) of 10^5 to account for the possible chain nature of some reactions. Since the irradiation occurs in an aqueous solution, the solute is also indirectly affected by the radiolysis of the solvent. The net effect of the products of the radiolysis of water (H, OH and HO_2 radicals and H_2O_2) is not readily predictable for a complex matrix, but the relatively low

TABLE 1

Retention of ^{56}Mn in neutron-irradiated geochemical matrices after a sea water—cation exchange elution (mean ± 1 standard deviation)

Matrix	Manganese complex	% ^{56}Mn retained in matrix
Manganese dioxide	δ-MnO_2	99.0 ± 0.30
Rhodonite	$MnSiO_3$	100.0 ± 0.01
Manganese nodules	δ-MnO_2, γ-MnOH	99.3 ± 0.91

TABLE 2

A comparison of the fraction of labile manganese determined in an intra-laboratory sediment standard by two different methods (mean ±1 standard deviation)

Method	Eluant	Labile Mn (%)
Stable Mn elution	0.05 M $CuSO_4$	33.3 ± 5.0
N.a.a. ^{56}Mn elution	sea water	33.8 ± 3.3

TABLE 3

Forms of filterable (0.4 μm) ^{56}Mn eluted from neutron-irradiated samples of an intra-laboratory sediment standard by sea water (mean ±1 standard deviation)

Form of manganese[a]	Total filterable ^{56}Mn (%)
Resin extractable, cationic	98.5 ± 0.3
Resin extractable, complexed	1.5 ± 0.3
Resin non-extractable, complexed	<0.1

[a]The efficiency of the Chelex resin extraction of cationic Mn(II) in filtered sea water which was determined with cationic ^{54}Mn was less (~1%) than 100%, and forms other than cationic Mn(II) may be extracted by the resin and then eluted with acid.

G values (1—10) of those products and the presence of dissolved oxygen limit their potential for altering the chemical composition of the matrix.

Conclusions

The applicability of this n.a.a. radiotracer technique is dependent on the proposition that the specific activities of the labile and non-labile forms of manganese produced by the thermal neutron activation of geochemical matrices are the same. Experimental data indicate that this is the case for the matrices considered, in spite of the Szilard—Chalmers effect. Theoretical calculations, additionally, indicate that the magnitude of radiation damage caused by this process is minimal.

Therefore, this technique represents a sensitive and accurate way of studying some of the phase transformations of manganese in the estuarine zone. Specifically, the manganese in sediments may be labelled with ^{56}Mn by neutron activation in order to trace fluxes from particulate phases in the estuarine zone; and the cationic manganese in the dissolved phase may be spiked with ^{54}Mn in order to trace fluxes to particulate phases simultaneously.

REFERENCES

1 K. K. Turekian, Geochim. Cosmochim. Acta, 41 (1977) 1139.
2 D. E. Robertson, in P. D. LaFleur (Ed.), Accuracy in Trace Analysis: Sampling, Sample Handling, Analysis, U.S. National Bureau of Standards Special Publication 422, 1976, p. 805.

3 E. K. Duursma, in J. D. Burton and P. S. Liss (Eds.), Estuarine Chemistry, Academic Press, London, 1976, p. 159.
4 D. DeSoete, R. Gijbels and J. Hoste, Neutron Activation Analysis, Wiley-Interscience, London, 1972, p. 7.
5 L. Szilard and T. A. Chalmers, Nature (London), 134 (1934) 462.
6 G. Friedlander, J. W. Kennedy and J. M. Miller, Nuclear and Radiochemistry, J. Wiley, New York, 1964, p. 209.
7 G. Harbottle, Ann. Rev. Nucl. Sci., 15 (1965) 89.
8 A. R. Flegal, in preparation.
9 J. P. Riley and D. Taylor, Anal. Chim. Acta, 40 (1968) 479.
10 H. J. M. Bowen and D. Gibbons, Radioactivation Analysis, Clarendon Press, Oxford, 1963, p. 166.
11 W. F. Libby, J. Am. Chem. Soc., 69 (1947) 2523.
12 C. W. Owens and W. C. Lecington, Inorg. Nucl. Chem. Lett., 11 (1975) 673.
13 D. J. Apers and G. Harbottle, Radiochim. Acta, 1 (1963) 188.
14 W. D. James, M. Jonghorbani and T. Baxter, Anal. Chem., 49 (1977) 1994.

Analytica Chimica Acta, 116 (1980) 365—374

ISOLATION OF THE SODIUM 589.0-NM LINE BY A VOIGT EFFECT FILTER

G. JOLLY and R. STEPHENS*

Trace Analysis Research Centre, Department of Chemistry, Dalhousie University, Halifax, Nova Scotia B3H 4J3 (Canada)

(Received 22nd October 1979)

SUMMARY

Rotation of plane polarised radiation by means of the Voigt effect provides a basis for an optical transmission filter. The performance of such a filter at 589.0 nm is examined with hollow-cathode and continuum sources. The Voigt effect filter in combination with a continuum source gives atomic absorption sensitivity similar to that obtainable with a hollow-cathode lamp; however, its signal-to-noise ratio is worse because of the low output of the continuum source used over the wavelength range occupied by the atomic absorption line.

When light from a resonance line source is incident on an atomic absorption cell which has been positioned between two crossed polarisers, the application of a magnetic field to the atom cell causes polarisation rotation of the resonance radiation to occur, and thereby permits the system to show partial optical transmission at the resonance frequencies. The effect will be referred to here as magneto-optic rotation (MOR). The magnetic field required for the observation of MOR may be either transverse or parallel to the optical axis; magneto-optic rotation observed in these two configurations is termed the Voigt or the Faraday effect respectively. The suitability of both Voigt and Faraday effects for the detection of atomic species has been investigated [1—4].

Because MOR gives rise to a partial transmission of those frequencies which lie in the immediate vicinity of the absorption lines of the vapour contained in the MOR cell, any such cell can be used as an optical filter capable of specific transmission of those frequencies. This particular application has not yet been examined for the purposes of analytical atomic spectrometry. Such an MOR filter is expected to show characteristics which include automatic frequency stability, predictable transmission spectrum, and a narrow bandwidth of the transmitted lines, comparable to the width of the absorption lines in the MOR cell.

An investigation of the characteristics of an MOR filter, set up for the sodium 589.0-nm line, is the subject of the present paper.

THEORY

The filter examined here utilized the Voigt effect. Therefore a transverse magnetic field configuration is assumed throughout the following discussion. To distinguish between vapour-phase sodium atoms in the filter and those in the flame atomiser considered later, the term 'atom concentration' will be applied exclusively to the former situation.

The properties of a Voigt effect filter can be adequately accounted for by the 'absorption only' model, described in detail elsewhere [5, 6]. This model gives the intensity, I_T, transmitted at any frequency ν as

$$I_T = \tfrac{1}{2} I_0 \sin^2\theta \cos^2\theta \left\{ \sum_{\substack{\text{all } \pi \\ \text{components}}} \exp[-\tfrac{1}{2}\kappa_i(\nu) c_a l] - \sum_{\substack{\text{all } \sigma \\ \text{components}}} \exp[-\tfrac{1}{2}\kappa_i(\nu) c_a l] \right\}^2 \quad (1)$$

where θ is the angle between either polariser axis and the magnetic field axis, $\kappa_i(\nu)$ is the molar Naperian absorption coefficient at a frequency ν of the ith component of the Zeeman absorption multiplet, c_a is the atom concentration, l the optical path length, and I_0 the unpolarised source intensity. Summations are taken over all the components of the transverse Zeeman multiplet of the line considered.

Assuming the zero field absorption line to be Gaussian, $\kappa_i(\nu)$ can be written as

$$\kappa_i(\nu) = \kappa_0 Z_i \exp[-a^2(\nu - \nu_0 + \Delta\nu_i)]^2 \quad (2)$$

where κ_0 is the peak absorption coefficient of the zero magnetic field line, Z_i the peak amplitude of the ith multiplet component relative to κ_0, $\Delta\nu_i$ the magnetic displacement of the ith multiplet component, ν_0 the frequency of the zero field line, and a is a constant, given by $a = 2(\ln 2)^{1/2}/\Delta\nu_0$, $\Delta\nu_0$ being the halfwidth of the line [7].

No polariser is completely effective in producing fully polarised light, with the result that some wavelength-independent background transmission always occurs through an MOR cell. If I_B is the magnitude of this background, then the total intensity, I_t, transmitted by a Voigt effect filter is given by

$$I_t = I_T + I_B \quad (3)$$

Substitution of eqns. (1) and (2) into eqn. (3) and assuming an optimum value of $\theta = 45°$ to maximise I_t, gives:

$$I_t = \frac{I_0}{8} \left\{ \sum_{\text{all } \pi} \exp[-\tfrac{1}{2} c_a l \kappa_i(\nu)] - \sum_{\text{all } \sigma} \exp[-\tfrac{1}{2} c_a l \kappa_i(\nu)] \right\} + I_B \quad (4)$$

Figure 1 shows the variations of I_t with ν for various values of the atomic concentration, c_a, calculated from eqn. (4). Values of Z_i and $\Delta\nu_i$ used in determining these data were those appropriate to the anomalous multiplet of the sodium 589.0-nm $^2P_{3/2}$—$^2S_{1/2}$ line (see Fig. 2). A value of $0.1 \times I_0$ was used for I_B; this is consistent with the absorption coefficient of the polarisers used (3×10^{-3}).

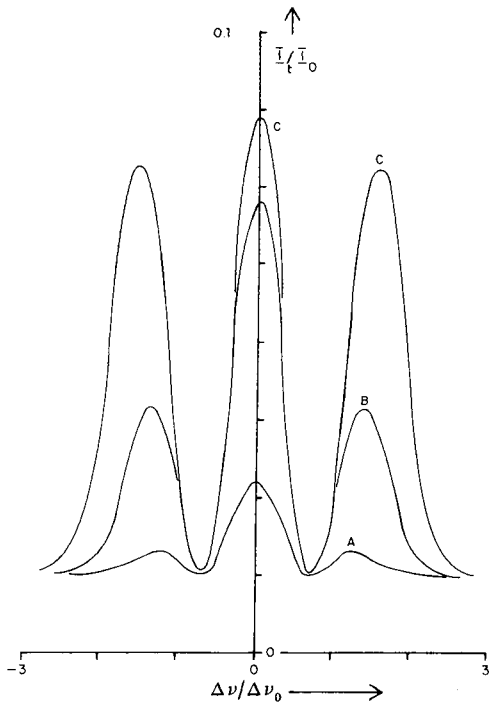

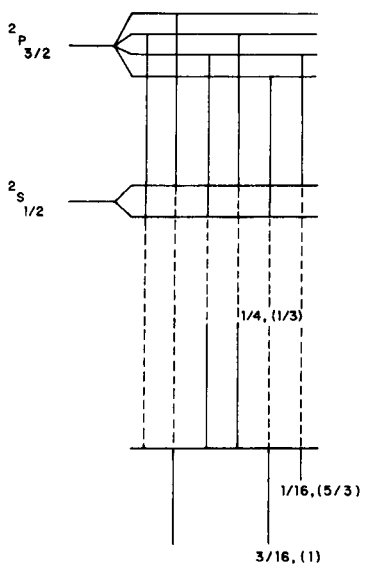

Fig. 1. Variations of I_t/I_0 when the source line is displaced by a value $\Delta\nu$ from the peak zero field absorption frequency ν_0. The MOR cell is assumed to be held at a fixed magnetic field strength, of a value such that the σ frequency shift of the normal Zeeman effect is $\Delta\nu_N$. Values of $\Delta\nu_N$ and $\Delta\nu_0$ were assumed to be equal. Curves A, B and C are for values of $\kappa_0 c_a l$ of 1, 4 and 10, respectively.

Fig. 2. Zeeman splitting of the Na 589.0-nm line. Numbers over each component represent its intensity relative to that of the zero field line when the intensity measurement is made in absorption with an unpolarised line. Numbers in parentheses represent the frequency shift relative to the σ frequency shift $\Delta\nu_N$ of the normal Zeeman effect.

A number of features are apparent from the curves shown in Fig. 1. First, and at the particular magnetic field strength shown, the transmission spectrum is that of a normal Zeeman triplet (although the σ displacement is quantitatively different from the normal value; also, separation of the π and σ envelopes of the transmission spectrum into the individual components of the absorption multiplet will eventually occur at sufficiently high magnetic field strengths). Secondly, π envelope transmission dominates at low atom concentrations while σ envelope transmission dominates at high concentrations. Thirdly, the σ component envelope frequencies show a dependence on atom concentration, being shifted away from the zero field line as atom concentration increases. Finally, continuum transmission from the finite absorption coefficient of the polarisers markedly degrades filter performance

at low atom concentrations; however, as atom concentration increases, this effect is correspondingly reduced. Thus the line-to-background transmission ratio of the filter improves as the atom concentration in the filter increases.

EXPERIMENTAL

Sodium was selected as a test element for an MOR filter, because of the particular simplicity with which atomic vapour cells can then be built, and because the *D* lines occur conveniently in the middle of the visible spectrum. The optical system used to test the sodium filter is shown in Fig. 3.

The sodium cell consisted of a 24 cm long by 2 cm diameter evacuated pyrex tube, into which sodium metal had been evaporated. Details of the construction of the device are given elsewhere [5]. A winding pattern for the heating element of the cell was found which localised the deposited metal at the centre of the tube and kept the windows clear. The cell was insulated with asbestos paper; copper—constantin thermocouples were inserted under the insulation, adjacent to the body of the cell. The thermocouples were connected in series, and their output used to control the heater current through a laboratory-built power supply. Orthogonal dichroic polarisers, with their transmission axes at 45° to the magnetic field axis, were mounted on both sides of the sodium cell to complete the MOR filter. The absorption coefficient of the polarisers used was 3×10^{-3}. The remaining optical components, and the electronics used to measure the MOR signal, were part of an existing Zeeman background-corrected spectrometer whose construction has been discussed elsewhere [8].

Because experimental work was to be carried out with a continuous source, and because the dichroic polarisers had finite absorption coefficients, the monochromator (McKee—Pedersen MP1018A; reciprocal dispersion 0.9 nm mm^{-1}) from the original Zeeman-corrected instrument was retained, to limit the bandwidth over which continuum background transmission of the filter would be observed.

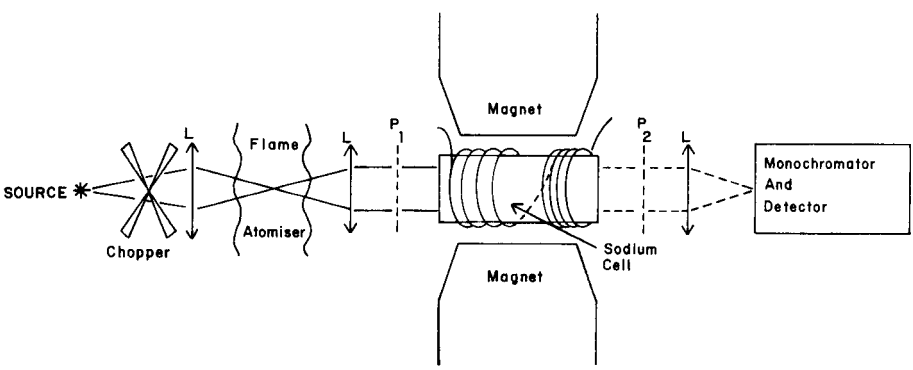

Fig. 3. Optical system used with the MOR filter. L, lens; P_1 and P_2, orthonormal polarisers.

The continuum light source used throughout this work was a 75-W quartz—halogen lamp.

RESULTS AND DISCUSSION

Transmission behaviour of the filter

Figure 4(A—C) show the observed intensities transmitted by the filter with changing source intensity, magnetic field strength and atom concentration. The zero of the transmitted intensity was set at the observed intensity transmitted at zero magnetic field strength in all cases (i.e., I_B was used for the intensity baseline). A monochromator slit of 1.6 mm was used to give the largest slit consistent with selective transmission of the 589.0-nm line. Thus, these intensity data represent the total filter output over all the Zeeman components of the 589.0-nm line, but without inclusion of the background transmission of the polarisers. Figure 4(A) shows that the intensity transmitted by the filter is directly proportional to source intensity. This is exactly as expected from eqn. (4).

Effects of magnetic field strength and c_a *on* I_T. To determine the effect of magnetic field strength two sources were used: the 75-W quartz—halogen continuum, and a sodium hollow-cathode lamp. In the former case, the

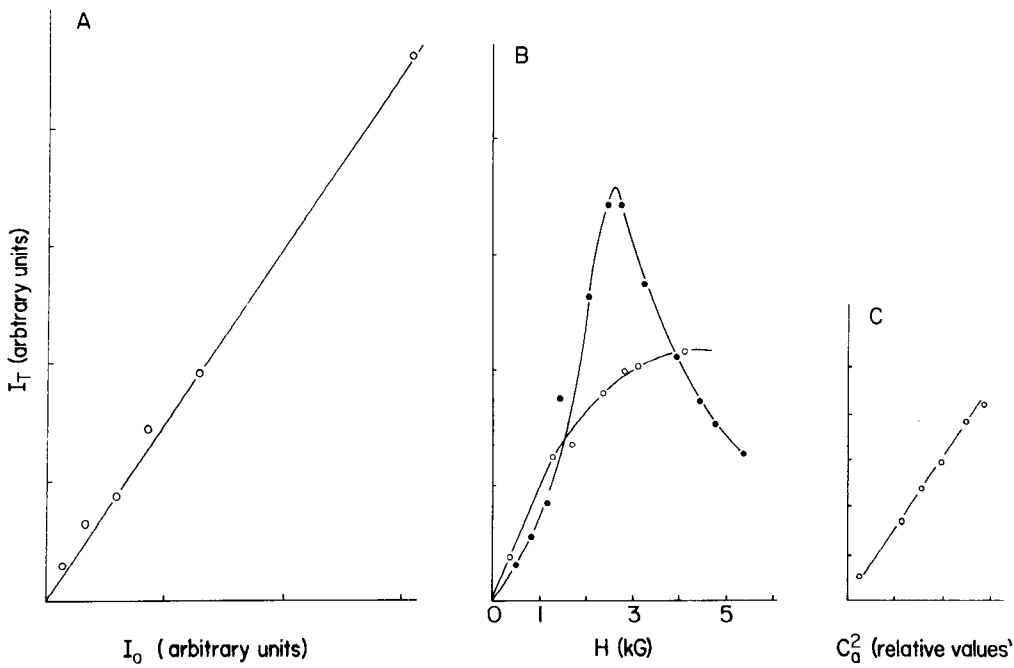

Fig. 4. Dependence of transmitted intensity (A) on source intensity; (B) on magnetic field strength for (•) hollow-cathode lamp and (○) quartz—halogen continuum; (C) on c_a^2 observed with the continuum source.

transmitted intensity rises to a plateau with increasing field strength; in the latter case the curve shows a maximum (Fig. 4B). This behaviour is due to the separation of the π components of an anomalous multiplet. As long as the magnetic field is low enough to maintain transmission over a single π envelope maximised at the zero field frequency (the type of situation shown in Fig. 1), the transmission envelope of the filter coincides with the hollow cathode emission line, and I_T increases with $\Delta\nu_i$ according to eqns. (1) and (2). However, at high field strengths the π transmission envelope breaks into the two separate π components, characteristic of the anomalous sodium absorption multiplet. These components are shifted in frequency from the hollow-cathode line, so that I_T starts to fall. In contrast, such frequency shifts do not matter with the continuum source, since the source emission intensity shows no significant variation over the frequency range considered. The existence of a plateau under such circumstances is then implicit in eqn. (4), since at high field strengths $\kappa_i(\nu)$ must be negligible for all π components if it is to be significant for any σ (owing to the large π—σ frequency separation), and vice versa. Thus the term within braces in eqn. (1) limits at one or the other summation term or at zero, according to the position of observation within the multiplet.

The dependence of I_T on atom concentration is expected to follow a square law [1—6], unless both the atom concentration and $\kappa(\nu)$ are simultaneously large. This follows directly from eqn. (4). Thus expansion of the exponential terms in eqn. (4) gives:

$$8\frac{I_t}{I_0} = \left\{\sum_{\text{all }\pi}\left[1 - \frac{1}{2}c_a l\kappa_i(\nu) + \frac{1}{8}c_a^2 l\kappa_i(\nu)^2 - \ldots.\right] - \sum_{\text{all }\sigma}\left[1 - \frac{1}{2}c_a l\kappa_i(\nu) + \frac{1}{8}c_a^2 l^2\kappa_i(\nu)^2 - \ldots.\right]\right\}^2 + 8I_B$$

$$\simeq c_a^2 l^2\left\{\sum_{\text{all }\pi}\kappa_i(\nu) - \sum_{\text{all }\sigma}\kappa_i(\nu)\right\}^2 + 8I_B \qquad (5)$$

Experimental values for c_a were determined by measuring the absorbance in the cell at various heater currents by using the hollow-cathode lamp, and assuming a linear relation between hollow-cathode absorbance data and absorbing atom concentration. This permitted a relative calibration curve for the cell to be obtained in terms of the heater current used. Values of I_T were then measured, using the continuum source, for various values of the cell heater current. The results thereby obtained are given in Fig. 4(C). It is apparent from this figure that the square law dependence of I_T on c_a, deduced for a monochromatic source in eqn. (5), is also exhibited by the continuum. This is as expected; integration of eqn. (5) over a wide emission profile will affect $\kappa(\nu)$, but is not likely to modify the c_a^2 term. It can be noted that the square law dependence of I_T on c_a is a major disadvantage when MOR is used directly for the analytical detection of atomic species, since it means that signal magnitudes fall off very rapidly with decreasing concentration, to

the detriment of detection limits. In the present application, however, the effect is of no particular importance, since c_a^2 is a completely controllable variable.

Atomic absorption results obtained with the filter and continuum source

Atomic absorption measurements for sodium were made in a conventional manner, by aspirating aqueous standard solutions into a standard, unmodified Varian-Techtron AA5 burner/nebuliser assembly. Values of I_T were measured in an identical manner to that used in the previous section, and the absorption signal determined by the reduction of I_T upon aspiration of the sodium solution. Thus the data below represent the effect of flame atomic absorption on the combined Zeeman components of the 589.0-nm line, but do not include the effect of the wavelength-invariant background transmission of the polarisers.

Effects of H *and* c_a *on the absorption signal.* Figure 5 shows percentage absorption signals found for a 2.5 ppm sodium solution aspirated into the flame with increasing magnetic field strength and for three different atom concentrations in the filter. It is clear that (a) optimum flame absorption sensitivity occurs at the intermediate filter atom concentration; sensitivity falls off as the atom concentration becomes very high or very low; and (b) apparently an optimum magnetic field strength exists at which maximum absorption sensitivity is obtained. These findings can be interpreted as follows.

It is apparent from Fig. 1 that the amplitude to halfwidth ratio of the π transmission line increases markedly as atom concentration increases. Since the π transmission line must always be broadened in comparison to its zero field value because of the magnetic displacement of the π components in the MOR cell, overlap between the π transmission line profile and the flame atomic absorption profile must be correspondingly improved as the amplitude to halfwidth ratio increases. Thus, atomic absorption sensitivity is expected to increase with c_a. However, as c_a increases, Fig. 1 shows the filter output to be increasingly contained within the two σ envelopes, thereby reducing atomic absorption sensitivity. The optimum condition therefore represents a compromise between these two effects.

Figure 5 shows absorption sensitivity at the intermediate and high c_a values to show a maximum with decreasing field strength, but to increase, up to the limit of measurement, for low c_a. If the zero magnetic field absorption frequency in the MOR cell exactly coincided with that in the flame it would be expected that the behaviour at low c_a would also be observed at higher values (since coincidence between the zero magnetic field line and the π and σ envelopes in Fig. 1 improves continuously as the field strength is reduced to zero). This is not the case; the results in Fig. 5 probably show the influence of a frequency shift in the sodium flame absorption profile, due to pressure broadening. Thus the maxima at intermediate and high c_a values are attributed to the increased absorption as

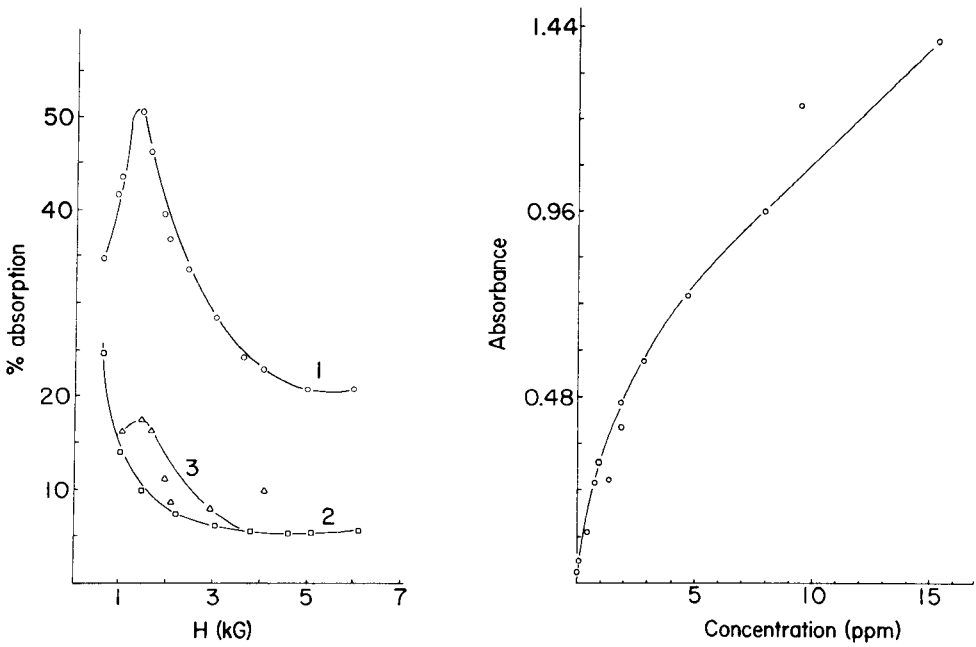

Fig. 5. Absorption by a 2.5 ppm soldium solution using the quartz—halogen source at increasing magnetic field strength across the filter. Curves 1, 2 and 3 represent intermediate, low and high values of c_a.

Fig. 6. Calibration curve obtained with the MOR filter and continuum source.

either one of the σ envelopes is displaced to the maximum of the flame absorption profile. A maximum is not observed when c_a is low because of the relatively low amplitudes of the two σ envelopes in this case (Fig. 1).

Calibration curve. It might be expected that the calibration curves given by the present system would be influenced by the Zeeman structure of the filter transmission spectrum. Such influence can for example be observed under certain circumstances with Zeeman background-corrected atomic absorption spectrometers. Accordingly, the filter was adjusted to give optimum flame absorption sensitivity, and a calibration curve (Fig. 6) was established by using suitably closely spaced calibration points. In fact no obvious influence of the Zeeman structure can be observed, apart from the marked curvature associated with the existence of more than one line within the optical bandpass of the system.

Sensitivity and detection limit. The lowest 1% absorption sensitivity concentration found with the MOR filter-continuum source combination was 0.005 ppm. This was almost identical to the corresponding value obtained by using a hollow-cathode lamp, a result which demonstrates the narrow transmission profile of the filter under optimum conditions. However, the detection limit in the former instance was only slightly

lower than the 1% absorption concentration, because of a lower signal-to-noise ratio. Two effects are responsible for the lower signal-to-noise ratios found with the filter. First, a quartz—halogen lamp radiates less power than a hollow-cathode lamp over the wavelength range occupied by an atomic absorption line. Therefore, because the source intensity is low, the signal-to-photon noise ratio of the present system is also inherently low. Secondly, the background polariser transmission, I_B, occupies the full bandpass of the monochromator. Thus it contributes to photon noise without adding significant power at the resonance frequencies. The influence of the first noise source can be reduced either by increasing source intensity or by increasing the monochromator slit width to improve the light throughput of the system. Reduction of the second noise source requires a compromise between monochromator slit width (since this governs the wavelength range over which I_B is observed), and the magnitude of the polariser absorption coefficient (which governs the size of I_B at any particular frequency). Thus the monochromator slit width can be increased if more efficient polarisers are used, and vice versa.

With the present apparatus, the slit width used (1.6 mm) gave about the optimum signal-to-noise ratio. Increasing the slit width to its maximum (5.5 mm) decreased the signal-to-noise ratio by a factor of five, most of which was attributed to the effect of I_B. In view of the preceding remarks, the signal-to-noise ratio of the present system could probably be appreciably improved by use of more efficient polarisers combined with a wide aperture optical system, even if the optical resolving power of the latter were lower than that of the monochromator used here. The most critical parameter in the design of an MOR filter intended for atomic absorption work appears to be the absorption coefficient of the polarisers which are to be used.

As expected, use of the MOR filter was found to give improved absorption sensitivity only with the continuum source. Combining the filter with the hollow-cathode lamp left absorption sensitivity unchanged, and served only to increase the background noise level.

Conclusions

The present results demonstrate the ability of an MOR filter to isolate the frequencies characteristic of the atomic species within the filter. The frequency stability and the width of the transmitted lines are sufficiently good to permit an analytically useful level of atomic absorption sensitivity to be obtained with these lines. Two adverse effects encountered are (1) a high photon noise level, and (2) the demand for very low polariser absorption coefficients to block unwanted frequencies. The former problem is aggravated by the limited transmission efficiency of the MOR filter; eqn. (1) shows this efficiency to have a peak value of only 12.5%. The latter problem becomes more apparent as the bandwidth of the secondary tuning element (e.g. the monochromator used here) increases. However, it does appear feasible to obtain useful performance from the MOR filter even when

the bandwidth of this secondary element is of the order of that available from an ordinary interference filter. Incorporation of an interference filter to replace the monochromator used would clearly represent a worthwhile simplification of the present apparatus, while considerably improving the aperture of the system.

One potential advantage that can be foreseen for an MOR filter is its optical simplicity. Thus the device can be inserted directly into an existing optical system without changing the optical axis and without causing any major perturbation to the focal properties of the system. The value of this simplicity in atomic absorption analysis can be seen, for example, when the problem of designing a multi-channel instrument is considered. A second possible advantage lies in the narrow optical bandwidth of the MOR filter, evident from the absorption data in Fig. 5. The high resolving power shown by the device is beyond the range of most commercially available monochromators and could be employed to advantage in emission or fluorescence determinations, for instance under circumstances where a line must be determined on top of a continuous background, or where selection of one line from a closely spaced multiplet is required.

The authors are indebted to the Natural Sciences and Engineering Research Council Canada for support of this work.

REFERENCES

1 D. A. Church and T. Hadeishi, Appl. Phys. Lett., 24 (1974) 185.
2 M. Ito, S. Murayama, K. Kayama and M. Yamamoto, Spectrochim. Acta, Part B, 32 (1977) 347.
3 R. Stephens, Anal. Chim. Acta, 98 (1978) 291.
4 K. Kitagawa, T. Shigeyasu and T. Takeuchi, Analyst, 103 (1978) 1021.
5 R. Stephens, Can. J. Spectrosc., 24 (1979) 105.
6 J. B. Dawson, E. Grassam, D. J. Ellis and A. D. Kersey, paper presented at the 8th ICAS/XXI CSI, Cambridge (U.K.), 1979 Abstract Handbook, p. 141.
7 A. C. G. Mitchell and M. W. Zemansky, Resonance Radiation and Excited Atoms, Cambridge University Press, Cambridge, 1934.
8 R. Stephens, Talanta, 25 (1978) 435.

Analytica Chimica Acta, 116 (1980) 375—381

CONTINUOUS SAMPLING OF DIALYSATE FOR THE ATOMIC ABSORPTION SPECTROMETRIC DETERMINATION OF COPPER AND ZINC FROM HEMODIALYSIS PATIENTS

S. LEVI and WILLIAM C. PURDY*

Department of Chemistry, McGill University, 801 Sherbrooke St. W., Montreal, Que. (Canada H3A 2K6)

(Received 6th November 1979)

SUMMARY

Procedures for the determination of copper and zinc concentrations in dialysates for patients undergoing hemodialysis treatment are reported. Representative samples are collected continuously during dialysis. Two designs of sample collectors are described. Copper and zinc are determined by flame a.a.s. after concentration of the metals from the dialysate solution by an APDC—MIBK extraction.

Since only about 5% [ca. 50 $\mu g\ l^{-1}$ (ppb)] of the copper and zinc in blood is not bound to protein [1], transfer of these metal ions to the blood can be expected when blood is dialyzed against solutions which contain more than 50 ppb of these ions. Copper poisoning of hemodialysis patients by the dialysis process has been investigated by several groups [2—6].

Dialysate copper and zinc levels have been measured on fractions of the dialysate [3—5] but not on the gross dialysate solution which drains at 500 ml min^{-1} for 4—8 h. To overcome the problem of the large volume of dialysate solution (60 l during 2 h), two designs for continuous sampling are proposed. These two sampling designs permit the determination of the overall effect of the dialysis process on the level of copper and zinc in the dialysate. These metal ions were determined by flame atomic absorption spectrometry (a.a.s.) after concentration by methyl isobutyl ketone—ammonium pyrrolidine-carbodithioate extraction [7].

EXPERIMENTAL

Avoidance of contamination

The following steps were taken to minimize the effects of contamination.

Nature of containers. Conventional polyethylene bottles were found to be the most suitable containers for copper and zinc sample and standard solutions. All extractions were carried out in polyethylene vessels which could be tightly sealed. The organic phase was aspirated directly from polyethylene bottles.

Cleaning procedure. All bottles and glassware were cleaned in the following manner. The vessels were soaked for 6 h in a (1+1) mixture of 6 M HCl and 7.5 M HNO_3 (Baker Analyzed Grade). After discarding the acid solution, the vessels were rinsed 3 times with distilled water and once with deionized water. They were then soaked for 12 h in deionized water. The deionized water was discarded and the vessels were rinsed 3 times with conductivity water (1.138×10^{-6} s cm^{-1}). Finally the vessels were dried either in a clean oven or at room temperature in a clean area by inverting them on fresh paper towels.

Sampling apparatus and tubing. These were cleaned in the (1+1) acid described above, and then connected to the dialyzer for 12 h before sampling. This was done to saturate the surfaces of the apparatus and tubing and avoid adsorption of copper and zinc during hemodialysis.

Standard solutions and reagents

For the standards, copper and zinc metal (Baker Analyzed Reagent) were dissolved in a minimum volume of nitric acid (Ultrex, J. T. Baker Chemical Co.) and hydrochloric acid (Ultrex) respectively, and diluted with conductivity water to yield a stock solution of a concentration of 1000 mg l^{-1} in the particular metal. Serial dilution of the stock gave secondary standards. These dilutions were done with a volumetric pipet of at least 5-ml volume to minimize volume errors.

Ammonium 1-pyrrolidinecarbodithioate (APDC; Baker Analyzed Reagent; suitable for a.a.s.) was used as an aqueous 2% (w/v) solution, which was prepared daily by dissolving 1 g of APDC in 50 ml of conductivity water and filtering to obtain a clear solution. 4-Methyl-2-pentanone (MIBK; 99.5%, Aldrich Chemical Co.) was saturated with conductivity water prior to use. The citrate buffer contained 1.2 M sodium citrate and 0.7 M citric acid (both Baker Analyzed Reagents) to yield a pH of 4.3.

Sampling apparatus

Because of the high flow rate of the dialysate (500 ml min^{-1}) during a hemodialysis procedure, it would be impractical to collect the whole solution for analysis. Therefore, two designs of sampling apparatus were developed (Fig. 1). All hemodialyses were carried out at the Royal Victoria Hospital, Montreal. Samples were collected continuously by connecting the dialysate-filled sampling apparatus to the dialyzer (membrane, 1-m^2 Viva Cell; delivering machine, Drake Willock Proportionating System). The samples were collected in 4-l polyethylene containers during 2 h of dialysis. (After 2 h, the concentration gradient across the dialyzer membrane becomes smaller and hence the active transport of the metal ions is insignificant.) For each determination two samples were collected: the sample, collected while the patient was on-line with the dialyzer, and the blank, collected while the patient was not on-line.

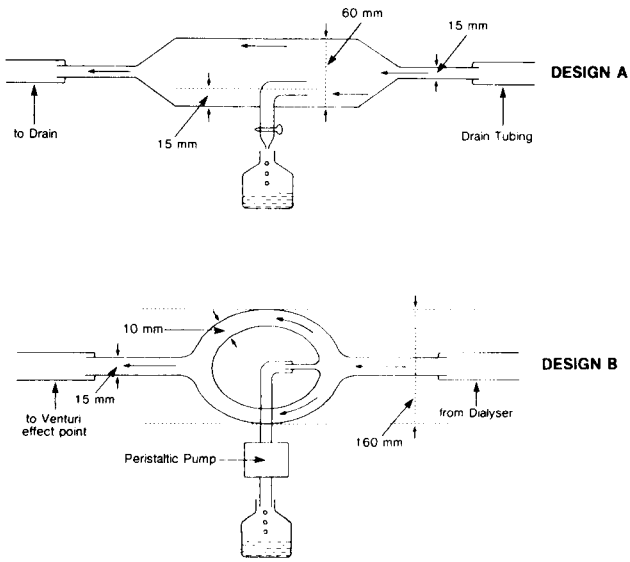

Fig. 1. Two designs of continuous sampling apparatus. Design A can be used only with a dialyzer for which negative pressure is provided by an electrical pump. Design B can be used with any type of proportioning dialyzer.

Procedure

Collected samples were stored at −2°C until analysis. To a 100-ml dialysate sample in a 125-ml polyethylene bottle was added 5 ml of citrate buffer, and the solution was shaken well. The APDC solution (2.00 ml) was added, and the solution was shaken and allowed to stand for 5 min. MIBK (10.0 ml) was then added, the bottle sealed and the solution shaken by a mechanical shaker for 5 min. After shaking, the solution was allowed to stand for 15 min. The organic phase was then raised by pouring into the bottle the appropriate volume of conductivity water to allow aspiration of the organic phase directly into the flame. Copper and zinc were determined on a Perkin-Elmer Model 603 atomic absorption spectrophotometer equipped with a deuterium background corrector, under the conditions recommended by the manufacturer.

RESULTS AND DISCUSSION

Studies were conducted to test whether the two designs of sampling apparatus gave representative samples. The validity of the proposed systems was checked by sampling copper solutions under conditions similar to those of actual sampling from the dialyzer. A 4-l mixing reservoir was used to feed a copper solution to each sampling apparatus. The flow of distilled water into the reservoir was maintained at 500 ml min^{-1} (the same as that used in the dialyzer) so that the volume of stirred solution in the dialyzer remained

constant. Over a 120-min period, 60 ml of an aqueous 100 ppm copper standard solution was added dropwise to the reservoir from a buret located on the reservoir. The drop rate was adjusted only at the beginning of the run so that the rate decreased constantly as the solution head fell. This resulted in a constantly changing copper concentration in the mixing reservoir.

Triplicate 260-ml samples were collected with the use of design A and triplicate 840-ml samples were collected with design B out of a total of 60 l of solution which passed through the system in 2 h. Atomic absorbance measurements were made on the MIBK extracts of these solutions and compared with those of the MIBK extracts of three 0.1-ppm copper standard solutions. These results are found in Table 1.

To strengthen the validity of these results and to show the general potential of the sampling system, the same tests were repeated with an aqueous dye solution. All conditions were the same as described above except that a dye solution (5% eriochrome red B, J. T. Baker Chemical Co.) was used in place of the copper solution. Duplicate 212-ml samples were collected by each sampling apparatus. Absorbance readings were taken on these solutions and compared with those of two solutions prepared by adding 200 μl of the dye solution to 144 ml of distilled water. These absorbance readings are found in Table 2.

These results indicate that both designs of sampling apparatus yield representative samples with a relative standard deviation (RSD) of less than 5%. The critical factor in this method of sampling is the maintenance of constant flow through the apparatus during the sampling.

The calibration plots obtained for standard solutions of the two metal ions after extraction with MIBK are linear over the ranges shown in Table 3. Since the day-to-day RSD was found to be near 1%, it is recommended that calibration graphs be obtained at the same time as actual determinations. The statistical parameters which characterize the calibration curves are given

TABLE 1

Comparison of absorbance values of MIBK extracts of 0.1 ppm copper standard solutions and of MIBK extracts of solutions from the two designs of sampling apparatus

	Sample	Absorbance	Mean
Design A	1	0.256	0.254
	2	0.252	
	3	0.254	
Design B	1	0.256	0.255
	2	0.251	
	3	0.258	
0.1 ppm standard copper solution	1	0.260	0.260
	2	0.258	
	3	0.262	

TABLE 2

Comparison of absorbances of solutions from the two designs of sampling apparatus and of diluted dye solution

Sample	Absorbance[a]	
Design A	0.125	0.127
Design B	0.124	0.127
Standard solution	0.120	0.124

[a]All absorbance measurements were made in the linear range.

TABLE 3

Statistical treatment of calibration curves[a]

Ion $y = ax+b$	r	SD slope	SD intercept	Concentration range (ppm)	RSD slope	CV
$Cu = 0.2563x + 0.1125 \times 10^{-2}$	0.99985	0.1504×10^{-2}	0.1263×10^{-2}	0—2.000	0.6	1.5
$Zn = 1.192x + 2.639 \times 10^{-3}$	0.99807	0.9566×10^{-2}	0.4211×10^{-2}	0—0.800	0.8	1.8

[a]y = absorbance; x = ppm; a = slope; b = intercept. The correlation coefficient (r) is given with the standard deviations of the slope and of the intercept, and the relative standard deviation (RSD) of the slope, calculated in the conventional manner from 11 points (Cu) and 7 points (Zn). The coefficient of variance (CV) was calculated from the absorption readings obtained for 10 aliquots of a 0.500 ppm standard of each metal.

in Table 3. The coefficient of variance was calculated at 0.500 ppm, in the middle of the concentration range.

Table 4 provides data on the determination of copper and zinc for 10 patients undergoing a 2-h hemodialysis against a dialysate prepared with tap water. Blanks were collected while the patient was not connected to the dialyzer. Table 5 contains the same information for patients undergoing hemodialysis against dialysate prepared with distilled water. The difference between the mean absorbance of the blanks and samples indicates the possibility of active uptake of copper and zinc when patients are dialyzed against tap water. In concentration terms, the difference is about 0.040 ppm of copper and about 0.015 ppm of zinc. Smaller differences between the absorbances of the blanks and the appropriate samples are found when patients are dialyzed against distilled water.

The normal concentration ranges of copper and zinc in the blood are 0.7—1.4 ppm and 0.8—1.2 ppm, respectively. If the differences of concentration between the blank and the sample for each element were totally transferred to the patient's blood, then during a 2-h dialysis against tap water the blood would be enriched by significant amounts of copper and zinc.

The sources of copper and zinc contamination were investigated. The

TABLE 4

Absorbance values for copper and zinc for patients undergoing 2-h hemodialysis against dialysate prepared with tap water

Patient No.	Copper[a]		Zinc[b]		Patient No.	Copper[a]		Zinc[b]	
	Blank	Sample	Blank	Sample		Blank	Sample	Blank	Sample
1	0.459	0.368	0.554	0.313	6	0.470	0.389	0.575	0.409
	0.455	0.365	0.550	0.310		0.470	0.385	0.580	0.403
2	0.544	0.345	0.586	0.361	7	0.468	0.409	0.598	0.401
	0.540	0.343	0.580	0.364		0.462	0.405	0.592	0.406
3	0.428	0.312	0.532	0.334	8	0.504	0.322	0.590	0.510
	0.423	0.310	0.537	0.335		0.500	0.320	0.596	0.506
4	0.455	0.312	0.644	0.405	9	0.453	0.428	0.618	0.495
	0.459	0.312	0.641	0.410		0.448	0.425	0.615	0.503
5	0.427	0.343	0.649	0.500	10	0.486	0.397	0.597	0.480
	0.425	0.349	0.645	0.508		0.492	0.392	0.587	0.475
					Mean	0.468	0.362	0.583	0.421

[a] An extracted 0.01 ppm copper standard gave an absorbance of 0.026.
[b] An extracted 0.01 ppm zinc standard gave an absorbance of 0.120.

TABLE 5

Absorbance values for copper and zinc for patients undergoing 2-h hemodialysis against dialysate prepared with distilled water
(Absorbances for standards were the same as in Table 4.)

Patient No.	Copper		Zinc		Patient No.	Copper		Zinc	
	Blank	Sample	Blank	Sample		Blank	Sample	Blank	Sample
11	0.151	0.147	0.312	0.200	16	0.165	0.160	0.340	0.199
	0.152	0.147	0.310	0.201		0.165	0.157	0.335	0.205
12	0.173	0.158	0.326	0.207	17	0.182	0.173	0.339	0.217
	0.170	0.159	0.330	0.211		0.185	0.174	0.342	0.211
13	0.245	0.137	0.315	0.213	18	0.188	0.184	0.346	0.218
	0.245	0.139	0.316	0.210		0.191	0.183	0.345	0.216
14	0.181	0.171	0.295	0.182	19	0.175	0.174	0.325	0.213
	0.185	0.175	0.290	0.178		0.178	0.170	0.321	0.210
15	0.164	0.153	0.300	0.181	20	0.186	0.171	0.337	0.220
	0.163	0.156	0.298	0.181		0.182	0.171	0.334	0.217
					Mean	0.171	0.163	0.323	0.205

dialysis solution was analyzed for copper and zinc by the standard-additions method with a microprocessor and concentration signal of the instrument [8]. The concentrations of copper and zinc in the dialysis solution were found to be 0.625 ppm and 0.205 ppm, respectively. This solution reached the membrane of the dialyzer after being diluted by a factor of 34 making

the concentration of copper and zinc at the membrane from the dialysate alone 0.0184 ppm and 0.0060 ppm, respectively.

Triplicate analyses of the distilled and tap water used in the Royal Victoria Hospital (Montreal) showed that these waters contained 0.04 ppm (Cu) and 0.02 ppm (Zn) and 0.120 ppm (Cu) and 0.03 ppm (Zn), respectively. The amounts of copper and zinc which come from the tubing and dialysis membrane when distilled water is run into the dialyzer can be found by subtracting the sum of the metal concentrations in distilled water and in the dialysis solution from the mean blank concentration obtained from Table 5. The same procedure can be used for the tap water data. These calculations indicate that the tubing and membrane contribute about 0.01 ppm of zinc and 0.03 ppm of copper for distilled water, and 0.015 ppm of zinc and 0.100 ppm of copper for tap water. The differences between the results are due to the leaching efficiencies of the tap- and distilled-water flows.

Conclusions

Two designs of sampling apparatus are described. The systems continuously and representatively sample the dialysate as the patient is undergoing hemodialysis. Studies on 20 patients indicate an active uptake of copper and zinc from the dialysate, prepared either with distilled or tap water. The uptake of copper from tap water is large enough to suggest the possibility that hemodialysis might lead to a significant increase of copper in the blood of dialysis patients. The determination of copper and zinc in the serum of these patients is under investigation.

We are grateful to Dr. D. Hollomby and Head Nurse M. Dattel of the Nephrology Division, Royal Victoria Hospital. We acknowledge the support of the Medical Research Council and the Natural Sciences and Engineering Research Council of Canada.

REFERENCES

1 D. R. Williams, An Introduction to Bioinorganic Chemistry, C. C. Thomas Co., Springfield, IL, 1976, p. 197.
2 J. Blomfield, J. McPherson and C. R. P. George, Br. Med. J., 2 (1969) 141.
3 J. Blomfield, S. R. Dixon, and D. A. McCredie, Arch. Intern. Med., 128 (1971) 555.
4 E. D. M. Gallery, J. Blomfield, and S. R. Dixon, Br. Med. J., 4 (1972) 331.
5 A. D. Manzler and A. W. Schreiner, Ann. Intern. Med., 73 (1970) 409.
6 P. Allain, H. -E. Thebaud, L. Dupouet, P. Coville, M. Pisant, J. Spiesser and P. Alquier, Nouv. Presse. Med., 7 (1978) 92.
7 J. D. Kinrade and J. C. Van Loon, Anal. Chem., 46 (1974) 1894.
8 C. W. Fuller, At. Abs. Newsl., 11 (1972) 65.

Analytica Chimica Acta, 116 (1980) 383—389

DETERMINATION OF PALLADIUM IN SILVER, COPPER, SELENIUM AND ANODE SLUDGE BY ATOMIC-ABSORPTION SPECTROMETRY AFTER EXTRACTION OF TRI-n-OCTYLMETHYLAMMONIUM TETRABROMOPALLADATE

IWAO TSUKAHARA* and MINORU TANAKA

The Furukawa Electric Co., Ltd., Central Research Laboratory, 2-9-15, Futaba, Shinagawa-ku, Tokyo (Japan)

(Received 15th November 1979)

SUMMARY

Palladium (>0.5 μg) is extracted as tri-n-octylmethylammonium tetrabromopalladate into n-butyl acetate and determined by flame atomic-absorption spectrometry of the extract. Extraction from hydrochloric or hydrobromic acid solution with tri-n-octylamine is also discussed. The method is applied to the determination of palladium in silver, copper, selenium and anode sludge.

The determination of palladium in silver, copper, selenium or anode sludge from copper refining is of importance in their metallurgical evaluation, but few practical methods for the determination of trace quantities of palladium in the above materials have been reported. Sen Gupta [1] has determined palladium in native silver by flame atomic-absorption spectrometry (a.a.s.), and Everett [2] has determined palladium in copper by a.a.s. with a carbon rod atomizer. Tsukahara [3] has recently published a highly sensitive spectrophotometric method for palladium in silver, copper and anode sludge, with 4,4′-bis(dimethylamino)thiobenzophenone (Thio-Michler's ketone, TMK). This method is somewhat tedious as a lengthy pre-separation of palladium from interfering elements such as copper, gold or platinum is needed. It is, therefore, desirable to develop a simple, rapid and sensitive method for the determination of trace quantities of palladium in the above materials.

The extraction behaviour of palladium with certain high-molecular-weight ammonium salts from various media has been surveyed and tetrahexylammonium iodide shown to be an excellent extractant [4]. The extraction of palladium with tri-n-octylmethylammonium chloride (Aliquat 336) [5] and tri-n-octylamine [3] have been successfully used for the flame photometric and spectrophotometric determinations of palladium, respectively. These investigations suggest that extraction of palladium with a quaternary ammonium salt could also be effectively used for its atomic-absorption determination, especially as a highly selective extraction of palladium is not needed for this

purpose. The present paper, therefore, describes an investigation of the extraction of palladium with tri-n-octylamine (TOA), tri-n-octylmethylammonium chloride (TOMACl) and tri-n-octylmethylammonium bromide (TOMABr) from hydrochloric or hydrobromic acid solutions in conjunction with its a.a.s. determination. The TOMABr extraction system is applied to the determination of trace quantities of palladium in silver, copper, selenium and anode sludge.

EXPERIMENTAL

Apparatus

A Hitachi Model 208 atomic-absorption spectrophotometer with a three-slot 100-mm long burner, a Hamamatsu TV Model L233-46Q palladium hollow-cathode lamp and a Hitachi Model 056 recorder were used with the following operating conditions: wavelength 244.8 nm; slit-width 0.18 mm (entrance) and 0.18 mm (exit); burner height position 2; lamp current 5 mA; air 14 l min^{-1} ; acetylene 1 l min^{-1}.

Reagents

TOA solution. Dilute 6 ml of TOA (Wako Pure Chemical Industries Ltd.) to 200 ml with n-butyl acetate.

TOMACl solution. Dilute 6 ml of TOMACl (Capriquat; Dojindo Laboratories) to 200 ml with n-butyl acetate.

TOMABr solution. Dilute 6 ml of TOMACl to 20 ml with n-butyl acetate. Transfer this solution to a separatory funnel and shake with two 40-ml portions of 3 M hydrobromic acid for 10 min each time (discard the aqueous layers). Dilute the organic layer to 200 ml with n-butyl acetate.

Standard palladium solution. Dissolve 0.500 g of palladium metal in 10 ml of aqua regia. Add 40 ml of (1 + 1) hydrochloric acid and make up to 500 ml with water. Dilute the solution to the desired concentration immediately before use.

Procedure for investigation of extraction conditions and interferences

Transfer a portion of standard palladium solution (10 μg of Pd) to a 100-ml separatory funnel. Add hydrochloric or hydrobromic acid to give a final concentration of 0.2 M and dilute to 75 ml with water. Extract palladium by shaking vigorously with 10.0 ml of the TOA, TOMACl or TOMABr solution for 5 min. Discard the aqueous layer. Spray the organic layer into the flame and measure the atomic-absorption signal.

Recommended procedures for the analysis of samples

Copper and selenium. Decompose 5 g of sample with 30 ml of hydrochloric acid and 10 ml of nitric acid (for copper) or with 30 ml of (2 + 1) hydrochloric acid and 20 ml of nitric acid (for selenium). Evaporate the solution on a steam bath to a syrup (for copper) or to moist dryness (for

selenium). Add 60 ml of water (for copper) or 8 ml of (1 + 1) nitric acid and 50 ml of water (for selenium), and heat gently to dissolve the salts. Transfer the solution to a 200-ml separatory funnel. Add 10.0 ml of 3 M hydrobromic acid and dilute to 150 ml with water. Shake vigorously with 10.0 ml of the TOMABr solution for 5 min. Discard the aqueous layer. Wash the organic layer by shaking with 50 ml of 0.2 M hydrobromic acid for 3 min. Discard the aqueous layer. Spray the organic layer into the flame and measure the atomic-absorption signal.

Silver. Decompose 2 g of the sample with 10 ml of (1 + 1) nitric acid. Add 20 ml of (1 + 1) hydrochloric acid and heat gently on a steam bath for 1 h. Transfer the solution and silver chloride precipitate to a 100-ml volumetric flask and dilute to the mark with water. Transfer an aliquot (20—50 ml) of the supernatant solution to a 200-ml separatory funnel and dilute to about 120 ml with water. Add 10.0 ml of 3 M hydrobromic acid and make up to 150 ml with water. Complete the determination as for copper and selenium samples.

Anode sludge. Decompose 1 g of the sample, previously dried at 250°C for 10 h, with 30 ml of hydrochloric acid and 10 ml of nitric acid. Evaporate to moist dryness on a steam bath. Add 1 ml of (1 + 1) nitric acid, 3 ml of (1 + 1) hydrochloric acid and 50 ml of water, and heat gently to dissolve the salts. Transfer the solution together with the residue to a 100-ml volumetric flask and dilute to the mark with water. Transfer an aliquot (10—25 ml) of the supernatant solution to a 200-ml separatory funnel. Add 8 ml of (1 + 1) nitric acid and 2.5 ml of 3 M hydrobromic acid, and dilute to 150 ml with water. Complete the determination as described above.

Calibration. Transfer portions of standard palladium solution (containing up to 15 μg of Pd) to 200-ml separatory funnels. To each solution and a blank (water), add 1 ml of (1 + 1) nitric acid, 3 ml of (1 + 1) hydrochloric acid and 10.0 ml of 3 M hydrobromic acid, and dilute to 150 ml with water. Treat these solutions as described above, measure the atomic-absorption signals, and plot against the amount of palladium.

RESULTS AND DISCUSSION

Extraction with TOA and TOMA

The optimal conditions for the extraction of palladium with TOA and TOMACl from hydrochloric acid and with TOA and TOMABr from hydrobromic acid solution were investigated by using the procedure described above, with variation of one parameter at a time.

The greatest extraction of palladium with TOA was obtained from 0.02—0.5 M hydrochloric or hydrobromic acid; with TOMACl the acid range was 0.02—1.0 M hydrochloric acid, but with TOMABr it was wider (0.02—2.0 M hydrobromic acid) (Table 1). Small differences in the a.a.s. signals were observed among the four extraction systems at the respective optimal hydrochloric and hydrobromic acid concentrations; the highest sensitivity was obtained with the TOMABr—HBr system (Table 1).

TABLE 1

Effects of acid and amine concentrations on the extraction of palladium (10 μg)

HCl or HBr conc. (M)	TOA or TOMA conc. (% v/v)	Extraction system and scale reading			
		TOA—HCl	TOA—HBr	TOMACl—HCl	TOMABr—HBr
0.02[a]	3.0	45.2	48.0	47.2	48.9
0.05[a]	3.0	45.0	47.9	46.9	49.1
0.10[a]	3.0	45.0	47.9	47.0	48.8
0.20	3.0	45.2	48.0	47.0	49.0
0.30	3.0	45.0	48.0	47.0	49.0
0.50	3.0	45.2	48.0	47.1	49.0
1.0	3.0	42.7	46.0	46.8	49.0
1.5	3.0	40.0	44.5	46.1	49.2
2.0	3.0	36.7	42.8	44.5	49.2
3.0	3.0	29.5	37.5	41.0	46.5
0.20	0.2	24.8	35.4	50.0	51.2
0.20	0.4	34.4	38.7		
0.20	0.6	40.7	45.9	49.8	50.9
0.20	0.8	44.4	50.0		
0.20	1.0	46.9	50.1	49.5	50.7
0.20	2.0	46.3	49.4	47.9	50.0
0.20	3.0	45.0	48.0	47.0	49.0
0.20	4.0	45.0	47.2	46.7	48.5
0.20	5.0	45.0	46.8	45.1	47.8
0.20	7.0	42.8	45.7	42.3	46.5
0.20	10	41.3	43.3	40.3	43.9

[a]5 ml of 1.5 M sulfuric acid were added to the aqueous phase to avoid the formation of an emulsion or turbidity.

The concentrations of TOA, TOMACl and TOMABr in n-butyl acetate were varied from 0.2 to 10% (v/v). The results (Table 1) show that in the TOMA extraction systems, the absorption signals decreased gradually with increasing TOMA concentrations over the whole concentration range tested; in the TOA systems, the signals increased rapidly up to 1% TOA, probably because of an increase in the extraction of palladium with increasing TOA concentration, and then gradually decreased as the TOA concentration increased from 1 to 10%. The gradual decrease is probably due to a lowering of the aspiration rate of the extract because of the increasing viscosity of the solvent with increasing TOA or TOMA concentration.

The signals were independent of the shaking time from 1 to 10 min in all the extraction systems.

Effects of other acids

The effects of sulfuric, nitric, perchloric and hydrochloric acids on the extractions were investigated. The results are given in Table 2. Sulfuric acid

TABLE 2

Effects of other acids on the extraction of palladium (10 μg)
(HCl or HBr concentration 0.2 M; TOA or TOMA concentration in n-butyl acetate, 3% (v/v).)

Acid	Conc. (M)	Extraction system and scale reading			
		TOA—HCl	TOA—HBr	TOMACl—HCl	TOMABr—HBr
None		45.0	48.0	47.0	49.0
H_2SO_4	0.5	45.0	48.0	46.8	49.3
	1.0	45.1	47.7	46.4	48.9
	2.0	45.3	48.2	45.5	48.9
	3.0	45.6	48.0	42.4	49.1
HNO_3	0.01	45.3	48.2	47.0	48.9
	0.03	44.8	48.0	47.3	48.8
	0.05	43.3	47.8	46.7	49.2
	0.10	37.5	48.0	43.7	48.9
	0.20	24.3	48.0	35.8	48.9
	0.30	16.0	48.0	25.6	49.2
	0.50	8.0	45.9	10.9	49.0
	1.0	3.1	32.7	0.0	42.8
	2.0	0.0	2.7	0.0	12.0
$HClO_4$	0.01	41.0	46.9	0.0	48.4
	0.02	10.8	44.0	0.0	31.6
	0.04	1.7	29.0	0.0	11.6
	0.06	2.2	20.6	0.0	5.4
HCl	1.0		47.8		49.0
	2.0		48.0		49.1
	3.0		48.0		49.0
	4.0		45.0		47.5
	5.0		40.8		41.2
	6.0		35.9		31.3

above 0.5 M lowered the a.a.s. signals in the TOMACl—HCl system, but not up to at least 3.0 M in the other systems. Nitric and perchloric acids interfered greatly with the extraction of palladium; the interfering effects of nitric and perchloric acids in the chloride extraction systems were greater than those in the bromide extraction systems. Hydrochloric acid up to 3.0 M had no effect in the bromide extraction systems.

Effects of other elements

On the basis of the above results, the system with 0.2 M hydrobromic acid, 3% TOMABr in n-butyl acetate and a 5-min extraction was adopted for the determination of palladium in the materials mentioned. The effects of various ions on the extraction and determination of palladium by this

system were examined; the above experimental procedure was used, but with an additional 3-min washing of the organic layer with 50 ml of 0.2 M hydrobromic acid.

There was no interference from 1 mg of Pt(IV); 5 mg of Al, Be, Ce(IV), Cr(III), Hg(II), Mg, Mo(VI), Ti(IV), Tl(III), V(V), Zr; 10 mg of Au(III), Cd, In; 50 mg of Bi, Ca, Co, Mn(II), Sb(III); 100 mg of As(III), As(V), Fe(III), Sn(IV), Te(IV); 1 g of Zn; or 5 g of Cu or Ni. Up to 1 g of selenium(IV) did not interfere but 5 g caused a negative error; this could be eliminated by adding 4 ml of (1 + 1) nitric acid to the aqueous phase, i.e., by extracting palladium from a 0.2 M hydrobromic—0.35 M nitric acid solution.

Up to 10 mg of silver did not interfere, though a silver bromide precipitate was formed on the addition of hydrobromic acid; it is, however, desirable to separate the solution and the precipitate before the extraction of palladium. More than 10 mg of lead caused a positive error; that from 10—50 mg of lead could be eliminated by extracting palladium from 150 ml of 0.05 M hydrobromic—0.35 M nitric acid solution instead of from 75 ml of 0.2 M hydrobromic acid solution. Up to 1 mg of thallium(I) did not interfere, but larger amounts caused a negative error.

TABLE 3

Analytical results for various samples

Sample	Pd added[a] (μg)	Total Pd found (μg)	Pd in sample (ppm)		Sample	Pd added[a] (μ)	Total Pd found (μg)	Pd in sample (ppm	
			A.a.s. (average)	TMK method				A.a.s. (average)	TMK metho
Silver metal[b]	0	23.6	12	12	Copper metal (electrolytic)[c]	0	<0.5	<0.1	<0.02
	0	25.6				0	<0.5		
	20.0	43.0				5.0	5.2		
	20.0	45.6				5.0	5.1		
	0	1.2	0.6	0.81	Blister copper[c]	0	0.9	0.2	0.17
	0	1.2				0	1.0		
	2.0	3.3				2.0	3.1		
	2.0	3.1				2.0	2.9		
	0	36.4	18	20		0	5.7	1.2	0.98
	0	36.0				0	5.7		
	30.0	65.2				4.0	9.7		
	30.0	67.7				4.0	9.9		
Selenium[c]	0	<0.5	<0.1			0	<0.5	<0.1	0.07
	0	<0.5				0	<0.5		
	5.0	5.1				5.0	5.4		
	5.0	5.1				5.0	5.4		
Anode sludge[d]	0	26.0	26	26	Crude copper[c]	0	4.1	0.8	0.73
	0	25.5				0	3.9		
	25.0	50.5				4.0	8.1		
	25.0	51.1				4.0	8.3		

[a]Palladium solution was added to solid sample before dissolution. [b]2-g sample. [c]5-g sample. [d]1-g sample.

Applications

Palladium in silver, copper, selenium and anode sludge was determined by the proposed method (Table 3). The amounts of palladium added to samples before the sample decomposition were recovered quantitatively. As little as 0.5 μg of palladium in a sample or in an aliquot of the sample solution could be determined. The palladium contents determined by the proposed method are in good agreement with those determined by the spectrophotometric method based on [3]. The proposed method is simple, rapid and sensitive.

REFERENCES

1 J. G. Sen Gupta, Anal. Chim. Acta, 63 (1973) 19.
2 G. L. Everett, Analyst, 101 (1976) 348.
3 I. Tsukahara, Bunseki Kagaku, 28 (1979) 253.
4 W. J. Maeck, G. L. Booman, M. E. Kussy and J. E. Rein, Anal. Chem., 33 (1961) 1775.
5 M. H. Campbell, Anal. Chem., 40 (1968) 6.

Analytica Chimica Acta, 116 (1980) 391—396

Short Communication

ION-SELECTIVE ELECTRODES RESPONSIVE TO CHLOROCOBALTATE(II) IONS

R. W. CATTRALL* and GEAT LEAN LEE

Department of Inorganic and Analytical Chemistry, La Trobe University, Bundoora, Victoria 3083 (Australia)

I. C. HAMILTON

Department of Chemistry, Footscray Institute of Technology, Footscray, Victoria 3011 (Australia)

(Received 13th August 1979)

Summary. The response characteristics of some electrodes sensitive to chlorocobaltate(II) ions are reported. The most reliable electrode, which showed near-Nernstian response in the range 10^{-1}—10^{-4} M cobalt(II), was obtained by using a membrane consisting of 35% poly(vinyl chloride), 5% Aliquat chloride, and 60% of the blue oil obtained by extraction of cobalt with Aliquat-336, with conventional internal reference system.

Several coated-wire ion-selective electrodes responsive to various halometal complex anions have been reported [1—3]. In each case, the Aliquat-336 salt of the appropriate complex anion was immobilized in a poly(vinyl chloride) membrane and applied to a platinum wire. A study of similar electrodes involving anionic chlorocobaltate(II) complexes is described below.

Experimental

Materials and equipment. Aliquat-336 (tricaprylylmethylammonium chloride; General Mills Chemical Inc.), poly(vinyl chloride) powder (Corvic 20-6506; I.C.I., A.N.Z.), tetrahydrofuran, anhydrous lithium chloride (both May and Baker, reagent grade), and hexane (commercial grade) were used as received. The disodium salt of EDTA (Ajax Chemicals Ltd.) and chloroform (B.D.H.) were of analytical-reagent grade, as were all acids used.

Potentials were measured at room temperature with an Orion Model 801 digital pH meter and a saturated calomel triple-junction reference electrode. The outermost compartment contained lithium chloride solution of the appropriate concentration, separated from the test solution by a very low-leak asbestos fibre junction. This was necessary to prevent precipitation of potassium tetrachlorocobaltate(II) at the junction. The other compartments contained saturated potassium chloride solution.

Conversion of Aliquat-336 to the tetrachlorocobaltate(II) salt. Conversion was done by solvent extraction of 10^{-1} M cobalt chloride from either lithium chloride or hydrochloric acid solution [2]. At least 5 M total chloride was required to obtain the third phase, which was a deep purple/blue oil.

Construction of electrodes. The cobalt-containing oils from these preparations were mixed with poly(vinyl chloride) in the appropriate ratio. The mixture was dissolved in tetrahydrofuran and dip-coated onto a platinum wire, or a cobalt bead attached to a platinum wire, or a silver chloride-coated silver wire as described previously [2]. A conventional membrane electrode was prepared by forming a film of the membrane mixture over the open end of a narrow glass tube (ca. 0.4 cm diam.) and allowing to dry in air; this electrode had an internal reference system consisting of a silver/silver chloride wire in an appropriate aqueous lithium chloride solution (saturated with silver chloride).

Determination of Cl/Co ratio in oil extracts. The oily third phases obtained by solvent extraction from different media were analysed for their cobalt and chloride contents to establish the stoichiometry of the extracted complex. Cobalt was determined by ashing the oil with (2 + 1) concentrated nitric and perchloric (60—70%) acids, evaporation, dilution with water and atomic absorption spectrometry. Chloride was determined by the oxygen flask method [4].

A Cl/Co ratio of 4:1 was expected for complete conversion of Aliquat chloride to the tetrachlorocobaltate(II) salt. Ratios of Cl/Co in the range 4.6—5.5 were found for the different extracts. The excess of chloride was apparently due to uncomplexed Aliquat chloride, since lithium was not detected in extracts and continual washing of extracts with hexane (in which Aliquat chloride is soluble) reduced the ratio to 3.9:1. Oils prepared by extraction from hydrochloric acid solutions were contaminated with this acid, as was expected from the work of Good et al. [5].

Results and discussion

Coated-wire electrodes. The characteristics of coated-wire electrodes based on Aliquat salts of halometal complexes depend very much on the method of preparation of the oily third phase and on the proportions of Aliquat salt and poly(vinyl chloride) used in the membrane [1—3]. Each particular system demands empirical testing to establish optimum responses. Greater than 40% poly(vinyl chloride) produces a very hard membrane with a high electrical resistance and sluggish response, whereas greater than about 70% of the oil yields a sticky membrane which has a much faster response.

For the cobalt system, oils prepared from 7 M lithium chloride solutions produced the best coated-wire electrodes; one electrode which used 10 M lithium chloride was satisfactory only after long conditioning. Membrane compositions of 70, 60, 65, and 55% of oily phase and 30, 40, 35, and 45% poly(vinyl chloride), respectively, were studied for a platinum wire substrate. The 60:40 composition produced the most satisfactory membranes.

The general characteristics of such electrodes on platinum, silver, and silver choride-coated silver substrates is shown in Table 1; in all cases, the detection limit was 10^{-4} M cobalt(II). Measurements reported were made in 7 M lithium chloride solutions. The use of hydrochloric acid solutions led to non-Nernstian behaviour presumably because of protonation of the $CoCl_4^{2-}$ species. The responses of these coated-wire electrodes are near-Nernstian in the 10^{-1}–10^{-4} M total cobalt(II) concentration range, but their reproducibility, both short and long term, is inferior to that observed for previous systems [1–3]. Calculation, based on the appropriate formation constants [6], of the concentrations of the anionic chlorocobaltate(II) complexes in 7 M lithium chloride solutions demonstrates the high sensitivity of the electrodes to these species as they represent only 0.001% of the total cobalt(II) present in solution.

Another feature of the electrodes is their long response times. Attempts to reduce response times by addition of 10% dinonylphthalate or bis-(2-ethylhexyl)-2-ethylhexylphosphonate plasticizers were unsuccessful. Better results were obtained by adding Aliquate chlorid directly to the membrane. Improved response was obtained with a membrane consisting of 60% oil, 35% PVC and 5% Aliquat chloride on an Ag/AgCl substrate, but the lifetime of this electrode was short because of dissolution of the silver chloride. Attempts to control the internal reference potential by using a Co^0/Co^{2+} couple obtained by coating membranes on a cobalt metal substrate were not successful; these electrodes displayed a similar response to those in Table 1 but suffered from serious drift and poor reproducibility.

Some of the problems associated with the performance of electrodes based on silver, silver/silver chloride and cobalt may be caused by chemical reactions in the membrane on those substrates. Evidence from u.v. and infrared spectrophotometry and electrochemical measurements suggests that metal corrosion reactions lead to formation of Aliquat hydroxide and tertiary amine decomposition products in the membrane; the reactions cause the

TABLE 1

Coated-wire electrode characteristics for the 60:40 oil/PVC membrane composition in 7 M lithium chloride solutions

Substrate	Slope (mV/pCo)	Reproducibility (mV)		Response time (min)[b]	
		Run-to-run[a]	Daily	High[Co]	Low[Co]
Pt	+27.0	2	10–20	3–5	10–15
Ag	+27.0	2	5–10	3–5	10–20
Ag/AgCl	+27.5; +29.5[c]	2	10	3–5	10–15
Pt[d] (10 M LiCl)	+28.5	1	10–20	5–12	–

[a]Consecutive values for the same solution in repeated measurement of a series of standards. [b]The time required to reach a potential value stable for 1 min. [c]Two electrodes. [d]The standard solutions contained 10 M lithium chloride.

membranes to change from blue to green with time. There is no evidence of formation of hydroxy-substituted cobalt species and the reactions are not observed in membranes coated onto platinum.

Unlike those systems studied previously [1–3], it does not seem possible to produce satisfactory chlorocobaltate(II)-sensitive coated-wire electrodes. This is in contrast to a recent paper [7] in which satisfactory coated-wire electrodes sensitive to tetrathiocyanatocobaltate(II) are reported. A significant factor, is, no doubt, the higher stability of the thiocyanatocobaltate(II) complexes, which allows the use of much lower ionic strength solutions.

Electrodes with an aqueous internal reference system. Conventional PVC membrane electrodes based on oils extracted from 7 M and 10 M lithium chloride with an internal reference system comprising silver/silver chloride electrode in aqueous lithium chloride (7 M or 10 M) saturated with silver chloride and 10^{-1} M in cobalt chloride were investigated; membrane compositions of 60% oil, 35% PVC and 5% Aliquat chloride, and 60% oil and 40% PVC were tested. Electrodes based on 10 M lithium chloride extracts showed no improvement over those based on 7 M lithium chloride extracts; indeed, problems with solubility of silver chloride in the internal reference increased. Alternative reference systems (e.g., $Pt/PtCl_4^{2-}$) were no better than Ag/AgCl at this high chloride activity. Results for electrodes based on 7 M lithium chloride are shown in Table 2; both types had a detection limit of 10^{-4} M cobalt(II). The electrodes showed a linear response in the total cobalt(II) concentration range 10^{-4}—10^{-1} M (Fig. 1) and have superior day-to-day reproducibility to the coated-wire electrodes. Response times are, however, still rather long, which is not surprising as this property is largely controlled by membrane resistance and the change in configuration would not affect this markedly. This viewpoint is supported by the superior results obtained for electrodes based on membranes containing 60% oil, 35% PVC and 5% Aliquat chloride in both coated-wire and conventional configurations. Membranes with larger proportions of oil and/or Aliquat chloride were not examined in detail, as they were sticky and unstable.

TABLE 2

Characteristics of electrodes containing an aqueous reference system

Membrane composition (%)			Slope (mV/pCo)	Reproducibility (mV)		Response time (min)
Oil	PVC	Aliquat Cl^-		Run-to-run	Daily	
60	40	—	+24.0	1—3	1	6—25
60	35	5[a]	+31.5	1	1—3	1—12

[a]One electrode with this composition, prepared more recently with an internal aqueous reference system which had been allowed to age for several weeks, gave response times of less than 1 min in the more concentrated solutions and up to 5 min in the more dilute solutions.

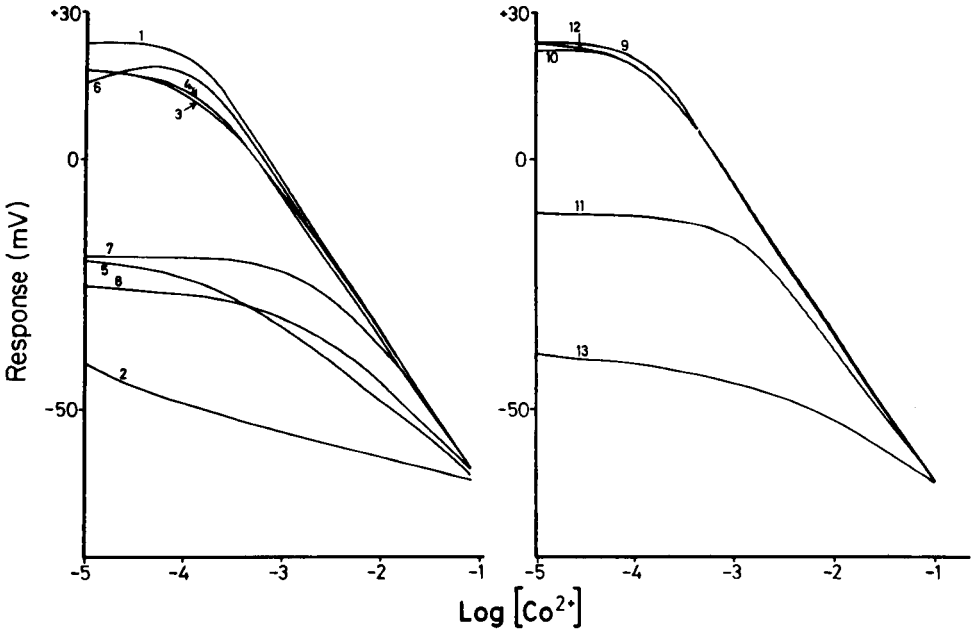

Fig. 1. Interference curves. (1) and (9) Co^{2+}; (2) 5×10^{-3} M Hg^{2+}; (3) 10^{-4} M Fe^{3+}; (4) 10^{-4} M Cu^{2+} and 10^{-1} M Ni^{2+}; (5) 5×10^{-4} M Cd^{2+}; (6) 5×10^{-2} M Cr^{3+}; (7) 5×10^{-2} M Mn^{2+}; (8) 10^{-3} M Zn^{2+}; (10) 10^{-2} M SO_4^{2-}; (11) 10^{-2} M I^-; (12) 5×10^{-2} M F^-; (13) 10^{-3} M ClO_4^-.

Electrodes based on extracts from 7 M lithium chloride with a 60:35:5 membrane composition and the aqueous Ag/AgCl reference system described above, were used for all work on interferences, pH dependence and potentiometric titrations. All measurements were carried out with 7 M lithium chloride test solutions.

In the pH study, no interference was observed in the pH range 1—4.5 for 10^{-1} M cobalt chloride solutions or in the range 1—5.5 for 10^{-2} M solutions. At higher pH values cobalt hydroxide precipitated. In strongly acidic solutions the electrode became insensitive as the chlorocobaltate(II) species became protonated. The results of other interference studies are shown in Fig. 1; these curves [8] were obtained for a fixed concentration of the interfering ion with varying total cobalt(II) concentrations. For strongly interfering ions, the fixed concentration was 10^{-3}—10^{-4} M and for weakly interfering ions, 10^{-1}—10^{-2} M. The interference curves show, as expected [1—3], that the strongly interfering ions are Cd^{2+}, Hg^{2+}, Zn^{2+}, Cu^{2+} and Fe^{3+}; Mn^{2+} and Cr^{3+} interfere less, and the interference by Ni^{2+} is small. Of the anions studied, strong interference occurs with perchlorate and iodide whereas sulphate, bromide and fluoride interfere weakly.

Potentiometric titrations. The titration of cobalt with EDTA containing 7 M lithium chloride was studied with the electrode as the end-point sensor. Since it was difficult to adjust the solution to pH 5—6, which is necessary for

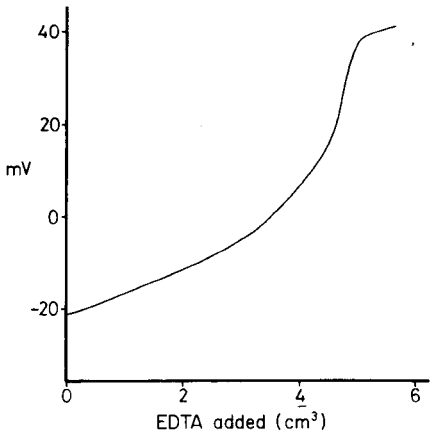

Fig. 2. The titration of 10 cm^3 of a ca. 5×10^{-3} M cobalt(II) solution with 0.01 M EDTA; initial pH 5.7.

the titration of cobalt without precipitation of cobalt hydroxide, the pH of the EDTA solution was adjusted to about 8 before the start of the titration. This kept the cobalt solution below pH 5.5 during the titration and gave a pH value of 6—6.8 at the end-point. Reasonably sharp inflections were thus observed in the titration curves even for very low concentrations of cobalt (Fig. 2). The control of the pH is crucial since too high a value will lead to precipitation of cobalt hydroxide whereas too low a value gives incomplete reaction with EDTA. With careful pH control, the method gives results similar to those obtained with a visual indicator. For example, repeated titrations of a ca. 5×10^{-3} M cobalt(II) solution with 10^{-2} M EDTA gave an average result of 4.89×10^{-3} M (0.5% r.s.d., $n = 6$) by the electrode method, compared with a result of 5.01×10^{-3} M (0.3% r.s.d., $n = 6$) by a conventional visual titration with xylenol orange as indicator.

We are grateful to the Australian Research Grants Committee for financial support and one of us (G.L.L.) thanks La Trobe University for the award of a Postgraduate Scholarship.

REFERENCES

1 R. W. Cattrall and Chin-Poh Pui, Anal. Chem., 47 (1975) 92.
2 R. W. Cattrall and Chin-Poh Pui, Anal. Chem., 48 (1976) 552.
3 R. W. Cattrall and Chin-Poh Pui, Anal. Chim. Acta, 83 (1976) 355; 87 (1976) 419; 88 (1977) 185.
4 I. M. Kolthoff and P. J. Elving, Treatise on Analytical Chemistry, Part I, Theory and Practice, Vol. 2, Interscience, New York, 1961, p. 1062.
5 M. L. Good, S. E. Bryan, F. F. Holland, Jr. and G. J. Maus, J. Inorg. Nucl. Chem., 25 (1963) 1167.
6 Stability Constants of Metal-Ion Complexes, Supplement No. 1, Spec. Publ. No. 25, The Chemical Society, London, 1971, p. 171.
7 K. Burger and G. Petho, Anal. Chim. Acta, 107 (1979) 113.
8 G. J. Moody and J. D. R. Thomas, Talanta, 19 (1972) 623.

Analytica Chimica Acta, 116 (1980) 397—401

Short Communication

THE USE OF TUNGSTEN TRIOXIDE IN THE COULOMETRIC DETERMINATION OF TOTAL CHLORINE IN ORGANIC AND INORGANIC MATERIALS

M. C. VAN GRONDELLE* and P. J. ZEEN

Koninklijke/Shell-Laboratorium (Shell Research B.V.), Amsterdam (The Netherlands)

(Received 19th October 1979)

Summary. Samples are placed on tungsten trioxide in a platinum boat for combustion or pyrolysis. Moistened oxygen is used as the combustion and carrier gas. The hydrochloric acid formed is titrated with electrolytically generated silver ions. Coals, spent catalysts, aqueous solutions and other organic and inorganic substances with chlorine contents in the range of 1 mg kg^{-1} up to several percent can be analysed reproducibly.

For the determination of traces [1, 2] or larger amounts [3] of chlorine in organic products, sample combustion in a quartz tube followed by on-line detection of the hydrogen chloride or chlorine formed, is well established. A serious drawback of this procedure, however, is its sensitivity to the presence of metals, which may retain chlorine in the combustion residue as involatile chlorides. This problem has previously been overcome by adopting a two-stage procedure comprising, e.g., decomposition of the sample via a Schöniger combustion or peroxide fusion, with subsequent determination of the chloride in aqueous solution by titration. As the latter methods are time-consuming, the possibility of a rapid on-line determination was investigated analogously to a recent study of sulfur determinations [4], several metal oxides being examined as releasing agents.

Experimental

Apparatus. A diagram of the apparatus is shown in Fig. 1. It consists of a platinum boat inlet system, a quartz combustion tube, an absorption vessel for the removal of water from the combustion gases and a cell controlled by a Dohrman microcoulometer for the titration with silver(I) ions. The sample inlet system and the quartz combustion tube are identical with those described for the determination of sulfur [4]; the arrangement results in a complete "flash-type" combustion of organic materials. The primary oxygen is moistened. The flow rates used for the primary and secondary oxygen streams are 75 and 225 ml min^{-1}, respectively. For organic substances 5-mg samples are taken; for inorganic materials the sample amount can be increased.

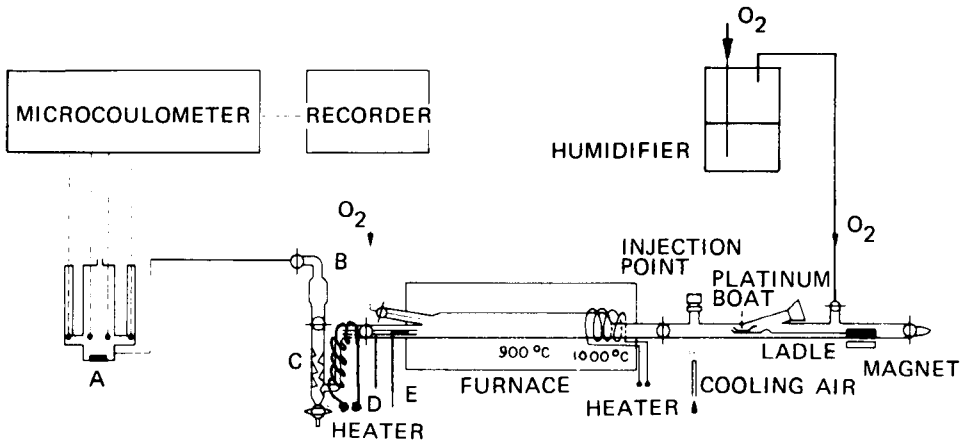

Fig. 1. Diagram of apparatus. (A) Titration cell and stirrer; (B) foam destroyer; (C) absorption vessel; (D) quartz outlet tube; (E) quartz wool plug.

General procedure. The sample is weighed or injected via a syringe into the platinum boat, which contains a layer of the reagent. The boat is moved into the furnace by means of a ladle and magnet. The "combustion" gases are dried by passing them through the absorption vessel, which contains 2 ml of 80% sulfuric acid. Finally, the chlorides formed are titrated with coulometrically generated silver ions. Any free chlorine formed is first reduced by hydrazine sulfate present in the cell electrolyte.

Choice and behavior of releasing agent. Several materials were tested as aids for the decomposition of inorganic chlorides at a furnace temperature of ca. 900°C; the results are given in Table 1. Generally, the results were good, but only tungsten trioxide and vanadium pentoxide proved entirely satisfactory. As tungstic oxide had previously performed well for the determination of sulfur [4], it was chosen again for all further work. It has the practical advantage that, unlike V_2O_5 which melts in the platinum boat during analysis, it remains as a powder and is easily removed from the boat.

TABLE 1

Comparison of reagents for the release of chlorine from aqueous NaCl solution (800 mg kg^{-1})

	Reagent					
	WO_3	V_2O_5	Cr_2O_3	Fe_2O_3	Co_3O_4	None
Recovery (%)	100	100	95—100	90—95	90—95	0
Elution time (min)	<1	<1	2	3—4	5	No peak

When tungsten trioxide was used, the following observations were made. Tungsten oxides condense in the cold outlet part of the quartz tube in amounts proportional to the amounts of chloride introduced. Presumably, the chlorine is initially transported as volatile oxyhalides (e.g. $WOCl_4$), which decompose or hydrolyse in the quartz tube to form hydrogen chloride, chlorine and involatile oxides. Mass spectrometric analyses of the cold outlet gases confirmed that only HCl and Cl_2 are present. In the analysis of sodium or potassium chloride solutions a reaction temperature of 700°C was found to be sufficient for releasing the chlorine within one minute. With solid samples such as silica-based catalysts, the diffusion of chlorine to the surface of the sample particles may limit the reaction velocity. Increasing the temperature to 1000—1100°C is then necessary.

Water vapour added to the primary oxygen stream greatly improves the reaction rate. Moistening reduces the elution time of the chloride peak from 5 to 1.5 min in the case of pure sodium chloride; even with aqueous sodium chloride solutions, the elution time is considerably shorter (< 30 s). Further addition of water is inconvenient as it necessitates more frequent replacement of the sulfuric acid in the absorption vessel. Another advantage of moistening the oxygen stream is a decrease of the chlorine formation ($2Cl_2 + 2H_2O \leftrightarrows 4\ HCl + O_2$), although chlorine cannot be completely avoided. Addition of a few milligrams of hydrazine sulfate to the cell electrolyte prevents chlorine from escaping titration.

Titration with silver(I) ions. The titration cell is essentially the same as that described by Dohrman [5]. However, as the titration is very light-sensitive, brown glass cells were preferred. The reference electrode is calomel: a platinum wire in a mixture of mercury and mercury(I) chloride. Its lifetime is much longer than that of the original silver—silver acetate reference electrode, which easily decomposes to form silver metal.

Owing to the low conductivity of the electrolyte, 70% (w/w) acetic acid, the titration of large amounts of chloride is a lengthy procedure. Experiments in which the electrolyte conductivity was increased by the addition of, e.g., trichloroacetic, sulfuric or perchloric acid [6] initially failed because of irreversible damage to the sensor electrode after several days of use. This resulted in baseline noise and negative baseline shifts. The best compromise was the addition of perchloric acid to the electrolyte up to a concentration of about 2%, just before its application. When not in use the silver sensor and generator electrode should be stored in water to minimize damage. For the determination of the lowest chloride concentrations, the perchloric acid can be omitted.

When some metal-containing samples were analysed, an increasing tendency to severe overshoot was observed. This phenomenon also occurred when small amounts (of the order of several mg kg^{-1}) of iron salts were added to the cell. To minimize the transport of metals to the titration cell and sulfuric acid scrubber, a piece of quartz wool was placed in the outlet tube just outside the furnace.

For the titration of small amounts of chlorine, the T520 Dohrman titration cell of the DE-20 system also gave excellent results. This cell is gas-stirred, has a volume of only 2 ml and comprises solid silver rod electrodes held in feed-through rubber-teflon septa. The stability of this cell, if protected from light, can be better than that of the standard cell by a factor of ten.

Results and discussion

Aqueous chloride test solutions ranging in concentration from 1 to 10,000 mg kg^{-1} were analysed. The recoveries (100%) and peak shapes are the same as those for organic test samples. Table 2 gives some results for inorganic metal halides with sample sizes of approximately 0.2 mg. Only mercury interfered, as the metal recombines with the halide prior to titration. Bromide and iodide give the same response as chloride, so that the method is in fact a procedure for the determination of total halogen except fluorine.

The method has been used for the analysis of a wide variety of samples. Table 3 compares the results of the proposed methods with those of alternative procedures. The results show good agreement.

The accumulation of some metal compounds in the cooler part of the outlet tube might lead to low results because of adsorption effects or chemical reactions. In practice, however, no such effect was found. Tungsten oxides are deposited throughout the system and in the outlet tube, forming an inert layer which prevents adsorption of chlorine. In fact, the recovery is more stable than was previously found with tungsten trioxide in the determination of organic samples. The colder part of the outlet tube should be cleaned or replaced whenever excessive amounts of deposit are visible, e.g. every two weeks. The outlet tube is an easily replaceable straight piece of quartz-tube [4]. The quartz tube can be used for about six months.

The limit of detection is about 1 mg kg^{-1} and is mainly governed by blank effects. Blanks can be minimized by washing the ladle and inlet system with water and acetone after analyses of samples with high chlorine contents. The weighing boat should not be exposed to the atmosphere for periods longer than are necessary for weighing. For analysis of aqueous solutions, blank effects can be reduced by injecting large samples and taking care that the water evaporates slowly.

For chlorine contents higher than 20 mg kg^{-1}, the standard deviation of the method proved to be 1.5% relative.

TABLE 2

Analyses of various inorganic halides

	NaCl	$CaCl_2$	$PbCl_2$	$HgCl_2$	$Ba(ClO_4)_2$	$ZnCl_2$ soln.	KBr	KI
Cl calculated (%)	60.7	64.0	25.5	26.1	21.1	1.05	67.1	76.4
Cl found	61.3	63.6	26.1	<5	21.8	1.06	67.0	76.9

TABLE 3

Analyses of various samples

Sample type	Chlorine content ($mg\ kg^{-1}$)		Sample type	Chlorine content (% w/w)	
	Found	Present		Found	Present
Acetone–water mixture, containing Cs	89	88	Catalyst A, Pt on Al_2O_3	1.33	1.31
Tap water Amsterdam, 1977	170	171	Catalyst B, Pt on Al_2O_3	0.65	0.64
Brine, 5% K, 3% Na, 2.4% Mg + Ca	2600	2650	Coal A, 19% ash	0.0044	0.005
Catalyst A, 7% Ag on silica	131	127	Coal B, 70% ash	0.0062	0.005
Catalyst B, 7% Ag on silica	21	17	Coal C, 5% ash	0.143	0.14
Polypropylene A, traces Na, Al, Ti	37	33	Coal D, 5% ash	0.25	0.23
Polypropylene B, traces Na, Al, Ti	73	77			

REFERENCES

1 W. Lädrach, F. van de Craats and P. Gouverneur, Anal. Chim. Acta, 50 (1970) 219.
2 F. C. A. Killer, in R. Belcher (Ed.), Instrumental Organic Elemental Analysis, Academic Press, London, 1977.
3 H. C. E. van Leuven, Fresenius Z. Anal. Chem., 264 (1973) 220.
4 M. C. van Grondelle and P. J. Zeen, Anal. Chim. Acta, 116 (1980) 335.
5 J. A. McNulty and L. W. Hoppe, Submicro Elemental Analysis by Micro-coulometry, Dohrmann Instruments, Mountain View, CA, 1969.
6 W. J. van Oort, G. Veenendaal, E. Buysman and B. Griepink, Fresenius Z. Anal. Chem., 284 (1977) 125.

Analytica Chimica Acta, 116 (1980) 403—406

Short Communication

METALLEXTRAKTION MIT *N*-THIOBENZOYL-*N*-PHENYLHYDROXYLAMIN

E. UHLEMANN*, B. MAACK und M. RAAB**

Pädagogische Hochschule "Karl Liebknecht" Potsdam, Potsdam-Sanssouci (D.D.R.)

(Eingegangen den 14. November 1979)

Extraction of metal ions with N-*thiobenzoyl*-N-*phenylhydroxylamine*

Summary. The extraction parameters $pH_{½}$ and K_{ex} for Mn, Fe, Co, Ni, Cu, Zn, Cd, and Pb with *N*-thiobenzoyl-*N*-phenylhydroxylamine are reported. *N*-Thiobenzoyl-*N*-phenylhydroxylamine extracts metals from more strongly acidic solutions than does *N*-benzoyl-*N*-phenylhydroxylamine. Iron(III) is extracted as a 1:2 chelate with the extractant, whereas iron(II) forms the expected tris chelate by oxidation. The other bivalent ions are extracted as their bis chelates.

Zusammenfassung. Die Extraktionsparameter $pH_{½}$ und K_{ex} für Mn, Fe, Co, Ni, Cu, Zn, Cd und Pb wurden bestimmt. *N*-Thiobenzoyl-*N*-phenylhydroxylamin extrahiert die Metalle aus stärker saurer Lösung als *N*-Benzoyl-*N*-phenylhydroxylamin. Bei der Extraktion von Eisen(III) werden überraschenderweise nur 2 Moleküle des Extraktionsmittels gebunden, während beim Eisen(II) durch Oxydation das erwartete Tris-Chelat entsteht. Alle anderen zweiwertigen Metalle werden als Bis-Chelate extrahiert.

N-Benzoyl-*N*-phenylhydroxylamin hat sich als Extraktionsmittel für Metallionen bereits bestens bewährt [1, 2], über des thioanaloge *N*-Thiobenzoyl-*N*-phenylhydroxylamin liegen dagegen nur wenige Angaben vor. Der Grund hierfür ist wohl in Schwierigkeiten bei der Darstellung der Substanz zu suchen. So verläuft die Synthese aus Phenylhydroxylamin und Thiobenzoylchlorid nur mit relativ geringer Ausbeute, und auch das Ausgangsprodukt Thiobenzoylchlorid ist nicht ohne Schwierigkeiten zugänglich [3, 4]. Ohne großen Aufwand und in guter Ausbeute kann *N*-Thiobenzoyl-*N*-phenylhydroxylamin durch Verwendung von Thiobenzoylthioglykolsäure als Thiobenzoylierungsmittel hergestellt werden [5]. Über die Darstellung von Metallchelaten und die Bestimmung von Komplexstabilitätskonstanten [4] sowie über die Verwendung zur gravimetrischen Bestimmung von Kupfer [6] und Eisen [7] wurde von anderer Seite berichtet; in dieser Arbeit wird die Extraktion von Metallen durch *N*-Thiobenzoyl-*N*-phenylhydroxylamin und das Verteilungsverhalten des Extraktionsmittels untersucht.

**Zentralinstitut für Ernährung der AdW der DDR, Potsdam-Rehbrücke.

Experimenteller Teil

Darstellung von N-*Thiobenzoyl*-N-*phenylhydroxylamin.* Thiobenzoylthioglykolsäure (18 g;0,1 mol) [8] werden in 360 ml 1 M Natronlauge gelöst. Dazu gibt man unter Rühren und Eiskühlung eine Lösung von Phenylhydroxylamin (10,9 g;0,1 mol) in 200 ml Wasser und läßt die Mischung einige Zeit stehen. Die Lösung trübt sich und nimmt eine orange Färbung an. Im Verlaufe von 30 min wird unter Kühlung mit verdünnter Salzsäure angesäuert. *N*-Thiobenzoyl-*N*-phenylhydroxylamin scheidet sich in Form gelber Kristalle ab. Ausbeute: 11 g (65%); Schmp. 101—102°C (Ethanol/Wasser).

Verteilungsverhältnis des N-*Thiobenzoyl*-N-*phenylhydroxylamins.* Zur Bestimmung des Verteilungsverhältnisses in Abhängigkeit vom pH-Wert wurden jeweils 10 ml einer 4×10^{-3} M Lösung von *N*-Thiobenzoyl-*N*-phenylhydroxylamin in Chloroform mit dem gleichen Volumen entsprechender Pufferlösungen der Ionenstärke 0,1 30 min geschüttelt: 10 min nach erfolgter Phasentrennung wurde die Extinktion der organischen Phase bei einer geeigneten Wellenlänge gemessen und daraus mit Hilfe der Extinktion der Ausgangslösung der Verteilungskoeffizient D berechnet. Die Auftragung von log D gegen pH entspricht der linearen Beziehung $\log D = \log (K_v/K_s) -$ pH aus der für $\log D = \sigma$, $\log K_v/K_s = 9{,}95$ leicht ermittelt werden kann.

Durchführung der Extraktion. Als Metallstandardlösungen dienten 4×10^{-5} M Lösungen der Metallnitrate, die außerdem 2×10^{-4} M Kaliumnatriumtartrat als Hilfskomplexbildner und 10^{-1} M Natriumnitrat zur Gewährleistung einer konstanten Ionenstärke enthielten. Zur Untersuchung der Zweiphasenverteilung wurden jeweils 10 ml 4×10^{-5} M wäßriger Metallsalzlösung mit 10 ml 4×10^{-3} M Lösung des Extraktionsmittels in Chloroform 30 min geschüttelt. Die Einstellung verschiedener pH-Werte erfolgte durch tropfenweise Zugabe von 1 M, 0,1 M und 0,01 M Salzsäure bzw. 1 M, 0,5 M, 0,2 M, 0,1 M und 0,01 M Natronlauge. Die Bestimmung des pH-Wertes der jeweiligen wäßrigen Phase wurde mit pH-Meßgerät (MV 84; Elektrodensystem GA 50 N/SE 20; VEB Präcitronic, Dresden) vorgenommen. Die Metallbestimmung erfolgte in einem Anteil der wäßrigen Phase. Dazu stand das Atomabsorptionsspektrometer AAS 1 (VEB Carl Zeiss, Jena) mit Hohlkatoden (VEB Narva, Berlin) zur Verfügung. Aus der Differenz der Ausgangskonzentration an Metall und des nach der Extraktion in der wäßrigen Phase verbliebenen Anteils konnten die Verteilungskoeffizienten ausreichend genau berechnet werden.

Eine Beeinflussung der Extraktion durch die zugesetzten Hilfskomplexbildner findet in den interessierenden pH-Bereichen nicht statt; nur beim Eisen(III) sind oberhalb pH 1,5 geringe Korrekturen erforderlich [9].

Ergebnisse und Diskussion

Die pH-Abhängigkeit der Extraktion von Mangan, Eisen, Cobalt, Nickel, Kupfer, Zink, Cadmium und Blei mit *N*-Thiobenzoyl-*N*-phenylhydroxylamin ist in Abb. 1 dargestellt. Auffällig ist hierbei das Vermögen zur Extraktion von Kupfer aus recht stark saurer Lösung, wobei allerdings mit Ansteigen

des pH-Wertes die Extraktionsausbeute — wahrscheinlich infolge von Redoxvorgängen — wieder abnimmt. Bemerkenswert gut wird auch Blei extrahiert.

Aus der Darstellung von log D gegen pH wurden als Extraktionskenngrößen die Zahl der bei der Extraktion freigesetzten Säureprotonen n, die pH-Werte hälftiger Extraction $pH_{½}$ und die Extraktionskonstanten K_{ex} bestimmt.

Ein interessantes Verhalten zeigt hier Eisen. Eisen(III) wird bereits bei sehr tiefem pH extrahiert. Die Darstellung von log D gegen pH ergibt eine Gerade der Neigung 2; im Extrakt liegt also nicht das erwartete Tris-Chelat vor, sondern wahrscheinlich ein Komplex der Zusammensetzung $FeL_2^+NO_3^-$. Derartige Komplexe konnten vor einiger Zeit auch in fester Form dargestellt werden [11], wohingegen die Tris-Komplexe präparativ nur bei höheren pH-Werten zugänglich sind. Bei Verwendung von Eisen(II)-sulfat erfolgt die Extraktion erst oberhalb pH 3, es entsteht aber in diesem Falle — wie das log D/pH-Diagramm ausweist (Abb. 2) — ein Tris-Chelat FeL_3 unter gleichzeitiger Oxydation des Eisen-Zentralatoms. Alle anderen zweiwertigen Metallionen werden als Bis-Ligand-Komplex extrahiert.

Die Kenngrößen für die Metallextraktion mit *N*-Thiobenzoyl-*N*-phenylhydroxylamin sind in Tab. 1 zusammengefaßt. Zum Vergleich wurden auch $pH_{1/2}$-Werte für *N*-Benzoyl-*N*-phenylhydroxylamin angegeben. Mit Ausnahme des Eisens weist die Thioverbindung in jedem Fall den kleineren $pH_{1/2}$-Wert auf, ist also für Extraktionen aus saurer Lösung besser geeignet. Die Ursachen sind vor allem in der höheren Komplexstabilität der Thioverbindungen zu suchen, wohingegen die Verteilungsverhältnisse der Extraktionsmittel nur von geringem Einfluß sind. Die Werte von log K_v/K_s betragen für *N*-Benzoyl-*N*-phenylhydroxylamin 10,48 [12] und für *N*-Thiobenzoyl-*N*-phenylhydroxylamin 9,95.

Die Extrahierbarkeit der zweiwertigen Übergangsmetallionen durch *N*-Thiobenzoyl-*N*-phenylhydroxylamin entspricht im wesentlichen der Irving—Williams-Reihe der Komplexstabilitäten, wenngleich die Unterschiede zwischen Nickel, Cobalt und Zink recht gering ausfallen.

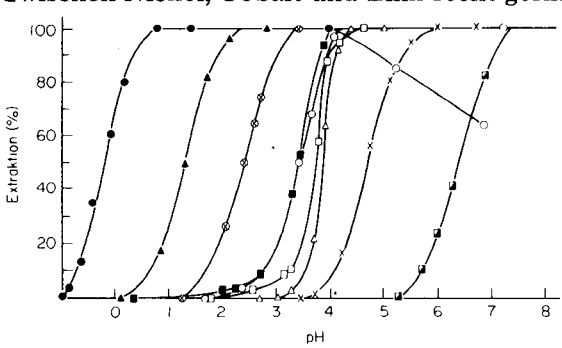

Abb. 1. Metallextraktion mit *N*-Thiobenzoyl-*N*-phenylhydroxylamin. (•) Cu; (▲) Fe(III); (⊗) Pb; (■) Ni; (○) Co; (□) Zn; (△) Fe(II); (×) Cd; (⧈) Mn.

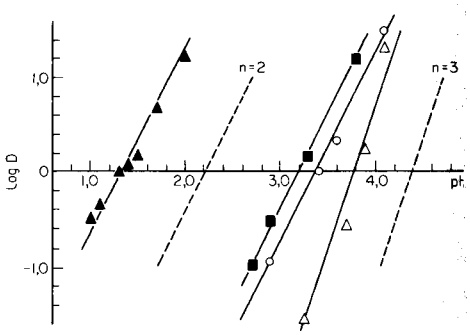

Abb. 2. Log D/pH-Diagramm für die Extraktion von (▲) Fe(III); (△) Fe(II); (■) Ni; (○) Co.

TABELLE 1

Extraktionsparameter für *N*-Thiobenzoyl-*N*-phenylhydroxylamin (TBPHA) im Vergleich mit *N*-Benzoyl-*N*-phenylhydroxylamin (BPHA)

	TBPHA		BPHA		TBPHA		BPHA
	$pH_{1/2}$	$\log K_{ex}$	$pH_{1/2}$ [10]		$pH_{1/2}$	$\log K_{ex}$	$pH_{1/2}$ [10]
Cu	−0,25	5,3	2,3	Zn	3,65	−2,5	7,85
Fe(III)	1,35	2,1	1,4	Fe(II)	3,80	−4,2	—
Pb	2,80	−0,8	6,1	Cd	4,70	−4,6	9,0
Ni	3,20	−1,6	7,65	Mn	6,30	−7,8	8,3
Co	3,55	−2,3	7,65				

LITERATUR

1 J. Stary, The Solvent Extraction of Metal Chelates, Pergamon, Oxford, 1964.
2 O. G. Koch und G. A. Koch-Dedic, Handbuch der Spurenanalyse, Springer-Verlag, Berlin—Heidelberg—New York, 1974.
3 G. A. Brydon und D. E. Ryan, Anal. Chim. Acta, 35 (1966) 190.
4 R. Dietzel und Ph. Thomas, Z. Anorg. Allg. Chem., 381 (1971) 214.
5 E. Uhlemann und B. Maack, Wirtsch. -Pat. DDR WP C 07 C/201 140.
6 R. M. Cassidy und D. E. Ryan, Anal. Chim. Acta, 41 (1968) 319.
7 I. D. Abraham, J. Abraham und D. E. Ryan, Anal. Chim. Acta, 48 (1969) 93.
8 F. Kurzer und A. Lawson, Org. Synth., 42 (1962) 100.
9 E. Uhlemann, B. Maack und M. Raab, Anal. Chim. Acta, 116 (1980) 153
10 J. Chwastowska, Chem. Anal., 12 (1967) 469.
11 A. J. Mitchell, K. S. Murray, P. J. Newman und P. E. Clark, Aust. J. Chem., 30 (1977) 2439.
12 D. Dyrssen, Acta Chem. Scand., 10 (1956) 353.

Analytica Chimica Acta, 116 (1980) 407—411

Short Communication

TIME-RESOLVED LASER-INDUCED FLUORESCENCE WITH HIGH-PERFORMANCE LIQUID CHROMATOGRAPHY FOR ANALYSIS OF POLYCYCLIC AROMATIC HYDROCARBON MIXTURES

J. H. RICHARDSON*, K. M. LARSON**, G. R. HAUGEN, D. C. JOHNSON and J. E. CLARKSON

General Chemistry Division, Lawrence Livermore Laboratory, University of California, Livermore, California 94550 (U.S.A.)

(Received 18th October 1979)

Summary. Time-resolved fluorescence is used to enhance the selectivity for polycyclic aromatic hydrocarbon mixtures by high-performance liquid chromatography. A pulsed laser is used as the excitation source. Only fluorophores with long fluorescence lifetimes (e.g. fluoranthene) are monitored if the delay between excitation and detection is sufficiently long. Limits of detection are of the order of 1—10 pg (5—50 fmol). The advantages are illustrated with a sample from the condensed steam distillate following a coal gasification experiment.

High-performance liquid chromatography (h.p.l.c.) has been used extensively to separate polycyclic aromatic hydrocarbon (PAH) mixtures. Detection has usually been by u.v. absorption [1, 2] or fluorescence with conventional sources [3, 4]. Laser-induced fluorescence has been used as the detection system following h.p.l.c. separation for several fluorophores [5, 6], with the lowest limits of detection, 750 fg, being obtained for aflatoxins [7]. Time-resolved laser-induced fluorescence techniques have been used to obtain sensitive detection of pure PAH compounds in aqueous solutions [8] and in matrix isolation [9]. This communication describes the use of this technique with h.p.l.c. to analyze PAH mixtures.

Experimental

Reagents. All PAH compounds were obtained from commercial sources and used without further purification: anthracene, azulene, 1,12-benzoperylene, fluoranthene, pyrene (all from Aldrich), and chrysene (Eastman Kodak, Baker, and Aldrich). The h.p.l.c. mobile phase was a 70:30 mixture of acetonitrile (Burdick and Jackson) and water (deionized distilled).

Instrumentation. A Waters Associates liquid chromatograph pump was used with a Whatman Partisil PXS 10/25 ODS column. Sample injection was done by using a sample loop operated by a rotary valve with a 20-μl injection volume. Deaerating the solvent reservoir with nitrogen had no appreciable

**Present address: Department of Chemical Engineering, University of Colorado, Boulder, CO 80309, U.S.A.

effect on the fluorescence lifetime or intensity. The sample chamber initially consisted of a Schoeffel flow-through cuvette. Somewhat better results were obtained with a windowless fluorescence cell similar to that described previously [7]; the eluent from the h.p.l.c. column flows in the gap between a stainless steel tube and a solid rod. The flow rate was 0.6 ml min^{-1}.

The fluorescence cell was contained in a light-tight sample chamber previously described [8, 10]. This sample chamber was designed for time-resolved laser-induced fluorescence, and has provisions for picking off a trigger pulse, spatial filtering and focusing of the excitation pulse, and right-angle fluorescence monitoring with focusing objectives and both spatial and wavelength filtering.

A Molectron UV-1000 nitrogen laser was used to excite the sample directly at 337 nm or to pump a Molectron dye laser used in the DL-200 configuration. The pulsewidths of both lasers were nominally 10 ns, with a 25-Hz repetition rate. Typical powers used were 1.5 kW at 337 nm (vastly attenuated, higher powers appeared deleterious) and 10 kW at 366 nm (with the dye laser with PBD). An RCA 8850 photomultiplier tube was used to monitor the resulting fluorescence. A Princeton Applied Research 162/163 boxcar averager with a 1-ns sampling head was used for data acquisition and signal averaging. Schott long-pass filters were used to attenuate undesired scatter. Typical effective time constants were 3 s.

A limit of detection for fluoranthene similar to that obtained with the pulsed laser was also obtained by using a SpectraPhysics 171 krypton ion laser. The constant-wavelength u.v. output (351/356 nm) was mechanically chopped; typically incident powers were 200 mW. The resulting modulated fluorescence signal was detected with a Princeton Applied Research HR-8 lock-in amplifier.

Results and discussion

Detection limits were approximately one order of magnitude lower by using the windowless fluorescence cell as opposed to the quartz cuvette. This result can be attributed to less scatter and fluorescence resulting from the windowless cell [6]. Figure 1 illustrates typical signal-to-noise (S/N) ratios near the limit of detection when the windowless cuvette was used. The modulated constant-wavelength krypton ion laser resulted in a S/N ratio similar to that obtained with the pulsed dye laser.

The calibration graph obtained for fluoranthene was linear for over three orders of magnitude. Figure 2 illustrates this linearity at the more dilute concentrations for both pyrene and fluoranthene. The last point obtained for fluoranthene corresponded to 0.2 pmol (40 pg); extrapolating to $S/N \approx 2$ yields a lower limit of detection of approximately 0.05 pmol (10 pg). Somewhat lower limits of detection resulted with pyrene. The last point obtained for pyrene corresponded to 0.06 pmol (12 pg); extrapolating to $S/N \approx 2$ yields a lower limit of detection of approximately 0.02 pmol (4 pg). These values lie between those recently obtained by other workers [3, 4].

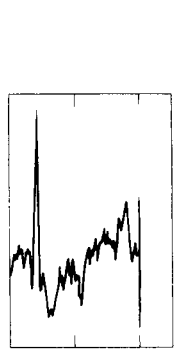

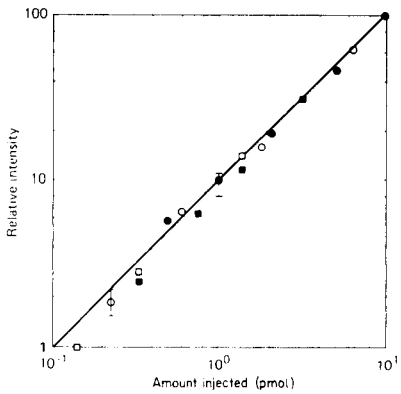

Fig. 1. H.p.l.c.—fluorescence chromatogram taken for 0.6 pmol of fluoranthene with the windowless fluorescence cell and pulsed dye laser excitation source near the limit of detection; λ_{ex} = 366 nm; 60 ns delay.

Fig. 2. Analytical working curves for fluoranthene (•,○) and pyrene (▪,□) near the limits of detection. Excitation wavelengths were 366 and 337 nm for fluoranthene and pyrene, respectively. (•,▪) Quartz cell; (○,□) windowless cell.

Figure 3 illustrates the use of temporal resolution in a mixture consisting of six PAH compounds. (The impurity found in chrysene was present regardless of the commercial source.) Increasing the temporal delay improves *S/N*, decreases Rayleigh and Raman scatter, and eventually results in the detection of only compounds with a long fluorescence lifetime. For example, in the mixture of PAH standards, anthracene and azulene have the shortest lifetimes, and are greatly reduced in magnitude after 45-ns delay. This enhancement in the resolution of PAH mixtures results from improving the selectivity of the detection system [9], and illustrates an advantage of pulsed lasers and gated detection systems over constant-wavelength lasers and the corresponding detection systems.

The advantages of temporal resolution for complex mixture analysis are illustrated in Fig. 4. This field sample was taken from the condensed steam distillate obtained during a coal gasification burn near Gillette, Wyoming (Hoe Creek No. 3) [11]. No additional or prior sample preparation was needed; the condensate obtained in the field was directly injected into the instrument. It is apparent that the largely unresolved chromatogram obtained at zero time delay shows considerably more resolution after 40-ns delay. The presence of fluoranthene, unrevealed at zero delay, is clearly indicated at 40-ns delay.

Most of the PAH compounds which have the greatest environmental and health interest have long fluorescence lifetimes; consequently the use of the time-resolved method proposed appears to have specific application in their determination. In general, the use of fluorescence techniques with pulsed lasers as a detection system for h.p.l.c. is seen to provide not only high sensi-

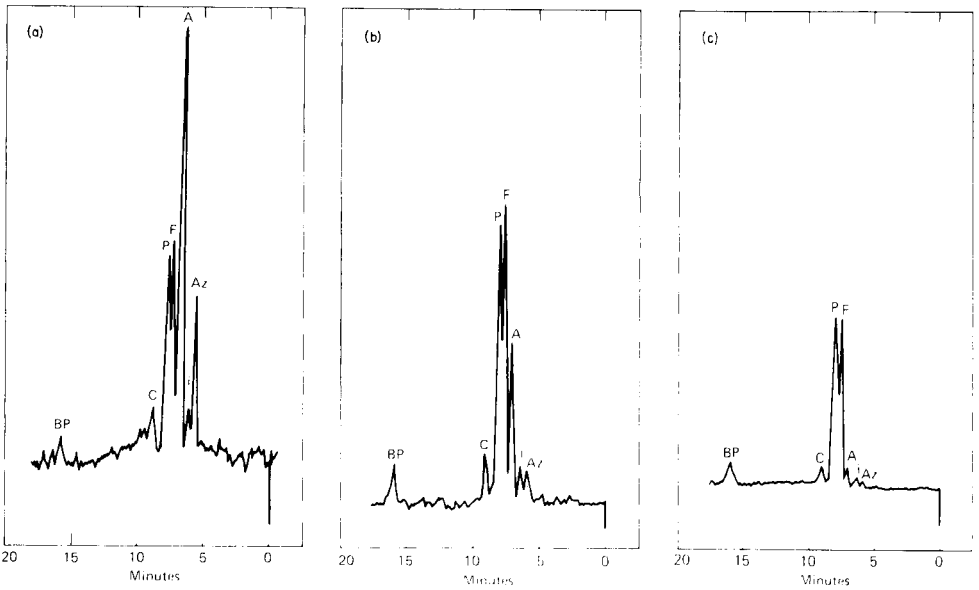

Fig. 3. Liquid chromatograms of six PAH standards illustrating the use of temporal resolution: A (anthracene, 3.2 ng), Az (azulene, 10 ng), BP (1,12-benzoperylene, 5.6 ng), C (chrysene, 46.8 ng), F (fluoranthene, 6 ng), i (impurity present in chrysene obtained from three different commercial sources), and P (pyrene, 2.8 ng). λ_{ex} = 337 nm. Delay times: (a) 0 ns; (b) 15 ns; (c) 45 ns.

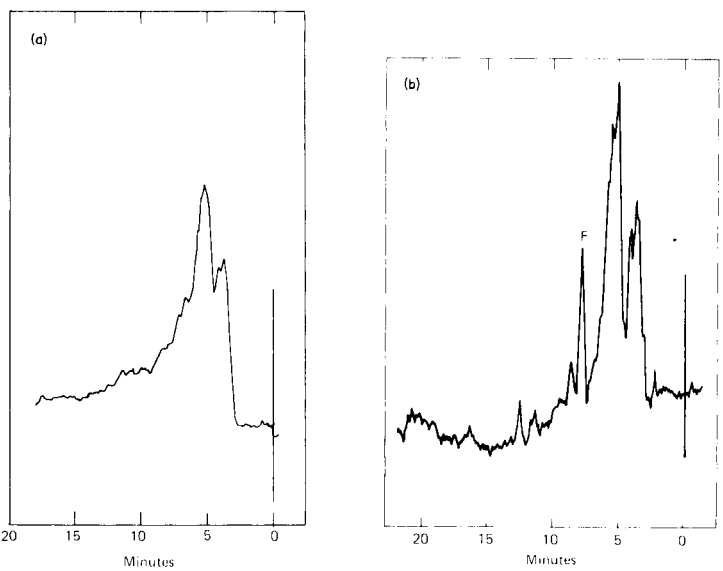

Fig. 4. Liquid chromatograms of field sample from coal gasification burn illustrating the advantages of temporal resolution; F (fluoranthene). λ_{ex} = 366 nm. Delay times: (a) 0 ns; (b) 40 ns.

tivity, but also an additional selectivity parameter which is useful in handling actual samples.

We thank S. B. Deutscher, D. H. Stuermer, and F. T. Wang for providing the coal gasification sample. This work was performed under the U. S. Department of Energy contract W-7405-Eng-48.

REFERENCES

1 T. Nielsen, J. Chromatogr., 170 (1979) 147.
2 A. M. Krstulovic, D. M. Rosie, and P. R. Brown, Anal. Chem., 48 (1976) 1383.
3 M. A. Fox and S. W. Staley, Anal. Chem., 48 (1976) 992.
4 B. S. Das and G. H. Thomas, Anal. Chem., 50 (1978) 967.
5 E. S. Yeung, Anal. Chem., 49 (1977) 1555.
6 L. W. Hershberger, J. B. Callis, and G. D. Christian, Anal. Chem., 51 (1979) 1444.
7 G. J. Diebold and R. N. Zare, Science, 196 (1977) 1439.
8 J. H. Richardson and M. E. Ando, Anal. Chem., 49 (1977) 955.
9 R. B. Dickinson, Jr. and E. L. Wehry, Anal. Chem., 51 (1979) 778.
10 J. H. Richardson, B. W. Wallin, D. C. Johnson, and L. W. Hrubesh, Anal. Chim. Acta, 86 (1976) 263.
11 For a description of the Lawrence Livermore Laboratory Underground Coal Gasification Project see R. W. Hill, C. B. Thorsness, D. R. Stephens, D. S. Thompson, and W. R. Aiman, presented at the Fourth Annual Underground Coal Conservation Symposium, Steamboat Springs, Colorado (July 17—20, 1978). Sponsored by the U.S. Department of Energy's Division of Oil, Shale, and In Situ Technology. (Also see internal report UCRL-50026-78-2.)

Analytica Chimica Acta, 116 (1980) 413—416

Short Communication

SPECTRAL PROPERTIES AND ANALYTICAL APPLICATION OF THE TERNARY COMPLEX OF LANTHANUM(III) WITH 1,10-PHENANTHROLINE AND EOSIN

K. A. IDRISS*, M. M. SELEIM, A. M. AWAD and M. S. ABU-BAKR

Department of Chemistry, Faculty of Science, Assiut University, Assiut (Egypt)

(Received 19th September 1979)

Summary. The pink lanthanum—(1,10-phenanthroline)$_2$—(eosin)$_2$ complex is used to determine 0.5—10 × 10^{-5} M lanthanum, either in aqueous solution or chloroform. In the presence of EDTA, only aluminium and cyanide interfere.

The formation of mixed-ligand complexes with fluorescein derivatives as the secondary ligand has been reported [1—4]. The colour reactions were particularly useful for determining copper(II) [5], cobalt(II) [6], and palladium(II) [7]. The present communication reports spectrophotometric studies of the mixed-ligand complex of lanthanum(III) with 1,-10-phenanthroline and eosin (2,4,5,7-tetrabromofluorescein). The formation of the coloured complex is instantaneous in acidic solution and the complex is easily extracted.

Experimental

Reagents and apparatus. Lanthanum(III) solutions were prepared from the analytical-grade nitrate, and standardized gravimetrically [8]. Solutions of 10^{-3} M 1,10-phenanthroline and eosin were prepared by dissolving the appropriate amount of the solid(Merck) in twice-distilled water. Other chemicals were all of analytical grade. Buffer solutions of pH 2.5—8 consisting of citric acid and disodium hydrogenphosphate were prepared as recommended [9]. Spectrophotometric measurements were made at room temperature (ca. 25°C) with a Unicam SP 8000 spectrophotometer with 1-cm silica cells.

Procedures. For aqueous media, a series of solutions was prepared containing 1 ml of 10^{-1} M EDTA, 0.5 ml of 10^{-3} M phenanthroline, 7.5 ml of 10^{-4} M eosin and 0—14 ml of 1 × 10^{-4} M lanthanum solution (25—180 μg La). The pH was adjusted to pH 4.0—4.5, and the solution made up to 25 ml with twice-distilled water. After thorough mixing, the absorbance was measured at 555 nm against a reagent blank similarly prepared but containing no lanthanum. For examining the effects of interfering ions, solutions of such ions were added before the lanthanum(III).

For extraction experiments, 0—14 ml of 2×10^{-5} M lanthanum solution (5—32.5 μg La), 1 ml of 10^{-1} M EDTA, 0.5 ml of 10^{-3} M phenanthroline, 1 ml of citric acid—phosphate buffer and 7.5 ml of 10^{-4} M eosin were mixed in 100-ml separatory funnels, and the volume made up to 25 ml. After adding 25 ml of chloroform (or nitrobenzene), the mixture was shaken vigorously for 5 min and allowed to stand for 10 min. The organic layer was transferred to a beaker containing sodium sulphate and thence to the spectrophotometer cell, where the absorbance was measured over the range 500—600 nm against a reagent blank taken through the procedure.

Results and discussion

The absorption spectrum of 5 ml of 10^{-4} M eosin diluted to 25 ml shows a peak at 510 nm (Fig. 1, curve 1). The presence of 5 ml of 10^{-4} M lanthanum produces no significant change in the colour or absorption spectrum, but on adding 0.5 ml of 10^{-3} M 1,10-phenanthroline the colour changes from orange-yellow to pink. The peak at 510 nm decreases, and a new peak appears at 555 nm. Maximum colour development was obtained at pH 4—4.5. Up to a 100-fold molar amount of EDTA relative to lanthanum had no effect on the sensitivity.

The effects of eighteen cations and 13 anions were investigated for interference in the presence of a 100-fold molar amount of EDTA relative to lanthanum. The results (Table 1) show that only aluminium(III) and cyanide interfere seriously under these conditions.

The stoichiometry of the ternary complex was determined by Job's method [10] and the mole ratio method [11]. The results shown in Figs. 2 and 3 indicate that the ternary complex is La : 2 (1,10-phenanthroline): 2 eosin, i.e. the normal charged chelate formed between lanthanum and 1,10-phenanthroline associates with the negatively charged eosin.

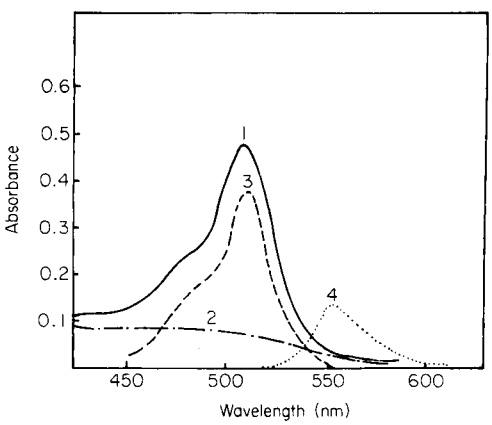

Fig. 1. Absorption spectra in aqueous solution of: (1) eosin, eosin and lanthanum, or 1,10-phenanthroline and eosin; (2) lanthanum and eosin measured against eosin; (3) lanthanum and eosin measured against lanthanum; (4) lanthanum, 1,10-phenanthroline and eosin measured against eosin and 1,10-phenanthroline.

TABLE 1

Effect of foreign ions on the absorbance of the lanthanum complex (at 555 nm) in the presence of EDTA

Ion added[a]	Absorbance vs. blank	Ion added[a]	Absorbance vs. blank	Ion added[a]	Absorbance vs. blank
—	0.180	—	0.180	—	0.180
Al(III)	0.380	Mg(II)	0.183	CO_3^{2-}	0.175
As(III)	0.183	Mn(II)	0.182	$C_2O_4^{2-}$	0.176
Ba(II)	0.178	Ni(II)	0.185	F^-	0.174
Ca(II)	0.184	Pb(II)	0.184	HPO_4^{2-}	0.175
Co(II)	0.182	Th(IV)	0.183	I^-	0.176
Cu(II)	0.185	U(VI)	0.182	NO_2^-	0.181
Cr(III)	0.176	Zn(II)	0.184	NO_3^-	0.182
Ce(III)	0.175	Br^-	0.177	S^{2-}	0.175
Fe(III)	0.179	Cl^-	0.176	SO_3^{2-}	0.184
Fe(II)	0.178	CN^-	0.060	SO_4^{2-}	0.185
Hg(II)	0.184				

[a]100-fold molar amount relative to lanthanum.

The extraction of ion-association complexes involving fluorescein derivatives is only achieved satisfactorily with chloroform or nitrobenzene. These solvents were also able to extract the present ternary complex. In combination with the use of EDTA as a broad-range masking agent, the extraction procedure provides an extremely selective and sensitive method for the

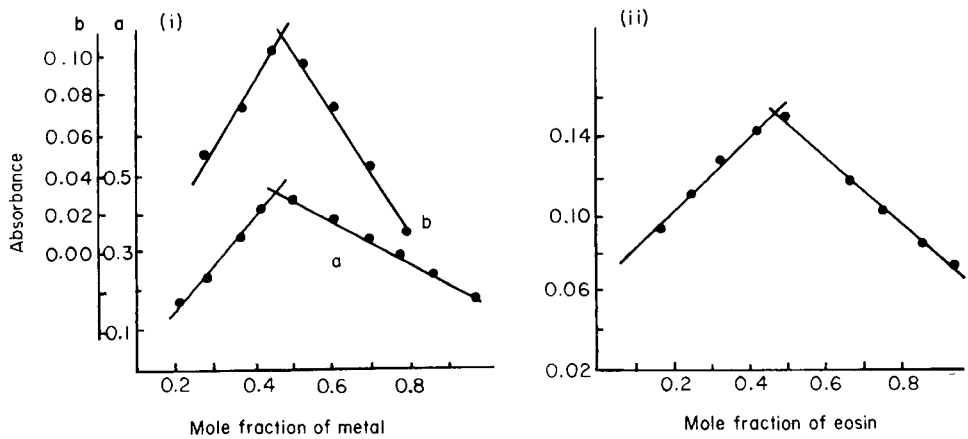

Fig. 2. Job plots. (i) (a) Eosin—La (1,10-phenanthroline in excess) with varying ratios of 1×10^{-4} M eosin and $La(NO_3)_3$ plus 1 ml of buffer and 1 ml of 10^{-3} M 1,10-phenanthroline per 25 ml; (b) 1,10-phenanthroline—La (eosin in excess) with varying ratios of 5×10^{-4} M 1,10-phenanthroline and $La(NO_3)_3$ plus 1 ml of buffer and 5.0 ml of 5×10^{-4} M eosin per 25 ml. (ii) Eosin—1,10-phenanthroline (metal in excess) with varying ratios of 5×10^{-4} M eosin and 1,10-phenanthroline plus 1 ml of buffer and 5 ml of 5×10^{-4} M La $(NO_3)_3$ per 25 ml.

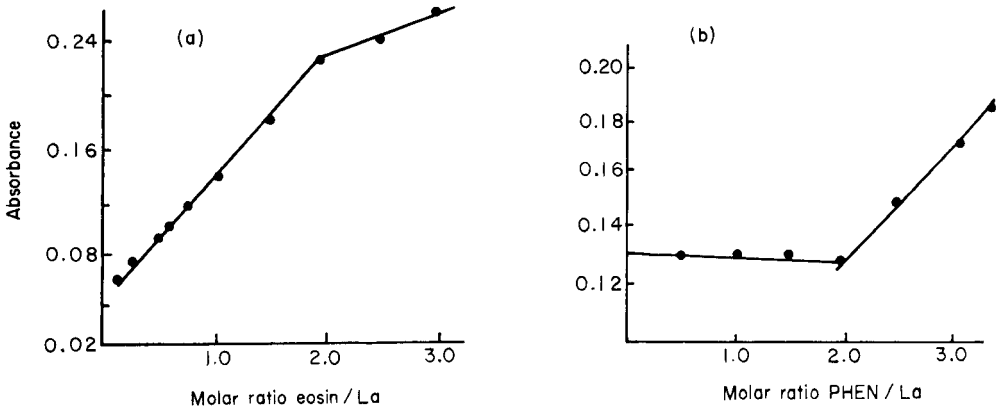

Fig. 3. Mole ratio plots. (a) Variation of eosin: 0.5—10 ml of 10^{-4} M eosin added to 4.0 ml of 10^{-4} M $La(NO_3)_3$, 1.0 ml of 10^{-3} M 1,10-phenanthroline and 1 ml of buffer per 25 ml. (b) Variation of 1,10-phenanthroline: 0.5—6 ml of 5×10^{-4} M 1,10-phenanthroline added to 2.0 ml of 5×10^{-4} M $La(NO_3)_3$, 8.0 ml of 5×10^{-4} M eosin and 1 ml of buffer per 25 ml.

determination of lanthanum. The spectrum of the extracted species is almost identical to that in aqueous solution. Calibration graphs obtained for the aqueous and organic systems were rectilinear over the ranges 0—5.25×10^{-5} M and 0—10.5×10^{-5} M, respectively. The molar absorptivities are 14,200 in aqueous solution and 38,100 l mol^{-1} cm^{-1} in chloroform.

REFERENCES

1 M. T. El-Ghamry and R. W. Frei, Anal. Chem., 40 (1968) 1986; Talanta, 16 (1969) 235.
2 N. S. Poluektov and M. A. Sandu, Zh. Anal. Khim., 25 (1970) 1510.
3 M. M. Tananaiko and L. I. Gorenshtein, Ukr. Khim. Zh., 40 (1974) 275; Izv. Vyssb. Uchebn. Zared Khim. Tekhnol., 18 (1975) 893.
4 M. M. Tananaiko and N. S. Bilenko, Zh. Anal. Khim., 30 (1975) 689.
5 B. W. Bailey, R. M. Dagnall and T. S. West, Talanta 13 (1966) 1661.
6 P. R. Haddad, P. W. Alexander and L. E. Smyth, Talanta, 23 (1976) 275.
7 R. M. Dagnall, M. T. El-Ghamry and T. S. West, Talanta, 15 (1968) 1353.
8 W. Scott and N. Furman, Standard Methods of Chemical Analysis, Van Nostrand, 6th edn., New York, 1962, p. 617
9 D. D. Perrin, B. Dempsey, Buffers for pH and Metal ion control, Chapman and Hall, 1974.
10 P. Job, Ann. Chim. (Paris), 9 (1928) 113; F. G. Sherif and A. M. Awad, Inorg. Nucl. Chem., 24 (1962) 79.
11 G. H. Yoe and A. L. Jones, Ind. Eng. Chem. Anal. Edn., 16 (1944) 111.

Analytica Chimica Acta, 116 (1980) 417—420

Short Communication

PHOTOMETRIC TITRATION OF VANADIUM(IV) WITH 8-HYDROXY-QUINOLINE-5-SULPHONIC ACID

G. DEN BOEF* and W. OZINGA

Laboratory for Analytical Chemistry, University of Amsterdam, Nieuwe Achtergracht 166, Amsterdam (The Netherlands)
(Received 17th December 1979)

Summary. Vanadium(IV) at concentrations of 10^{-2}—10^{-4} M can be titrated at pH 5—6; the 1:2 metal—ligand complex is formed. Back-titrations with copper(II) solution and reverse titrations are also feasible. Absorbances are measured at 385 nm.

In previous papers, the usefulness of titrations of metal ions with ligands forming 1:2 complexes has been discussed [1, 2] and the determination of copper(II) with 8-hydroxyquinoline-5-sulphonic acid (HQS), based on 1:2 complex formation, has been described [3]. During the latter investigation, vanadium(IV) was found to interfere, which suggested that vanadium(IV) might be determined with HQS or a similar ligand. Screening of the data for the stability constants of the complexes of vanadium(IV) with various ligands [4] indicated that a number of ligands could be suitable for titrations, viz. tiron, HQS, 1,2-dihydroxybenzene, salicylic acid and sulphosalicylic acid. Of these five ligands, only HQS seemed likely to be useful for the photometric titration of vanadium(IV) at low concentration levels. The other ligands were less suitable, because the spectral properties of their complexes with vanadium(IV) did not allow photometric end-point detection. Table 1 gives the stability constants of the complexes of HQS with several metal ions.

TABLE 1

Stability constants of complexes of metal ions with HQS [4]

Metal ion	Log K_1	Log K_2	Metal ion	Log K_1	Log K_2
V(IV)	11.8	—	Co(II)	8.8	7.1
Cu(II)	11.5	10.1	Fe(II)	8.4	6.7
Cd(II)	7.7	6.5	Fe(III)	11.6	11.2
Zn(II)	7.5	6.6	Mn(II)	5.6	5.2
Pb(II)	8.5	7.6	Ni(II)	9.0	7.7
U(VI)	8.5	7.1	Cr(III)	11.0	10.0
Th(IV)	9.6	8.7	H^+	8.5	3.9

Although the literature does not contain a value for the stability constant of a 1:2 complex of vanadium(IV) with HQS, the absorption spectra in the near-u.v. for solutions of HQS and 1:1 and 1:2 mixtures of vanadium(IV) and HQS prove that a 1:2 complex is formed. At pH about 5 these spectra are quite similar to those measured for copper(II) and HQS. At 385 nm, the most suitable wavelength for photometric indication, the ligand does not absorb whereas the molar absorptivities for V(IV)HQS and $V(IV)(HQS)_2$ are 8500 and 4000 l mol^{-1} cm^{-1}, respectively. As the molar absorptivity for $V(IV)(HQS)_2$ is about twice that for V(IV)HQS, the photometric titration curve for vanadium(IV) with HQS at 385 nm will show a linear increase until a twofold amount of HQS with respect to vanadium(IV) has been added, after which the absorbance will remain constant provided that the $V(IV)(HQS)_2$ complex is completely formed at the equivalence point. It has been demonstrated [2] that 99% formation of ML_2 is realized at the equivalence point when $K_2'c \geqslant 10^2$, where K_2' is the second conditional stability constant of the complex formed between metal ion M and ligand L, and c is the concentration of the metal ion. Although the exact value is unknown, it can be concluded from Table 1 that $\log K_{V(IV)(HQS)_2}$ is not less than 10.0.

The side-reaction coefficients $\alpha_{L(H)}$ for HQS, calculated with the protonation constants of the ligand, have the logarithmic values 6.45, 4.6, 3.5, 2.5 and 1.5 for pH values of 3, 4, 5, 6 and 7, respectively. This means that titrations of vanadium(IV) in the concentration range 10^{-4}—10^{-5} M are possible only in the pH range 5—6. When acetic acid—acetate buffers are used to adjust the pH, the side-reaction coefficient of vanadium(IV) with acetate should be taken into account in calculating the conditional stability constants of the vanadium(IV)—HQS complexes. However, no data are available for the stability constants of vanadium(IV) with acetate. The use of pH values above 6, to increase the conditional stability constants, is not advisable because hydroxides of other metal ions might be formed and because the absorption spectrum of the ligand becomes similar to those of the complexes at high pH values. In practice, the titration of 10^{-4} M vanadium(IV) at pH 5 appeared to be the lower limit of determination.

The determinations were carried out at this pH value. Figure 1 shows a typical titration curve.

Direct titrations

Procedure. Transfer 8—10 ml of a solution containing about 50 μg of vanadium(IV) to the titration cell. Add 1 ml of a concentrated acetic acid—acetate buffer solution pH 5 (final concentration of acetic acid + acetate is 0.1 M). Set the wavelength at 385 nm. Titrate with 10^{-2} M HQS. The equivalence point is found by the intersection of the two straight parts of the titration curve. A Zeiss PMQ II spectrophotometer was used.

Results. The standard deviation for a single determination is about 2%. As the stability constants of other metal ions with HQS are appreciable, although generally smaller than those of vanadium(IV), the selectivity of the method

is rather limited. Cadmium(II) or manganese(II) may be present in tenfold amounts, and zinc(II), lead(II), cobalt(II) or uranium(VI) in equal amounts with respect to vanadium(IV) without interfering. The presence of equal amounts of iron(II) and chromium(III) eauses positive errors of about 10%. Nickel(II) and copper(II) interfere. Chromium(III) reacts slowly with HQS.

Back-titrations and reverse titrations

Vanadium(IV) can be determined by addition of HQS in excess and back-titration with copper(II), as expected from theoretical considerations [5]. On the addition of HQS in excess, $V(IV)(HQS)_2$ is formed. The excess of HQS reacts with copper(II) to form $Cu(II)(HQS)_2$. Further addition of copper(II) breaks up the less stable of the two complexes, resulting in a sharp break in the titration curve. An example of such a titration curve is given in Fig. 2.

The reverse titration of HQS with vanadium(IV) also gives sharp end-points (Fig. 3). This curve might be of practical significance for the method mentioned below.

Oxidation—reduction titrations

The colour formation of vanadium(IV) with HQS could be useful to indicate the end-points of titrations based on the oxidation of vanadium(IV) to vanadium(V) or on the reduction of vanadium(V) to vanadium(IV). In the former case, the colour of the V(IV)—HQS complex would disappear gradually, resulting in a break in the absorbance curve at the end-point; in the latter case, the colour of the complex would appear, again resulting in a break, provided that HQS is present in excess. These methods would be expected to be more selective, if suitable reductants and oxidants could be found. At the pH value necessary for the end-point indication, i.e. 5–6, the only re-

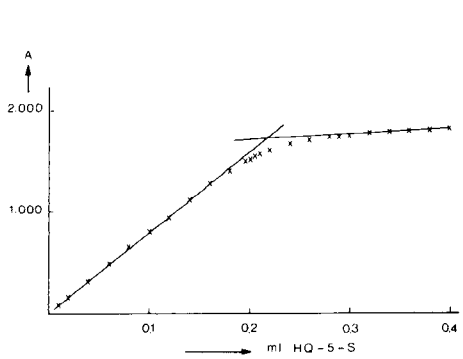

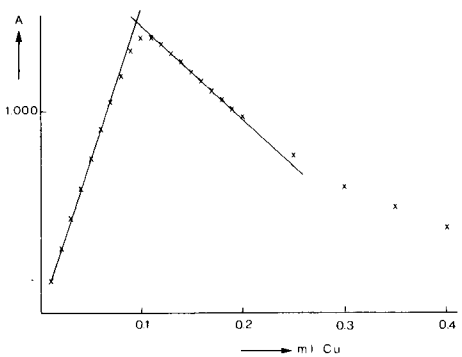

Fig. 1. Photometric titration curve of 10^{-4} M vanadium(IV) with HQS in acetic acid—acetate buffer pH 5 at 385 nm.

Fig. 2. Photometric curve of the back-titration of a solution containing 10^{-4} M vanadium-(IV) and 4×10^{-4} M HQS with copper(II) at 385 nm.

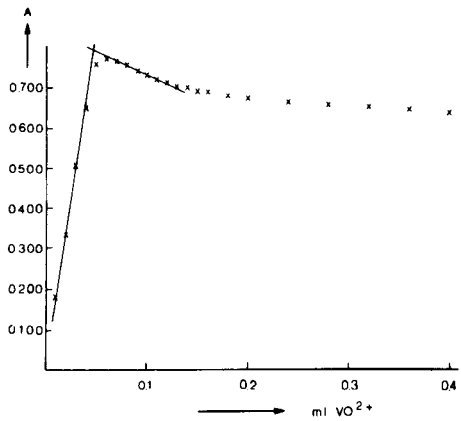

Fig. 3. Photometric titration curve of 10^{-4} M HQS with vanadium(IV) in acetic acid—acetate buffer pH 5 at 385 nm.

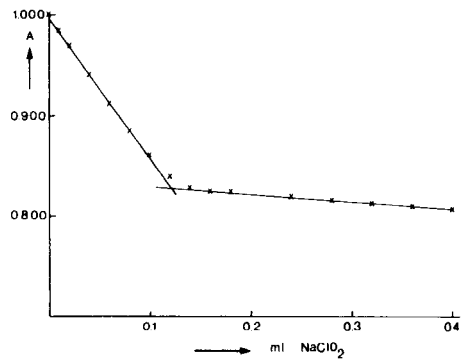

Fig. 4. Photometric titration curve of a solution containing 10^{-4} M vanadium(IV) and 4×10^{-4} M HQS, with 2.5×10^{-3} M sodium chlorite at 385 nm.

agent which gave suitable titration curves (Fig. 4) was sodium chlorite. At 40°C, the titration reaction is fast and the reproducibility is good but the stoichiometry is poor. A solution to the problem might be the coulometric oxidation of vanadium(IV) or the coulometric reduction of vanadium(V) in the presence of HQS.

REFERENCES

1 F. Freese, G. den Boef and G. J. van Rossum, Anal. Chim. Acta, 58 (1972) 429.
2 F. Freese and G. den Boef, Anal. Chim. Acta, 60 (1972) 131.
3 G. J. van Rossum and G. den Boef, Anal. Chim. Acta, 61 (1972) 144.
4 L. G. Sillén and A. E. Martell, Stability Constants, Spec. Publ. No. 17, The Chemical Society, London, 1964; Suppl. No. 1, Spec. Publ. No. 25, The Chemical Society, London, 1971.
5 G. J. van Rossum and G. den Boef, Anal. Chim. Acta, 76 (1975) 443.

Analytica Chimica Acta, 116 (1980) 421—425

Short Communication

CATALYTIC END-POINT INDICATION IN REDOX TITRATIONS

SIEGBERT PANTEL and HERBERT WEISZ*

Lehrstuhl für Analytische Chemie, Chemisches Laboratorium der Universität, Freiburg i.Br. (Federal Republic of Germany)

(Received 19th November 1979)

Summary. The applicability of catalytic end-point indication to redox titrations is demonstrated by the determination of 3—30 μmol of ascorbic acid (in 22.5 ml of solution) with standard dichromate solution; the chromium(VI)-catalyzed oxidation of *o*-dianisidine with hydrogen peroxide serves as indicator reaction. Oxidizing substances, such as vanadium(V), thallium(III) or cerium(IV) can be determined by addition of excess of ascorbic acid and back-titration.

Catalytic end-point indication in titrimetric analysis is based on the fact that the first drop of titrant in excess is not used for a stoichiometric reaction with the indicator, but acts as catalyst for the indicator reaction. Consequently, a very small excess of the titrant suffices to catalyze large amounts of the indicator reagent mixture. Such catalytic end-points are therefore markedly sensitive and very easily detected [1]. This principle is quite different from the catalimetric titration method described by Yatsimirskii [2], in which a number of identical batches of reactants and catalyst (or inhibitor) are treated with different amounts of inhibitor (or catalyst) and the catalytic activity of the various systems is measured. The concentration of the inhibitor (or catalyst) to be determined is evaluated by a graphical extrapolation to the point where the catalytic activity starts or stops decreasing.

It could be said that catalytic end-point indication involves a so-called open system, whereas the catalimetric titration is based on a closed system.

The principle of catalytic end-point indication was described in 1960 by Erdey and Buzas for luminescent end-points [3]; in 1965 Vaughan and Swithenbank [4] described an acid—base titration using a base-catalyzed polymerization for end-point indication. Since then, this principle has been applied for numerous determinations of various ions, as well as for acids and bases in non-aqueous media. Several reviews demonstrate the interest taken in this method [5—13]; there are also several more recent applications [14—25]. Table 1 gives a systematic representation of the various techniques so far applied. Redox titrations are mentioned only in brackets, as no example seems to have been described previously.

In the case of redox titrations several conditions for the indicator reaction

TABLE 1

Catalytic end-point indication methods in which a catalyst (K) is added to a mixture of an inhibitor (i) and the components of the reaction catalyzed ($A + B$)

Examples:
Precipitation: $K = I^-$, A = Ce(IV), B = As(III), $i = Ag^+$
Complexation: K = Co, A = tiron, $B = H_2O_2$, i = EDTA
Stoichiometric reaction (titration reaction): $i + K \rightarrow \langle iK \rangle$
Catalyzed reaction (indicator reaction): $A + B \overset{K}{\rightarrow} C$
Inhibition of catalyst: precipitation, complexation, (redox)
Method of monitoring indicator reaction (disappearance of A or B or appearance of C): visual, potentiometric, photometric, biamperometric, thermometric
Determination method: direct, indirect (back), reversed, substitution, non-aqueous

must be fulfilled. First, the titrant must exhibit reasonable catalytic activity only in one, well-defined, oxidation state and this oxidation state must be applicable for the stoichiometric titration reaction involved. Secondly, the stoichiometric reaction must be distinctly faster than the catalyzed indicator reaction and the reactants of the latter must not react with the substance to be determined.

These conditions are fulfilled in the titration of ascorbic acid with dichromate solution, using the chromium(VI)-catalyzed oxidation of *o*-dianisidine with hydrogen peroxide [26] as indicator reaction. The oxidation product of *o*-dianisidine colours the solution brownish-red. This indicator reaction proceeds very slowly without catalysis, whereas chromium(VI) oxidizes ascorbic acid [27] quickly under the optimum conditions for the indicator reaction. The components of the indicator reaction do not interfere. As ascorbic acid is readily oxidized by air in the presence of traces of metal ions, the titration is done in the presence of EDTA; citric acid is added to activate the catalyst. The titration curve rises slowly before the end-point (Fig. 1, AB) because chromium(III) as well as its EDTA complex absorb in the spectral range applied.

Oxidizing substances that do not interfere with the indicator reaction or the monitoring system, may be determined by addition of ascorbic acid, and back-titration of the excess with standard dichromate solution.

Reagents and apparatus

Solutions were prepared, as far as possible, from analytical-grade reagents with deionized-distilled water. The concentration of the stock solution of ascorbic acid was checked daily by iodimetric titration [27]. From this stock solution, standard and sample solutions were prepared by dilution.

The apparatus used consisted of a photometer, an automatic burette and a strip-chart recorder. The photoelectric colorimeter (Model J, B. Lange, Berlin) was fitted with a blue filter (λ_{max} = 415 nm), a temperature-controlled (rotary thermostat) cuvette holder, and a magnetic stirrer beneath the cell

compartment. The cylindrical cuvette was of 30-mm diameter and 40-ml capacity. The Tölg burette (W. K. Becher oHG, Mainz) used was set at 0.02435 ml min^{-1}. The glass capillary of this burette was fitted tightly into the cover of the cell compartment (to minimize entry of light) with the tip almost at the bottom of the cuvette. The mV-range of the recorder (Servogor RE541; Metrawatt GmbH, Nürnberg) was set so that the full range corresponded to 0—100% absorbance on the photometer scale. The reaction temperature was 25 ± 0.1 °C and the recorder speed 300 mm h^{-1} in all cases.

Determination of ascorbic acid with dichromate

To the cuvette were added 0.5 ml of 0.05 M disodium-EDTA solution, 0.5 ml of *o*-dianisidine solution (3 mg ml^{-1} in 0.5 M HCl), 0.1 ml of aqueous citric acid solution (10 mg ml^{-1}), and 0.5—5 ml of standard ascorbic acid solution (1 mg ml^{-1}) for preparing a calibration graph or a suitable amount of a sample solution. After dilution to 22 ml and thermostating for 3 min, 0.5 ml of hydrogen peroxide solution (2 mg ml^{-1}) were added; the automatic addition of potassium dichromate solution (1 mg Cr ml^{-1}) and the recorder were started simultaneously. The recorder plots were evaluated by drawing two tangents to the linear parts of the curves, to give the point of intersection B (Fig. 1a). This end-point is not identical with the equivalence point of the titration. The equivalence point should correspond to the point when the linear portion starts to curve upwards; this point cannot be seen with sufficient accuracy here. Therefore, a calibration graph was drawn by plotting the abscissa intercepts (corresponding to the distance AB in Fig. 1a) versus ascorbic acid concentrations (Fig. 1b). The intersection of the graph with the ordinate gives the difference between the equivalence point and the end-point B.

Some results for the determination of ascorbic acid are given in Table 2.

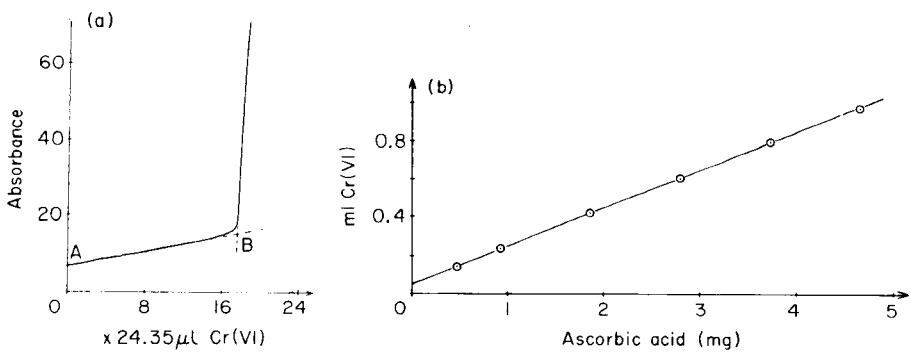

Fig. 1. (a) Recorder plot for the determination of 2 mg of ascorbic acid in 22.5 ml of solution with standard dichromate solution (1 mg Cr ml^{-1}). (b) Calibration graph for the determination of ascorbic acid.

TABLE 2

Titration of ascorbic acid (mg/22.5 ml) with dichromate by the catalytic end-point indication method

Given	0.60	1.23	1.40	1.86	2.33	2.42	3.26	3.61	4.61	4.66
Found	0.61	1.24	1.42	1.85	2.32	2.42	3.27	3.59	4.59	4.61

Determination of oxidants (vanadium(V), thallium(III) and cerium(IV)) with ascorbic acid

The solution of the oxidant to be determined was treated with an appropriate excess of ascorbic acid for 5 min in the presence of 100 μmol of di-sodium EDTA (heating was used if necessary [27]). Then the pH was adjusted to 3.0, the indicator reaction mixture was added as described above, and the excess of ascorbic acid was back-titrated with standard dichromate solution.

Vanadium(V) or cerium(IV) (5—50 μmol) and thallium(III) (2—20 μmol) could be determined in this way. The calibration graphs were almost linear, but the reproducibility was not as good as in the determination of ascorbic acid itself.

REFERENCES

1 H. Weisz and U. Muschelknautz, Fresenius Z. Anal. Chem., 215 (1966) 17.
2 K. B. Yatsimirskii, Kinetic Methods of Analysis, Pergamon Press, Oxford, 1966.
3 L. Erdey and I. Buzas, Anal. Chim. Acta, 22 (1960) 524.
4 G. A. Vaughan and J. J. Swithenbank, Analyst, 90 (1965) 594.
5 J. Barthel, Thermometric Titration, J. Wiley, New York, 1975.
6 J. Jordan, J. K. Grime, D. H. Waugh, C. D. Miller, H. M. Cullis and D. Lohr, Anal. Chem., 48 (1976) 427 A.
7 E. J. Greenhow, Chem. Rev., 77 (1977) 835.
8 H. A. Mottola, Talanta, 16 (1969) 1267; Crit. Rev. Anal. Chem., 4 (1975) 229.
9 H. Weisz, Angew. Chem., 88 (1976) 177.
10 H. Müller and G. Werner, Z. Chem., 16 (1976) 304.
11 T. P. Hadjiioannou, Rev. Anal. Chem. Isr., 3 (1976) 82.
12 G. G. Guilbault, in I. M. Kolthoff and P. J. Elving (Eds.), Treatise on Analytical Chemistry, 2nd edn., Vol. 1(I), 1978, p. 663.
13 A. M. Albrecht-Gary and J. P. Schwing, Les Méthodes Cinétiques en Chimie Analytique, in Les Techniques de l'Ingénieur, Paris, in press.
14 S. Abe and S. Kon, Bunseki Kagaku, 25 (1976) 846.
15 N. Hotta, Toyama Kogyo Koto Semmon Gakko Kiyo, 10 (1976) 1.
16 S. Pantel and H. Weisz, Fresenius Z. Anal. Chem., 281 (1976) 211 and references therein.
17 N. Hotta, Toyama Kogyo Koto Semmon Gakko Kiyo, 11 (1977) 83.
18 T. P. Hadjiioannou, M. A. Kouparis and C. E. Efstathiou, Anal. Chim. Acta, 88 (1977) 281.
19 T. P. Hadjiioannou and M. M. Timotheou, Mikrochim. Acta, (1977) (I) 61.
20 T. P. Hadjiioannou and E. A. Piperaki, Anal. Chim. Acta, 90 (1977) 329.
21 F. F. Gaal, B. F. Abramovic, F. B. Szebenyi and V. D. Canic, Fresenius Z. Anal. Chem., 286 (1977) 222.
22 F. F. Gaal, B. F. Abramovic and V. D. Canic, Talanta, 25 (1978) 113.

23 N. Kiba and M. Furosawa, Anal. Chim. Acta, 98 (1978) 343.
24 M. Ternero, F. Pino, D. Perez-Bendito and M. Valcarcel, Anal. Chim. Acta, 109 (1979) 401.
25 A. G. Hens, M. Ternero, D. Perez-Bendito and M. Valcarcel, Mikrochem. Acta, (1979) (I) 375.
26 J. F. Dolmanova, G. A. Zolotova, L. V. Tavasova and V. M. Peshkova, Zh. Anal. Khim., 24 (1969) 1035; Chem. Abstr., 71 (1969) 87341.
27 A. Berka, J. Vulterin and J. Zyka, Newer Redox Titrants, Pergamon Press, Oxford, 1965.

Analytica Chimica Acta, 116 (1980) 427—431

Short Communication

THE ATOMIC ABSORPTION SPECTROMETRIC DETERMINATION OF LITHIUM ISOTOPE ABUNDANCES BY DIRECT MEASUREMENT OF THE ABSORBANCE RATIO

J. F. CHAPMAN, L. S. DALE* and H. J. FRASER

Australian Atomic Energy Commission, Research Establishment, Lucas Heights, New South Wales 2234 (Australia)

(Received 14th November 1979)

Summary. A specially designed amplifier allows direct measurement of the absorbance ratio. The unit simultaneously monitors the attenuation of both a natural-lithium and a ^{6}Li-enriched hollow-cathode lamp, which are aligned in the optical axis of the instrument. The attenuations are converted to absorbances, the ratio of which is proportional to the relative isotope abundance. The stable signals obtained permit rapid determinations at natural abundance levels, with a relative standard deviation of 3%.

The determination of lithium isotope abundances by atomic absorption spectrometry based on the ratio of absorbances, obtained independently, from hollow-cathode lamps of natural lithium and enriched lithium-6 has been described by Wheat [1]. Chapman and Dale [2] adapted a dual-beam attachment to measure simultaneously the two absorbances and used the absorbance difference as a measure of the abundance. This overcame variations obtained in the ratio technique arising from fluctuations in flame conditions when independent measurements were made. The disadvantages of this procedure were the dependence of the absorbance difference on total lithium concentration, and the difficulty in measuring small differences which were both positive and negative, with the instrument amplifier.

These problems could be overcome by measuring the absorbance ratio directly, i.e., simultaneous measurement of the individual absorbances. However, to enable such measurements to be made with a dual-beam, single-detector spectrometer, it was necessary to design a ratio amplifier. Such a device was constructed and operated with a commercial atomic absorption spectrometer as described below.

Ratio circuit

The function of the circuit is to obtain an output voltage V_0 where $V_0 = \log I_a/\log I_b$, I_a and I_b being the phototube output currents produced by the two lamps. Initially I_a and I_b are set equal to I_{ref}, the reference current. When the lamp currents are attenuated by lithium atoms in the flame, then

$I_a = I_{ref} \exp(-k_1c_1l)$ and $I_b = I_{ref} \exp(-k_2c_2l)$, where c_1 and c_2 are the concentrations of the absorbing species, k_1 and k_2 are the absorption coefficients, and l is the path length. It follows that $\ln I_a/\ln I_b = (\ln I_{ref} - k_1c_1l)/(\ln I_{ref} - k_2c_2l)$; hence $\log I_a/\log I_b = (\log I_{ref} - 0.43\, k_1c_1l)/(\log I_{ref} - 0.43\, k_2c_2l)$. The circuit makes it possible to set $\log I_{ref} = 0$. Hence $\log I_a/\log I_b = k_1c_1l/k_2c_2l$; since $k_1 = k_2$, and l is constant, $\log I_a/\log I_b = c_1/c_2 = V_0$.

Experimental

Electronic circuit. A schematic diagram of the circuit is shown in Fig. 1. The amplifiers A_2, A_4 and log module IC2 form one log converter used to find $\log I_a$ (channel 1). Log I_b is found in a similar way in channel 2. The amplifiers and log modules are Teledyne Philbrick models 1026 and 4358, respectively. After amplification by A3, A6 (Precision Monolithic Incorp. Model OP07CJ), these signals are averaged, with a time constant of 0.15 s, before entering the divider circuit A8 (Analog Devices Model AD434A). The output of A8 is scaled to read $\log I_a/\log I_b$ directly on a digital voltmeter.

The input current to A2 is switched, by a CMOS quad bilateral switch IC1, to be equal to I_a while lamp A is off. The input to channel 2 (I_b) is controlled in a similar manner. Control of the CMOS switches is obtained from the lamp control voltage waveforms.

Initially, with no absorber in the light path, I_a and I_b are both set to I_{ref} by adjustment of either the lamp intensities or the EHT supply to the photomultiplier to obtain zero output voltage V_{01}, V_{02} from amplifiers A3 and A6. Errors in measurement can be kept low by operating within the range —0.1 to —0.3 V for V_{01} and V_{02}. These limits represent absorbances of 0.2—0.5.

Atomic absorption measurements. All measurements were made on a

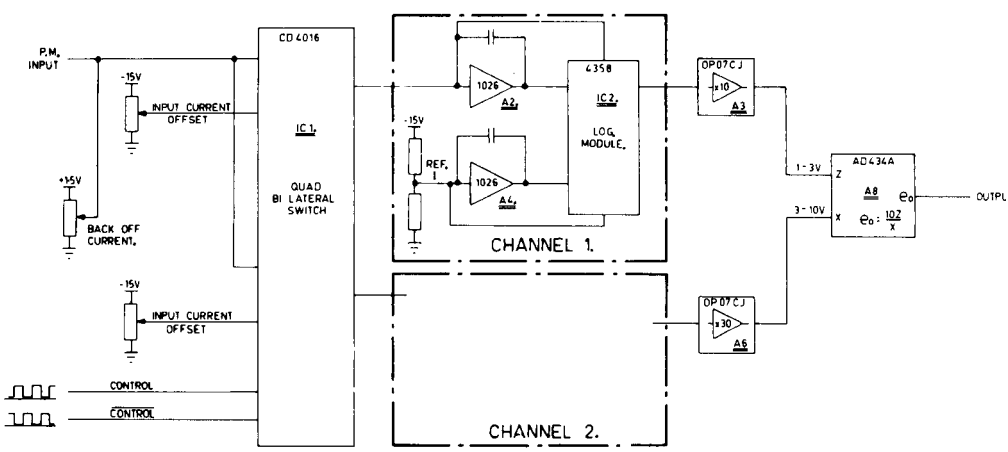

Fig. 1. Schematic diagram of ratio circuit.

Varian-Techtron Model AA5 atomic absorption spectrometer. Hollow-cathode lamps of natural lithium and enriched lithium-6 (Varian Techtron Pty Ltd., Springvale, Victoria) were operated at around 7 mA. The spectral bandpass was 0.2 nm. The photomultiplier was a R446 (Hamamatsu Co., Japan). The high voltage for the photomultiplier was derived from the IM5 amplifier unit, which also supplied the triggers for the lamp supplies. The output of the photomultiplier was fed to the input of the ratio circuit.

The air—acetylene flame was adjusted to yield maximum sensitivity. The concentration of lithium in the test solutions was 2 mg l^{-1}. Preparation of standards has been described previously [2].

The spectrometer was aligned by peaking on the photomultiplier output produced by the enriched lithium-6 hollow-cathode lamp which was mounted in the off-axis position of the lamp turret. The zeros of the two lamp outputs were then set by fine adjustment of the lamp currents. To facilitate this adjustment, a selector switch allowed each channel to be monitored on the digital voltmeter. A warm-up time of about 30 min was allowed.

Since the output from the photomultiplier consisted of both the modulated hollow-cathode lamp outputs plus a d.c. signal from the emission of lithium radiation from the flame, a back-off supply had to be used at the input to the ratio circuit. With this, the d.c. level could be removed so that only the signals from the lamps were measured. The degree of back-off was determined by measuring the d.c. photocurrent on a digital multimeter with a 1-MΩ resistor across the photomultiplier output while aspirating a lithium solution (2 mg l^{-1}) into the flame with the lamp outputs blanked off. The d.c. component entering the ratio circuit was then reduced to zero by selecting the appropriate current from the back-off supply.

Although the absorbance ratio could be read directly on the digital voltmeter, it could also be conveniently displayed on a strip-chart recorder to obtain calibrations over the concentration range 0—99.3 atom-% lithium-6. However, for abundance measurements near the natural level where standards covering a much narrower concentration range were used, optimum performance was achieved by feeding the output into a voltage-to-frequency converter which was connected to a scaler—timer and printer. This enabled the signal to be integrated, resulting in improved precision.

Results

The output of the ratio circuit yielded extremely high stability; Fig. 2 is a recorder trace of several standards run over a period of about 10 min. To permit statistical assessment of the stability, the output signal for a 66.6 atom-% lithium-6 standard was integrated by the counting technique with repetitive 2-s count times. The relative standard deviation was 0.35%.

A typical calibration for 0—99.3 atom-% lithium-6 is shown in Fig. 3. Some curvature is evident, similar to that obtained when independent measurements are used in the ratio technique.

To assess the suitability of the procedure for determining abundances near

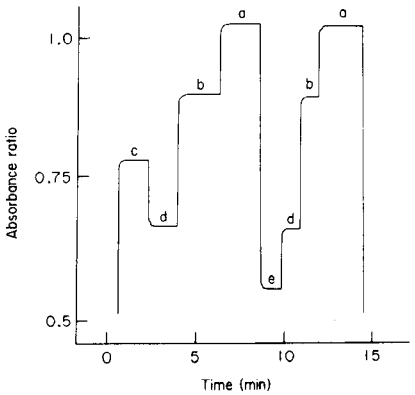

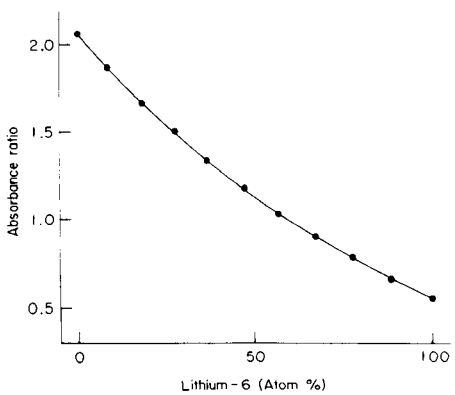

Fig. 2. Stability of output of ratio circuit. Absorbance ratio versus time for various lithium isotopic abundances: (a) 56.6, (b) 66.9, (c) 77.4, (d) 88.2, (e) 99.3 atom-% lithium-6.

Fig. 3. Typical calibration. Absorbance ratio versus lithium isotope abundance in the range 0—99.3 atom-% ^{6}Li.

the natural level, a set of standards was prepared ranging between 0 and 10 atom-% lithium-6. The calibration obtained with these standards by the counting technique with a 10-s count time was a straight line; the correlation coefficient was 0.997. A sample of analytical-grade lithium carbonate was analysed with respect to these standards and a mean value of 7.4 atom-% lithium-6 was obtained for 10 separate analyses; the standard deviation was 0.2 atom-% (1σ). This may be compared with the standard deviation of 0.5 atom-% obtained when the same sample was analysed by the absorbance ratio technique but with separate measurements of the absorbances.

Effect of total lithium concentration. This aspect was tested over the concentration range 1.5—4 mg l^{-1} which, under the conditions described, corresponded to an absorbance range of 0.2—0.5 which was also the optimum working range of the ratio circuit. At the 50 atom-% lithium-6 abundance level with the integration technique, where the relative standard deviation of counts was typically 0.4%, no significant difference in the ratio was observed. It was, however, necessary to measure the d.c. emission level from the flame for each concentration and make the appropriate adjustment to the back-off current to reduce the d.c. component to zero.

Discussion

The very stable output of the ratio circuit made it possible to carry out lithium isotope abundance determinations with a precision approaching that of thermal-ionisation mass spectrometry. However, to achieve this, it was necessary to pay particular attention to the optical alignment of the lamps and, more importantly, to allow a sufficient warm-up period for the electronics to stabilise to minimise drift after the zeros of the two channels had

been set. The counting technique for signal integration was necessary to achieve this level of precision. This procedure, unlike mass spectrometry, permits fairly rapid determination of abundances, with relatively simple instrumentation.

Although the procedure has been shown to be independent of concentration, the linearity of response of the ratio circuit imposes a restriction on the concentration range that can be used. This is of no great disadvantage because samples requiring analysis are usually stoichiometric compounds and a solution can be easily prepared with a total lithium concentration falling within the linear response range.

The authors thank Mr. W. O. Hill for constructing the ratio amplifier.

REFERENCES

1 J. A. Wheat, Appl. Spectrosc., 25 (1971) 328.
2 J. F. Chapman and L. S. Dale, Anal. Chim. Acta, 87 (1976) 91.

Analytica Chimica Acta, 116 (1980) 433—437

Short Communication

DETERMINATION OF MINOR AND TRACE ELEMENTS IN SILICATE ROCKS BY INDUCTIVELY-COUPLED PLASMA EMISSION SPECTROMETRY

HIROSHI UCHIDA*

Industrial Research Institute of Kanagawa Prefecture 3173, Showa-machi, Kanazawa-ku, Yokohama 236 (Japan)

TETSUO UCHIDA and CHUZO IIDA

Laboratory of Analytical Chemistry, Department of Engineering Science, Nagoya Institute of Technology, Gokiso-cho, Showa-ku, Nagoya 466 (Japan)

(Received 9th October 1979)

Summary. Samples (0.5 g) are decomposed with mixed acids in a sealed teflon vessel. After suitable treatment, barium, cobalt, chromium, copper, lithium, nickel, scandium, strontium, vanadium and zirconium are determined sequentially. The method is satisfactory for a variety of standard silicate materials.

The inductively-coupled plasma (i.c.p.) seems to be the best excitation source in emission spectrochemical analysis for major, minor and trace elements in silicates because of its high sensitivity, wide dynamic range and comparative freedom from chemical and ionization interferences [1, 2]. Solution viscosity tends to affect results [1, 3] but it has been shown [4] that decomposition with a mixture of hydrochloric and hydrofluoric acids in a sealed teflon vessel is satisfactory for the interference-free determination of major and minor elements in silicates. The present communication deals with the determination of minor and trace elements by i.c.p. emission spectrometry after decomposition of the silicate in a sealed teflon vessel. Almost all minor and trace elements are completely dissolved by the proposed method. Barium, scandium, strontium, vanadium and zirconium, which are not easily determined by atomic absorption spectrometry, can be determined accurately and reproducibly.

Experimental

Instrumentation and operating parameters. The instrumentation was the same as that employed previously [4]. Operating conditions were also identical, except for the carrier gas flow rate. The rate (0.85 l min^{-1}) had to be increased for stable nebulization, because the salt concentration of the sample solution was higher than that obtained in analysis for major and minor elements.

Reagents and standard solutions. Stock solutions of aluminum, iron, calcium, magnesium, sodium and potassium were prepared [4]. Commercially-available standard stock solutions for atomic absorption spectrometry (1000 ppm) were used for Ba, Co, Cr, Cu, Li, Ni, Sr and V. Scandium stock solution was prepared by dissolving scandium oxide (99%) in nitric acid. Zirconium metal powder (99%) was dissolved in nitric and hydrofluoric acids, and the acids were expelled by heating the solution with sulfuric acid. Hydrochloric, nitric, sulfuric and perchloric acids were super-special grade, and hydrofluoric acid was reagent grade. All chemicals were obtained from Wako Pure Chemical Co.

Working standards were prepared by suitable dilution and appropriate mixing of stock solutions. The concentrations of minor and trace elements in these standards, which contained as matrix elements aluminum (600 ppm), iron (600 ppm), calcium (500 ppm), magnesium (400 ppm), sodium (200 ppm) and potassium (200 ppm), were in the range 5.0—0.05 ppm, with corresponding blank solutions. Each of these mixed standard solutions contained 4 ml of hydrochloric acid and 2 ml of perchloric acid per 100 g of solution. All dilutions were done gravimetrically on a top-pan balance.

Decomposition. To the teflon vessel [4, 5] were added 0.5 g of powdered sample (accurately weighed), 4 ml of hydrofluoric acid and 2 ml of aqua regia. After the vessel had been sealed and left to stand for 16 h at room temperature, the contents were transferred to a teflon beaker and evaporated nearly to dryness at 95°C on a hot-plate. The solution was fumed with 2 ml of perchloric acid at 190°C to remove tetrafluorosilicate and excess of hydrofluoric acid, and then cooled. After addition of 2 ml of concentrated hydrochloric acid and 30 ml of water, the residue was dissolved by heating at 95°C. Finally the solution was transferred to a polypropylene bottle, diluted with water to 50 g, and weighed.

The choice of spectral lines is discussed below.

Results and discussion

In the determination of trace elements by i.c.p. emission spectrometry, the analytical lines must be chosen carefully to avoid spectral interferences. The lines generally recommended for the determination of the ten trace elements are shown in Table 1 together with their detection limits. The detection limits are the concentrations corresponding to an intensity twice the standard deviation of the background obtained from the blank solution containing only matrix elements. In the absence of spectral interferences, concentrations five times the detection limit could be determined with a relative standard deviation of about 10%.

The powdered silicate samples (0.5 g) could be decomposed with small amounts of hydrofluoric acid and aqua regia in the teflon vessel at room temperature after 16 h [5]. In the present work, fluorosilicate was removed, to decrease the salt concentration of the sample solution and so provide more reproducible nebulization. The effects of temperature on the decompo-

TABLE 1

Analytical lines and detection limits

Species	Analytical line (nm)	Detection limit in silicate (ppm)	Species	Analytical line (nm)	Detection limit in silicate (ppm)
Ba	455.4	0.17	Ni	341.5	1.8
Co	345.3	2.6	Sc	361.4	0.068
Cr	267.7	0.59	Sr	407.7	0.013
Cu	327.4	0.91	V	310.2	0.67
Li	670.8	0.19	Zr	349.6	0.31

sition were examined for all the elements listed at room temperature and at 50, 90 and 130°C. For the decomposition at 90 and 130°C, a novel design of teflon-lined stainless-steel bomb [6] was used. The effect of heating was not significant except for zirconium in JG-1 and chromium in MRG-1, for which the contents in leached fractions increased with an increase in temperature. Nevertheless, even at 130°C, the recoveries did not reach 100%; they were only 53% for zirconium and 83% for chromium. Complete decomposition of various rock samples at room temperature for determinations of copper, nickel, zinc and cadmium by atomic absorption spectrometry was confirmed earlier [5]. Thus, decomposition at room temperature is recommended for convenience.

The calibration graphs obtained were linear up to 5 ppm for synthetic solutions. The results for a wide variety of rocks are summarized in Table 2 with accuracies and reproducibilities obtained from 6 analyses. The results are in reasonable agreement with reported values. Features of individual elements are as follows.

Barium. Barium is a minor element in most silicates, but is not easily determined by atomic absorption spectrometry because of chemical and ionization interferences. With the plasma, sensitivity is good and there is no interference.

Cobalt. Spectral interferences make it difficult to determine trace amounts of cobalt by the plasma method, as is clear from significant differences between found and reported values in JB-1 and MRG-1 (Table 2). The atomic lines above 340 nm were less sensitive, but suffered less spectral interference than the ionic lines below 260 nm.

Chromium. Chromium ionic lines are sensitive, and significant spectral interferences were not found at the 267.7-nm line. However, chromium in MRG-1 and AGV-1 could not be brought into solution completely by the method proposed, and the reproducibilities were poor for the other two samples; the causes of these problems are not clear.

Copper. Though the 324.7-nm line is more sensitive than the 327.4-nm line, the latter was preferred because of less interference from other elements present, except in the case of JG-1.

TABLE 2

Analytical results with accuracies and precisions for minor and trace elements in standard rock samples

Rock	Metal	Reported value (ppm)	Value found (ppm)	Recovery (%)	R.s.d. (%)
JG-1	Ba	466[a]	463	100	2.2
	Co	6.4	—	—	—
	Cr	52.7	51.1	97	16.6
	Cu	3.9	—	—	—
	Li	94	86.4	92	2.8
	Ni	8.2	7.9	96	10.0
	Sc	6.5	5.4	83	2.8
	Sr	184.1	185	101	0.6
	V	24	24.9	104	2.7
	Zr	111	29.0	26	11.6
JB-1	Ba	490[a]	486	99	1.1
	Co	39.1	45.6	117	3.3
	Cr	405	406	100	6.6
	Cu	55.7	56.1	101	1.9
	Li	11.4	10.7	94	2.6
	Ni	135	140	104	2.2
	Sc	26	26.3	101	1.2
	Sr	435.2	434	100	1.1
	V	211	215	102	2.6
	Zr	153	142	93	2.2
MRG-1	Ba	55[b]	46.7	85	4.4
	Co	87	125	144	8.7
	Cr	420	308	73	1.1
	Cu	135	140	104	1.4
	Li	4	3.9	98	6.2
	Ni	200	196	98	0.8
	Sc	48	50.3	105	2.1
	Sr	260	271	104	0.6
	V	520	533	103	2.2
	Zr	100	110	110	3.2
AGV-1	Ba	1208[c]	1200	99	1.6
	Co	14.1	13.8	98	7.5
	Cr	12.2	7.4	61	4.5
	Cu	59.7	61.2	103	1.6
	Li	12	12.4	103	1.4
	Ni	18.5	17.4[d]	94	8.4
	Sc	13.4	13.0	98	3.7
	Sr	657	658	100	2.1
	V	125	124	99	1.7
	Zr	225	238	106	3.9

[a]Reported by Ando et al. [7]. [b]Reported by Abbey et al. [8]. [c]Reported by Flanagan [9]. [d]351.5 nm used as analytical line.

Lithium. As for other alkali metals, there is no suitable ionic line and atomic lines must be used. The emission intensity of lithium at 670.8 nm is fairly sensitive and there is no significant spectral interference so that agreement with reported values is good.

Nickel. Ionic lines are unsuitable for the determination of nickel in silicates as in the case of cobalt. For the determination of nickel in AGV-1, zirconium emission at 341.466 nm interferes with the nickel emission at 341.477 nm. Thus, 351.5 nm was used in this case.

Scandium. Scandium can be determined very sensitively by i.c.p. emission spectrometry. Even at the trace level, the results are in fair agreement with reported values.

Strontium. Ionization interference was not observed; the results agree well with reported values and reproducibility is good.

Vanadium. Spectral interferences were often observed with vanadium ionic lines. The 292.4, 309.3, 310.2, 311.1 and 311.8 nm lines were investigated. The 310.2-nm line was found to be suitable because of less spectral interference, except from large amounts of nickel.

Zirconium. Zirconium is difficult to determine by atomic absorption spectrometry because of the formation of the monoxide in chemical flames; in i.c.p. spectrometry, the ionic lines give good sensitivity. The most sensitive 343.823-nm line cannot be used because of spectral interference from the Fe 343.831-nm line.

Conclusions

The inductively-coupled plasma is suitable for the determination of minor and trace elements in silicate rocks. For barium, chromium, scandium, vanadium and zirconium, which are difficult to determine by flame atomic absorption spectrometry, sensitivity is high and chemical and ionization interferences are not observed. However, a spectrometer with great resolving power is necessary in order to reduce spectral interferences. The proposed method for the decomposition of silicate rocks gives complete dissolution of almost all minor and trace elements. Mixed standard solutions are simply prepared in the same matrix solution.

The authors express their gratitude to Dr. I. Kojima for useful discussions.

REFERENCES

1 S. Greenfield, H. M. McGeachin and P. B. Smith, Anal. Chim. Acta, 84 (1976) 67.
2 D. J. Kalnicky, V. A. Fassel and R. N. Kniseley, Appl. Spectrosc., 31 (1977) 137.
3 H. Uchida and H. Matsui, Bunko Kenkyu, 27 (1978) 110.
4 H. Uchida, T. Uchida and C. Iida, Anal. Chim. Acta, 108 (1979) 87.
5 T. Uchida, M. Nagase, I. Kojima and C. Iida, Anal. Chim. Acta, 94 (1977) 275.
6 C. Iida, T. Uchida and I. Kojima, Anal. Chim. Acta, 113 (1980) 365.
7 A. Ando, H. Kurasawa, T. Ohmori and E. Takeda, Geochem. J., 8 (1974) 175.
8 S. Abbey, A. H. Gillieson and G. Perrault, A. Report on the Collaborative Analysis of Three Canadian Rock Samples for Use as Certified Reference Materials, 1975.
9 F. J. Flanagan, Geochim. Cosmochim. Acta, 37 (1973) 1189.

ANALYTICA CHIMICA ACTA, Vol. 116 (1980)

AUTHOR INDEX

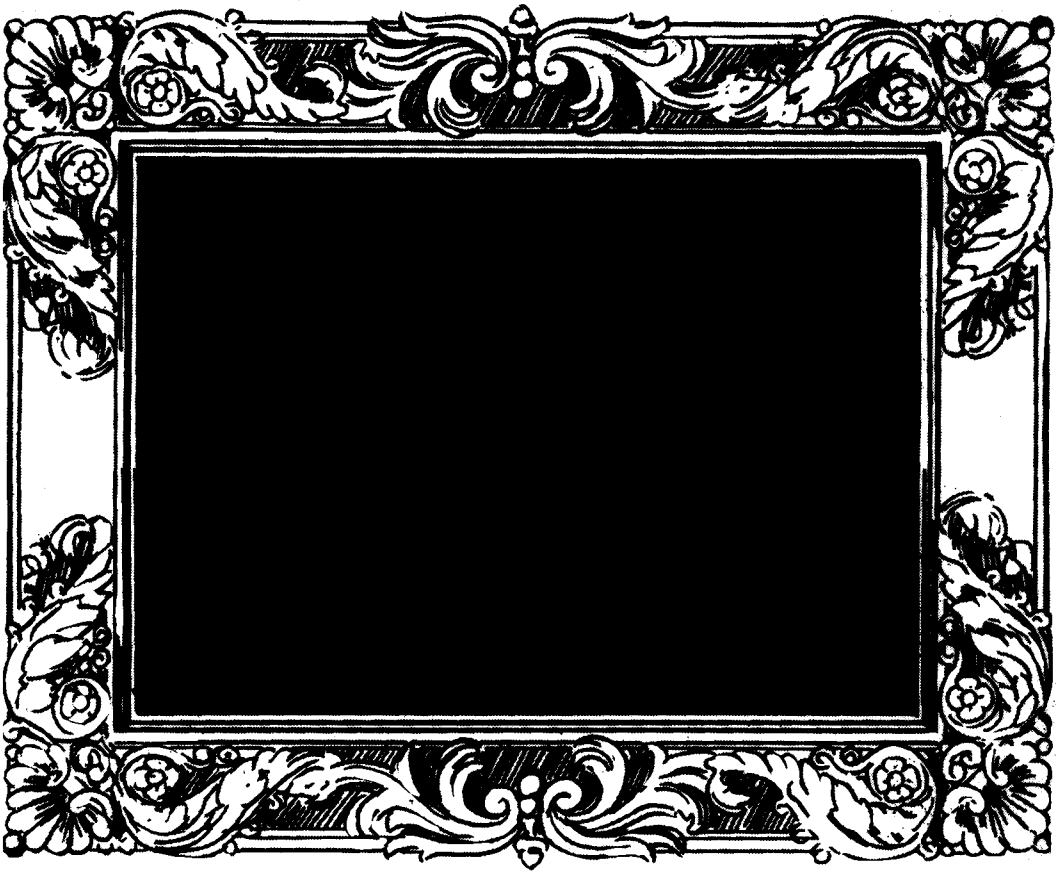

What Industry would be without computers.

Computers?
You as an engineer don't need them as toys. Playing is for kids and Einsteins. But you need them badly as tools.
You want to forget about them as soon as you can. But not sooner. You and your company thrive on them. Or worry about them.
Read Computers in Industry, from cover to cover, 4 times a year and subscribe to it. You need it more than you know. And so does your Industry.

COUPON FOR A FREE COPY

For a free copy of a recent issue of **Computers in Industry,** please write or complete the coupon and return it directly to the publisher:

North-Holland Publishing Company
Attn: Mr. J. Dirkmaat
P.O. Box 211
1000 AE Amsterdam, The Netherlands

Name: _____

_____

Address: _____

_____

_____

6054 NH

Evaluation and Optimization of Laboratory Methods and Analytical Procedures

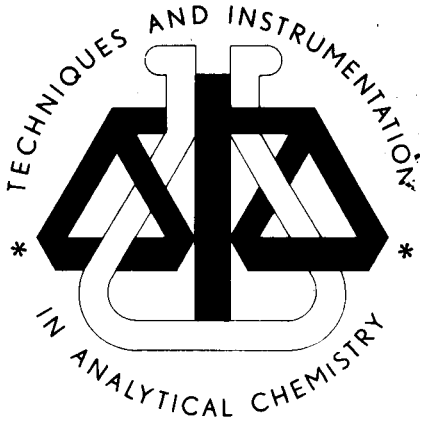

A Survey of Statistical and Mathematical Techniques

D.L. MASSART, A. DIJKSTRA *and* L. KAUFMAN.

with contributions by S. Wold, B. Vandeginste *and* Y. Michotte

Techniques and Instrumentation in Analytical Chemistry - Volume 1

This book provides detailed treatment, in a single volume, of formal methods for optimization in analytical chemistry. It is a comprehensive and practical handbook which no analytical laboratory will want to be without.

All aspects of optimization are discussed, from the simple evaluation of procedures to the organization of laboratories or the selection of optimal complex analytical programmes. Quantitative discrete analysis as well as qualitative and continuous measurement techniques are evaluated.

The book consists of 30 chapters divided into 5 main parts.The main sections are: Evaluation of the Performance of Analytical Procedures, Experimental Optimization, Combinatorial Problems, Requirements for Analytical Procedures, and Systems Approach in Analytical Chemistry.

This work will be of practical value not only to those involved with optimization problems in analytical chemistry, but also to those in related fields such as clinical chemistry or specialized fields such as chromatography. Because it discusses the application of many mathematical techniques in analytical chemistry, this book will also serve as a general introduction to the new field of Chemometrics.

Oct. 1978 xvi + 596 pages US $57.75/Dfl. 130.00 ISBN 0-444-41743-5

ELSEVIER

P.O. Box 211,
1000 AE Amsterdam
The Netherlands

52 Vanderbilt Ave
New York, N.Y. 10017

The Dutch guilder price is definitive. US $ prices are subject to exchange rate fluctuations.

7113

(continued from back cover)

CONTENTS

(continued on inside page of cover)

Printed in The Netherlands.